

“ex duobus oculis pars unica”



2nd International Tsunami Field Symposium

IGCP Project 495

Quaternary Land-Ocean Interactions:
Driving Mechanisms and Coastal Responses

Ostuni (Italy) and Ionian Islands (Greece) 22-28 September 2008



Project 495

Palaeotsunami imprints along the coasts of the Central Mediterranean Sea

Field Guide

by

Giuseppe Mastronuzzi ¹

Paolo Sansò ²

Helmut Brückner ³

Andreas Vött ⁴

Cosimo Pignatelli ¹

Riccardo Caputo ⁵

Donato Coppola ^{6, 7}

Daniela Di Bucci ⁸

Umberto Fracassi ⁹

Simon Matthias May ⁴

Maurilio Milella ¹

Gianluca Selleri ^{2, 10}

¹ Dipartimento di Geologia e Geofisica, Università degli Studi “Aldo Moro”, Bari, Italy;

² Dipartimento di Scienza dei Materiali, Università del Salento, Lecce, Italy;

³ Faculty of Geography, Philipps-Universität Marburg, Germany;

⁴ Department of Geography, Universität zu Köln, Germany;

⁵ Università degli Studi di Ferrara, Dipartimento di Scienze della Terra, Ferrara, Italy;

⁶ Museo di Civiltà Preclassiche della Murgia Meridionale, Ostuni (BR), Italy;

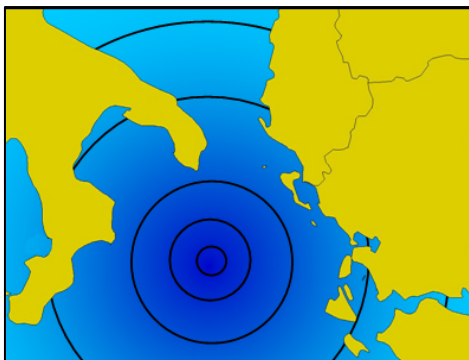
⁷ Dipartimento di Beni Culturali, Musica e Spettacolo, Università degli Studi “Tor Vergata”, Roma, Italy;

⁸ Dipartimento della Protezione Civile, Roma, Italy;

⁹ Istituto Nazionale di Geofisica e Vulcanologia, Roma, Italy;

¹⁰ G.D.S. – Geo Data Service s.r.l., Taranto, Italy.

Preface



The dramatically increasing extension of human presence in coastal areas makes them particularly prone to low frequency – high magnitude events, such as tsunamis and or exceptional sea-storms. Due to the global climate change areas where extreme events were uncommon in the past, will be affected more frequently by high-energy coastal dynamics (for instance: Gianfreda et al., 2005; Emanuel, 2005; Bourrouilh-Le Jan et al., 2007; Fita et al., 2007). Moreover the recent floods of Myanmar (2008), Bangladesh (2007), USA (2005) and Philippines (2004) remind us that numerous coastal areas in the world are highly vulnerable.

The tsunami that occurred on December 26th, 2004 was the largest event that ever occurred in history. About 300.000 persons died in Indonesia, Thailand, and other countries in

Asia and Africa facing the Indian Ocean. Large coastal areas were completely flooded and coasts were strongly modified and even destroyed (for instance: Lavigne et al., 2006; Richmond et al., 2006; Umitzu et al., 2007; Paris et al., 2007; 2008; Srinivasalu et al., 2007). Tsunami waves caused also tremendous damage of infrastructure facilities and the environment (Gunatillake, 2007) producing economic, social and politic changes (Sukma, 2006; Clarck, 2007; Gaillard et al., 2008). The causes for the incredibly long list of casualties seems to be related to the scarce research on tsunamigenic areas and also on tsunami propagation and potential tsunami effects on coasts. Nevertheless, underrating the use of morphological/sedimentological evidence for the determination of tsunami target areas and for setting up a chronology of past events could make future impacts even more destructive. The large growth of tsunami science in the last few years produced dozens of field research performed along different coasts all over the world; they permit to identify a big number of tsunami relics. However, there are still few geological studies focusing on field evidence of tsunami events that occurred in the late Holocene.

An active debate exists concerning the discrimination between tsunami and sea storm effects. The main task is to improve our knowledge on coastal wave dynamics and on the local effects of wave propagation, but also to improve our knowledge of the past climate about wind-generated wave. Such scientific efforts are justified by the importance of tsunami risk assessment; their acceptance is being directly linked to the frequency and intensity of such events in the study area. However, informing on the tsunamis risk assessment along a coastal area is to define its overall vulnerability.

Many tsunami occurred before the Andaman – Sumatra 2004 event and killed thousands of people along many coasts of the world (for instance: Baptista et al., 1993; Yeh et al., 1993; 1995; Shimamoto et al., 1995; Tsuji et al., 1995a; 1995b; Imamura et al., 1995; Shuto & Matsutomi, 1995; Pelinovsky et al., 1997; Maramai & Tinti, 1997). These phenomena are rarely taken into account by planners, with the exception of particular high-developed areas where modern structures and procedures seek to mitigate the tsunami risk (Narayan et al., 2005; Cochard et al., 2008). During the past years, worldwide catalogues of tsunami events were elaborated for different regions of the world (NGDC, 2008; ITIC, 2008; ICMMG, 2008; USGS, 2008); they comprise far more than 2000 events for the past 4000 years (Scheffers & Kelletat, 2003); field data was hardly incorporated into these catalogues (Scheffers & Scheffers, 2007).

High-magnitude, low-frequency events are considered to have played an important role in the evolution of many coastlines (for instance: Dawson, 1994; Bryant, 2001). In fact, tsunami are able to modify coastal system erasing or destroying their previous architectures. Already Heck (1947) reported that large boulders were transported far inland by the December 8th, 1908 tsunami in the Strait of Messina (Sicily). Geomorphological effects of catastrophic wave impacts have been reported since the 1990s by, for instance, Kawana & Pirazzoli (1990) and Nishimura & Miyaji (1995) for Japan; Jones & Hunter (1992) for the Cayman Islands; Bryant et al. (1996), Bryant & Young (1996) and Young et al. (1996), for the southeastern coast of Australia; Hearty (1997; 1998) for the Bahamas; Mastronuzzi & Sansò (2000; 2004) and Scicchitano et al. (2007) for Italy. In particular, geological research focused on the signature of tsunamis represented by anomalous sand layers encountered within lagoonal muds (for instance Atwater, 1987; Bourgeois et al. 1988; Minoura & Nakaya, 1991; Minoura et al., 1997; Bondevik et al., 1997a; 1997b; Goff & Chagué-Goff, 1999; Dawson & Smith, 2000; De Martini et al., 2003; Vött et al., 2007a; 2008a; 2008b). However, palaeotsunamis can also be detected by the presence of unusually sized coastal landforms, i.e. huge washover fans at the back of a sandy coastal barrier (for instance: Andrade, 1992; Gianfreda et al., 2001; Ruiz et al., 2005; Vött et al., 2006a; Switzer et al. 2006; de Lange & Moon, 2007) or accumulations of large boulders – isolated, in fields or in berms – near the coastline.

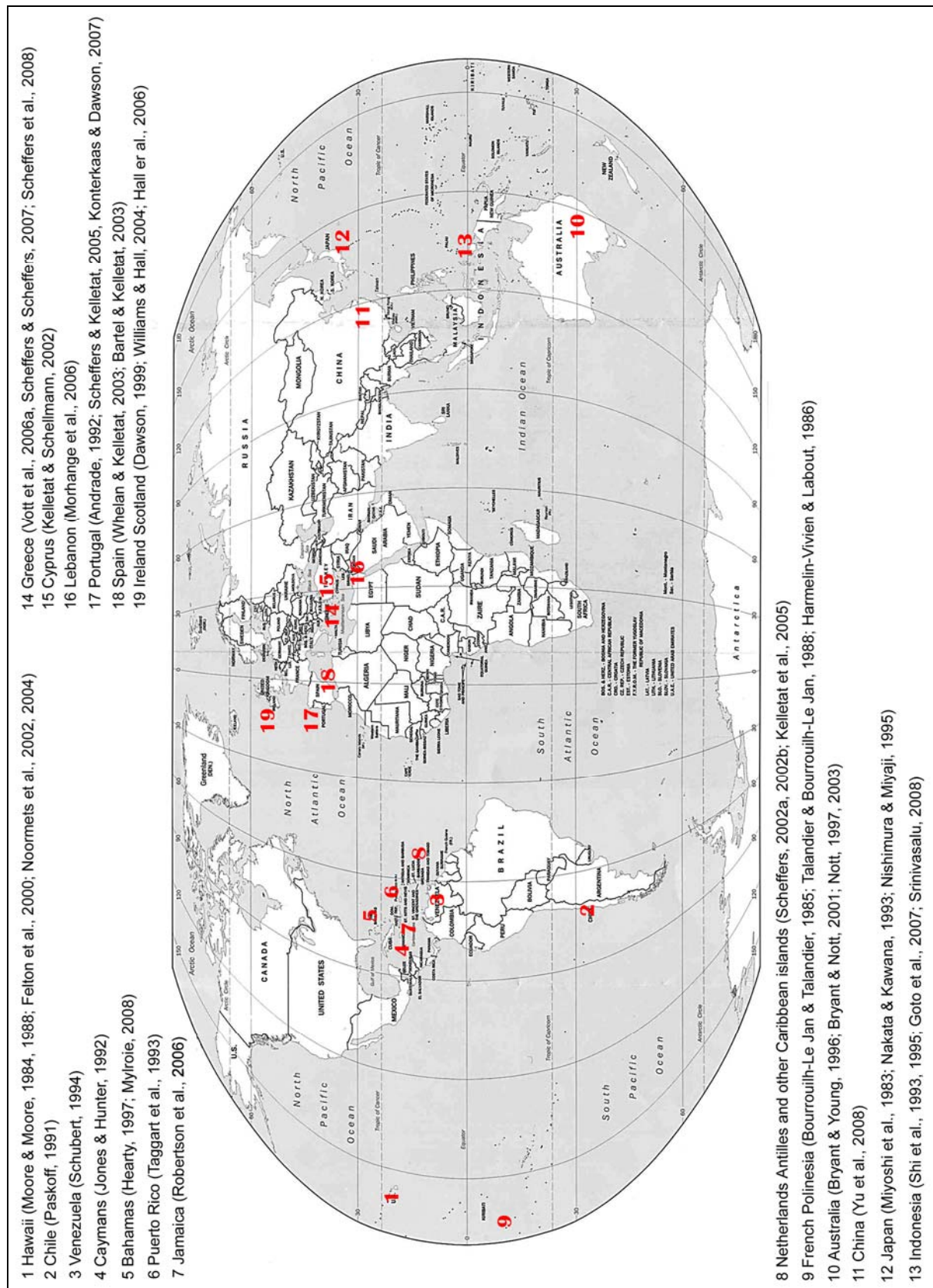


Figure 1 – Localities around the world that show boulders deposits due to impact of tsunami, sea storms and hurricanes.

Boulders assemblage is present along numerous rocky coasts all around the coast of the world (Fig. 2.18): in Hawaii (i.e.: Moore & Moore, 1984; 1988; Felton et al., 2000; Noormets et al., 2002; 2004); Chile (i.e.: Paskoff, 1991); Venezuela (i.e.: Schubert, 1994); the Caymans (i.e.: Jones & Hunter, 1992); the Bahamas (i.e.: Hearty, 1997; Mylroie, 2008); Puerto Rico (i.e.: Taggart et al., 1993); Jamaica (i.e.: Robertson et al., 2006); the Netherlands Antilles and other Caribbean islands (i.e.: Scheffers, 2002a; 2002b; Kelletat et al., 2005); French Polynesia (i.e.: Bourrouilh-Le Jan & Talandier, 1985; Talandier & Bourrouilh-Le Jan, 1988; Harmelin-Vivien & Labout, 1986); Australia (i.e.: Bryant & Young; 1996; Bryant & Nott, 2001; Nott, 1997; 2003); China (Yu et al., 2008); Japan (i.e.: Miyoshi et al., 1983; Nakata & Kawana, 1993; Nishimura & Miyaji, 1995); Indonesia (i.e.: Shi et al., 1993; 1995; Goto et al. 2007; Srinivasalu et al., 2008); Greece (Vott et al., 2006a; Scheffers & Scheffers, 2007; Scheffers et al., 2008); Cyprus (i.e.: Kelletat & Schellmann, 2002); Lebanon (i.e.: Morhange et al., 2006); Portugal (i.e.: Andrade, 1992; Scheffers & Kelletat 2005; Konterkaas & Dawson, 2007); Spain (i.e.: Whelan & Kelletat, 2003; Bartel & Kelletat, 2003) and Ireland, Scotland (i.e.: Dawson, 1999; Williams & Hall, 2004; Hall et al., 2006) (Fig. 1).

Boulder deposits are present along numerous rocky coasts in the world; their accumulation is attributed to tsunami but also to exceptional storm events (for instance: Mastronuzzi & Sansò, 2004; Williams & Hall, 2004; Hall et al., 2006); in other cases, it is known that boulders were emplaced by hurricanes (Scheffers, 2002a; 2002b; 2004). However, this debate is still going on involving all the scientific aspects connected to tsunami sciences. Notwithstanding the recent increase of tropical like-cyclones in Mediterranean (for instance: Ernst & Matson, 1983; Rasmussen & Zick, 1987; Reale & Atlas, 1998; Pytharoulis et al., 1999; Gianfreda et al., 2005; Emanuel, 2005; Monserrat et al., 2006; Beck et al., 2007; Fita et al., 2007; Meehl et al., 2007; Ullmann et al. 2007), this area is characterized by the absence of hurricane-like storms and thus represents an ideal laboratory for determining the true capacity of tsunamis and their effects on the coasts.

The main objectives of this book are: **(i)** present selected morphological, sedimentological and chronological data associated to tsunami impacts all around the coasts of Apulia (Italy) and Ionian Island (Greece); **(ii)** compare them with the historical series of wave climate data; **(iii)** discuss whether storm or tsunami events can be made responsible for boulder emplacement.

The Conference Organizers

Giuseppe Mastronuzzi

Dipartimento di Geologia e Geofisica
Università degli Studi “Aldo Moro”
Bari - Italy

Helmut Brückner

Faculty of Geography
Philipps-Universität Marburg
Marburg/Lahn - Germany

Paolo Sansò

Dipartimento di Scienza dei Materiali
Università del Salento
Lecce - Italy

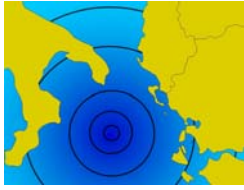
Andreas Vött

Department of Geography
Universität zu Köln
Köln - Germany

Note

The present book has been realized as the result of the implementation of texts and new data coming from different sources. Pictures are in part unpublished; text are original and/or in part derived or reprinted by the following official publication listed in alphabetical order:

- Caputo et al. (2008). Rend. On line Società Geologica Italiana, 1, Note Brevi, www.socgeol.it, 62-67.
- Gianfreda et al. (2001). Natural Hazard and Earth System Sciences, 1, 213-219.
- Gravina et al. (2005). *Mediterranéé*, 1-2, 107-117.
- Mastronuzzi et al. (2004). Risk Analysis IV, Wessex Institute of Technology Press, 681-689.
- Mastronuzzi et al. (2006). *Zeitschrift für Geomorphologie*, NF Suppl. Bd., 146, 173-194.
- Mastronuzzi et al. (2007). *Marine Geology*, 242, 191-205.
- Mastronuzzi G., Sansò P. (2000). *Marine Geology*, 170, 93-103.
- Mastronuzzi G., Sansò P. (2002). *Journal of Quaternary Science*, 17 (5-6), 593-606.
- Mastronuzzi G., Sansò P. (eds) (2003). *GI2S Coast*, Research Publication, 5, 184 pp.
- Mastronuzzi G., Sansò P. (2004). *Quaternary International*, 120, 173-184.
- Mastronuzzi G., Sansò S. (2006). *Geografia Fisica e Dinamica Quaternaria*, 29 (2), 83-91.
- Pignatelli et al. (2008). *Memorie Descrittive della Carta Geologica d'Italia* (in press).
- Vött et al. (2006a). *Zeitschrift für Geomorphologie N.F. Suppl. Bd.*, 146, 139-172.
- Vött et al. (2006b). *Geoarchaeology*, 21/7, 649-664.
- Vött et al. (2007a). *Méditerranée*, 108, 43-57.
- Vött et al. (2008a). *Quaternary International*, 181, 105-122.
- Vött et al. (2008b). *Global and Planetary Change* (accepted).
- Vött et al. (2008c). *Proc. Int. Conf. Honouring Wilhelm Dörpfeld*, August 6-9, 2006, (in press).
- Zander et al. (2006). *Geografia Fisica e Dinamica Quaternaria*, 29 (2), 33-50.



2nd International Tsunami Field Symposium

IGCP Project 495

Quaternary Land-Ocean Interactions:
Driving Mechanisms and Coastal Responses

Ostuni (Italy) and Ionian Islands (Greece) 22-28 September 2008



Project 495

CHAPTER 1

Central Mediterranean Area: An Overview

Brückner H., Mastronuzzi G., Pignatelli C., Sansò P., Vött A.

1.1. Introduction

The coasts of the central Mediterranean Sea are characterized by numerous indentations. Its major part is the Ionian Sea, a deep semi-closed basin, enclosed by Tunisia to the W, Sicily to NW, the peninsulas of Calabria and Apulia in southern Italy to the N, Greece to E-NE and North Africa to S. The Otranto Channel connects the Ionian and the Adriatic Seas; the Sicily Channel joins the Ionian Sea to the western Mediterranean basin. Only towards the SE there is an open sea connection to the Ionian Basin with the Eastern Basin (Fig. 1.1).



Figure 1.1 - Map concerning the Central Mediterranean Basin. (NASA Satellite Image, Modified).

The Mediterranean area is frequently affected by tsunami impacts as reported by earthquake and tsunami catalogues (for instance Ambraseys, 1962, 1965; Antonopoulos, 1979; Caputo & Faita, 1984; Bedosti & Caputo, 1987; Guidoboni & Tinti, 1987; 1988; Tinti & Maramai, 1996; Tinti et al., 1995; 2004; Soloviev, 1990; Soloviev et al., 2000). These catalogues are based upon historical and archival descriptions and on seismological data. During the past decades, new data deriving from systematic geological (geomorphological and sedimentological) and (geo-)archaeological studies have permitted to improve these catalogues (for instance Guidoboni & Comastri, 2007; Tinti et al., 2007).

Since Heck's (1947) study on geomorphological effects of the December 1908 Messina tsunami waves a large number of geomorphological surveys have been performed in the central Mediterranean yielded further evidence of palaeotsunami impact.

Along the Ionian coasts of southern Italy, boulder fields and/or boulder ridges were identified and studied in Sicily (Scicchitano et al., 2007) and in Apulia (Mastronuzzi & Sansò, 2000, 2004; Mastronuzzi et al., 2007a) and attributed to different tsunami that occurred in historical time. Vött et al. (2006a, 2007a, 2008a) identified tsunamigenically dislocated boulders, fields of scattered blocks and stones from the littoral zone, tsunami-prone washover fans etc. along the northern coasts of the island of Lefkada in Greece. Moreover, sedimentological and geo-archaeological studies were carried out in Sicily (for instance: Barbano et al., 2007; Smedile et al., 2007; Pantosti et al., 2008; Scicchitano et al., 2008), in Apulia (for instance: Gianfreda et al., 2001; De Martini et al., 2003; Gravina et al., 2005) and in northwestern Greece (for instance: Vött et al., 2008a; 2008b). These studies allowed to complete the list of tsunami events based on data coming from sediment cores and palaeoecological analyses.

1.2. Geomorphological and sedimentological traces of tsunami impact in the central Mediterranean area

Along the coast of southern Italy and western Greece, several sites are characterized by the presence of geomorphological and sedimentological evidence of palaeotsunami impact. They are characterized by out-of-place layers and out-of-size landforms.

For instance, allocthonous sandy/gravel layers were found intercalating dune or in back dune, lagoonal or coastal lake deposits. Analyses of biological indicators (molluscs, foraminifera, etc.) further allow to reconstruct the inundation limit; ¹⁴C-AMS age helped to determine local tsunami chronologies.

Out-of-place layers were detected along the eastern coast of Sicily not far from Messina and in the lagoonal area near Augusta and Messina. Based on radiocarbon analyses and archaeological data tsunami landfalls were found for 17 AD, the IV century, 4th of January, 1169, 1st of January, 1693, 6th of February 1783 and 12th of December 1908; some more pre-historic tsunami were identified (Barbano et al., 2007; Smedile et al., 2007; Pantosti et al., 2008; Scicchitano et al., 2008).

In Apulia, out-of-place layer were identified near the Gargano promontory, around the Lesina Lake and near Manfredonia in the Siponto area. Some of these findings were ascribed to the tsunami from 30th of July, 1627; some other deposits were accumulated by older events maybe during the IV century and in prehistoric time (De Martini et al., 2003).

In Greece, tsunami traces were found in the lagoonal area near Lefkada Island and in the Voulkaria coastal lake (Vött et al., 2006a; 2007a; 2008a; 2008b).

Out-of-size landforms are represented by mega-boulders and sand by washover fans. The study of boulder and berm positions may indicate the limit of the maximum flooding.

The scattering causal depositional event of these boulders along the coast is still a matter of debate and yet is generally attributed to extreme waves. Some of them are considered result of the impact of tsunami on the coasts (i.e.: Scheffers & Scheffers, 2007; Mastronuzzi et al., 2007; Vött et al., 2008c). However, in some cases there are evidences that boulders emplacement and/or reworking has been caused by storms and/or hurricanes (Scheffers, 2002a, 2002b; 2004; Mastronuzzi & Sansò, 2004; Williams & Hall, 2004; Hall et al., 2006; Hansom et al., 2008). At present, no physical or morphological criteria have been identified to distinguish between the morpho-sedimentological effects of severe storms, hurricanes, cyclones and tsunami. Recent papers indicate that morphological characters as row of imbricated boulders previously considered diagnostic of tsunami depositional processes, can be produced by a sequence of distinct storms (Mastronuzzi & Sansò, 2004; Williams & Hall 2004); so far, there are evidences that boulders have been emplaced inland and then reworked by different events (Mastronuzzi & Sansò, 2004; Noormets et al., 2004). Even less is known on the normal high energy wave processes that characterize rocky coasts in their sub-aerial or underwater parts (Felton & Crook, 2003; Le Roux et al., 2004; Felton et al., 2006).

Along the Italian coast, tsunamigenically dislocated boulders were found between Augusta and Siracusa in Sicily and near Crotone in Calabria. Along the Maddalena Peninsula, near Siracusa, tsunami boulders rest on a large terrace at 5 m above sea level which is ascribed to MIS 5 (Scicchitano et al., 2007) and on gently sloping

rocky coasts. Boulders are up to 150 t in weight and are arranged in isolated elements or small groups composed of a few imbricated elements. The surface of the boulders is usually covered by biogenic encrustations (serpulids, balanids, *Lithophaga* sp.) suggesting a mid or sub-littoral origin. Radiocarbon data, compared to historical catalogues, suggest that at least three tsunamis produced by local sources struck the Ionian coast of south-eastern Sicily on 4th of February, 1169, on 11th of January, 1693, and during the strong earthquake in the Strait of Messina on 28th December, 1908 (Scicchitano et al., 2007) (Fig. 1.2).

Along the eastern side of the Crotone peninsula, flanked by a staircase of marine terraces referred to MIS 9 and MIS 5, isolated boulders cover a well developed wave cut platform stretching at approx. 1 m above biological sea level (a.b.s.l.) raised by recent co-seismic events (Pirazzoli et al., 1997). The maximum weight of these boulders is estimated to 3 tons. Unfortunately, no bioconcretions are present and so it is impossible to assess the age of the scattered boulders.

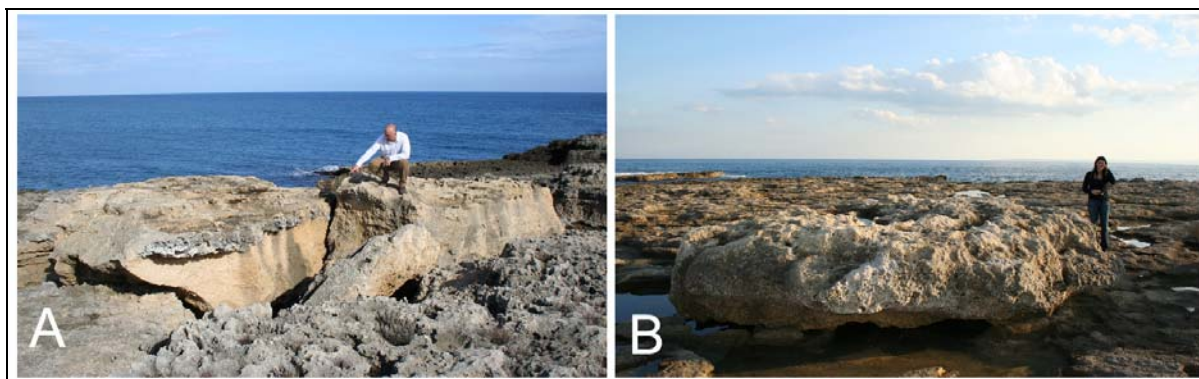


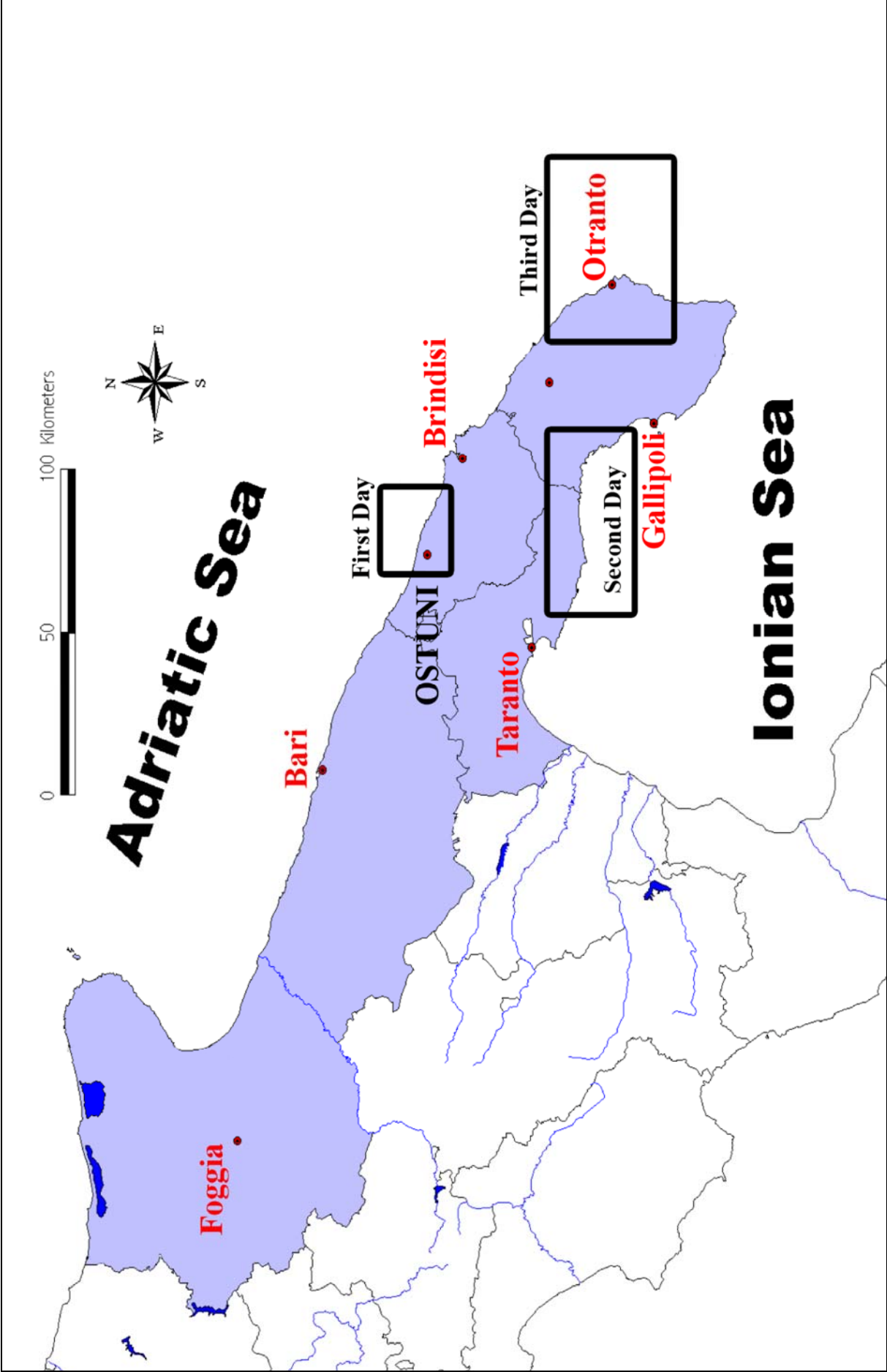
Figure 1.2 – Boulder deposits in Southeastern Sicily. **A)** Punta della Maddalena (Siracusa); **B)** Penisola Monte Tauro (Augusta).

Sparse boulders, boulder fields, boulder berms and sand berms were also identified between Taranto, Capo Santa Maria di Leuca and Brindisi and Ostuni, up to Bari in Apulia, along both Ionian and Adriatic coasts. Radiocarbon analyses as well as archaeological and historical data reveal at least four different tsunami events that occurred on 4th December, 1456, on 6th April, 1667, on 20th February, 1743 and on 24th April, 1836 (Mastronuzzi & Sansò, 2000, 2004; Mastronuzzi et al., 2007).

Washover fans were identified in the Lesina coastal lake, in the northernmost part of Apulia region. Analyses performed on biological remains indicate that they were formed by the tsunami events that occurred on 493 AD and on 30th of July, 1627; another strong tsunami affected the area in prehistoric times building a large washover fan (Gianfreda et al., 2001; Gravina et al., 2005).

In the Lefkada-Preveza coastal zone in northwestern Greece, a series of palaeotsunami deposits were discovered by Vött et al. (2006a, 2007a, 2007b, 2008a, 2008b; May et al., 2007). These sediments, partly interrelated, attest to multiple tsunami landfall since the mid-Holocene. Tsunamite types comprise dislocated mega-blocks both on land and under water, washover fan deposits (chevrons), run up/backwash layers, a breakthrough channel and suspension deposits in a near-coast freshwater lake environment. Recent studies along the shores of the quiescent lagoonal waters of the nearby Sound of Lefkada revealed geo- and bio-scientific evidence of multiple tsunami influence since, at least, around 2800 cal BC and document strong impact on the long-term coastal evolution (Vött et al., 2008b). Tsunami findings from the inner sound correlate well with those known from the Preveza-Lefkada outer-sound area. Tsunami events were dated by means of radiocarbon dating and age determination of diagnostic ceramic fragments; tsunami landfalls were found for around 2800 BC, 1620 BC, 1000 BC, 350 BC and 800-1000 AD (Vött et al., 2006a; 2007a; 2008a; 2008b).

APULIAN FIELD TRIP
23-25 September 2008





2nd International Tsunami Field Symposium

IGCP Project 495

Quaternary Land-Ocean Interactions:
Driving Mechanisms and Coastal Responses

Ostuni (Italy) and Ionian Islands (Greece) 22-28 September 2008



Project 495

CHAPTER 2

Geological, Geodynamic and Morphological features of Apulia (Italy)

*Mastronuzzi G., Pignatelli C., Sansò P., Selleri G.,
Caputo R., Di Bucci D., Fracassi U., Milella M.*

2.1. Geological and geodynamic setting

Southern Italy is placed in the centre of a complex tectonic mosaic that justifies the presence of numerous different seismically active structures and a number of active volcanoes (Channel et al., 1979; Favali et al., 1993).

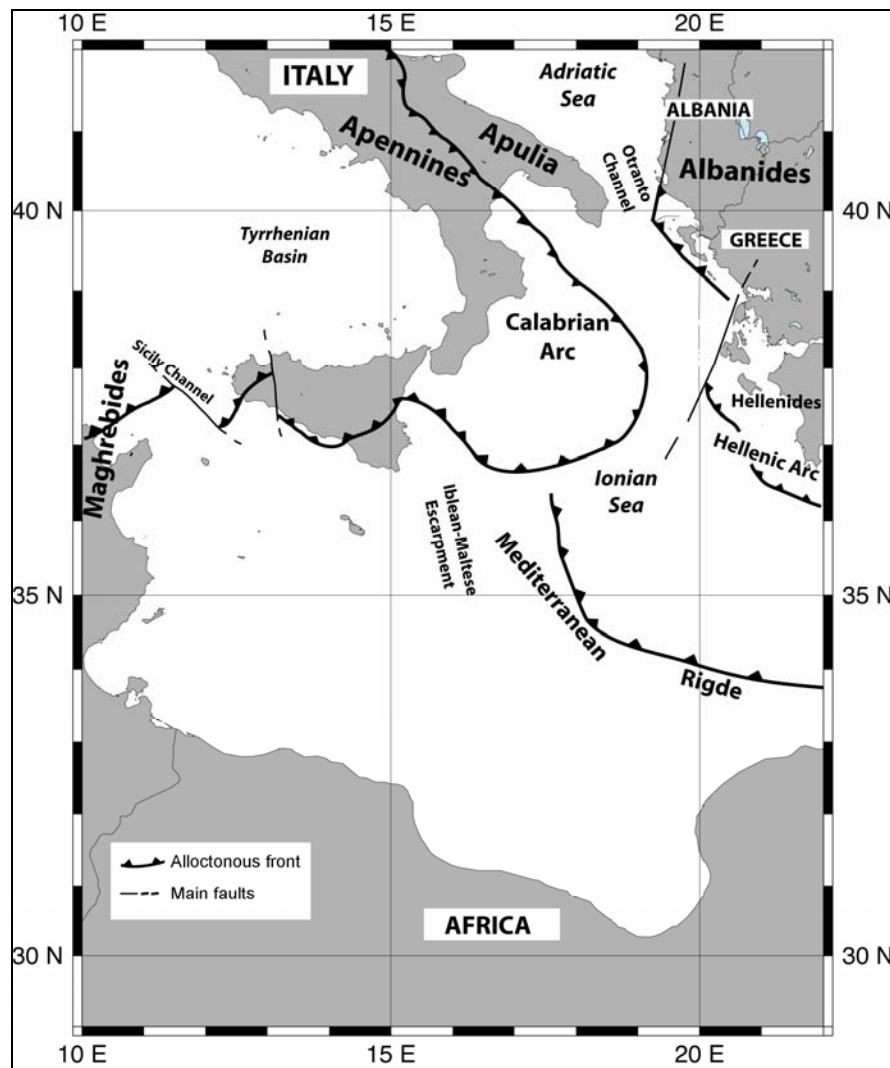


Figure 2.1 - Main geodynamic features of the Central Mediterranean Basin and surrounding areas.

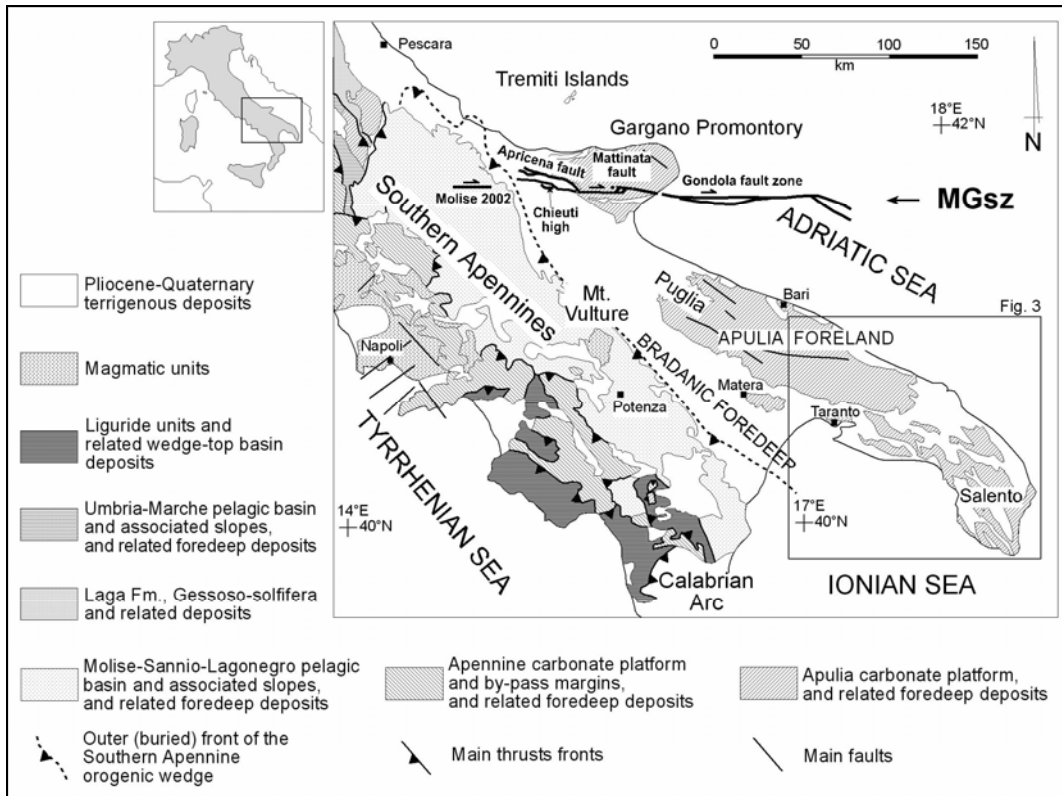


Figure 2.2 - Geological sketch map of Southern Italy (Calabrian Arc excl.). The Mattinata-Gondola shear zone (MGsz) is also shown.

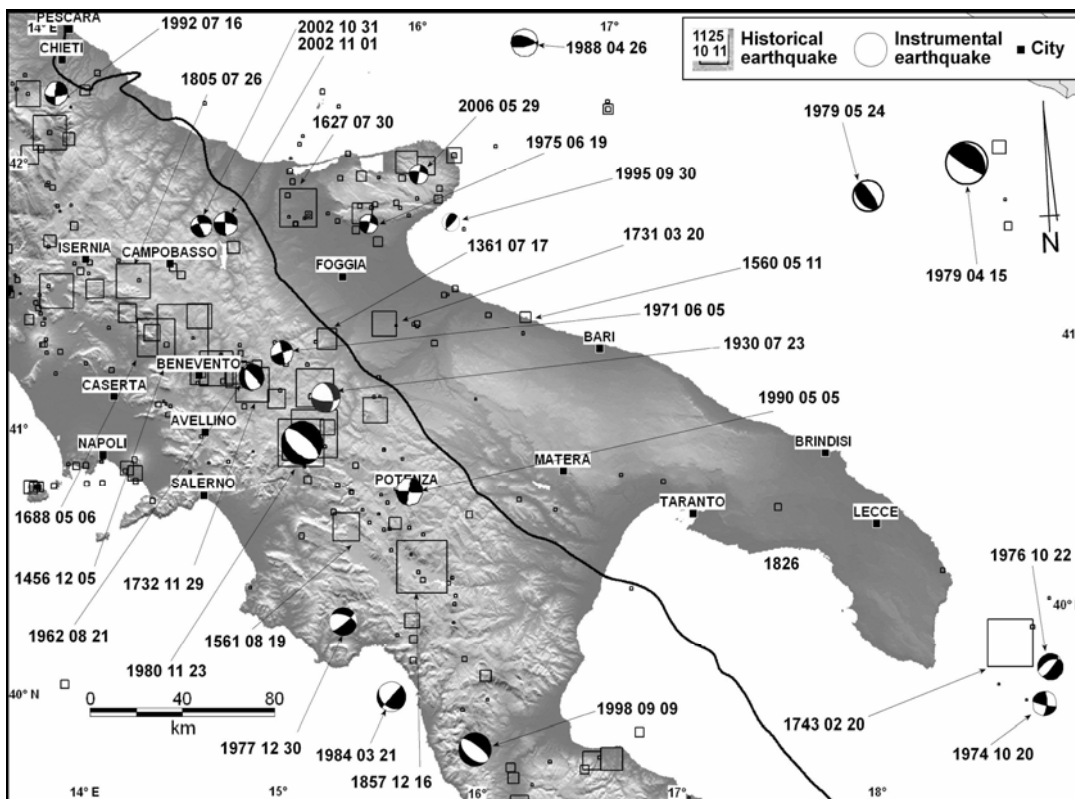


Figure 2.3 - Historical and instrumental earthquakes of the Central and Southern Apennines ($M > 4.0$; Gruppo di lavoro CPTI, 2004; Vannucci & Gasperini, 2004; Harvard CMT Project, 2006; Fracassi & Valensise, 2007). The size of the square Symbols is proportional to an equivalent magnitude derived from intensity data. The black thick line is the outer buried front of the Southern Apennines as in Fig. 2.2 (from Caputo et al., 2008).

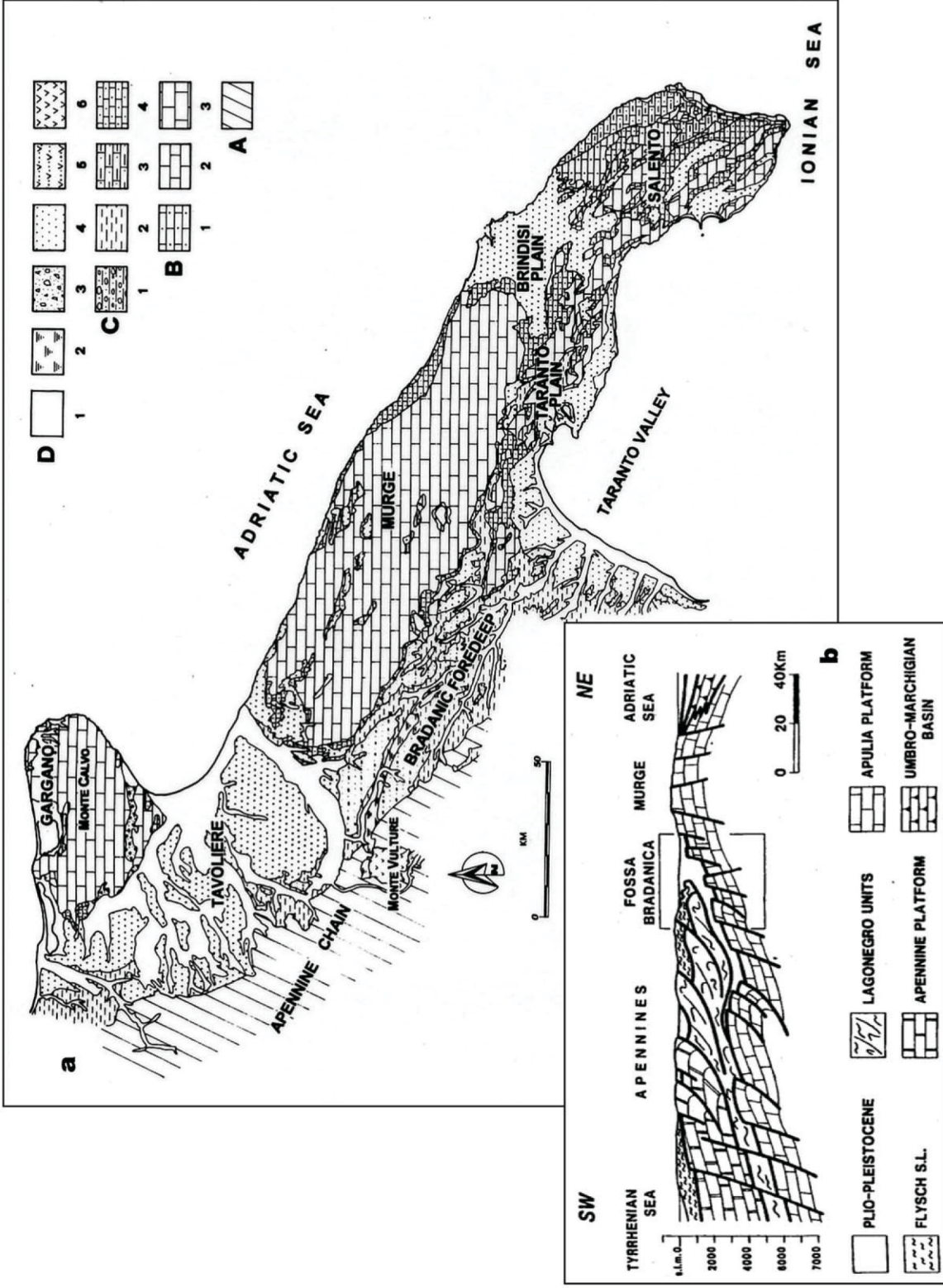


Figure 2.4 – Geological map and geological cross section of Puglia region. **A.** Apenninic Units; **B.** Apulian Foreland; **1** – Open shelf carbonate sequences, Miocene; **2** – Calcarenes and calcilutites, Paleocene – Oligocene; **3** – Limestones and dolomites, Cretaceous; **C.** Foredeep: **1** – Sands and conglomerates; Lower Pleistocene; **2** – Clay; Lower Pleistocene; **3** – Calcarenes and calcilutites; Pliocene; **4** – Calcarenes; Middle Pliocene – Lower Pleistocene; **D.** Quaternary: **1** – Alluvial, beaches and coastal dune deposits; Upper Pleistocene – Holocene; **2** – Lacustrine terraces deposits; Lower – Middle Pleistocene; **3** – Slope deposits; Late Pleistocene; **4** – Marine terraced deposits; Middle-Upper Pleistocene; **5** – Volcano sedimentary deposits; **6** – Volcanic deposits (from Caldara et al., 1998; Sella et al., 1988).

The Ionian Sea, the Otranto Channel and the southern Adriatic Sea are surrounded by the Albanides and by the Hellenic chain to the E-NE and by the Apennines and by Calabro-Peloritan Arc to the W-NW. The Apennines and Calabro-Peloritan Arc are characterized by extensive seismic activity while compressive seismic activity is present in the Albanides and the Hellenides. According to the distribution of earthquakes epicentres (Fig. 2.1), important active structures have been recognised in the area of Ionian sea (for instance: Lort, 1971; Anderson & Jackson, 1997; Bianca et al., 1999; Argnani & Bonazzi, 2005) as far as the Iblean-Maltese scarp located off-shore between Sicily and Malta or the Kefalonia scarp (Argnani & Bonazzi, 2005).

Indeed, in 1743 the southern portion of the Adriatic foreland was hit by a severe earthquake sequence, but these events have been positively located off-shore (I_{\max} =IX-X, M =6.9; Gruppo di Lavoro CPTI, 2004; Guidoboni & Ferrari 2004). This conclusion is also supported by the study of the deposits recognized in the southernmost part of Apulia and referred to this earthquake (Mastronuzzi & Sansò 2004; Mastronuzzi et al. 2007a).

The Apulia region corresponds to the only emerged part of the Adriatic foreland of both the Apennines and Dinarid/Hellenides chains (Fig. 2.2). The Adriatic foreland has long been considered a tectonically and seismically “stable” area; in effect, only in its central sector it is characterized by significant historical and instrumental seismicity (Boschi et al., 2000; Gruppo di Lavoro CPTI, 2004; Castello et al., 2005; Fig. 2.3), both off shore (active Mesoadriatic strip; Console et al., 1993) and on-land (Molise-Gondola shear zone; Di Bucci et al. 2006; Fig. 2.2). Recently some seismogenic faults have already been identified (DISS Working Group, 2007, and references therein).

Northern Apulia is the locus of rare but destructive historical earthquakes (Gruppo di Lavoro CPTI, 2004), occasionally associated with surface faulting (Piccardi, 2005) and possibly with coseismic uplift of limited parts of the coastal area (Mastronuzzi & Sansò 2002a). Moreover, all around the Apulian coast the MIS 5.5 (~125 ka) deposits are variously uplifted; the correlate coastline is displaced from the Ionian side to the Adriatic one, indicating different tectonic behaviour during the Middle-Late Pleistocene (for instance Bordoni & Valensise, 1998; Ferranti et al., 2006).

Seismites have been recognized in Upper Pleistocene deposits along the central and southern Adriatic coasts, testifying to the occurrence of strong ground shaking, that has been associated with Late Pleistocene earthquakes whose epicentres were located no more than 40 km far from the coast (Moretti & Tropeano, 1996; Tropeano et al. 1997; Moretti, 2000). In contrast, only one moderate historical earthquake occurred with epicentre in Southern Apulia (1826 Manduria earthquake, I_{\max} =VI-VII, M =5.3; Gruppo di Lavoro CPTI, 2004; Fig. 2.3).

Notwithstanding, active tectonics is still not well understood, because **(1)** no data are available on the active stress fields, neither from breakout nor from earthquakes; **(2)** GPS data suggest very little strain, in the order of 10 nanostrain per year (Serpelloni et al., 2005); **(3)** recent geomorphological studies indicate different tectonic behaviour in the Middle-Upper Pleistocene (Mastronuzzi et al., 2007b; Ferranti et al., 2006).

On the other hand, faults are rare and all characterized by small displacement values, whereas extension joints prevailing in most of the investigated sites, are frequently well exposed and organised in sets. Preliminary results of an original structural analysis carried out by mean of mesostructural detailed analysis, indicate that Southern Apulia has been affected by mild but recurrent and discernible brittle deformation throughout the Middle and Late Pleistocene (Di Bucci et al., 2007; Caputo et al., 2008).

2.1.1. Tectonic outline

The Adriatic foreland is shared among key mountain chains of the Central Mediterranean, i.e., the Albanides, the Dinarides, and the Apennines of peninsular Italy. The latter fold-and-thrust belt is a Late Cenozoic-Quaternary accretionary wedge, which forms part of the Africa verging mountain system in the Alpine-Mediterranean area. In the Southern Apennines, this wedge is formed by east-to-northeast verging thrust sheets deriving from palaeogeographic domains of alternating carbonate platforms and pelagic basins (for instance Mostardini & Merlini, 1986; Patacca & Scandone, 1989; Fig. 2.2). The most external of these domains is represented by the Apulia Platform, a ~6 km-thick succession of neritic Mesozoic carbonate rocks (Ricchetti, 1980). In turn, this succession is partially overlain by mainly terrigenous marine deposits of Cenozoic age (Patacca & Scandone, 2004b). The Apulia Platform and its underlying basement are partly involved in the orogenic wedge (Menardi Noguera & Rea, 2000; Butler et al., 2004), partly form the foreland inflected below the outer front of the Apennines (Mostardini & Merlini, 1986), and partly form the Adriatic foreland *sensu stricto*, both on-land and off-shore (Gargano, Central Apulia, Salento and Southern Adriatic Sea; Fig. 2.2). Southern Apennines migrated toward the Adriatic foreland up to the beginning of the Middle Pleistocene, when the motion of the wedge front is reported to have ceased (Patacca & Scandone, 2004b). Meanwhile, SW-NE-trending extension became dominant over the core of the Apennines, probably as a result of a geodynamic change that took place around 800 ka (for instance: Cinque et al., 1993, Hippolyte et al., 1994).

This tectonic regime is still active, as demonstrated by breakout and seismicity data (Montone et al., 2004), and accounts for large earthquakes generated by NW-SE–striking normal faults straddling the topographic divide of the Southern Apennines (Gruppo di Lavoro CPTI, 2004; DISS Working Group, 2007 and references therein; Fig. 2.3). In contrast, recent instrumental evidence shows that to the northeast of the Apennines ridge the SW-NE extension is associated with NW-SE horizontal compression (Vannucci & Gasperini, 2004; Boncio et al., 2007; Del Gaudio et al. 2005; 2007).

For instance, the unusual 2002 Molise earthquakes (Figs. 2.2 and 2.3) supplied living evidence that, in the frontal part of the chain, large upper crustal NW-SE normal faults give way to deeper E-W, right-lateral, seismogenic faults (Di Luccio et al., 2005). Major EW–oriented shear zones have been described in literature roughly between the latitudes 40°30'N and 42°30'N, both on-land and off-shore (Di Bucci & Mazzoli, 2003; Valensise, et al. 2004; both with references). They extend for tens of kilometres below the outer front of the Southern Apennines orogenic wedge and, toward the east, below the foredeep deposits up to the foreland. Their present-day activity is interpreted as due to the reactivation of inherited zones of weakness. Among them, the best constrained is referred to as Molise-Gondola shear zone, that has a clear geologic and seismogenic signature (MGsz; Di Bucci et al. 2006, with references; Fig. 2.2). Further south, another regional E-W lineament extending between Potenza and Taranto has been recently interpreted as active and seismogenic (DISS Working Group, 2007), as it includes the source area of a series of M5+ earthquakes that were caused by right lateral slip on E-W planes at 15-23 km depth (1990-1991 Potenza earthquakes; Boncio et al., 2007, with references; Fig. 2.3).

Assessing whether the southernmost portion of Apulia is tectonically active is made more difficult by the following circumstances: (1) seismicity is low, widespread and seemingly trendless; (2) no information on the active stress field is available from breakout data; (3) geomorphological studies indicate that the southernmost tip of the study area underwent uplift during the Middle Pleistocene, followed by a relative stability during the past 330 ka (Mastronuzzi et al., 2007b), while the Taranto area has been uplifted at 0.14-0.25 mm/a since the Late Pleistocene (Bordoni & Valensise, 1998; Belluomini et al., 2002; Ferranti et al., 2006).

2.1.2. Quaternary setting

Although considered as a stable area, the Apulia portion of the Adriatic foreland shows geological and morphological evidence linked to the build-up of the Apennines and Dinarides chains and the eustatic sea level changes in Pleistocene times. Therefore, the detailed analysis of the Southern Murge Plateau and Salento Peninsula provides a complex Quaternary evolution, marked by a number of transgression and regression cycles, that are partly controlled by tectonic activity.

2.1.3. Bradanic foredeep cycle

From Late Pliocene to Middle Pleistocene, the Apulia region was marked by relative sea level stages higher than the present one.

During this period, the area stretching between the foreland and the Southern Apennines chain, was submerged by the palaeo-Adriatic Sea and characterized by bioclastic calcarenites deposition (Calcareniti di Gravina Formation; for instance Iannone & Pieri, 1979; D'Alessandro & Iannone, 1982; 1984; Tropeano et al., 2002 and references therein; Fig. 2.4), which toward the Taranto Gulf shaded into grey-bluish clayey marls (Argille subappennine Formation; for instance Marino, 1996; Ciaranfi et al., 2001; Maiorano et al., 2007, and references therein). According to Ciaranfi et al. (1988; 2001), this sedimentary event could be referred to the Bradanic foredeep cycle, eventually closed by coarse terrigenous deposits. During the Lower-Middle Pleistocene almost the entire Salento was under subaerial conditions since bioclastic massive calcarenite heteropic to gray-bluish silty clays have been referred exclusively to the latest Early Pleistocene by Bossio et al. (1991, and references therein) or to the Bradanic foredeep cycle, i.e. to the Pliocene-Lower Pleistocene stratigraphic interval (Tropeano et al., 2004).

A considerable number of studies is available for the Bradanic foredeep (Ciaranfi et al., 2001; Maiorano et al., 2007 and references therein), whereas very few data have been collected on the silty-clay deposits frequently exposed, at the bottom of the Marine Terraced Deposits (see next subsection), along the coast between Brindisi and Lecce, or near Taranto (i.e. Ricchetti, 1967; 1972). In the former zone, along the Adriatic coast, Coppa et al. (2001) provided an Early-Middle Pleistocene age for a succession exposed along the coast South to Brindisi. Near Taranto, along the Ionian side of the Salento Peninsula, the most recent age obtained for an ash layer interbedded in the silty clay constrains its deposition at ~1.2 Ma (Capaldi et al., 1979), but recent studies on the nannoplankton and foraminifera indicate most likely a Middle Pleistocene age (Mastronuzzi & Sansò, 1998; Antonioli et al., 2008).

2.1.4. Marine Terraced Deposits

Bioclastic, sandy-calcareous sediments, rarely up to 15-20 m thick, referred as Marine Terraced Deposits and ascribed to the Middle-Late Pleistocene, crop out all around the Murge Plateau and in the Salento Peninsula, up to an elevation of 300-400 m (Ciaranfi et al., 1988; Fig. 2.5). Often, marine sediments are associated with well-cemented aeolian deposits, arranged in a continuous dune belt. These covers formed during several marine transgressions, which partly affected the eastern and southern part of the Salento Peninsula (Mastronuzzi et al., 2007b).

The best known are those located along the coast stretching from Taranto to Gallipoli, and referred to the latest Middle Pleistocene and/or to the Last Interglacial Period (for instance Hearty & Dai Pra, 1992; Belluomini et al., 2002 and references therein), as well as those belonging to the Middle-Upper Pleistocene succession recognized in the internal parts of the Salento between Lecce, Gallipoli and Leuca (D'Alessandro & Palmentola, 1978; D'Alessandro et al., 1994; D'Alessandro & Massari, 1997).

Along the Ionian side, the most recent units are represented by algal biocalcareous facies rich in tropical fauna (i.e.: *Strombus bubonius*, *Cardita calyculata senegalensis*, *Patella ferruginea*, *Hyotyssa hyotis*, etc.) and reef build-ups bio-constructed by *Cladocora caespitosa*. This fossil content, combined with an impressive set of relative (amino acid racemisation) or absolute (U/Th ratio) age determinations, indicates a tropical environment of Late Pleistocene age, that corresponds to the MIS 5.5 (Fig. 2.6). Deposits referred to sub-stages more recent than MIS 5 are also locally exposed (Hearty & Dai Pra, 1992; Belluomini et al., 2002, and references therein).

Marine terraced deposits, arranged in a staircase decreasing seaward, crop out extensively also along the Ionian coast of Basilicata. Here algal and biocalcareous facies are replaced by terrigenous sandy deposits with pebbles, rarely associated to marine palaeontological remains.

The local presence of the *Strombus bubonius* in the deposits nearest the Apulia, also if not well preserved, permit to ascribe them to a generic Upper Pleistocene may be to the MIS 5.5 (Boenzi et al., 1985; Caldara, 1987).

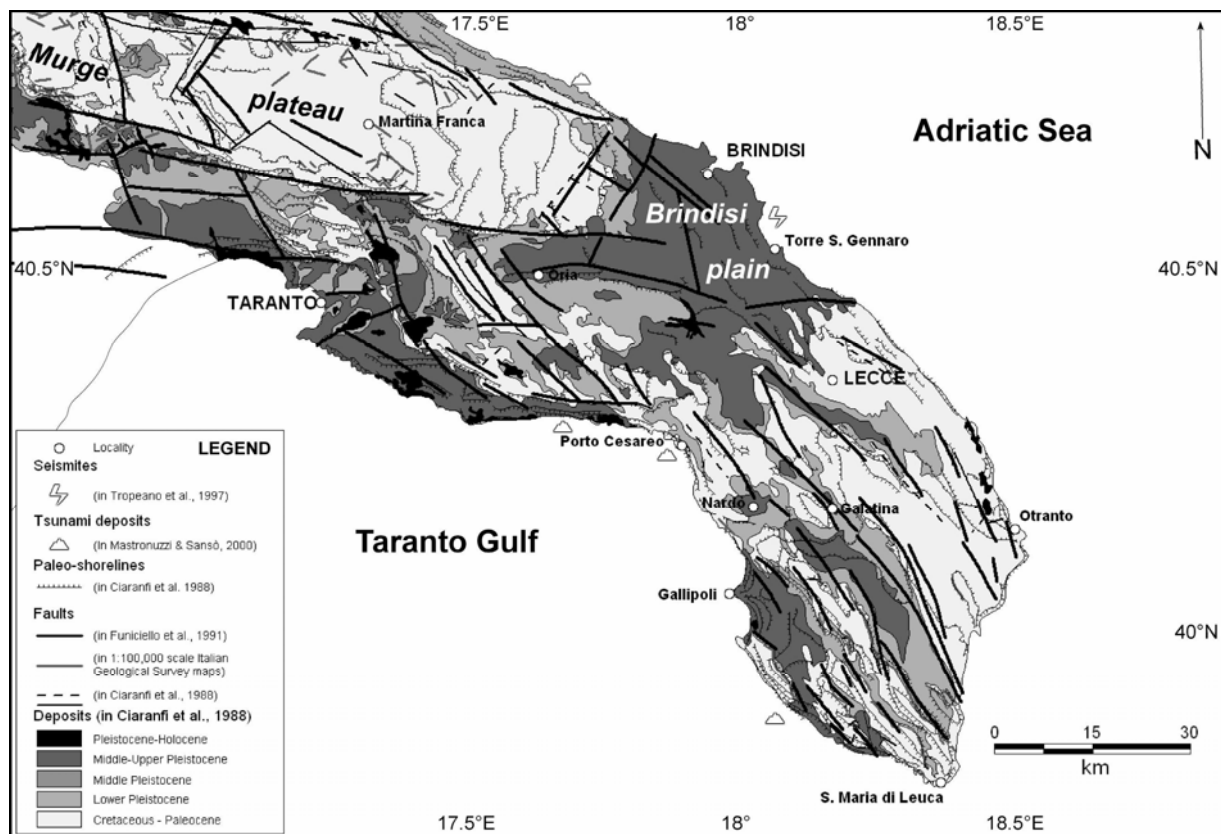


Figure 2.5 - Geological sketch of the Salento Peninsula (redrawn, data from sources mentioned in the legend). The Apulia carbonate platform (of Cretaceous-Paleocene age) outcrops primarily in the topographic highs to the N and NW (the Murge Plateau) and toward the SE sector of Salento. Lower to Upper Pleistocene deposits outcrop in the Brindisi Plain, along the coast from Porto Cesareo to Taranto and S of Gallipoli. Pleistocene to Holocene deposits can be found only in few localities, mostly on the western sector of the studied area but for the Otranto surroundings.

These attributions fit well with those performed by Brückner (1980) which ascribed the shaping of the three lowermost terraces to the MIS 7, MIS 5.5 and MIS 5.1. Recent studies aimed to establish a reliable chronostratigraphic frame for the terrace flight of Metaponto indicate that OSL analyses need of Th/U, AAR or ESR control (Zander et al., 2003; 2006).

Along the Adriatic side of the Murge Plateau and of the Brindisi Plain, well-cemented sterile calcarenites with rare bioturbations are exposed, ascribed to a beach/dune environment.

The absence of fossil remains did not allow any biostratigraphic correlation or absolute age determination. A rough chronological constraint is provided by a man-splinted flint found in the colluvium underlying the beach-dune deposits and ascribed to the Middle Palaeolithic- Mousterian Age. This suggests a Late Pleistocene age, corresponding to a generic MIS 5, for the overlying marine deposits (Marsico et al., 2003).

Finally, three generations of dune belts have been referred to the Holocene (Fig. 2.6). In some places they are associated with beach sediments, which can be recognized along several tracts of the Southern Apulia coast (Mastronuzzi & Sansò 2002b).

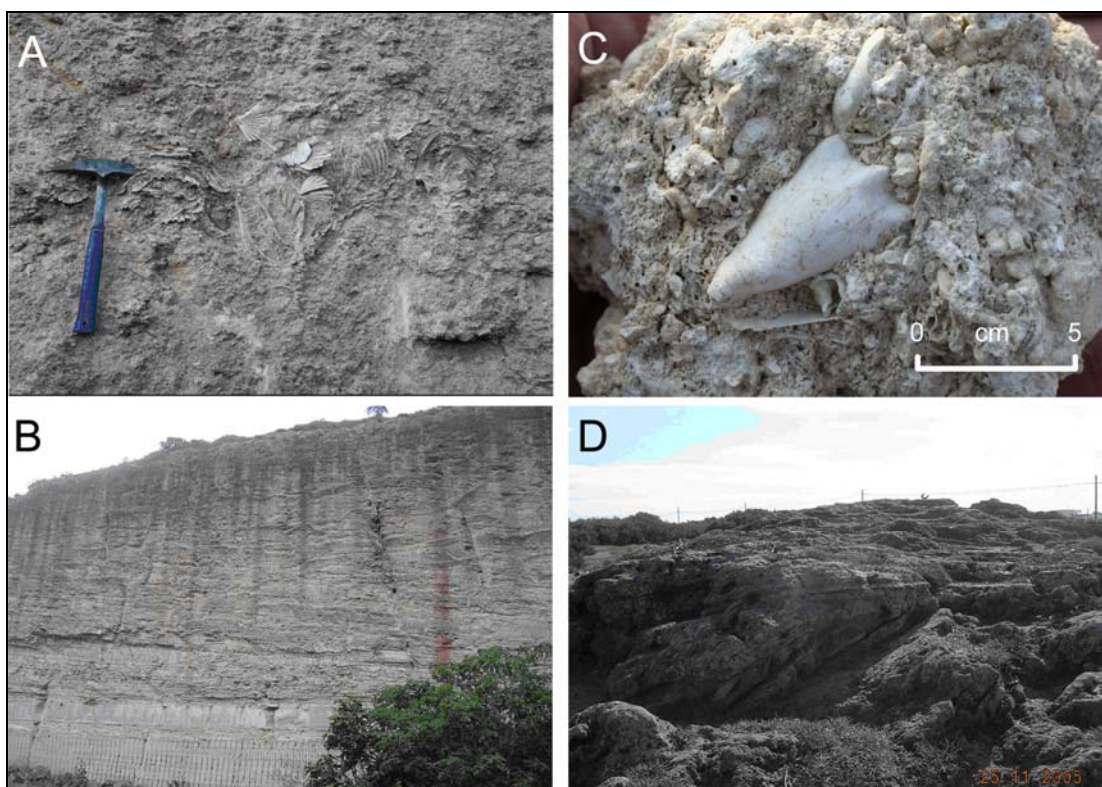


Figure 2.6 - Examples of deposits: **A)** Gravina fm. marine calcarenites, late Lower Pleistocene near Grottaglie (Ta); **B)** Marine Terraced Deposits, late Middle Pleistocene in the Gallipoli (Le) area; **C)** Marine calcarenites with *Strombus bubonius*, Upper Pleistocene from Taranto area (=MIS 5.5); **D)** cemented dune near Ostuni (Br), Holocene.

The oldest dune generation is the most developed; it is represented by aeolian, poorly cemented, bioclastic sands which retain some *Helix* sp. specimens. A number of radiocarbon age determinations on *Helix* sp., integrated with geomorphological and archaeological data, suggest that these dunes formed about 6.5 ka BP, during the maximum flooding event (Flandrian transgression). The second generation of dune belts, made up of loose brownish sands alternating with soil horizons, formed during the Greek-Roman Age. Finally, the last phase of dune formation has been ascribed to Medieval times.

2.1.5. Quaternary vertical motions

Within the Quaternary long-term uplift of the Adriatic foreland, which started in the latest Early Pleistocene (Pieri et al., 1996) or during the Middle Pleistocene (Ciaranfi et al., 1983), different landscape units indicate a not homogeneous morphotectonic evolution of the Murge Plateau and Salento Peninsula (Bordoni & Valensise, 1998; Ferranti et al., 2006). This evolution is also accompanied by evidence of pre-, sin- and post-sedimentary tectonic activity, recognised for instance in Pleistocene deposits exposed in the surroundings of Bari and Brindisi (Moretti & Tropeano 1996; Moretti, 2000).

The Murge Plateau is bordered by a staircase of well developed marine abrasive/sedimentary terraces, suggesting that the origin of the plateau is related to the superimposing effects of the eustatic sea level changes to a long-term regional uplift. On the contrary, the Salento Peninsula, although characterized by a set of horst and graben affecting the Mesozoic bedrock (locally named "Serre"; Palmentola, 1987), produced by a complex interaction between tectonics and eustatism. For example, the Sabbie a Brachiopodi sedimentation has been related to a pronounced subsidence occurred at least in the western and inner parts of the Salento Peninsula during the Middle Pleistocene (D'Alessandro et al., 1994). A subsequent uplift was then responsible for the emersion of wide sectors of the peninsula. Recent studies proved that the uplift-rate strongly decreased at MIS 9.3, about 330 ka BP (Mastronuzzi et al., 2007b). Since then, maximum values of the uplift rate have been recorded only in the Taranto area (0.25 mm/a; Ferranti et al., 2006), whereas they taper to zero in the southernmost part of the region (Dai Pra & Hearty 1988; Hearty & Dai Pra 1992; Belluomini et al., 2002). Finally, a slow subsidence seems to characterize at present the Adriatic side of the Apulia region (Mastronuzzi & Sansò, 2002c; Marsico et al., 2003; Lambeck et al., 2004).

The different uplift rates of the entire area have been interpreted as consequence of the reaching of the thick continental lithosphere of the Apulian swell in to the Apeninic subduction hinge; this caused a larger resistance to the flexure. The subsequent slowing down of the eastward rollback of the subduction hinge and the penetration of the slab induced the buckling of the foreland that was less intense in the central part of Adriatic sea and more intense, although differentiated, in the Apulia (Doglioni et al., 1994) (Fig. 2.7).

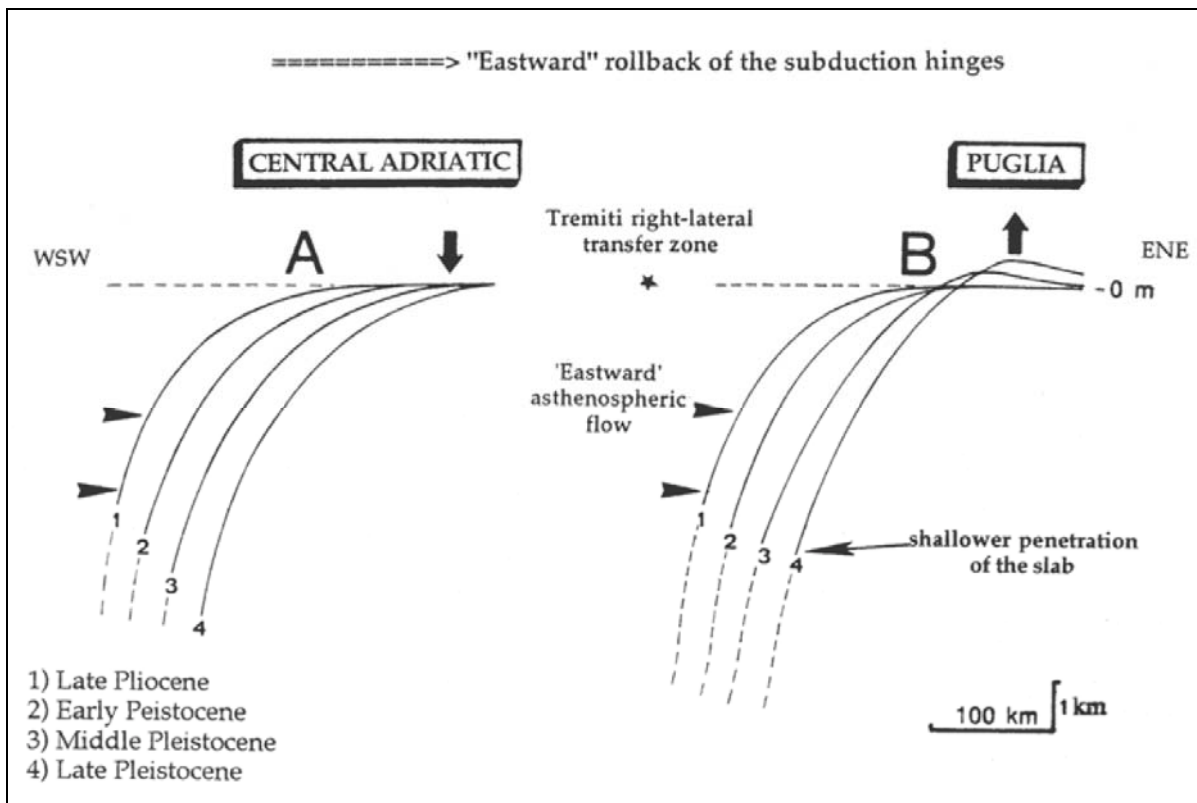


Figure 2.7 - Comparison of the different evolutions of the subduction hinge rollback of the central Adriatic and Puglia region (from Doglioni et al., 1994).

2.2. Apulian Coastal morphology

2.2.1. Introduction

Most densely populated coastal areas of the globe are subject to the average rising of the sea (Nicholls & Leatherman, 1995; Nichols et al., 1995; Douglas et al., 2001) due to eustatic and steric worldwide factors and amplified by local factors; it can be estimated in some mm per year (Pirazzoli, 1996; Douglas, 2001). Data provided by satellites ERS-1 and Topex-poseidon have shown the same trend for the eustatic sea level with an increase of about 0,5-2,0 mm per year (Pirazzoli, 1998; Pirazzoli & Tomasin, 1999; Cabanes et al., 2001).

The dynamics of the Apulian coast is the result of complex interactions between emerged and submerged morphological elements, hydrologic and oceanographic factors, climatic and sea-weather conditions.

Human impact has to be added to these interactions, at least since the Greek–Roman age. Particularly in the last decades, anthropogenic pressure has strongly altered the dynamics of the coastal environment. Hydraulic works have affected all the drainage basins reducing the contribution of alluvial deposits to the coast and inducing a negative sedimentary budget. Harbour facilities and coast defence works modify and impede the longshore transport of sediments. As a consequence of this, several tracts of Apulian coast are interested by severe erosion and environmental problems, rendering them vulnerable even to small environmental changes.

2.2.2. The continental shelf

The Ionian basin reaches in its central part a depth of approx. 4000 m (Senatore et al., 1982). Along numerous tracts it is bordered by steep continental slopes incised by canyons, whose heads marked the shelf break, in some cases placed less than 1 km far from the coastline. In fact, the Calabria region shows a narrow continental shelf, less than 3 km wide or locally absent.

Several important submarine landslides along the Calabrian slope have been surveyed (Colizza et al., 2005) or hypothesized as a consequence of earthquakes occurring inland (Mastronuzzi & Sansò, 2000). Offshore the narrow eastern Sicilian shelf, Pareschi et al. (2006) indicate the occurrence of large landslide along the steep continental slope. Moreover, large landslides affecting the north African continental slope have been reported by Cita and Aloisi (2000). Similar situation is recognisable all around the Ionian coast of Greece. North to Lefkada island the isobath 1500 m is no more than 3 km far.

The continental shelf of Puglia region shows very variable width (Fig. 2.8). Along the Adriatic coast the shelf width ranges from 18 km near Otranto up to 60 km at the Manfredonia Gulf, sloping about 1,5%. On Ionian side of Apulia the shelf is very narrow reaching the maximum width of 20 km between Porto Cesareo and S. Maria di Leuca where it is characterised by three submerged terraces. The shelf shows its minimum width of about 5 km in front of Bradano River mouth.

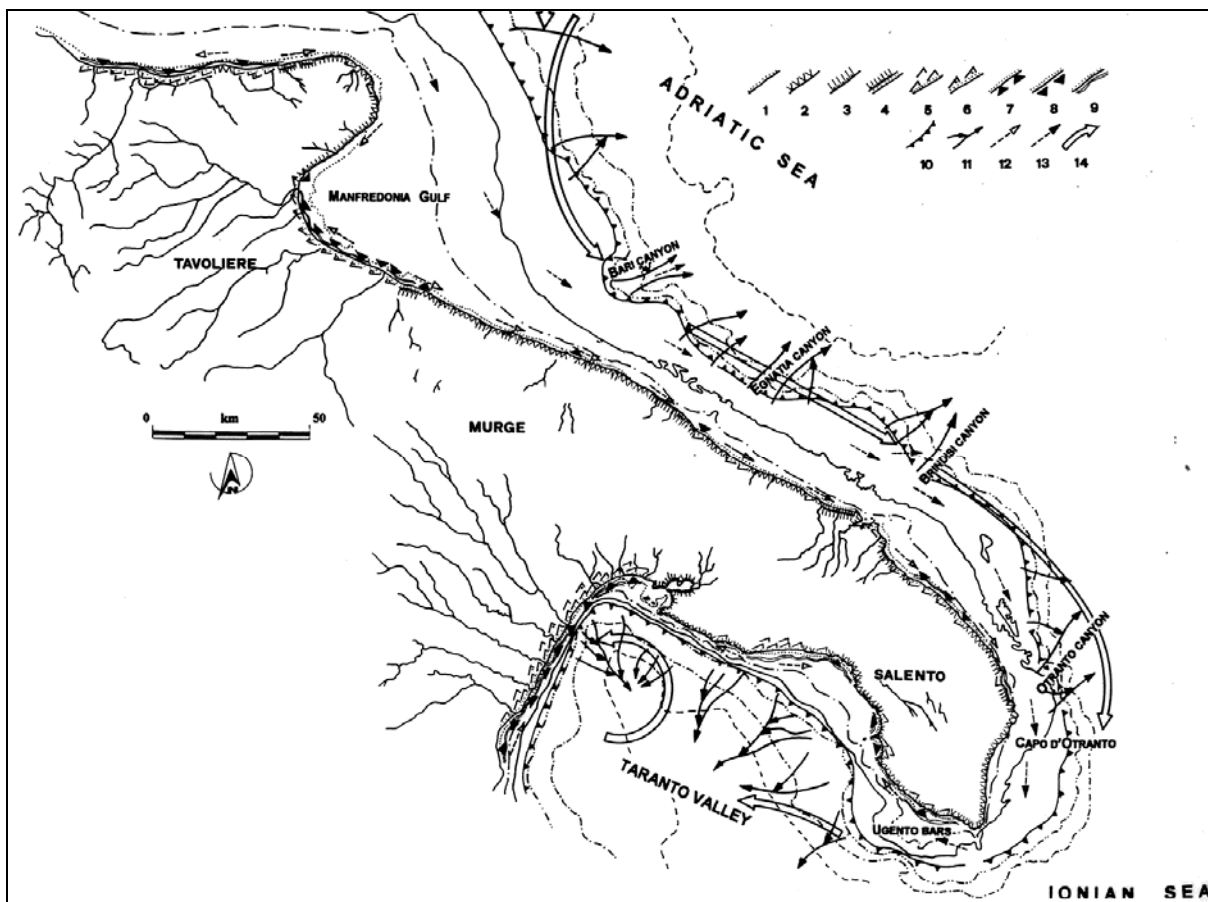


Figure 2.8 - Nearshore features and submarine morphology of coastal area of Puglia. 1 – sand/pebble beach; 2 – sloping rocky coast; 3 – cliff; 4 – cliff with beach at the foot; 5 – dune belts; 6 – dune belts affected by human activity; 7 – shoreline recession; 8 – shoreline progradation; 9 – bars; 10 – shelf break; 11 – submarine canyon; 12 – inshore sediment drift direction; 13 – offshore sediment drift direction; 14 – marine surface current (from Caldara et al., 1998).

The shelf break is placed at about 100-110 m along the Ionian side and at about 160-200 m of depth along the Adriatic one (Senatore et al., 1982; Caldara et al., 1998).

The continental shelf is covered by coastal sands (down to 10-15 m of depth), by silt and clay (down to 125 m of depth) and by sands again from 125 m of depth to the shelf break. These last sediments are relict sands marked by littoral (D'Onofrio, 1972; Taviani, 1978) or lagoonal fauna (Fabbri & Gallignani, 1972), partly reworked by postglacial transgression (Hesse et al., 1971). Their deposition has been related to the Middle Pleistocene (Aiello et al., 1995) or to the last glacial low sea level stand (Colantoni et al., 1975; Colantoni & Gallignani, 1978).

The composition of sediments placed on the Adriatic continental shelf mirrors the lithology of the influent drainage basins; it is marked out by heavy minerals coming from the Monte Vulture, a Pleistocene volcano placed in the drainage basin of Fortore River. The present sedimentation rate in the inner part of shelf has been estimated about 4mm/yr (Van Straatten, 1985).

Along the Ionian side, shelf sediments are constituted to the south of Taranto mainly by bioclastic material whereas in front of Metaponto plain silty-sands have been detected by Pennetta (1985).

Posidonia oceanica meadows form large patches on the inner shelf, generally where fine sands occurred (surroundings of Gallipoli, Torre Canne-Brindisi coastal tract); it is replaced off-shore by coralligenous (Fig. 2.9). These biocenoses play a key role in the nourishment of beaches since they are the main source of bioclastic sands, overall in the present situation because of the scarce sediment input of main rivers.

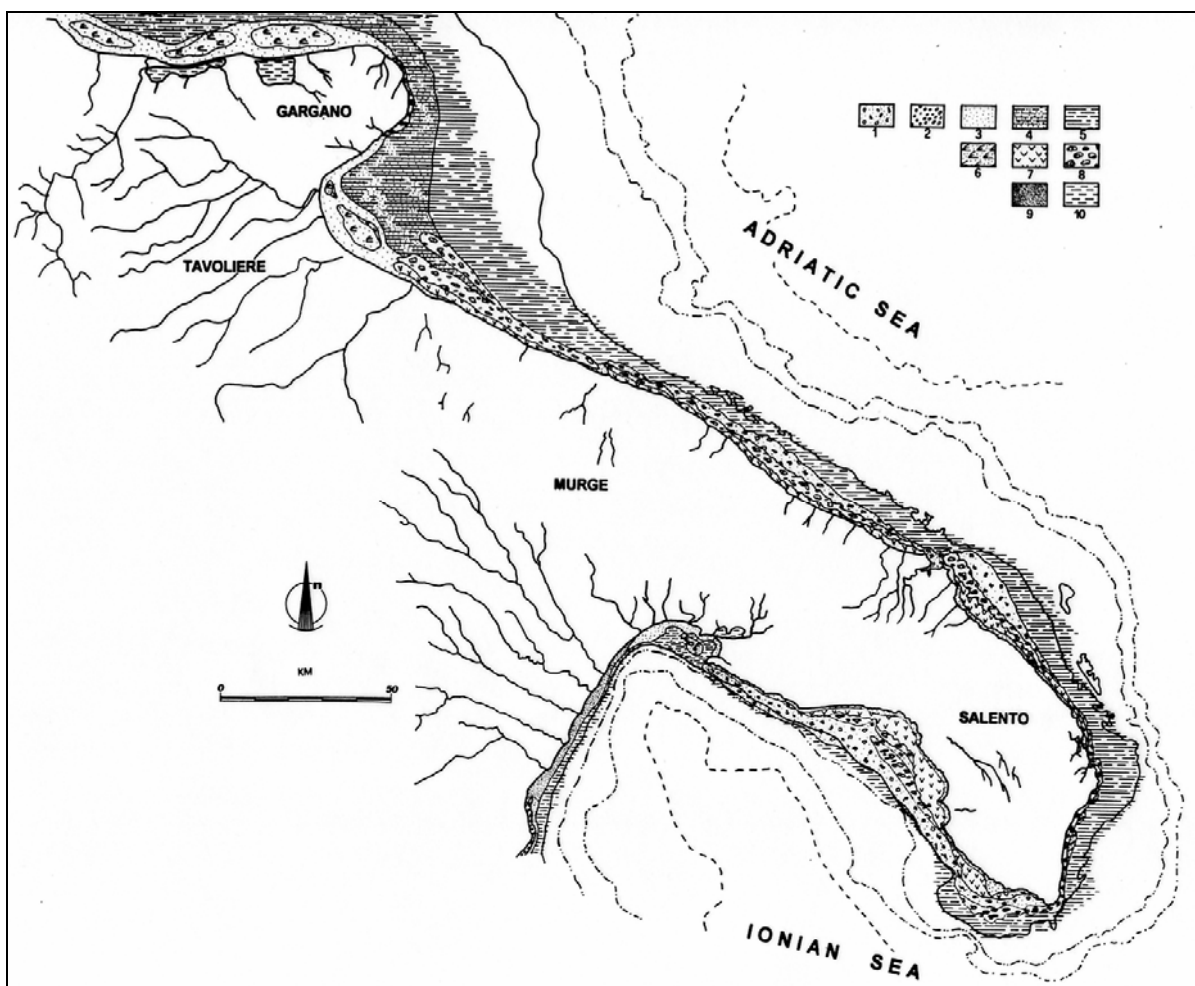


Figure 2.9 - Benthic sedimentary characteristics and biological assemblage along the shelf of Puglia region (Damiani et al., 1988). Biocoenosis terminology from Pérès (1967) and from Pérès & Picard (1964). 1 – coastal detritic bottoms (DC); 2 – pebbles beach sediments; 3 – fine well-sorted sands (SFBC); 4 – transition between SFBC and VTC; 5 – terrigenous mud (VTC); 6 – *Cymodocea nodosa* meadows; 7 – *Posidonia oceanica* meadows (HP); 8 – coralligenous; 9 – coarse terrigenous sands; 10 – superficial muddy sands in sheltered areas (SVMC); eurhaline and eurythermal in brackish waters (LEE) (from Caldara et al., 1998).

2.2.3. Hydrogeological features

The Puglia coastal area receives alluvial sediments from drainage basins extending over areas with different geological characteristics (Fig. 2.4).

Very permeable limestones crop out on Gargano, Murge and Salento areas; the drainage network is there poor developed as rain water rapidly infiltrates underground through joints and sink-holes feeding a karstic aquifer. Phreatic waters reach the sea through the numerous coastal springs, some ones submerged.

Rivers flowing on Tavoliere and Ionian areas crosses very impermeable, erodible rocks. As a consequence, they are characterised by well-developed drainage basins and by important discharge and load. However, the natural discharge has been dramatically reduced both by the intense exploitation of rivers for agricultural, civil and hydroelectrical uses, as well as by land reclamation and hydraulic works carried out mainly along the coastal area stretching from Manfredonia to Barletta and near Metaponto (Fig. 2.10).

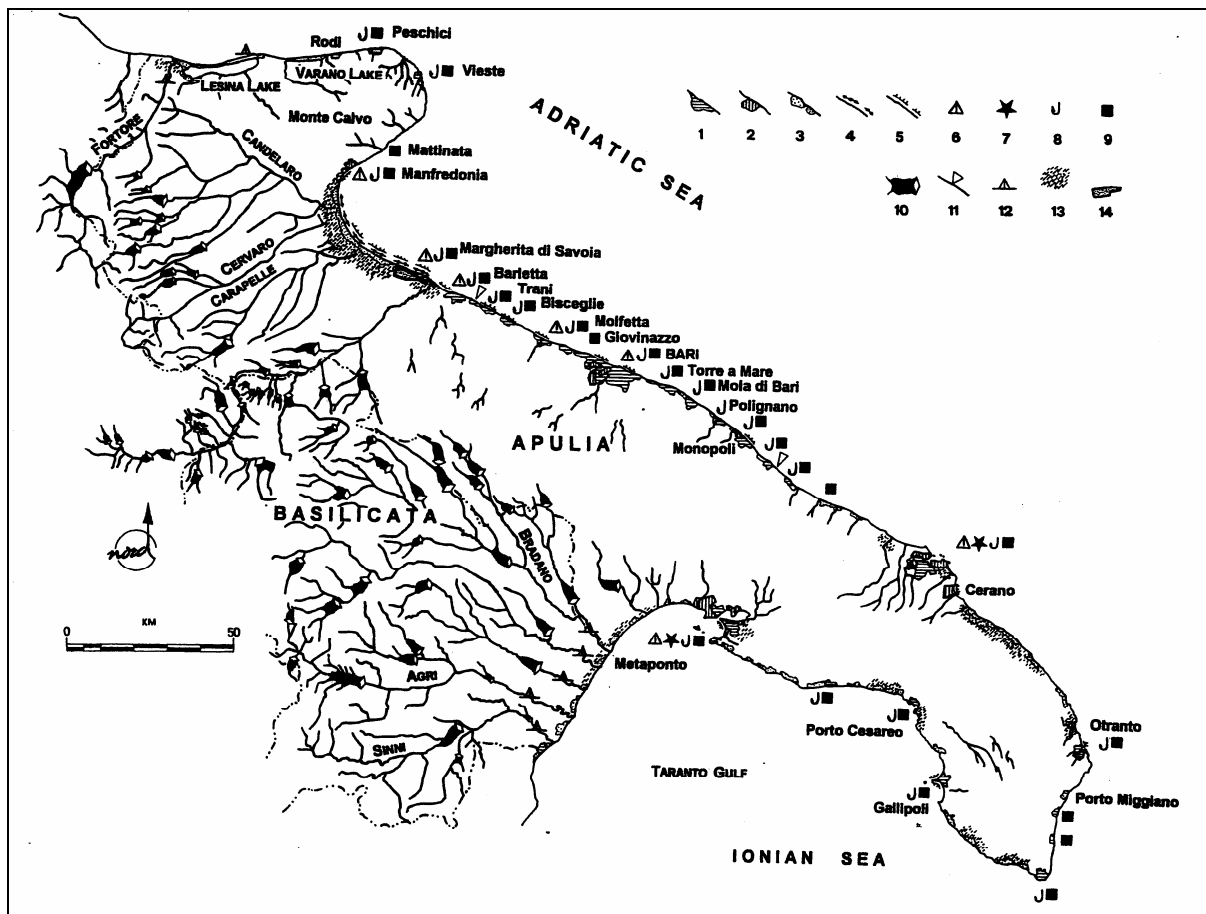


Figure 2.10 - Human activities influencing the coastal area of Puglia. 1 – urbanised coastal area; 2 – large industrial facilities; 3 – touristic coastal area; 4 - coastal defence works on land; 5 – coastal defence works at sea; 6 – industrial harbour; 7 – military harbour; 8 – fishing harbour; 9 – touristic harbour; 10 – dams and relative catchments; 11 – quarry waste materials dumps; 12 - quarries in river bed and on beach; 13 – reclaimed land; 14 – salina (from Caldara et al., 1998).

2.2.4. Meteo-marine features

The Ionian and Adriatic basins are exposed to the strong winds generate by the seasonal prevalence of Siberian and Azores anticyclones. They generate winds that have main directions from N-NE or S-SE, respectively. The last one has the longest fetches with the Azores anticyclones stable in this area of the Mediterranean sea: approx. 990 nautical miles from northern coast of Egypt to the Maddalena Peninsula (Ionian coast of Sicily), and approx. 630 nautical miles from the Gulf of Sidra (Libya) to the Torre Squillace (Ionian coast of Apulia) (Fig. 2.11).

Data recorded by buoys of RON (Rete Ondametrica Nazionale), (Corsini et al., 2002) are available since 1989. Wave data in the northern Ionian Sea are recorded by Catania, Crotone and Monopoli buoys (Fig. 2.12); this

latter one is located in Southern Adriatic sea between Bari and Brindisi but its location and the general climatic features allow its data to be used for the northern Ionian Sea exposed to ENE.

The integration of RON data with Italian Navy wave and/or wind data covering the last 60 years allows the frequency of sea storms during the last years to be reconstructed (Istituto Idrografico della Marina, 1982). Storm frequency records in the central area of the Mediterranean Sea during the last 50 years show that the wind speeds between 15 and 20 knots are decreasing. However, sea storms due to wind speeds between 11 and 14 knots and more than 27 knots are increasing along the Adriatic and Ionian coasts. In particular the frequency and duration of extreme gales between 5 and 7 Beaufort have been established for 5 anemometric stations placed along southern Italian coasts (Palascia near Otranto, Santa Maria di Leuca, and San Vito Pugliese near Taranto in Apulia, Capo Colonne in Calabria and Torre Avolos in Sicily, see Fig. 2.11).

The main sea storms come from directions N-NE and S-SE for the coastal Ionian stations of Capo Colonne and Capo San Vito: the first station shows that gales occur specially in winter months and have an average duration of approx. 40 hours; the latter station primarily measured sea storms concentrated in January with S-SSE wind direction and a duration of approx. 35 hours.

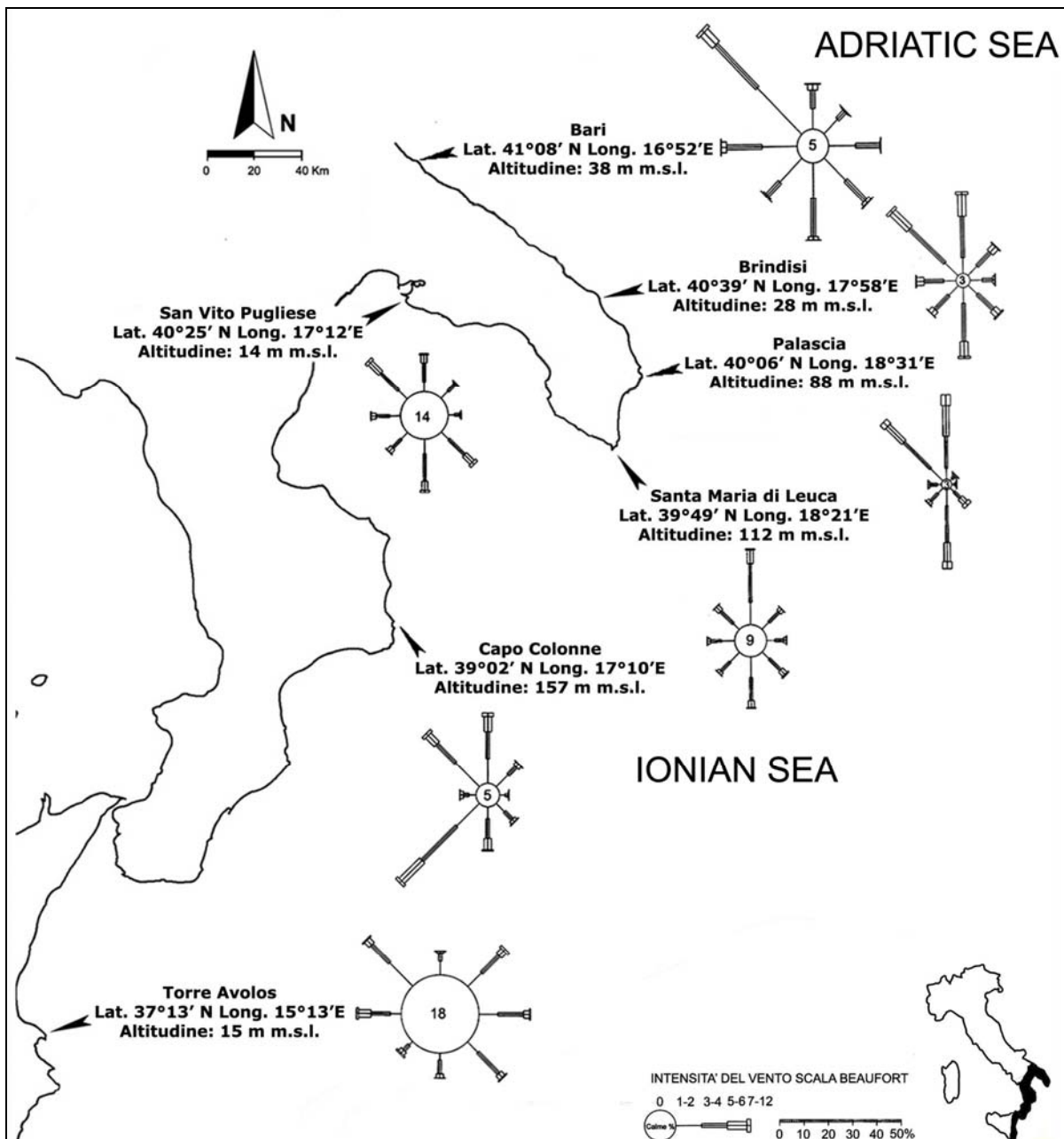


Figure 2.11 - Main fetch sectors and annual distribution of winds in Southern Italy; black arrows indicate meteorological stations; grey arrows indicate the direction of longest fetch in the considered coastal sector.



Figure 2.12 – Position of Rete Ondametrica Nazionale (RON) buoys.

The stations located in southern Apulia (Santa Maria di Leuca and Palascia) show important sea storms coming from the S-SW in October and January with the most limited fetch sector and duration of approx. 28 hours.

The Torre Avolos station shows the maximum fetch; it has recorded sea storms coming from the E-NE direction during wintery months with 35 hours of duration.

An evaluation from RON records of Catania, Crotona and Monopoli buoys covering the time period between 01/07/1989 and 31/12/2001 (Arena, 1999) of annual extreme offshore waves has been carried out to Catania buoy recorded a maximum offshore wave height of 6.3 m in February 1999 from the E-SE with a period of 11.1 sec. A similar offshore wave with the same period and height of 6.2 m coming from SE has been recorded at Crotona buoy in February 1994.

Finally, the Monopoli buoy recorded in January 1995 an offshore wave height of 5.2 m with a period of 10.0 sec coming from the NE (Tab. 2.1).

The return times of these offshore waves have been evaluated (Fig. 2.13; Tab. 2.1) for each buoy by using Gumbel distribution. For a return time of 50 years, the offshore waves of Catania, Crotona and Monopoli buoys can reach peaks approx. 1.3% higher of the maximum wave height recorded.

Puglia stretches between two marine basins, the Ionian and the Adriatic basins, each one characterised by peculiar morphological features. The current pattern is influenced by the interaction between waters belonging to the Ionian and Adriatic basins. The effect of earth's rotation forces waters entering in the Adriatic Sea from the south to flow northward along the western coast of Canale d'Otranto (see Fig. 2.8).

	H_{50} (m)	T_p (sec)	$\alpha^{\circ}N$	T_R (years)	1	20	50
Catania Buoy 37°26'24'' N - 15°08'48'' E	6,3	11,1	104	H_{50} (m)	3,97	6,21	6,89
				T_p (sec)	10,43	13,05	13,74
				T_m (sec)	8,82	11,04	11,62
Crotona Buoy 39°01'06'' N - 17°13'12'' E	6,2	11,1	135	H_{50} (m)	4,37	6,39	7,01
				T_p (sec)	10,01	12,11	12,68
				T_m (sec)	8,24	9,96	10,43
Monopoli Buoy 40°58'30'' N - 17°22'36'' E	5,2	10	61	H_{50} (m)	3,79	5,38	5,86
				T_p (sec)	8,87	10,57	11,03
				T_m (sec)	7,44	8,86	9,25

Table 2.1 - Extreme wave features recorded by the buoys of Catania, Crotona and Monopoli (Ba) of Rete Ondametrica Nazionale (RON); referring to the period between 07/01/1989-12/31/2001. Parameters of return time (T_R) calculated for the buoys indicated applied to the Gumbel formula; T_p = maximum peak period; T_m = mean period (Arena, 1999; Mastronuzzi et al., 2006).

After having received the waters coming from Po River, the current bends to the south-east flowing along the eastern Italian coasts. The current detaches from the coastline only in correspondence of Manfredonia Gulf because of the effect of E-W elongated Gargano Promontory which forces the current to describe a wide bend before reaching the coast again near Bari. A northwestward flowing counter-current forms in the Manfredonia Gulf.

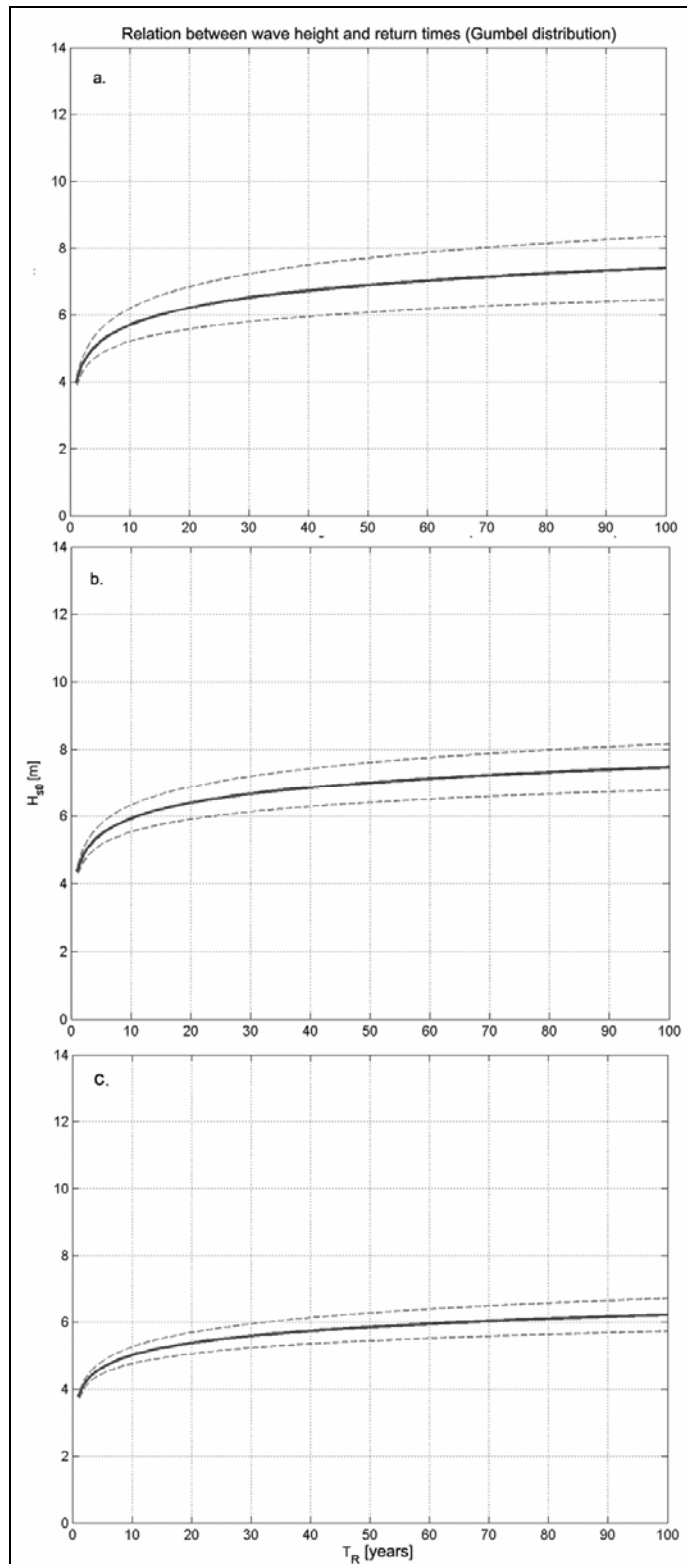


Figure 2.13 - Gumbel charts related to the Catania (a), Crotona (b) and Monopoli (c) buoys.

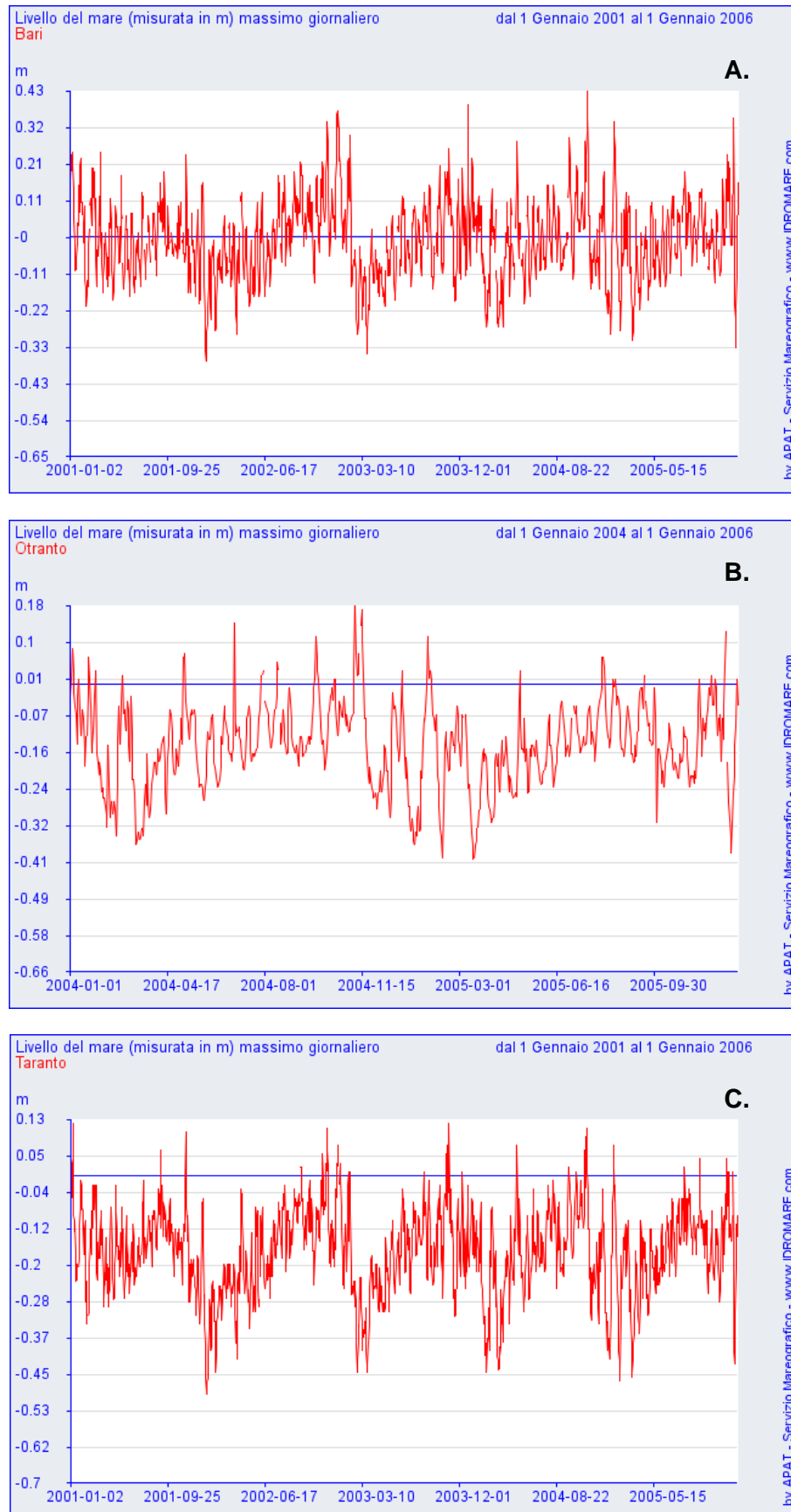


Figure 2.14 - Daily tidal range in the 2001-2006 period. **A.** Bari Station; **B.** Otranto Station; **C.** Taranto Station.

To the south of Bari the current flows toward the Canale d'Otranto where reaches the speed of 4 knots (Istituto Idrografico della Marina, 1982).

The amount and the speed of waters which enter in the Ionian sea depend on meteorological conditions, mainly to the atmospheric pressure of eastern Mediterranean Sea. The current, once overcome Capo S. Maria di Leuca, enters in the Taranto Gulf flowing northward along the western coast of Salento peninsula, giving place to a counterclockwise flow strongly influenced by smaller seasonally currents.

In the Adriatic Sea winds blow mainly from NW and subordinately from S-SE. They induced a similar pattern in the wave climate with the most frequent waves coming from the N-NW and, at lesser extent, from the S-SE. According to Simeoni (1992) more than 61% of waves shows an height smaller than 0,5 m whereas only 0,9% of them are higher then 2,5 m. The long shore drift of sediment occurs from the NW to the SE, at exception of Margherita di Savoia-Barletta coastal tract where the drift is oriented toward the NW.

The Ionian coast is exposed to the Scirocco wind, blowing from the SE, which is locally the most frequent and the strongest one. It induces a long shore drift of beach sediment from the SW to the NE.

The coast of Puglia region is affected by a maximum annual tide range of 1 m along the Adriatic coast at Vieste and of 0,6 m along the Ionian coast at Taranto; the maximum day tides are 0,7 m and 0,5 m, respectively (Fig. 2.14).

2.2.5. Coastal types

The Apulia coast is characterised by the alternation of cliffs, rocky sloping coasts, plain and convex, and beaches (see Figs. 2.8 and 2.15).

Regarding the cliffs and the sloping rocky coasts, plain or convex, there are different works inherent the evolutionary dynamics of these coastal types along the Apulia coast. Generally these show a withdrawal rate extremely varying depending on the structural arrangement and the lithology of the rocky bodies (Fig. 2.16).

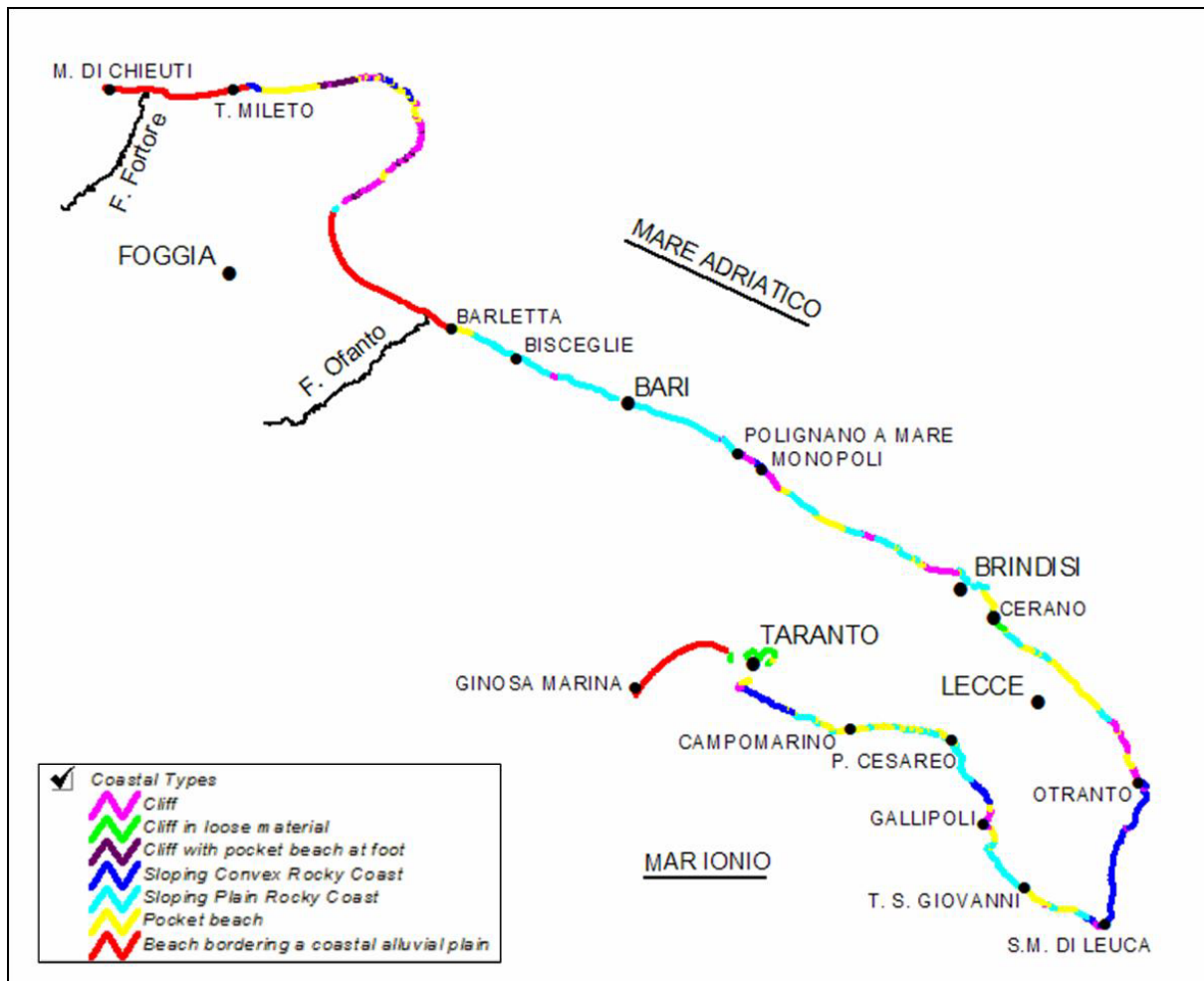


Figure 2.15 - Different morphological types of coast in Apulian region (Milella et al., 2008).

Some cliffs, modelled on moving back fractured Mesozoic limestone and on sediments of late Pleistocene, are located between Vieste and Manfredonia (Zezza, 1981), on the southern part of the Gargano promontory. Other cliffs in withdrawal are extended for brief lines on fractured limestones between the cities of Barletta and Bisceglie. Between Bisceglie and Monopoli, on the cliffs are modelled on limestone and calcareous sandstone and have been produced by the strong withdrawal of a sloping plain rocky coast (Maracchione et al., 2001). Near Cerano, south of Brindisi, the cliffs are carved in sandy-clayey deposits and they show rates of average withdrawal during the last 150 years of about 1-1,5 m/year (Gentile & Monterisi, 1994). In the Salento peninsula, cliffs carved in calcareous sandstone characterize the northern coast of Otranto. This appears to be affected by mass movements determining rates of average withdrawal of about 0,2 m/year (Mastronuzzi et al., 1992; Sergio, 1999). Other cliffs in rapid withdrawal are localized near Porto Miggiano (Zezza & Bruno, 1991).

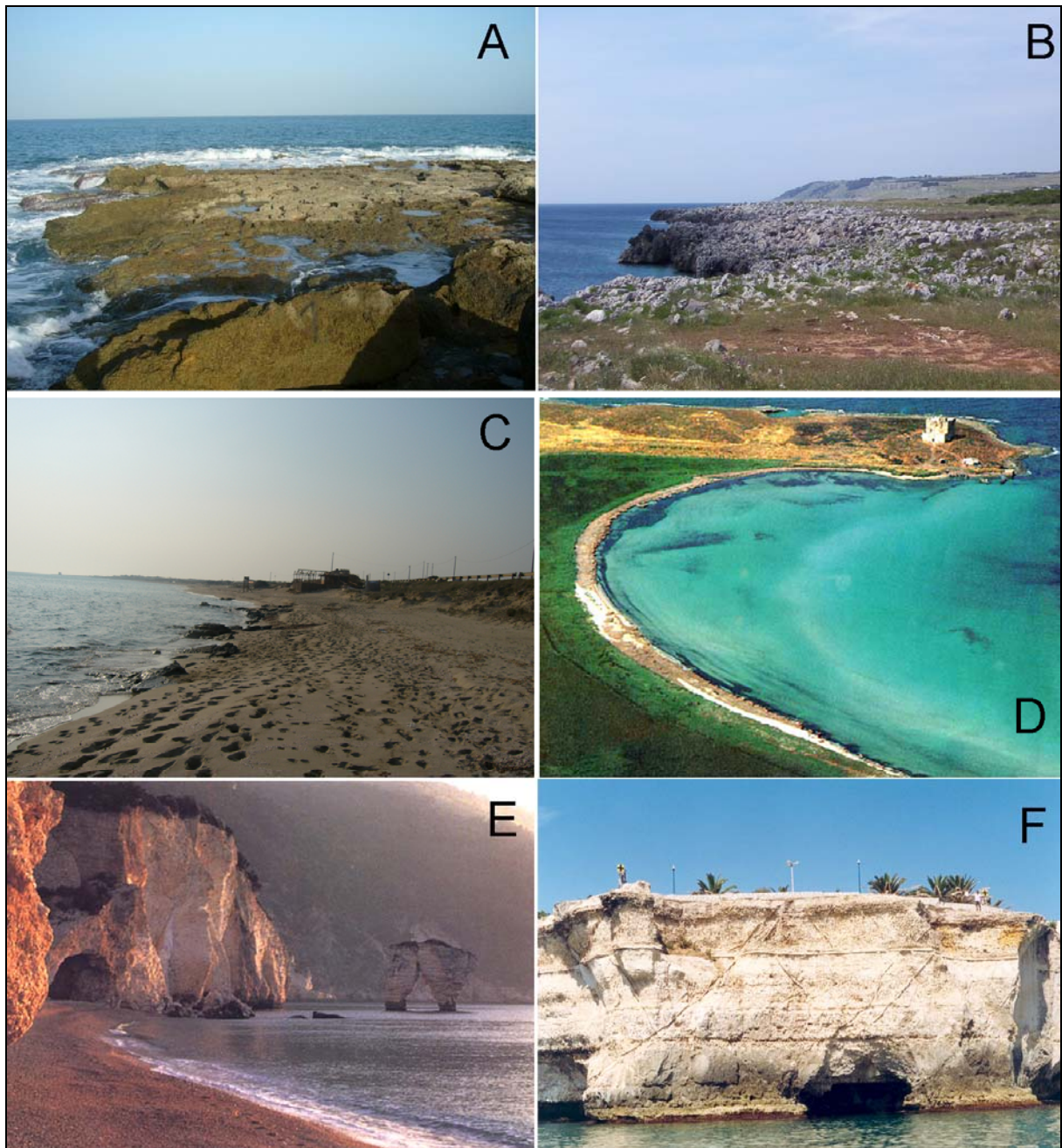


Figure 2.16 – A view of different morphological types of coast in Apulian region: **A.** Gently sloping coast in Polignano-San Vito (Ba); **B.** Rocky coast with a convex profile in the southernmost part of Salento near Otranto (Le); **C.** Beach with recent dune belt in Bagnara locality (Ta); **D.** Pocket beach in Torre Guaceto (Br); **E.** Cliff with beach at the foot in Baia delle Zagare (Fg) locality; **F.** Cliff in Roca locality near Lecce.

The cliffs bordering the Mar Grande of Taranto are modelled on sandy clays and show a rate of withdrawal of about 0,8 m/year (Mastronuzzi & Sansò, 1998). The sloping coasts, plain and convex, are the most widespread morphological type in the region. The sloping convex rocky profile, mainly located to the south of Otranto, on the Adriatic side, and to the south of Taranto, on the Ionian one, are constituted by a steep subaerial slope, in some places mantled by slope deposits as in Otranto – Capo S. M. di Leuca coastal tract.

The sloping plain coasts, from Barletta to Brindisi, on the Adriatic side and some tract from Campomarino and S.M. di Leuca, on Ionian side, are made up of a low, gently platform cut through terraces calcareous sandstones, on Plio-Pleistocene calcareous sandstones as well as on Mesozoic limestones.

The retreat rate of this type of coast is generally low; in the Taranto area it has been estimated at about 0,06 m/year (Mastronuzzi & Sansò, 1998). Several types of waves dominated sedimentary coasts occurring in Apulia region as showed in Fig. 2.17 and Fig. 2.18.

Long beaches border wide alluvial coastal plains near the mouth of the river Fortore, between Manfredonia and Barletta and in the Metaponto area in the Gulf of Taranto.

The Fortore river formed a cuspidate delta which produced the closing of Lesina and Varano coastal lakes during Roman age (Mastronuzzi & Sansò, 2002c). During the last decades, the delta area underwent to a severe coastal erosion so that beaches have been replaced by cliffs shaped on dune deposits (Fig. 2.19).

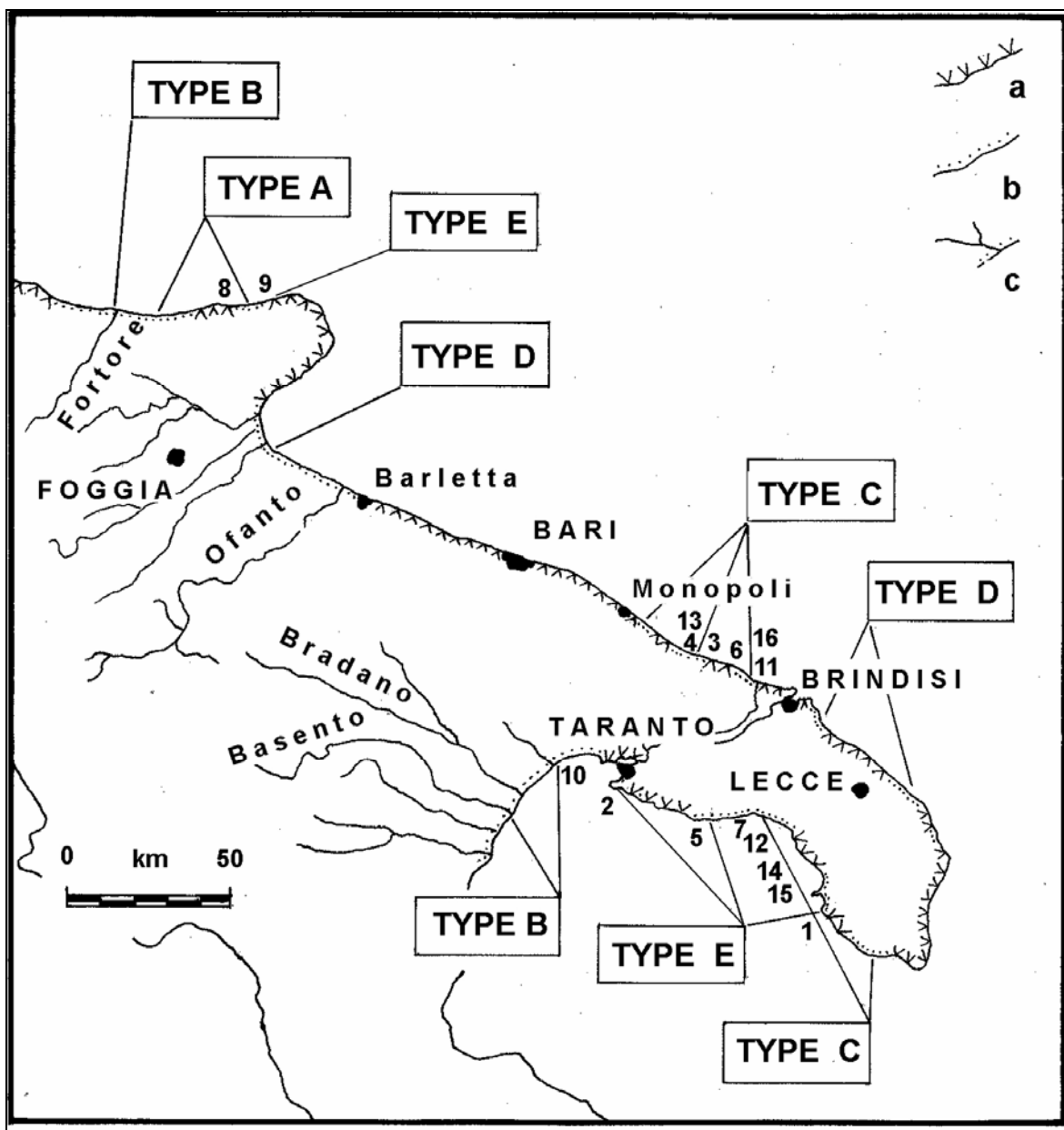


Figure 2.17 - Geographical distribution of wave-dominated sedimentary coasts. a – rocky coasts; b – beaches; c – river mouth.

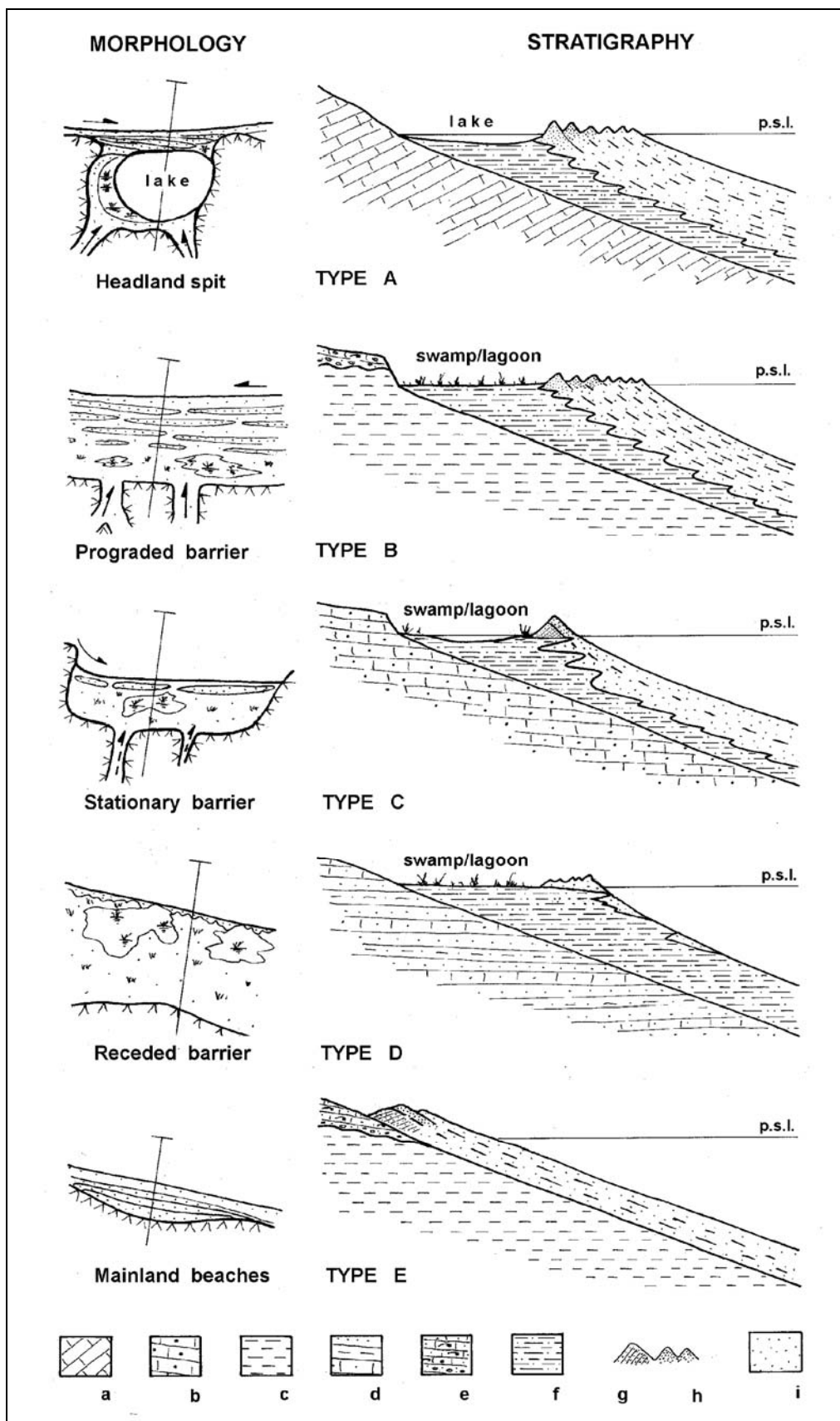


Figure 2.18 - Types of wave dominated sedimentary coasts occurring along in Apulian region. **a** – limestones; **b** – calcareous sandstones; **c** – clay; **d** – sands interbedded with clays and arenites; **e** – raised beach deposits; **f** – back dune deposits; **g** – Mid – Holocene and **h** – Greek dune belts; **i** – beach sediments.

Beaches placed at the south of Gargano promontory, between Manfredonia and Barletta, are about 60 Km long and nourished by materials carried by the Ofanto, Carapelle, Cervaro and Candelaro rivers.

In the past they were bordered by coastal dunes which have been completely removed by erosion or levelled by human and in some cases replaced by small artificial dunes for protecting the back dune areas. These beaches progradated until the end of the last century. However, since the '60s of the last century they have been affected by severe erosion with average retreat rate in the Ofanto mouth area of about 2 m/year (Pennetta L., 1988).

Beaches in the Metaponto area (Taranto Gulf) stretch for about 90 km (25 km of them in Puglia region) and are fed mainly by the solid load of Bradano, Basento, Sinni and Agri rivers. They were in accretion until about 40 years ago and bordered landward by 2 km wide strip of dune belts, up to 15 m high, which limited to the back large swamps. The entire area was interested by land reclamations works, extensive and intensive agriculture and by urbanization. At present, beaches are very narrow and border small cliffs in dune or backdune deposits. The mean retreat rate for the last 40 years has been estimated in about 3-4 m per year (Amore et al., 1988).

Pocket beaches characterize the coasts of Gargano, Murge and Salento areas. They occupy the numerous small bays which indent the general rocky and straight coastline. Along the Adriatic coast they are fed by relict sediment of Holocene age and by biogenic material. Ionian beaches are supplied by bioclastic sediments coming from *Posidonia* meadows and coralligenous covering the sea bottom in front of them.

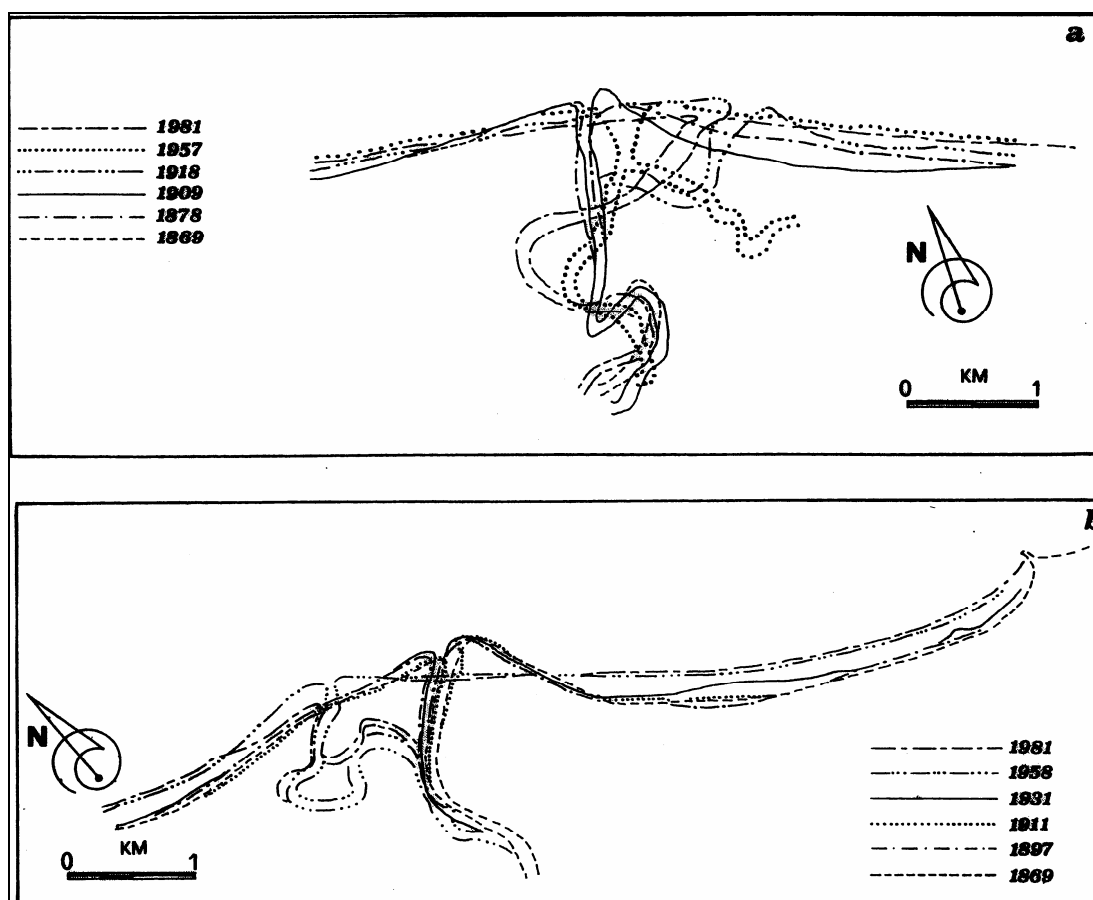


Figure 2.19 - Recent modifications of shoreline in the surroundings of (a) Fortore River mouth and of (b) Ofanto River mouth (from Caldara et al., 1998).

2.2.6. Causes of coastal erosion

Erosion affects several tracts of Puglia coastline, both on rocky coasts and beaches. However, while the former represents a severe problem only on some spots, the latter have raised very diffuse problems during last forty years (Fig. 2.20).

Clearly the greatest shoreline variations, both positive and negative, are recorded in correspondence of the beaches. In fact, those moving back cover a length of about 112 km, equal to 48% of the total one of the beaches; those stable represent 26% of the total one, equal to a general length of about 59 km; those advancing finally, extend for a length of about 59 km, equal to 26% of the total one of the beaches.



Figure 2.20 – Cliffs shaped on dune and/or on backdunes deposits are evidences of beaches in strong erosion near the Bradano River mouth.

The withdrawal of the Apulian beaches is a spread phenomenon along the whole coast. Nevertheless we have some lines where this phenomenon has reached wide and serious dimensions: the areas of delta of the principal apulian rivers (Fortore and Ofanto), along the whole Manfredonia Gulf and in correspondence of a lot of pocket beach, above all the one present along the Adriatic coast. From the collected data and especially from the comparison among the shoreline restored in different epoches, obviously where available, it seems evident that the lines in progress and, partly the stable ones, have had such trend because they represent build-up zones of sediments eroded in adjacent areas. It is, for instance, the case of Margherita di Savoia beach and that north of Barletta, which has received in these years the contributions from the intense erosion of the river Ofanto delta, or of Torre San Giovanni beach (Marina di Ugento, Lecce), that seems to be in progress to expenses of a neighbouring line of the same beach (De Santis, 2005).

The causes of the coastal erosive processes are manifold, some of them are natural, other ones have been induced by man; particularly these last ones are visible above all along the sandy coasts, much more sensitive to erosion in comparison to the rocky ones.

The drainage basins which influence the Apulian coast stretch mainly in the Tavoliere (Fortore, Candellaro, Cervaro, Carapelle and Ofanto) and in the Ionian (Bradano, Basento, Agri, Sinni) areas, most of them having their head on the Apennine chain. These rivers are characterized by variable discharge linked to the great difference between the maximum and minimum values of annual mean rainfalls. Nevertheless, the load is high because of the high rates of denudation which characterize the drainage basins of these rivers, mostly shaped in the very erodible rocks of Apennine Chain and foredeep.

During last forty years a sensible decrease of load of these rivers has been recorded (Fig. 2.21). This decrease is partly due to climatic variations but above all to the numerous dams built in their drainage basins (Mastronuzzi et al., 1997). The construction of these dams started in the fifties and continue until present days.

The Ofanto river, the longest Apulian river, about 134 km long, with a basin of about 2898 km², has been involved in the realization of 20 dams (basin of Locone, basin of Capacciotti, basin of Rendina, basin Conza, etc.) which can altogether store about 250 m³ of water. As a consequence of these interventions, the Ofanto has reduced its solid contribution to the outlet from about 2×10⁶ ton/year during the period 1935-1961 to about 0,6×10⁶ ton/year in the period 1967-1976 and to about 0,2×10⁶ ton/year during the last 20 years (Caldara, 1996; Caldara et al., 1998). A similar situation occurs along the Ionic coast. Likewise the same situation has occurred for the Bradano river where, the construction of the St. Giuliano dam (107×10⁶ m³ of basin) in 1958, has reduced the solid load to less than 10% (Cotecchia et al., 1977). The same happens for the other rivers which flows in the Taranto Gulf whose drainage basins have been interested by numerous dams (see Fig. 2.8). Furthermore, the presence of numerous harbour structures, which interest about the 5% of the whole coastal perimeter, and of diffuse coastal defence works impede the long shore drift of materials and the natural nourishment of beaches far from sediment input points.

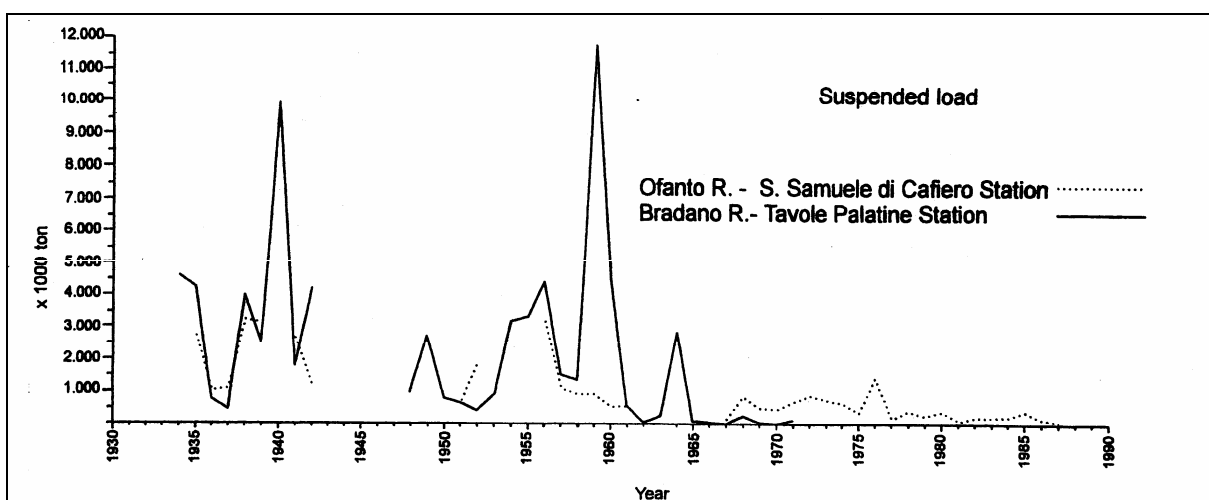


Figure 2.21- Suspended load trend of main rivers of Puglia (from Caldara et al., 1998).



Figure 2.22 – The cleaning of the beach to remove the *Posidonia oceanica* leaves contribute to determine a negative sedimentary budget. Here an illegal accumulation of this cleanness is exposed in an olive plantation with about other 80 mass. Every 2,5 kg of debris only about 400 gr. are represented by leaves and algae; 2.1 kg are represented by sands.

During the last years the incorrect management of the beaches as touristic resource has increased the deficit of sedimentary budget of most of them (Fig. 2.22).

Finally, the growing urbanisation of coastal area gives to the coastal system an extreme rigidity so that it can not modify its morphological features in response to environmental changes (wind climate, short-term climatic changes, sea level changes and so on) becoming a very fragile system.

The redistribution of the already scarce sediments delivered to the coast by the rivers is strongly hindered by the presence of dock and urban structures, which involve about 10% of the whole Apulia coastal perimeter, and by diffused coastline protection works, which prevent the sediments long-shore transport and the natural supply of the beaches.

2.3. The effects of the impact of catastrophic waves on the coasts of Apulia

The most striking morphological evidence of the impact of catastrophic waves recognised all around the coastal perimeter of Apulia is represented by boulders isolated, imbricated and/or sparse in fields or arranged in berms. The entire Apulian coast, from North to the South, preserves geological evidence of the impact of extreme catastrophic waves. They are represented by sedimentological and morphological data, sometimes coupled, that characterize the coastal landscape. The origin of these waves has been object of several studies aimed to define the difference between geomorphological effects of tsunami vs exceptional sea storm (i.e.: Mastronuzzi & Sansò, 2004;

Mastronuzzi et al., 2006). The central Mediterranean is a microtidal area characterized by low frequency of hurricane or tropical cyclone; however, one must stress that in the Ligurian Sea was generated on 23 February 1887 a meteorological tsunami to which is ascribed the death of one people in Marseille (Tinti & Maramai 1996; Eva & Rabinovich, 1997; see also: Pelinovsky et al., 2001; 2002; Monserrat et al., 2006). Moreover, since the '90s of XX century in the Central Mediterranean basin the number of like-tropical cyclone is fastly increasing (Rabinovich & Montserrat, 1998; Gianfreda et al. 2005; Fita et al. 2007). On the other hand, the attribution of important morphological consequence to seiches occurred in the seas around the Apulia, is generally neglected. On the other hand, sea surge generated by severe storms occurring in time of conjunction tides can break the barrier and shape washover fans that can modify the backbarrier drainage system. If surge is not enough high and energetic to break the barrier, it can create chevron in the dune system.

Extreme catastrophic waves are generally considered as effects of hurricanes, severe storms with very long cycle or tsunami approaching to the coasts. In the first two cases waves are highly frequent and, possible, with high run up; in the latter case a very fast sea surge characterised by low frequency and high run up occurs (Mörner, 1988; 1996). Few studies about the impact of tsunami on coastal dune belt are present in the scientific literature which mainly focuses on mechanisms of tsunami origin, propagation and deformation or on physical modelling of tsunami run-up and flooding. Sedimentological evidence of tsunami impact is represented by out-of-place layers; they are mainly marine sand/pebbles layers sandwiched in backdune, lagoonal or coastal lake sediments; more rarely they can be represented by marine sandy layers apparently wedged in sandy dune deposits. Their recognition is difficult and impossible without subsoil exploration managed by mean of geophysical investigation or by direct sampling by mean corer (Dawson, 1994; Bryant, 2001).

Geomorphological evidence ascribed to tsunami impact are represented by out-of-size depositional coastal landforms, and, but less representative, erosive landforms. Few examples exist in the world of pure erosive effects of tsunami impact; generally they are represented by collapse accumulation at the foot of high cliff, consequence of rock slide activated by tsunami or by denudational large surfaces marked by additional metric or decimetric microlandforms (Dawson, 1994; Bryant, 2001). For their prove nature it is very difficult to attribute erosive forms to a known paleo-tsunami due to the difficulty to date them.

Traditionally, the main morphological effects of tsunami on rocky coasts are represented by the detachment of large boulders in the nearshore zone and their deposition farther inland (Dawson, 1994, 2000; Nott, 2006), and by the sculpturing of bedrock resulting in the production of both smooth, small and large scale features (Bryant & Young, 1996; Bryant, 2001).

In synthesis, along the Apulian gently sloping rocky coast, features ascribed to tsunami impact are represented by boulder accumulations; otherwise, tsunami washover fans have been found along the sandy coasts. From North to the South will be presented four areas characterised by different evidence of extreme catastrophic waves that have been interpreted as produced by tsunami.



**CHAPTER
3**

The Fortore River Area

Mastronuzzi G., Sansò P.

3.1. An introduction

The Fortore River deltaic area, is placed on the NW of the Gargano Promontory (Fig. 3.1). This last is one of most seismic areas of Italy and is also the most uplifted part of Apulian foreland. During historical times has been struck by several earthquakes with epicentres placed both onshore and offshore some of which have been responsible for the generation of large tsunamis (for instance Tinti et al., 1995; Boschi et al., 1997; Gruppo di Lavoro CPTI, 2004). In particular, the most severe historical event struck this area the 30th July 1627, reaching the XI MCS grade and being responsible for the generation of a large tsunami that hit the northern coast of Apulia and Molise producing severe damage. Different are the hypothesis about the localisation of the epicentre of generative earthquake, but at present there are not agreement between different Authors (Panza et al., 1991; Tinti & Platanesi, 1996; Salvi et al., 1999; Patacca & Scandone, 2004a) (Fig. 3.2).

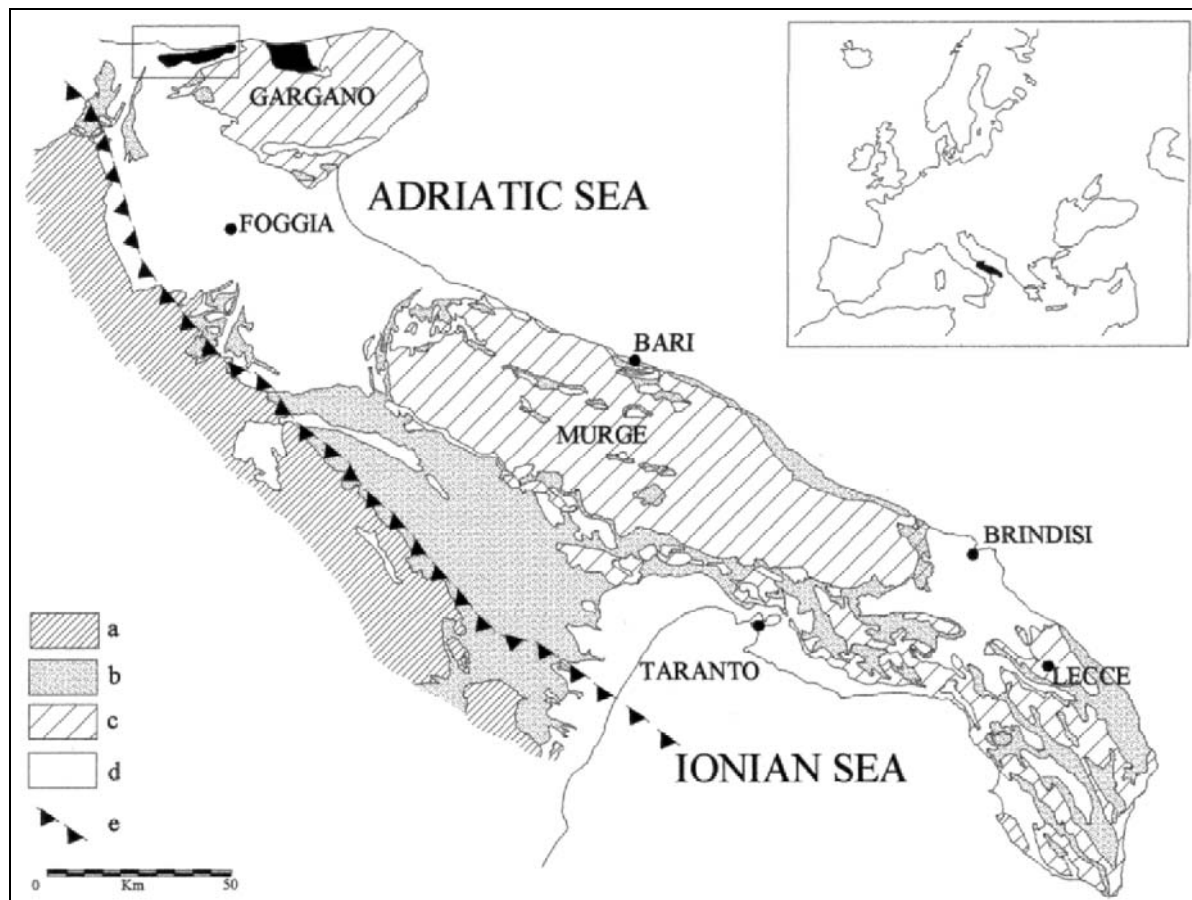


Figure 3.1 – Ubication of studied area. **a** – Apennine chain units; **b** – Apennine foredeeps units; **c** – Apulian foreland units; **d** – Pliopleistocene cover; **e** – compressive front of the southern Apennine chain. Box: Fortore River coastal plain.

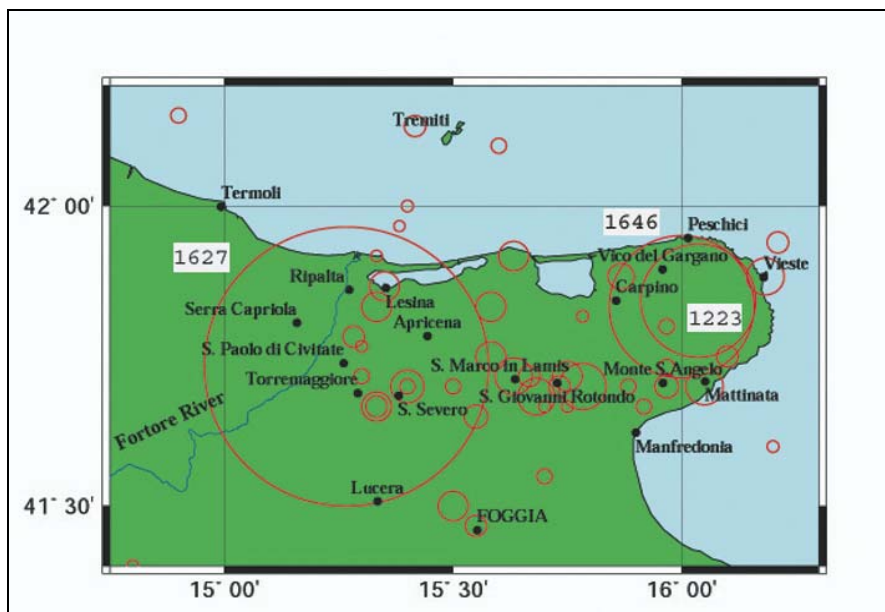


Figure 3.2 - Spatial distribution of seismicity throughout the Gargano Promontory; black circles represent the focal volumes of damaging earthquakes documented from AD 1000 to 1980 (after Del Gaudio & Pierri, 2001).

3.2. Geomorphological features

The Fortore River area comprises three main morphological unit (from West to East): the Fortore River coastal plain, the Punta delle Pietre Nere head and the Lesina Lake coastal barrier (Figs. 3.1 and 3.3).

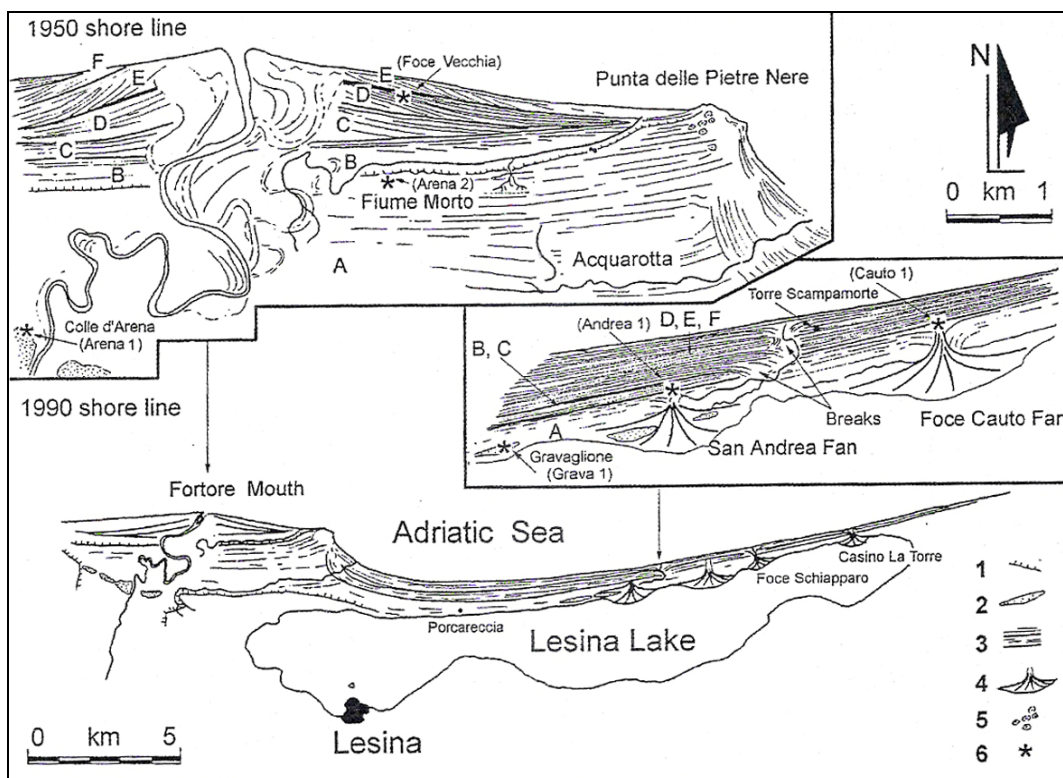


Figure 3.3 – Geomorphological sketch of Fortore River coastal plain and Lesina sandy barrier. Capital letters indicate morphological Units Legend 1. Middle Holocene cliff shaped in pre-Holocene conglomerate; 2. Colle d'Arena – Garavaglione dune belt; 3. Late Holocene dune belts; 4. tsunami washover; 5. sinkholes in the gypsum units; 6. location of dated samples.

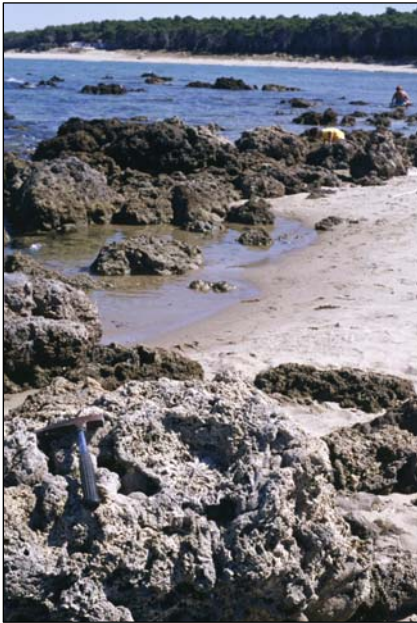


Figure 3.4 - A general view of the bioherm made of calcified worms, calcareous algae, Vermetids and *Cladocora caespitosa* (L.), cropping out at Punta delle Pietre Nere locality; near the hammer a large globular colony of *Cladocora caespitosa* - 0.60 m of diameter - is recognisable.

The first one stretches between 6 m of elevation and the present sea level, at the foot of a low cliff shaped in correspondence of the maximum Holocene transgression; it is lengthened for about 30 km from Marina di Chieuti, placed on the eastern side of the Apenninic Chain, to the Punta delle Pietre Nere head. It is made of terrigenous sands carried to the coast by Fortore and Biferno rivers and transported alongshore from West to East. The sandy deposits are arranged in a complex of swamps, dune belts and beach ridges, cut by short relict fluvial channels (i.e.: Mastronuzzi et al., 1989; Gravina et al., 2005). An impressive Late Holocene uplift rate has been recognised thanks to the individuation of raised beach sediments at about 2 m above p.s.l. dated back to (Mastronuzzi & Sansò, 2002).

Punta delle Pietre Nere is a small outcrop of igneous rocks, black limestones of Upper Triassic and deformed deposits of gypsum (i.e.: Cotecchia & Canitano, 1954; Guerricchio, 1983; Ortolani & Pagliuca, 1987; Bigazzi et al., 1996). A strong uplift rate of Punta delle Pietre Nere since the mid-Holocene has been estimated by Mastronuzzi & Sansò (2002) dating a Holocene bioherm constituted by corallinae algae and large globular colonies of *Cladocora caespitosa* (L.) (Fig. 3.4).

Furthermore, some biogenic encrustations (Fig. 3.5) and erosive marks affecting the bioherm surface would indicate that the uplift of this area follows a "seismic cycle" (Fig. 3.6); it is composed of a slow pre-seismic subsidence of the coastal area, rapidly increasing about one century before a large earthquake, followed by coseismic uplift, more than 0.5 m in elevation (Mastronuzzi & Sansò, 2002).

The Lesina Lake is divided from the Adriatic Sea by a sandy coastal barrier, about 22 km long and showing a mean elevation of 3 m. The lagoonal system has developed after the Holocene climatic optimum due to the growth of a steady littoral sandy ridge, first NW-SE then W-E oriented, on which dune ridges developed, led to the genesis of a lagoon behind the dunes. De Pippo et al. (2001) suggest that its origin is linked to the progressive development of composite littoral spits inside a shallow-water marine bay.

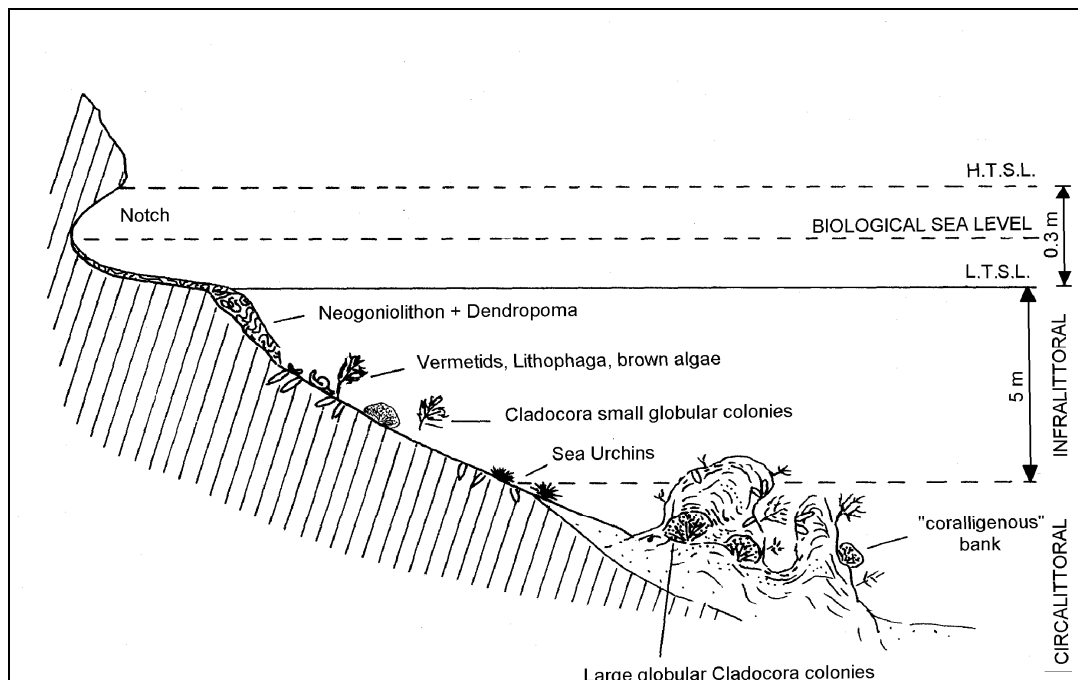


Figure 3.5 - Distribution of erosion and bioconstruction at the Northern coast of Gargano reconstructed by bibliographic data and underwater survey; dotted lines indicate variable levels. At Punta delle Pietre Nere locality the limit between infralittoral and circalittoral zone is placed at about 5 - 15 m below sea level and marked by "coralligene - like" bio-constructed formations.

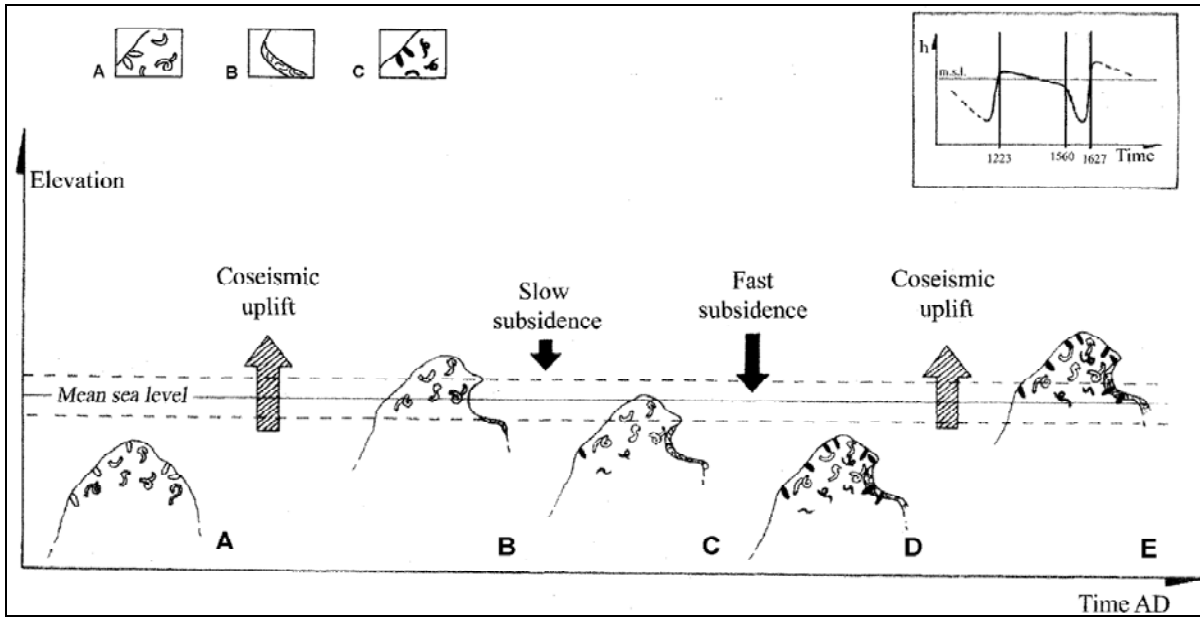


Figure 3.6 - Model of the vertical movements occurred during historical times in response of major earthquakes recorded at the locality of Punta delle Pietre Nere. In the box window is schematically reported a relative sea level curve for northern Gargano coast during last millennium. A - Vermetids and *Lithophaga* sp. (first colonization); B - *Dendropoma* sp. encrustation; C - Vermetids and *Lithophaga* sp. (second colonization).

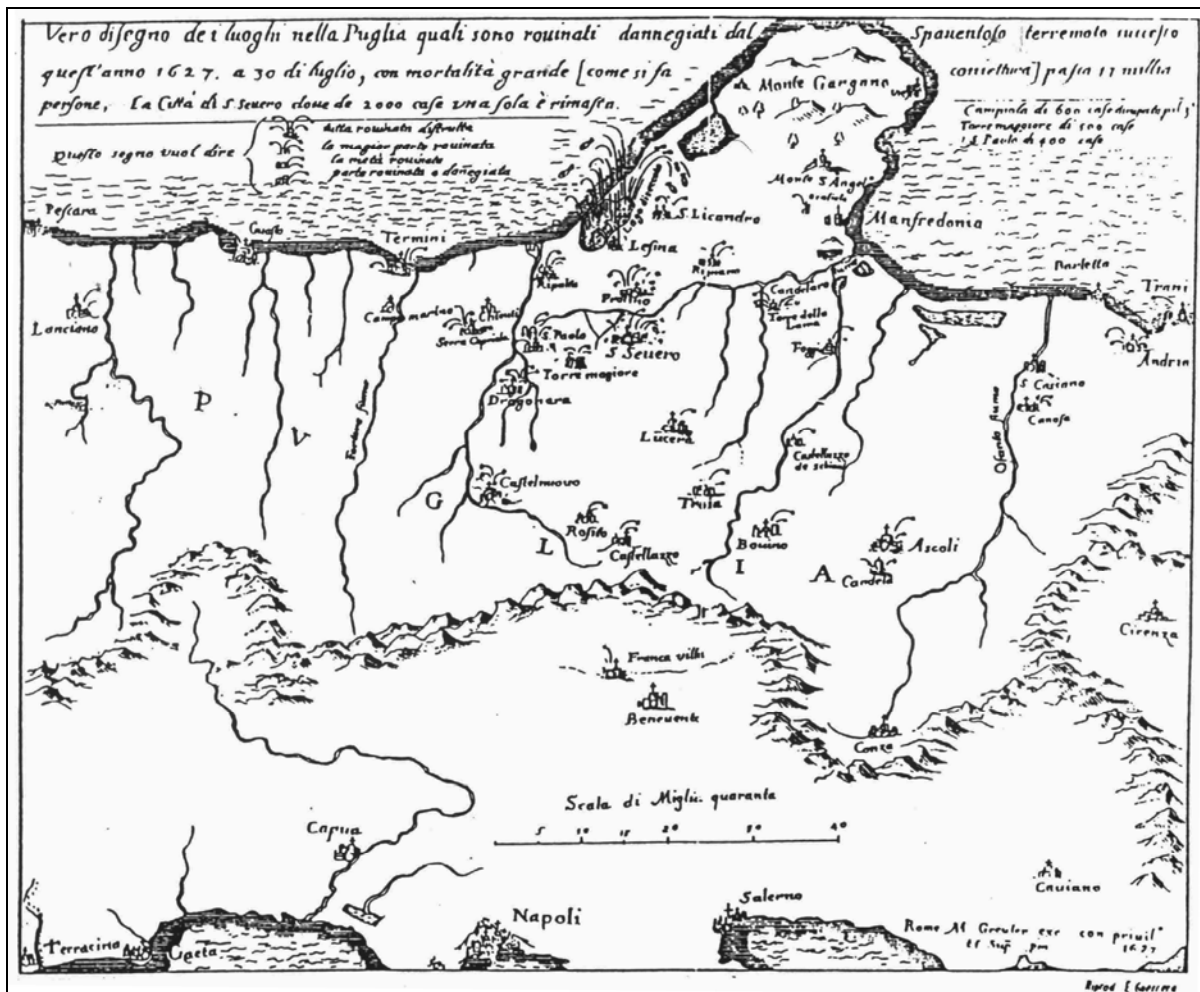


Figure 3.7 - The effects of the 30 July 1627 earthquake and tsunami described in the Magini's map (1627).

Gianfreda et al. (2001) carried out a detailed morphological analysis integrated by some radiocarbon age determinations. They individuated on the Lesina coastal barrier two huge washover fans (Sant'Andrea and Foce Cauto washover fans) which are the effects of two large tsunamis previous to the 1627 event (Fig. 3.7). Age determinations of the first dune belt closing the two washovers apex allowed to refer their development at about 2430 years BP (Sant'Andrea fan) and at about 493 AD (Foce Cauto fan). De Martini et al. (2003) recognized three distinct sandy layers interbedded into a marsh sequence occurring in the coastal plain. The most recent layer would have been deposited by the 1627 tsunami whereas the most ancient event would be 3639-3350 years BC.

3.3. The influence of large seismic events on the coastal landscape evolution

The available geomorphological and geochronological data set suggests that the morphological evolution of Fortore River coastal plain and Lesina Lake coastal barrier has been strongly influenced by strong seismic events that produced coseismic vertical movements and devastating tsunamis (Fig. 3.8).

The nature and the similarity of the surveyed effects related to each of these events strongly suggest their attribution to the activity of a seismogenic structure placed close to Punta delle Pietre Nere head. In fact, similar studies carried out in the Eastern Mediterranean (Stiros et al., 1992; Pirazzoli et al., 1991; 1994a; 1994b; Pirazzoli, 2005) along coastal areas that have been affected by slow pre-seismic subsidence and coseismic uplift - as well as large tsunamis (Pirazzoli et al., 1999) generally correlate these effects to the activity of nearby important seismogenic faults able to produce earthquakes with magnitude greater than 6.

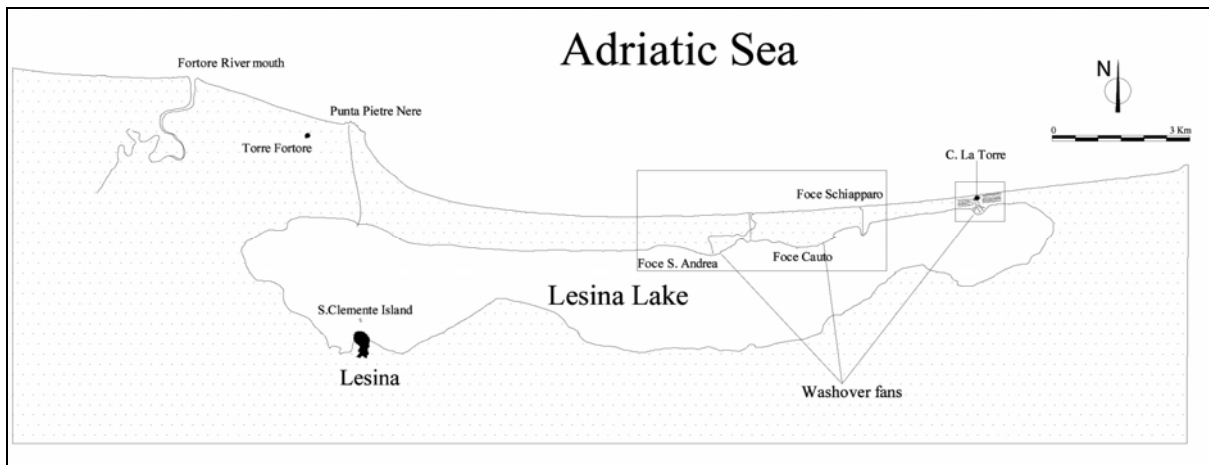


Figure 3.8 - Geographic position of the Lesina coastal barrier and washover fans.

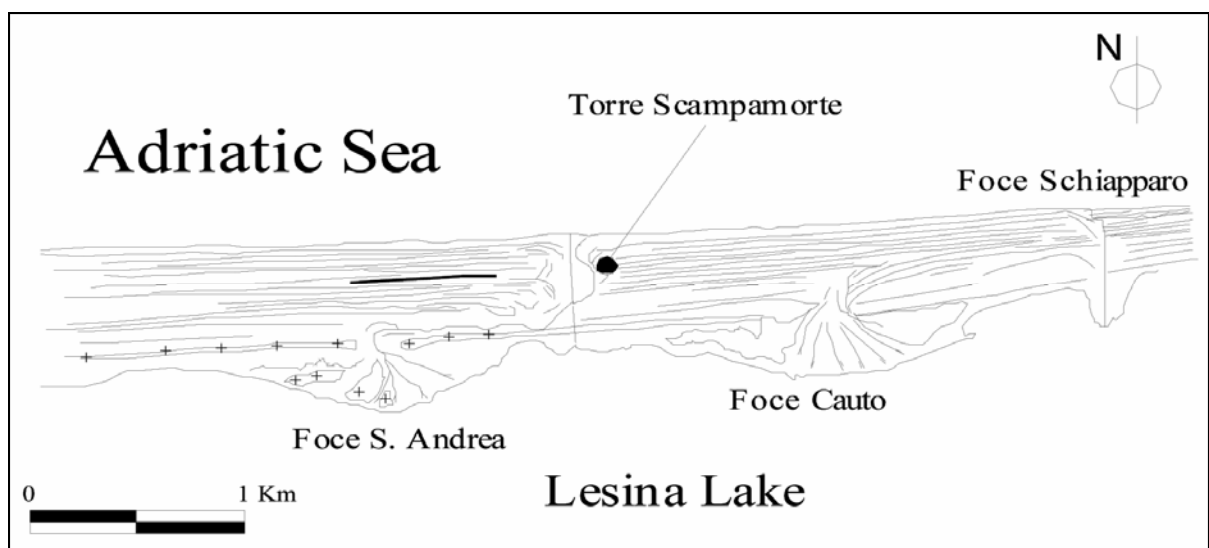


Figure 3.9 - Dune ridges and washover fans on the Lesina coastal barrier in the area of Sant'Andrea and Foce Cauto.

The morphology of the Lesina coastal barrier (Figs. 3.8 and 3.9) indicates that at least three tsunamis struck the northern coast of gargano promontory in historical times. Each one deposited a washover fan 100000 to 750000 m² in area that escludes the action of storm waves restricted by small, semi-enclosed state of the Adriatic Sea and by small tidal range (about 1 m). The washover fans were formed by catastrophic tsunami wave focused at distinct points coseismic cracking that developed into narrow, long breaches through coastal barrier ridges (Fig. 3.10 A). The formation of cracks was noted during the earthquake of the year 1627 at several localities near the epicentre, affecting the alluvial deposits and sands of the Fortore River lower valley and coastal plain (Molin & Margottini, 1981). These marks are similar to those reported following the Japan Sea earthquake and tsunamis of 26 May 1983 (Minoura & Nakaya, 1991). Here, cracks that formed in the Japan Sea, allowed tsunami to rush into the back barrier area. At the Lesina coastal barrier, during the second event, tsunami waves overtopped the coastal barrier levelling ridges and scoured a number of erosive grooves, similar to those reported by Sato et al. (1995) and McSaveney et al. (2000) during tsunami events. Sea water ran through the cracks, forming a narrow throat and a wide washover fan at the inner edge of the coastal barrier. At the same time, the seaward edge of the coastal barrier was most likely cliffed and a significant amount of barrier sediment was moved offshore forming sub-marine bars (Fig. 3.10 B). This is similar to processes observed by Maramai & Tinti (1997) during the June 1994 Java tsunami, and by Minoura & Nakaya (1991) in the offshore area soon after the Japan Sea earthquake and tsunami of 26 May 1983. Normal wave climate was the final factor responsible for the transport of submarine bars onshore, causing the recovery of the coastal barrier and the formation of new dune ridges. These closed the washover throat and buried the cliff (Fig. 3.10 C). The first recorded seismic event struck this area about 465 BC producing important effects on the coastal landscape evolution. This event interrupted most likely the progradation of the coastal plain which followed the maximum post-glacial ingression marked out by the cliff constituting the inner margin of the coastal plain. This phase of progradation started at about 3000 years BC and produced a wide coastal plain and the Colle d'Arena-Gravaglione dune belt which most likely constituted the first core of Lesina Lake coastal barrier. During this phase, the area was most likely affected by a differential uplift testified by the uplift of the bioherm with *Cladocora caespitosa* at Punta delle Pietre Nere head and by the beach level of Arena 2 sample (Tab. 3.1; Fig. 3.11). The uplift is marked by higher value on the Apenninic side as testified by the strong asymmetry of Fortore River lower valley. In this period the Fortore River has a negligible solid load so that it did not form a delta and the coastal plain is composed by straight, parallel ridges. Its final tract is forced by W-E littoral drift to runs parallel to the shoreline, flowing in an area to the East of Punta delle Pietre Nere.

The 465 BC earthquake produced the coseismic uplift of Punta delle Pietre Nere which from this moment on constitutes a small promontory dividing the Fortore River coastal plain from the Lesina Lake coastal barrier. Pre-seismic subsidence is suggested by the strong erosion of Fortore River coastal plain and the shaping of the small cliff which at present divides unit A from unit B (Fig. 3.3); subsidence is recorded also in area of Lesina Lake, where a large tsunami struck the coastal barrier producing severe erosion and the formation of Sant'Andrea washover fan (Fig. 3.11). This event was followed by the progradation of units B and C; these units merge on Lesina coastal barrier whereas a discontinuity into dune ridge pattern can be recognized in the area of Fortore river coastal plain (Fig. 3.3).

The second seismic event occurred in 493 AD and produced the large tsunami responsible for the Foc Cauto washover fan development and the partial erosion of the small cuspidate delta of Fortore River. This last one developed during the Roman Age in response to the solid load increase most likely due to the intense deforestation of Apulia and Basilicata regions since 400 BC (Boenzi et al., 2000; Gravina et al., 2005). Interestingly, the collated data confirm the occurrence of 493 AD strong earthquake on the Gargano Promontory, that is not documented historically and then is not reported in the most recent catalogues (e.g. Boschi et al., 1997), but it is described in one of the most important medieval sacred legend, that one of Monte Sant'Angelo. Moreover, this study would place the seismogenetic structure that produced the 493 AD event in the Punta delle Pietre Nere area and not along the Monte Sant'Angelo fault as suggested by Piccardi (1998, 2005).

Important coseismic movements produced by the following 1087 AD large earthquake can be inferred by the analysis of bioconcretions of *Vermetid sp.* (sample 1DOD: 734 – 1249 AD 2 σ calibrated age; Tab. 3.1) detected at Punta delle Pietre Nere (Mastronuzzi & Sansò, 2002). Rapid changes of Lesina Lake level in this date are also suggested by the local legend related to the pilgrimage of Matilde di Canossa to the Monte Sant'Angelo sanctuary (Vocino, 1930).

Lastly, the 30th July 1627 strong earthquake produced the last important coseismic uplift of Punta delle Pietre Nere head as testified by the emergence of the bioconcretions of *Lithophaga sp.* (1DOE sample: 1443 – 1677 AD 2 σ calibrated age; Tab. 3.1). This uplift was preceded by a century of rapid subsidence which caused the submergence of the intertidal colonies of *Dendropoma sp.* and their consequent death (PN 1 sample: 1115 – 1446 AD 2 σ calibrated age; Tab. 3.1) (Mastronuzzi & Sansò, 2002) as well as the strong erosion of Fortore River cuspidate delta.

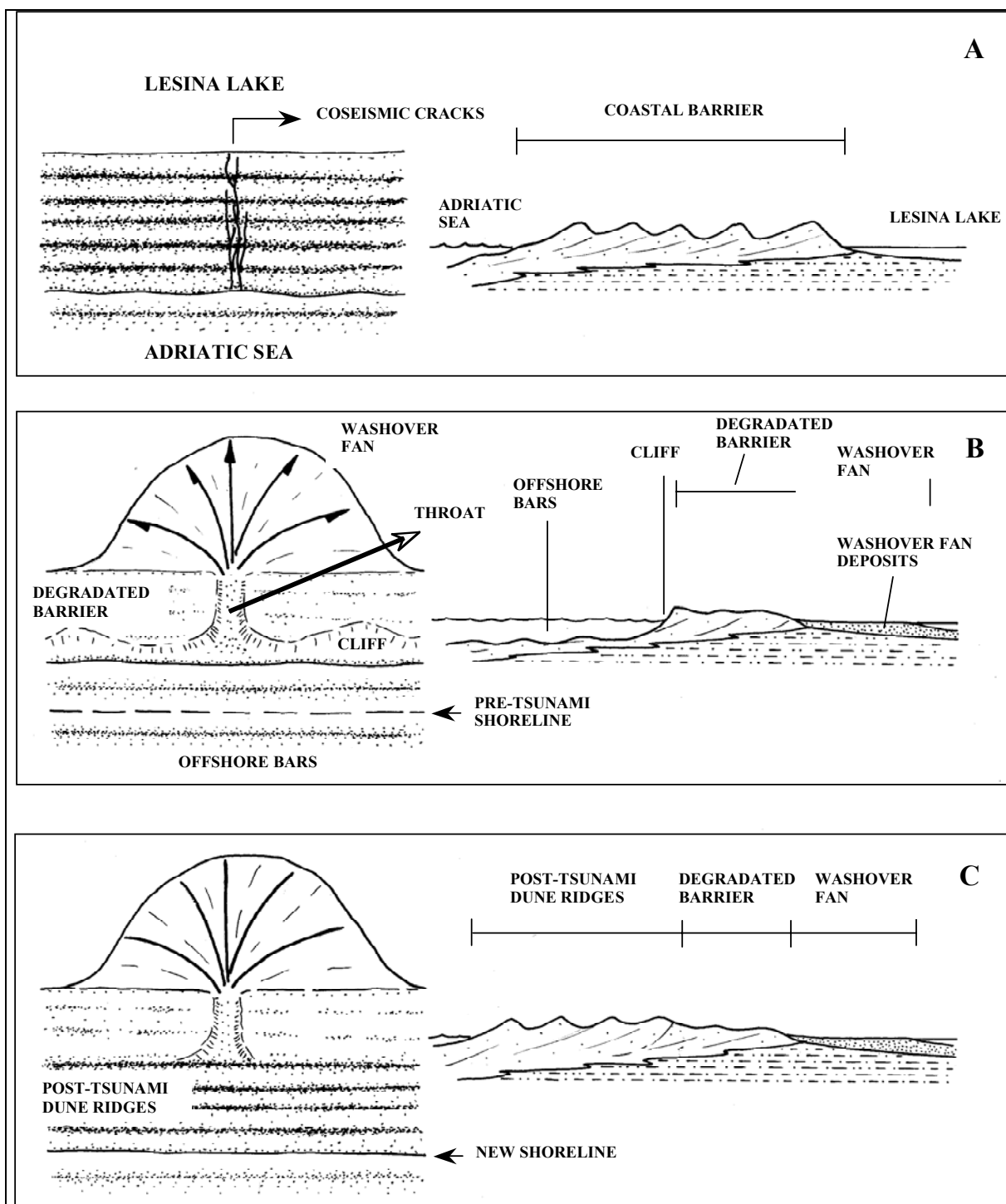


Figure 3.10 - Geomorphological model of tsunami impact on the Lesina coastal barrier. **A** - coseismic cracks formed in the coastal barrier dune ridges during an earthquakes; **B** - tsunami waves flatten the coastal barrier ridges. Sea water running through the cracks shapes a narrow throat and a wide washover fan at the inner edge of the coastal barrier. At the same time, a cliff is cut at the seaward edge of the coastal barrier and significant amounts of barrier sediments are moved offshore forming submarine bars; **C** - normal waves are the final factor responsible for the transport of submarine bars sediments onshore, causing the recovery of the coastal barrier with new dune ridges forming and closing the washover throat.

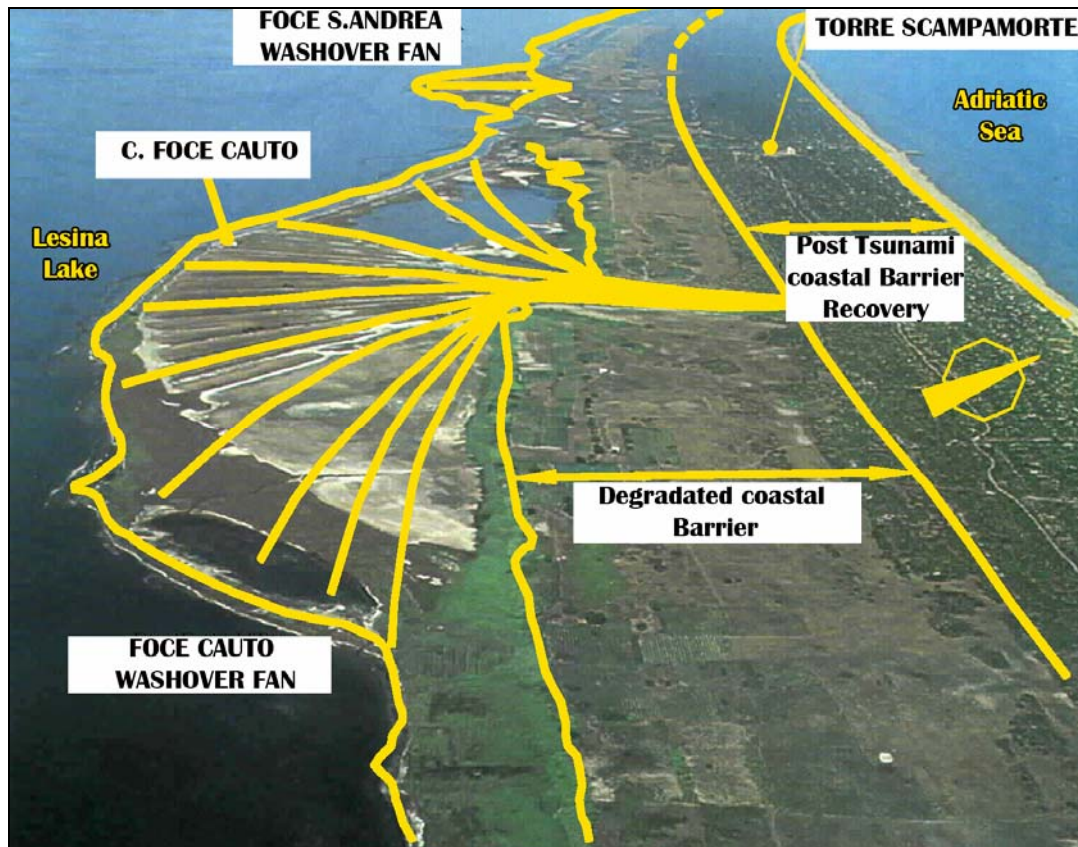


Figure 3.11 - The geomorphological interpretation of the Lesina coastal barrier in the area of Foce Cauto.

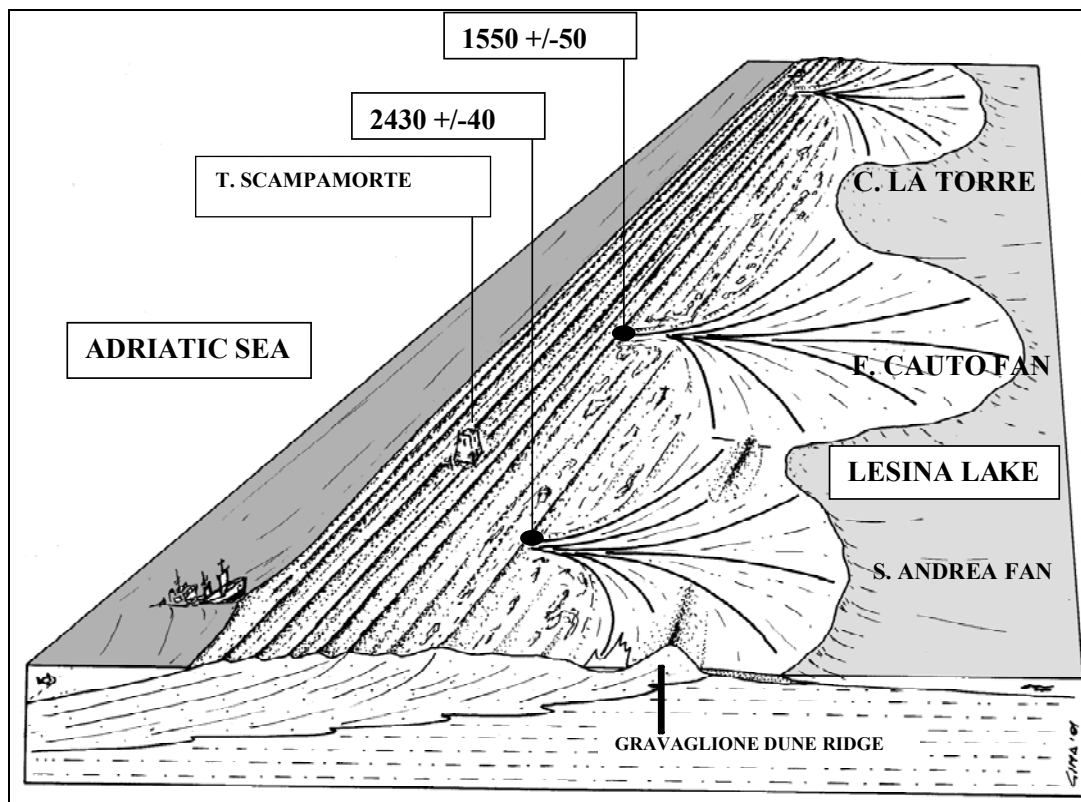


Figure 3.12 - Geomorphological sketch of the Lesina coastal barrier. The position of samples dated by means of AMS radiocarbon age determinations is also reported.

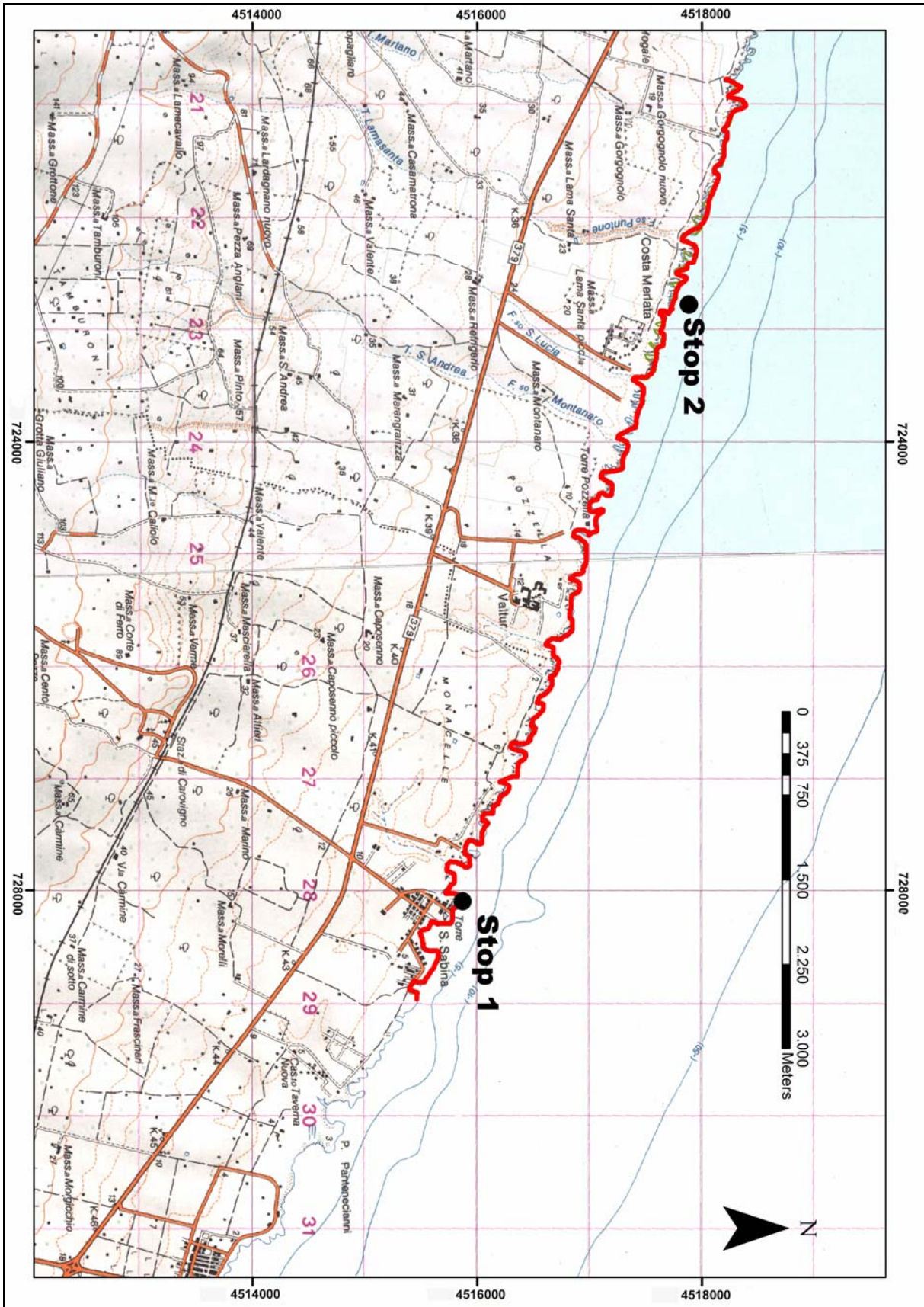
Sample	Laboratory N°	Specimen	Elevation m a.p.s.l.	Conventional age (yr BP +/-σ)	δC _{PDB} %	Calibrated age AD/BC Atmospheric (1 σ)	Calibrated age AD/BC Atmospheric (2 σ)	Ref.
Fortore River coastal plain								
Foce Vecchia	GX-27752-AMS	<i>Helix</i> sp	1,5	1590 ± 190	-7,3	311 - 642 AD	22 – 783 AD	B
Arena 2	GX-27751-AMS	<i>Lima</i> sp	2	3030 ± 190	-2,4	923 – 423 BC	1216 – 208 BC	B
Arena 1	GX-25750-AMS	<i>Helix</i> sp	7	4340 ± 80	-8,0	3035 - 2888 BC	3138 - 2861 BC	B
Lesina Lake coastal barrier								
Cauto 1	GX-28021-	<i>Pomatia</i> sp	2	1550 ± 50	-8,6	433 – 495 AD	410 – 609 AD	A
Andrea 1	GX-28020-	<i>Rumina</i> sp	3	2430 ± 40	-7,4	542 – 410 BC	597 – 402 BC	A
Grava 1	GX-28022-	<i>Pomatia</i> sp	6	4450 ± 40	-7,2	3324 – 3233 BC	3143 – 3008 BC	C
Punta delle Pietre Nere								
1DOE	GX-6369-AMS	<i>Lithophaga</i> sp	0,93	880 ± 40	-2,9	1487 – 1624 AD	1443 – 1677 AD	B
PN1	GX-27061-	<i>Dendropoma</i> sp	0,77-0,88	1210 ± 70	-3,3	1227 – 1390 AD	1115 – 1446 AD	B
1DOD	GX-26368-	<i>Vermetid</i> sp.	0,95	1520 ± 110	-0,2	873 – 1150 AD	734 – 1249 AD	B
PPN3	GX-28709-	<i>Cladocora caespitosa</i>	0,5	5950 ± 110	-3,6	4442 – 4162 BC	4557 – 3990 BC	B

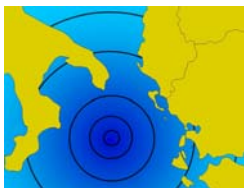
Table 3.1 - Samples dated by AMS ¹⁴C and by ¹⁴C on the Fortore River coastal plain. Radiocarbon age determinations were performed on coral and shell samples at Geochron Laboratories, Krueger Enterprises Inc., Cambridge, Massachusetts, USA. Samples were cleaned thoroughly in an ultrasonic cleaner and then leached with dilute HCl to remove additional surficial material which may have been altered to be sure only fresh carbonate material was used. The cleaned samples were then hydrolyzed with HCl, under vacuum, and the carbon dioxide was recovered for analysis. The ages obtained are based on the Libby half-life (5570 yr) for ¹⁴C. The error is 1 sigma as judged by the analytical data alone. The modern standard is 95% of the activity of N.B.S. Oxalic Acid. The age is referenced to the year AD 1950. The conventional radiocarbon ages have been calibrated using the CALIB 5.0 software (Stuiver et al., 2005). The marine reservoir correction for marine samples (Arena2, 1DOD, 1DOE, PN1, PPN3 samples) has been made using the ΔR values of 118 ± 60, obtained from the available sample nearest to Gargano promontory, a specimen of *Chlamys varia* coming from Barletta, South Adriatic (Stuiver et al., 1998) (Legend: A – Gianfreda et al. 2001; B – Mastronuzzi & Sansò, 2002a; C – Gravina et al., 2005).

3.4. Conclusions

The geomorphological analysis of Fortore River coastal plain and Lesina Lake coastal barrier points out some important effects of large seismic events on the coastal landscape of Northern Apulia. In particular, it shows that seismic events able to affect the morphological evolution of the coastal landscape have a return period of about one-thousand year. They are accompanied by vertical movements according to a “seismic cycle” which have been often recorded in seismic coastal areas (Thatcher, 1984; Taylor et al., 1990; Ward & Valensise, 1994; Stiros & Pirazzoli, 1995; Hamilton et al., 2005). These events produced coseismic vertical movements identified in the area of Lesina village and Punta delle Pietre Nere head and large tsunamis whose effects are still recognizable on the Lesina Lake coastal barrier and on the Fortore mouth coastal plain. The presence of a seismic deformation cycle has been detected on the Punta delle Pietre Nere bioherm. Moreover, a strong differential uplift of the northern Gargano coastal area during the Holocene has been inferred. The area to the West of Punta delle Pietre Nere, in fact, is affected by strong uplift (about 1.5 mm/a) whereas the area of the Lesina Lake shows subsidence.

FIRST DAY
23 September 2008





2nd International Tsunami Field Symposium

IGCP Project 495

Quaternary Land-Ocean Interactions:
Driving Mechanisms and Coastal Responses

Ostuni (Italy) and Ionian Islands (Greece) 22-28 September 2008



Project 495

CHAPTER 4

The Ostuni-Carovigno coastal area

Coppola D., Mastronuzzi G., Pignatelli C., Sansò P.

4.1. The Bari-Brindisi coast

Along the Adriatic side of Apulia the coast stretching between Bari and Brindisi for about 120 km is shaped on sequence of Mesozoic limestone and Cenozoic sandstone (D'Alessandro & Iannone, 1982; 1984). It is characterised by alternance of cliffs, gently sloping rocky coasts and deep and narrow bay corresponding to floated sapping valleys (Caldara et al., 1998; Mastronuzzi & Sansò 2002c; Mastronuzzi et al., 2002). Large boulder accumulations have been recognized in various sections of gently sloping rocky coasts. The boulders generally consist of large slabs of Pleistocene calcareous sandstones, their maximum size being approximately $2.9 \times 2.4 \times 0.7 \text{ m}^3$, with a volume of 4.8 m^3 and weighing up to approximately 8 t. The principal features of the boulder accumulations surveyed are as follows: **i** - the boulders often consist of slabs of calcareous sandstones (unit weight = 1.62 tm^{-3}) carved out along strata planes and joints in the nearshore area, and subsequently were accumulated farther inland; these slabs are often imbricated in small groups of several elements, or form parallel rows which are not oriented at right angles to the coastline, but instead are usually aligned in accordance with the direction of the wave approach to the coast responsible for their deposition; **ii** - most of the boulders have been carved out from an area close to the supratidal zone, which can be ascertained from the presence of wide, flat rock pools and by barnacles on the surface of the boulders; due to the tilting of the transported boulders, rock pools have been subsequently modified by new, horizontal solution pools formed because of karstic processes; **iii** - some boulders were carved out from the midsublittoral zone, which is confirmed by the presence of biogenic encrustations (*Vermetids*, *Serpulids* and *Bryozoa* colonies) and boring bivalves (*Lithophaga*) that have colonised their surface; **iv** - the boulder detachment and transportation occurred after the Middle Ages, as most boulders rest on medieval quarries or cover other man-made structures; in some cases, boulders have been found inside Messapic graves dating back to the 6th century B.C.



Figure 4.1 – Main localities along Adriatic side of Apulia that show tsunami and/or sea storms boulders accumulation.



Figure 4.2 – **a**) Boulders coming from the sublittoral zone cover medieval quarries near Mola di Bari (BA); **b**) A row of emblicated boulders in Polignano-San Vito (BA) locality; **c**) A view of a boulder at Egnatia (BR) locality showing a new, subhorizontal generation of karstic rock pools which cuts the former one suggesting only one single phase of transport; **d**) A boulder placed on an ancient quarry in Torre Santa Sabina (BR) area.

The largest of the boulder accumulations (composed of more than 10 elements) was found in the areas of Mola di Bari and Polignano villages as well as at Egnazia archaeological area (Fig. 4.1). To the south of Mola di Bari village, boulders were recently carved from the sublittoral zone (Fig. 4.2 a), confirmed by the presence of bioencrustations on their surfaces, and transported as much as 10m from the coastline and up to 1m above sea level.

Near Polignano village (S.Vito locality), numerous imbricated boulders measuring up to 2.2x1.9x0.9 m³ are sited up to 2.5m above m.s.l. and 50m from the coastline. Most boulders were detached from the supratidal zone as indicated by the presence of bioerosive rock pools. In some places boulders form rows composed of up to seven elements (Fig. 4.2 b).

At Egnatia locality imbricated boulders are placed up to 2m above mean sea level. Their surface is affected by tilted solution pans which have developed at the bottom new horizontal pans. It is evident that the boulders have not moved after the initial detachment and transportation (Fig. 4.2 c). They often cover the floor of medieval quarries (Fig. 4.2 d).

4.1.1. The boulder accumulation at Torre Santa Sabina: STOP 1

An accumulation of about 80 boulders has been found at the coastal town of Torre Santa Sabina, which lies approximately 30 km to the northwest of Brindisi. A detailed topographical survey of this boulder accumulation and surrounding coastal area was carried out with the intention of obtaining data concerning the direction and the strength of waves responsible for boulder transportation and deposition (Fig. 4.3).

The coast is generally composed of a rocky platform, partly corresponding to the last interglacial transgression surface. It is shaped on Plio-Pleistocene calcareous sandstones that are affected by a system of long subparallel fractures, sealed by laminated calcitic filling. The filling is about 5–15 cm thick, vertically laminated and more resistant to weathering and erosion than the bedrock. According to Magagnosc (1984) similar structures are formed in semi-arid regions in response to local earthquakes. Moreover, seismogenic structures have been found in marine sediments of the last interglacial period cropping out in this coastal area (Moretti & Tropeano, 1996; Moretti, 2000). Their presence suggests that this region has been affected by active tectonics during recent times. The network composed of vertical fractures and sub-horizontal stratification of the Plio-Pleistocene rocks determine the size of the carved blocks. The platform, gently sloping seaward, is placed between 0.5 and 2m above m.s.l. and shows a mean slope lower than 4°.

In greater detail, the platform surface is affected by weathering micro- and meso-landforms in correspondence with its seaward limit. Wave erosion has shaped in its easternmost part a short, wide channel open to the NNE direction. The detailed submerged profile of the coast was derived from direct scuba surveying (Fig. 4.4). It is marked by an irregular, steep surface which joins the low tide platform, up to 8m wide, to a sandy plain placed at a depth of approximately 4.5 m. This surface is variable in length (from 12 to 22 m) and in mean slope (from about 14% to 25%). It is also marked at several points by deep potholes, and to a large extent it has been colonised by brown algae. Some boulders, with the major axes up to 4m in length, rest on this surface.

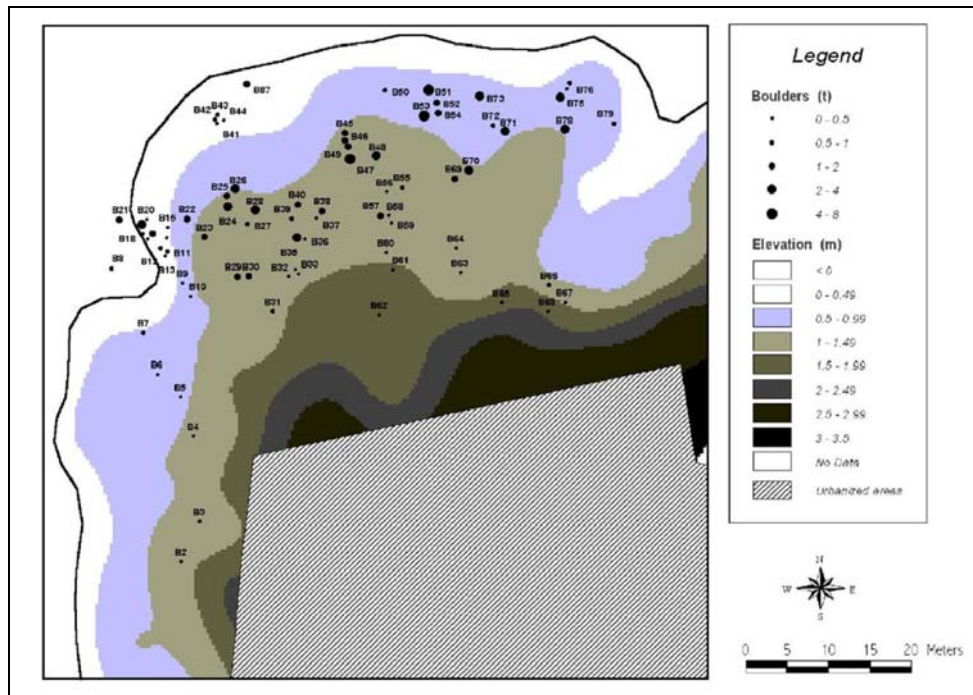


Figure 4.3 - Digital elevation model of the coastal platform, position and weight of boulders surveyed at Torre Santa Sabina locality.

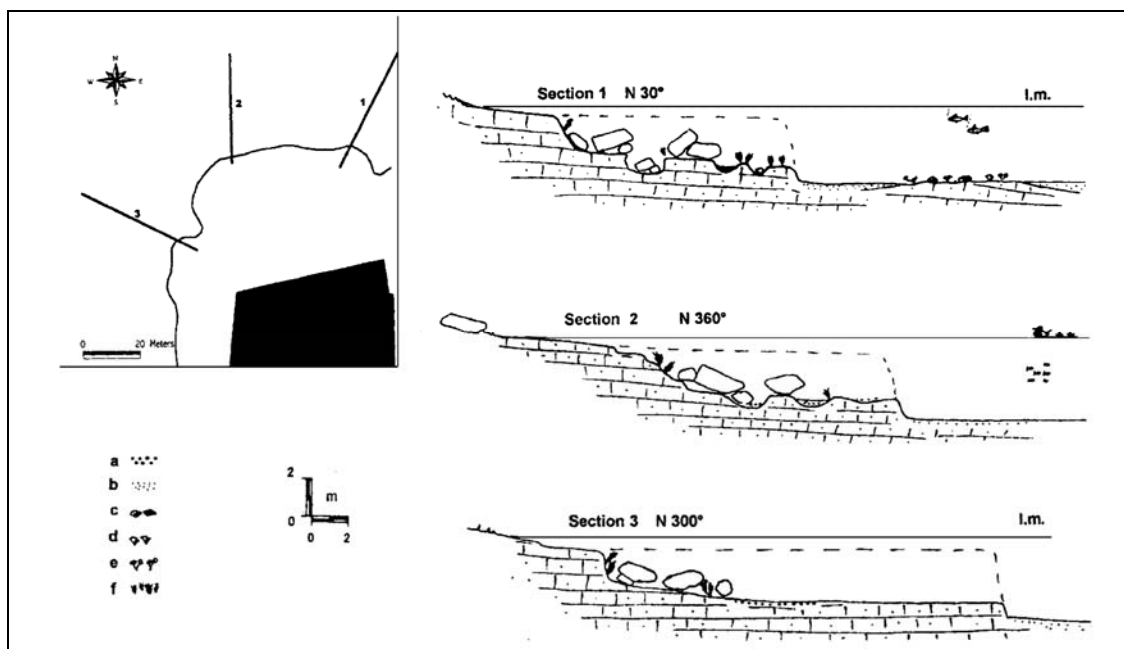


Figure 4.4 - Submerged profiles at Torre Santa Sabina locality. Legend: a - coarse sand; b - fine sand; c - *Cladocora caespitosa*; d - *Padina pavonica*; e - *Acetabularia acetabulum*; f - brown algae.

Many of them were moved recently as can be ascertained from the lack of colonisation or by the presence of white, unweathered rock on some parts of their surface. A total station was used to survey the position, altitude, size, and the A-axis direction of each boulder, as well as the detailed topography of the emerged rocky platform itself. Boulders are scattered along a strip stretching from the coastline to a maximum altitude of 2 m. However, the largest boulders are concentrated along a narrow belt WSW–ENE oriented, between 0.5 and 1.5m above m.s.l. The largest boulders are slabs of calcareous sandstones (A-axis>B-axis>>C-axis) with sizes up to 2.9x2.4x0.7 m³ and weighing up to 8 t. They are generally arranged in small groups of three or four elements, often imbricated and disposed in lines. The surfaces of some boulders were colonised by marine organisms living in the mid-infra littoral zone as *Dendropoma* sp. and bored by *Lithophaga* shells. In a few cases, biogenic encrustations can be observed at the lower face of boulders, indicating that they must have been overturned during their transportation. Boulder covers man-made features (most likely small salt pools) which most probably date back to the late Middle Ages.

Samples of vermetids were gathered from the surface of four imbricated elements (B47, B46, B49, B45) (Figs. 4.5 A-B) and their age established by using radiocarbon dating techniques. With the exception of B47, the other boulders are overturned. The conventional ¹⁴C ages of the samples are 610±60, 540±60, 1200±80 and modern age, respectively (Tab. 4.1).

We anticipate that the age of boulders B45 and B49, the youngest elements of an imbricated row, should be younger or very similar to that of B47 and B46. The older conventional age obtained for boulder B49 can be explained either by boulder reworking, pollution from older fossil remains or particles of Plio-Pleistocene bedrock included within the *Dendrophoma* encrustation.

The calibration of radiocarbon age determinations, carried out using Calib 4.3 software and adopting a ΔR value of 43±48 (Stuiver et al., 1998), yielded calibrated age ranges from 1667 to 1843 AD for boulder 47 and from 1797 to 1904 AD for boulder 46. On 4 January 2002, shortly after the detailed topographical survey was carried out, a severe sea storm developed due to strong NE winds whose velocity exceeded 30 knots. The National Wave Measuring Service (Servizio Ondametrico Nazionale) buoy at Monopoli, which is stationed few kilometers to the NW of Torre Santa Sabina area, recorded waves reaching a significant heights of up to 4.8m and with a peak period of 8.3 s moving in a N43E direction (Fig. 4.6 a). These wave statistics indicate that this extreme event was one of the most severe storms at sea recorded along this coastal area since the 1990s (Fig. 4.7). During this sea storm, one single boulder was detached, transported landward for about 1.6 m, and eventually deposited at 0.5m a.s.l. The boulder has a triangular shape (2.2m at its base, 1.3m in height and about 0.7m thick) and weighs 1.4 t.

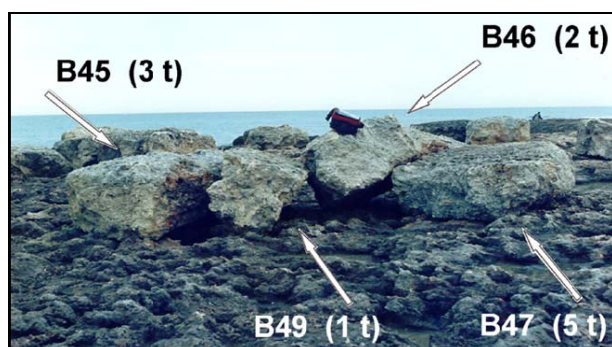


Fig. 4.5 A - Imbricated boulders at Torre Santa Sabina locality (Brindisi).



Figure 4.5 B – A view of the biological encrustation recognisable on boulder B46. Samples of *Vermetids* placed on *Dendrophoma* colonies were gathered from the surface of four imbricated elements.

Samples	Laboratory ID	Approximate Weight (tonns)	Overturned	Specimen	Method	Conventional ¹⁴ C age (yr BP ± 1σ)	δ ¹³ C _{PDB}	Calibrated Age AD
B47	GX-28869	5	N	<i>Dendropoma</i> sp.	14 C	610 ± 60	+0.4%	1667 - 1843
B46	GX 28868	2	Y	<i>Dendropoma</i> sp.	14 C	540 ± 60	-0.1%	1797 - 1904
B49	GX-29669	1	Y	<i>Dendropoma</i> sp.	14 C	1200 ± 80	+0.4%	-
B45	GX-29790	3	Y	<i>Dendropoma</i> sp.	AMS 14 C	103 ± 0.43 % of modern 14 C	+0.4%	-

Table 4.1 - Samples dated by 14 C at Torre Santa Sabina; age calibration for marine samples was performed by mean of CALIB 4.3 software and adopting ΔR values of 43±48 (Stuiver & Reimer, 1998). Analyses were performed at Geochron Laboratoires Krueger Enterprises Inc. (Cambridge, Massachusetts, U.S.A).

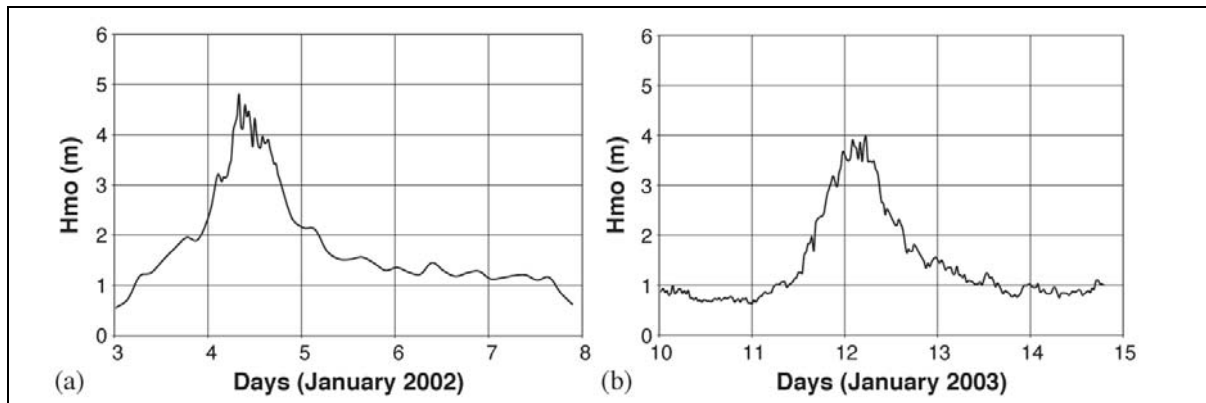


Figure 4.6 - Significant waves height (Hmo) recorded at Monopoli buoy (RON—Rete Ondametrica Nazionale): (a) from 3 to 8 January, 2002; (b) from 10 to 15 January, 2003.

The biogenic colonization present at the base of the boulder indicates that it was carved out from the midlittoral-sublittoral zone, and that it was overturned during transportation. The place where the boulder was detached from has been identified by means of scuba survey (Fig. 4.8).

During another storm at sea, which occurred on 12 January 2003, the boulder was moved once again by storm waves with a significant wave height of 4m and peak period of 9.1s moving in a N49E direction (data from Monopoli buoy, RON - Rete Ondametrica Nazionale/ National Wave Measuring Service) (Fig. 4.6 b). The boulder was transported for about 20m in NE-SW direction, colliding at first with the B42 and B43 imbricated boulders before stopping against the B15-16-17-18-19-20 imbricated boulders group, where it is now established as a new imbricated element with its upper face dipping parallel to the direction of movement (Fig. 4.9).

Finally, during the storm that hit the Santa Sabina area on February 2008, approaching from NE some boulder no more than $0.8 \div 1$ t were scattered inland up to about 30 m inland from the adlittoral area (Fig. 4.10).

An attempt to determine the approach direction of the actual waves responsible for the boulders' accumulation has been made by measuring the spatial distribution of elongated boulders' major axis (A-axis) (49 elements), and assuming the A-axis to be parallel to the crest of waves responsible for depositing the boulder and ignoring as of no great relevance any disturbance due to a few irregularities in the surface of the rocky platform.

The boulders' A-axis (Fig. 4.11) show a bimodal distribution marked by two frequency peaks at N80E and at N110E orientations which should indicate directions of wave approach of N350E and N20E, respectively.

Furthermore, although the spatial distribution is of a complicated pattern (Fig. 4.12), it does clearly indicate that boulders with different A-axis orientation intersect with each other at several points and that some groups of imbricated boulders are made up of elements belonging to both sets.

The figure for the wave energy necessary for the carving out and transportation of the boulders was obtained by plotting the distance of boulders from the coastline, measured orthogonal to the A-axis direction, and in relation to boulder weight.

In general, data are dispersed in an area enveloped by a polynomial function (Fig. 4.13). In detail, boulders transported by waves approaching the coast with N350E direction are in several cases much heavier than those transported by N20E wave trains.

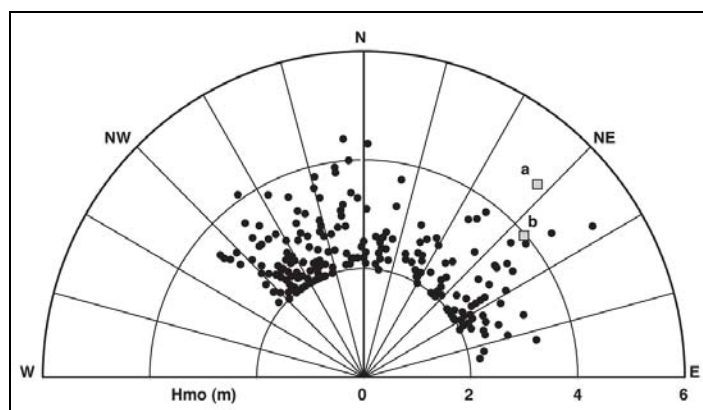


Figure 4.7 - Azimuth distribution of waves higher than 2m recorded since 1990. Grey boxes indicate the storm waves characteristics of 4 January, 2002 (a) and of 12 January, 2003 (b).

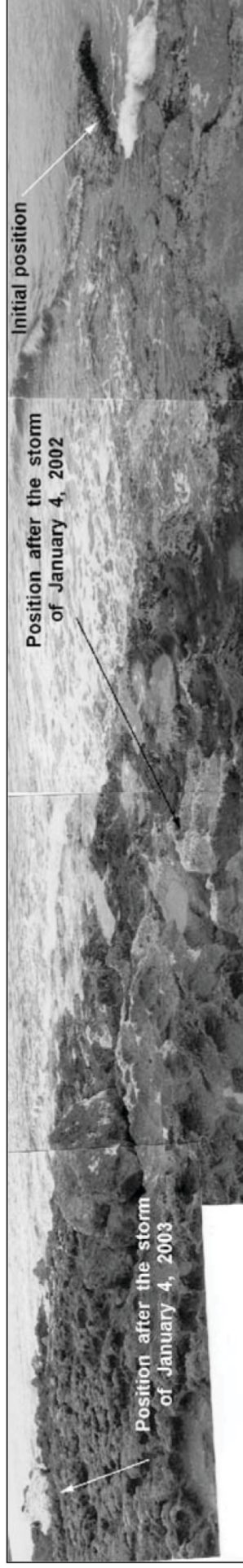


Figure 4.8 - The path of B87 boulder from original position in midlittoral-sublittoral zone (white arrow on the right) to the present position (white arrow on the left); note in foreground the B42 and B43 emblicated boulders hit by B87 and the abrasion of the rocky platform along the path.

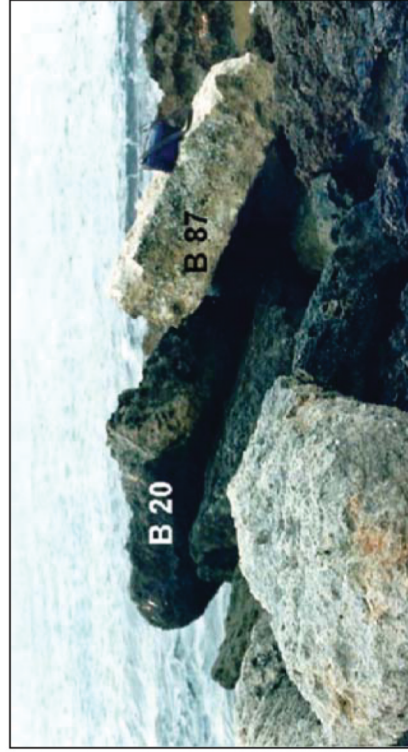


Figure 4.9 - A view of the B87 boulder on B15-16-17-18-19-20 imbricated group.

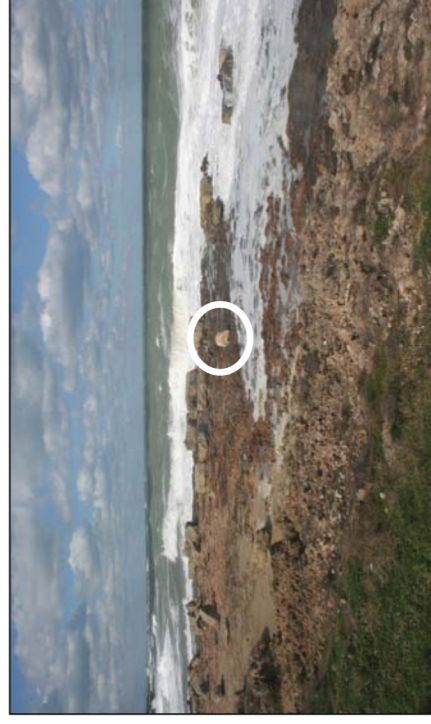


Figure 4.10 - A sea storm of the 8 February 2008 that have moved smaller boulders hanging their position and scattered inland from the adlittoral zone the boulder evidenced by the white circle.

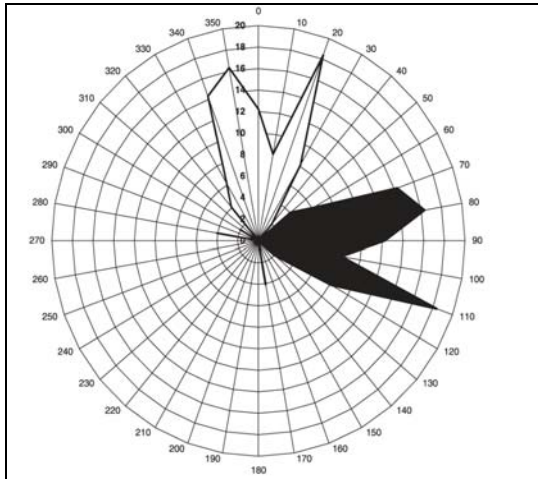


Figure 4.11 - Frequency of A-axis direction at Torre Santa Sabina locality (black) and frequency of approaching waves direction (white).

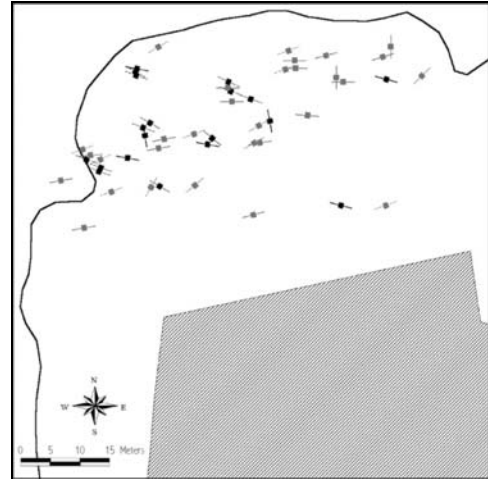


Figure 4.12 - Distribution of A-axis of elongated boulders at Torre Santa Sabina locality. Different colours of symbol outline the two different classes of directions of wave approach.

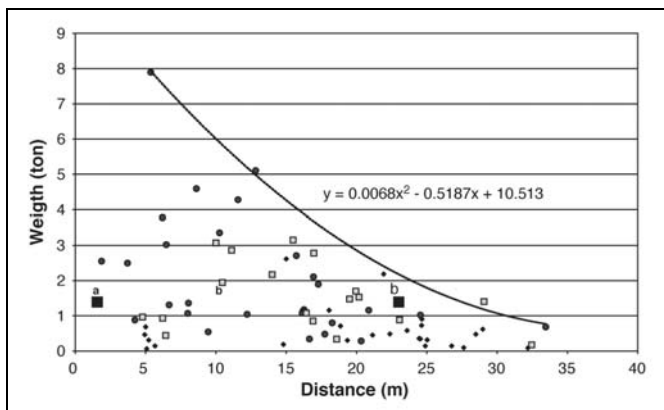


Figure 4.13 - Distance of boulders from the coastline, measured normally to the A-axis direction, in relation to boulder weight; data are dispersed in an area enveloped by a polynomial function. In detail, boulders transported by waves approaching the coast with N350E direction are in several cases much heavier than those transported by N20E wave trains. Legend: circles—elongated boulders with NNW oriented A-axis; gray squares—elongated boulders with NNE oriented A-axis; rhombs—boulders not elongated; black square — (a) position of B87 boulder after the 4 January 2002 storm, (b) position of B87 boulder after the 12 January 2003 storm.

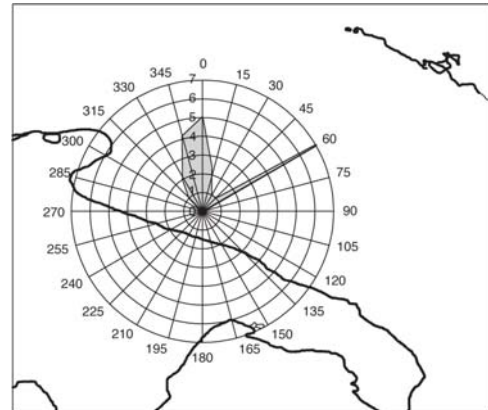


Figure 4.14 - Frequency distribution of highest waves ($H_{mo} > 3.5$ m) recorded at Monopoli buoy (RON - Rete Ondametrica Nazionale) from 1989 to 1999.

4.1.2. Discussions

The detailed survey carried out concerning the occurrence of large boulder accumulations along the Adriatic coast of southern Apulia allows us to define the processes responsible for their formation and to evaluate their significance as indicators of catastrophic waves. In general, the large boulder accumulations studied in our survey share characteristics of others which have been commonly described in other coastal regions of the world. These latter accumulations have often been related to catastrophic waves, but it has generally proven difficult to make any distinction between the action of storm waves and that of tsunami.

The detailed topographical survey of boulder accumulations placed along the Adriatic coast of southern Apulia reveals an interesting pattern in the A-axis orientation of the boulders. Elongated boulders show their major axis orthogonal to two directions, N350E and N20E (with a greater dispersion around the first direction), which can be considered as the approach directions of wave trains responsible for these large boulder accumulations. Moreover, the intersection observed between boulders or groups of boulders with differing A-axis orientation would suggest that boulder accumulations are not the result of any single or coupled particular extreme wave events, but that they are more likely to be the product of numerous high-energy wave trains,

coming from the NNW and the NNE. The same wave trains would also have been responsible for the movement of boulders previously carved out and transported during preceding extreme storms or tsunamis.

Furthermore, the relationship established between the relative weight of the boulders and their distance from the coastline indicates that waves approaching the coast from the NNW, may be related to tsunami events, which were much stronger than those arriving from the NNE. The frequency of the highest waves recorded by the Monopoli buoy of Servizio Ondametrico Nazionale during the period 1989–1999 (Inghilesi et al., 2002) (Fig. 4.14), clearly shows that storm waves approached the studied coastal area from two distinct direction, N0E and N60E, with the major dispersion around the first direction. This bimodal distribution is clearly reflected by the A-axis orientation of elongated boulders. The small differences existing between the direction of storm waves and those which can be deduced from the actual orientation of the boulders, could be related to the local effects of wave refraction.

A hydrodynamic approach was adopted by Nott (1997) to determine whether tsunami- or cyclone-generated waves were responsible for the deposition of fields of well-imbricated boulders (up to 290 t in weight) along the coast of Cairns inside the Great Barrier Reef, Australia. The minimum height required by tsunami or breaking waves to render them capable of initiating the transportation of boulders is determined by the means of two equations which take into account the forces necessary to overturn boulders in the surf zone

$$H_w \geq (\rho_s - \rho_w / \rho_w) \cdot 8a / [(a \cdot c / b^2) \cdot C_d + C_l]$$

where H_w is the wave height at breaking point

$$H_t \geq (\rho_s - \rho_w / \rho_w) \cdot 2a / [(a \cdot c / b^2) \cdot C_d + C_l]$$

where H_t is the tsunami wave height and ρ_w the density of water at 1.02 g/ml, ρ_s the density of boulder (in Torre Santa Sabina locality ranging from 1.56 to 1.65 tm^{-3}), C_d the coefficient of drag: 1.2, C_l the coefficient of lift: 0.178, g the gravitational constant, a the A-axis of boulder, b the B-axis of boulder, c the C-axis of boulder.

Applying these proposed equations to the boulders at Torre Santa Sabina, one can calculate a maximum breaking wave height of about 24m and a tsunami height of 1.5m (Tab. 4.2).

In accordance with the equations proposed by Nott (1997), the transportation of boulder B87, detached during the storm which occurred at the beginning of 2002, would imply a breaking wave height of approximately 9.3 m. This value should be compared with that calculated on the basis of the statistics concerning the wave characteristics supplied by the Monopoli buoy in deep water and according to the equation proposed by Sunamura and Horikawa (1974):

$$H_b/H_o = (\tan\beta)^{0.2} \cdot (H_o/L_o)^{-0.25}$$

where H_b is the breaking wave height; H_o the wave height in deep water; β is the slope of sea bottom; L_o the wave length in deep water. A breaking wave height of 7.5m is calculated when taking into account the mean submarine slope of 1.9% in front of Torre Santa Sabina coastal area.

Boulder	A-axis (m)	B-axis (m)	C-axis (m)	Volume (m^3)	Weight (t)	Storm wave height (m)	Tsunami height (m)
B87	2.2	1.3	0.6	0.9	1.4	9.3 (7.5)	—
B24	2.4	1.8	0.5	1.9	3.1	19.5	1.2
B51	2.9	2.4	0.7	4.9	7.9	22.7	1.4
B79	3.3	2.2	0.5	2.6	4.3	23.8	1.5
B78	1.7	2.7	0.6	1.9	3.1	24.1	1.5

Table 4.2 - Largest boulders' size and weight (adopting unit weight = 1.62 tm^{-3}) and tsunami and storm wave heights required to their transport according to Nott (1997) equations. B87 boulder was detached from sublittoral zone and transported by a breaking wave 7.5m high during the storm of 4 January, 2002. During the storm of 12 January 2003 it was transported farther inland for about 20m (Fig. 4.8) and imbricated on a larger boulder (Fig. 4.9).

These computations demonstrate that Nott's equations when applied in the case of Torre Santa Sabina, tend to underestimate the power of storm waves. The very large boulders of Torre Santa Sabina could be transported by wind-generated breakers with a height of about 23m or by a tsunami with a surge 1.5m high. Breaking waves of about 23m height can be produced by deep water waves which should have a significant height of 11m and a peak period of about 22 s. Recent surveys and correlated hydrodynamical condition (Mastronuzzi et al., 2006) suggests that it is very unlikely that waves with such characteristics could be generated in the semi-enclosed Adriatic Sea. Wave data recorded by the Monopoli buoy indicate that the most severe storm during the last ten years was marked by waves with H_{mo} (significant height in deep water) = 5.1m and peak period T_p = 10s with N57E direction. Waves with these characteristics do not produce breaking waves any higher than 8.6 m.

Furthermore, a significant height in deep water of about 6.5 m has been calculated from Monopoli buoy data for storm waves in the southern Apulia area for a return period of 100 years (Corsini et al., 2002). This figure corresponds to a breaking wave height of about 12 m, capable of overturning a boulder weighing about 2.5 t. Taking into account all these considerations, it can be surmised that the detaching and depositing of very large boulders (weight >2.5 t), could be the effect of the runup of unreported tsunami occurred during the last three centuries. However, no tsunami have been reported for the Adriatic coast of southern Apulia in the course of the last five centuries, notwithstanding the fact that numerous tsunami-generative earthquakes have taken place in the southern Adriatic and northern Ionian regions during the last millennium. A sea withdrawal was observed at Brindisi harbour during a strong earthquake which occurred on 20 February, 1743, although there was no inundation following it (Tinti & Maramai, 1996). Perhaps, the lack of historical chronicles concerning these events may be due to the low height of seismic sea waves, as suggested by the Torre Santa Sabina boulders, and to the absence of settlements in these coastal areas until very recent times.

A further enigma is posed by the presence of the stone-walled coastal tower of Santa Sabina. This tower, which was built very close to the coastline during the 16th century, would almost certainly have been affected by a tsunami run-up, and it is likely that news of any damage would be mentioned in the local chronicles.

According to the chronological and morphological data at our disposal, two distinct tsunami may have struck the Adriatic coasts of southern Apulia. The first to take place would be linked to the strong earthquake that struck Ragusa (modern day Dubrovnik) on 6 April 1667. The epicentre of the earthquake, which was accompanied by a destructive tsunami, was located a few kilometers offshore the Dalmatian coast, about 190 km NNE of southern Apulia coast (Guidoboni & Margottini, 1988). The second tsunami most likely was produced by the strong earthquake which hit southern Apulia on 20 February 1743. The areas most severely affected by this earthquake are those at the southeastern border of the studied area, along a strip of land stretching from Taranto to Brindisi which was affected by an “increase of intensity” (Margottini, 1981). The previously mentioned sea withdrawal in the harbour of Brindisi during this earthquake could support the hypothesis of the generation of a tsunami. At present, the epicentre of this earthquake is placed between the Capo Santa Maria di Leuca in Apulia and the island of Corfù also thank to studies performed on evidence of the related tsunami recognised between Otranto and Capo Santa Maria di Leuca (Mastronuzzi et al., 2007).

While bearing in mind all of the uncertain factors cited here above, a model possibly capable of providing an explanation for the formation of large boulders accumulation observed at Torre Santa Sabina could be developed as follows. In an initial phase, boulders would have been carved out during major sea storms, from the midlittoral zone for the most part, capsized and deposited on the seaward limit of the rocky platform.

Unreported tsunami would have been responsible for the detachment of the largest boulders. Further severe storms would have caused the sliding of the same boulders along the even surface of the rocky platform. This latter process would have required less energy than that unleashed in the initial phase, and would have determined the development of “packed” assemblages of boulders made up of rows or group of imbricated elements. This would also account for the particular distribution of the A-axis of elongated boulders, as observed in our survey.

4.1.3. Conclusions

The detailed survey of boulder accumulations occurring along the Adriatic coast of southern Apulia allows some conclusions to be drawn:

(a) the observed large boulder accumulations can be considered as the cumulative effects of several extreme storm wave events superimposed on the earlier effects of one or two tsunami run-up occurrences.

(b) It is highly probable that the largest boulders (more than 2.5 t in weight) were initially carved out and transported to the seaward edge of a rocky platform by tsunami, and then moved again during following extreme sea storms events and accumulated together with storm-generated boulders in a typical assemblage.

(c) Certain particular aspects of boulder accumulations such as imbrication, arrangement in groups or rows, etc., are not distinctive of tsunami run-up, given that these features can also be accounted for by the action of storm waves.

(d) The direction of A-axis of elongated boulders is orthogonal to the direction of their transport, whereas the dipping of imbricated boulders runs parallel to that direction. **(e)** Assuming a sufficient knowledge of local wave climate and tsunami history, the equations proposed by Nott (1997) can be used to identify and single out those boulders transported by storm waves from similar boulders resulting from the action of tsunami.

(f) It is most likely that one or two tsunami have struck the Adriatic coast of southern Apulia in recent centuries. The first tsunami would have been produced by the earthquake of 6 April 1667, which destroyed Ragusa on the Dalmatian coast (modern Dubrovnik).

The second tsunami would have accompanied the strong earthquake that struck southern Apulia on 20 February, 1743.

4.2. The Costa Merlata Area: STOP 2

4.2.1. Anthropogenic vs catastrophic origin of an enigmatic bioclastic deposit

The coastal region stretching from Torre San Leonardo to Torre Guaceto is marked by a staircase of abrasion platforms extended from about 120 m to the present sea-level. It is shaped on the Calcareniti di Gravina formation (D'Alessandro & Iannone, 1982; 1984) except the lowermost surface, placed 2-3 m above sea-level, covered by Late Pleistocene marine terraced sediments ascribed to the MIS 5 (Marsico et al., 2003). The flight of steps is backed, landward, by the Ostuni Scarp which divides the coastal area from the Murge Plateau; the Scarp of Ostuni gradually decreases in height towards the SE, disappearing near Torre Guaceto.

Marine terraces are cut by a hydrographical network composed of short sapping valleys, locally named lame (Mastronuzzi & Sansò, 2002c; 2003). Some of them have their mouth below present sea level producing a very indented coastline that justify the name of this locality: Costa Merlata means “battlemented coast”.



Figure 4.15 – General view of the Costa Merlata deposit.



Figure 4.16 – A detailed view of the deposit; fragment shells are very abundant with a prevalence of *H. reticulata* and *C. vulgatum*.

In the area near the small airport, on the top of a small head high no more than 2 m above present biological sea level, the coast is marked by the presence of a coarse sandy without any antropic settlements composed exclusively by small fragments and/or entire shells of marine molluscs (Figs. 4.15 and 4.16). It is about 0.35 m thick and overlay a 0.20 m thick red soil which cover the calcarenitic basement (Fig. 4.17). Inside the deposit hundred thousands of gastropod – prevailing – and bivalve shells can be found. The most abundant gastropods are represented – in order of prevalence by *Hinia reticulata*, *Columbella rustica*, *Cerithium vulgatum* and *Bittium reticulatum*; well represented are also *Murex brandaris*, *Astraea rugosa*, *Cyclope neritea*, *Conus sp*, *Patella sp*, *Gibbula sp*, and bivalves as *Venus sp*, *Arca sp*, *Mytilus sp*, *Ostrea sp*, *Tellina sp* and rare *Cerastoderma sp*. Shell size ranges from large specimens of *Bittium* and *Ceritium*, frequently up to 5-6 cm long, to the smaller specimens of *Gibbula* no more than 0,5 cm sized. In this area, bioclasts are the largest part of the sediment; entire shells constitute about the 40% of the total. Along the northern perimeter of the little head a coarse sand exclusively composed by shell fragments is recognizable; also in this deposit antropic settlements are absent.

The faunal assemblage suggests a shallow infralittoral environment of brown algae, on hard substrata with limited sandy areas.

Two AMS age determinations were performed on two specimens of *H. reticulata*. They yielded an uncalibrated age of about 3.3 ky BP (Tab. 4.3).

Sample	Lab. Code	Radiocarbon Age (BP)	$\delta^{13}\text{C}$ (‰)	Elevation a.p.m. s.l.
CM1	LTL1785A	3194 ± 50	-1.0 ± 0.2	1.3
CM2	LTL1786A	3573 ± 40	-0.8 ± 0.1	1.3

Table 4.3 - AMS age determinations performed on two specimens of *H. reticulata* sampled in Costa Merlata area. Analyses were performed by CEDAD – Centro di Datazione e Diagnostica, Università del Salento, Lecce.



Figure 4.17 – The section which supplied specimens of *H. reticulata* dated by means of AMS.



Figure 4.18 – The top surface of Costa Merlata deposits retains flints, pottery fragments and bronze nails. The mollusc *C. neritea* (in the center) and large specimens of *H. reticulata* and *C. vulgatum* (on the left) can be recognised.



Figure 4.19 – A detailed view of the deposit's top surface; flints, entire shells, bioclasts and calcarenitic pebbles are easily recognisable.

The uppermost part of the sediment is also characterised by the presence of human artefact fragments represented by flints, pottery and bronze nails (Figs. 4.18 and 4.19).

The archaeological survey supplied sparse, rare lithic industries which can be referred to a Late Pleistocene Palaeo-Epipalaeolithic frequentation. The top surface of the deposit is marked by a circular fireplace print and charcoal fragments (Figs. 4.20 and 4.21). The occurrence near the fireplace of long bronze nails with quadrangular section and of small fragments of historical age suggest that this area was used as a fishermen's camp during working waitings and for water supplying from the nearby still active springs.

The arrangement of shells in the sediment and the occurrence of small-mean size specimens seem to exclude the anthropic selection due to fooding. A good example of an anthropic accumulation of shells had been surveyed at Apani rocks, placet along the Adriatic coast to the east of Torre Guaceto promontory (Fig. 4.22) placed about southeasternward. Here, a Middle Bronze Age fireplace (half of II millennium BC) is marked by the occurrence of large bivalve shells, mostly *Cardium sp.*, along with burned and limed remains of domestic fauna (Figs. 4.23 A and 4.23 B). The presence of shells marked by medium-large and uniform size is a characteristic feature of proto-historical fireplaces since shells for human alimentation were surely selected avoiding small specimens that were only used in particular cases with ornamental purposes.

For example, in the surveyed site numerous specimens of *Cyclope neritea*, a small mollusc living in brackish waters and in the sandy or silty infralittoral, occur (cfr Fig. 4.18). In Agnano site near Ostuni, the headdress of Osuni 1 Grave (Gravettian age, about 24.410 ± 320 B.P. - Gif 9247) (Coppola et al., 2008) was realized with six hundreds of bored *Cyclope neritea*.

Research carried out along the Adriatic coast of Apulia indicate that this bivalve is mostly likely absent in the present coastal environment. On the contrary, numerous specimens of *Cyclope neritea* have been detected at the surveyed site and at Torre Guaceto, impressive site referred to the Bronze Age, so that it was still diffuse during the II millennium BC along the western Adriatic coast of Brindisi (i.e.: Coppola 1977; Coppola & Costantini 1987).

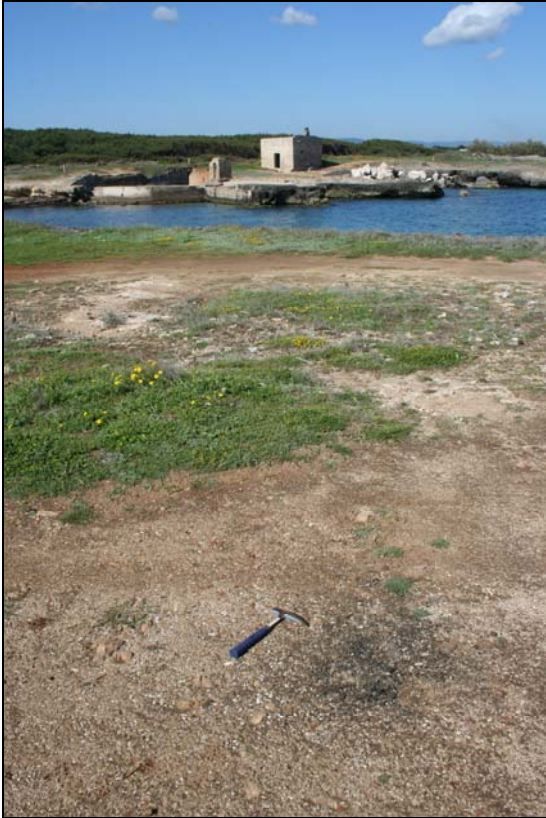


Figure 4.20 – A view of the fireplace remains surveyed on the deposit's top surface.



Figure 4.21 – A particular of the burned fireplace print.



Figure 4.22 – Apani rock: general view of the Bronze Age archaeological fillings and of the room curved in to the calcarenite.

4.2.2. Discussions

At a first look, the general characters of the Costa Merlata deposit could indicate an anthropic origin: shells were accumulated in a “Hidden” by fishermen living here during the Bronze age. However, a number of considerations allow to reconsider this hypothesis.

The first one is that Costa Merlata deposit is composed of a mixture of species of different size from large shells to small ones.



Figure 4.23 – Apani rock: **A.** The Bronze Age fireplace remains put in evidence by wave swash; **B.** A particular of the fossiliferous content.



Figure 4.24 – The present bioclastic sand doesn't cover the gently sloping rocky coast but mark the landward margin of a tiny pocket beach.

This character can derive from the particular type of fishing adopted, may be using carcass; but it does not justify the presence of some – subordinated in quantity – bivalves that don't attach on carcass. Archaeological research at Torre Guaceto suggests that humans preferred to eat mussels from large shells.

Moreover, the northernmost part of the promontory is characterised exclusively by presence of coarse bioclasts suggesting a deposition conditioned by waves rather than anthropic selection.

On the other hand, it is important to highlight that about 3.1 – 3.5 ky BP sea level was about 3-4 meters lowest than present position (Auriemma et al., 2004; 2005) and, consequently, the studied area was more distant from the shoreline than today and about 6 m above related past sea level. It is very difficult that a large quantity of shells was moved onshore by men to perform subsequently a selection of edible specimens.

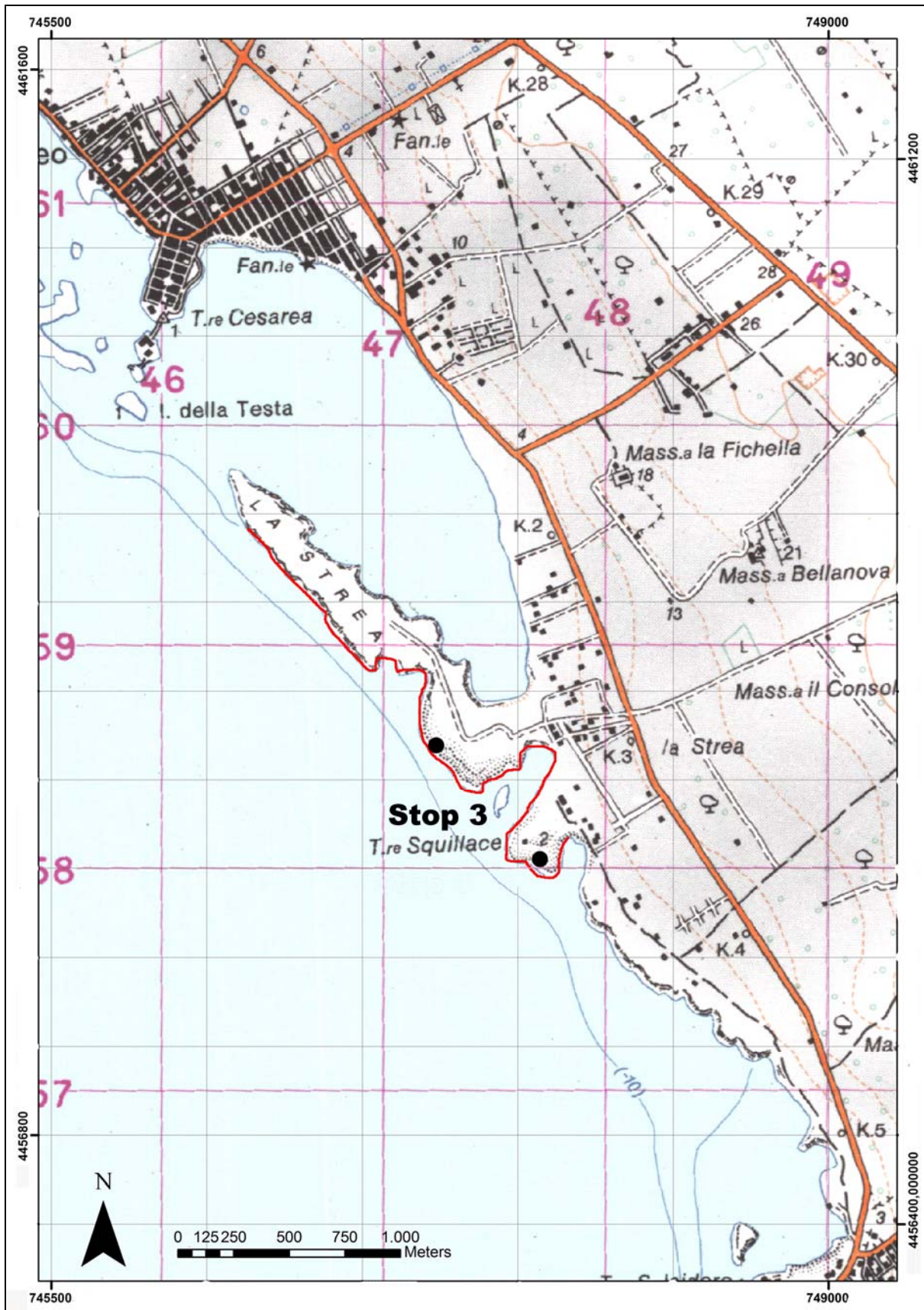
Present storm waves are able to accumulate coarse sands on the foreshore but not on the gently sloping rocky coasts. (Fig. 4.24).

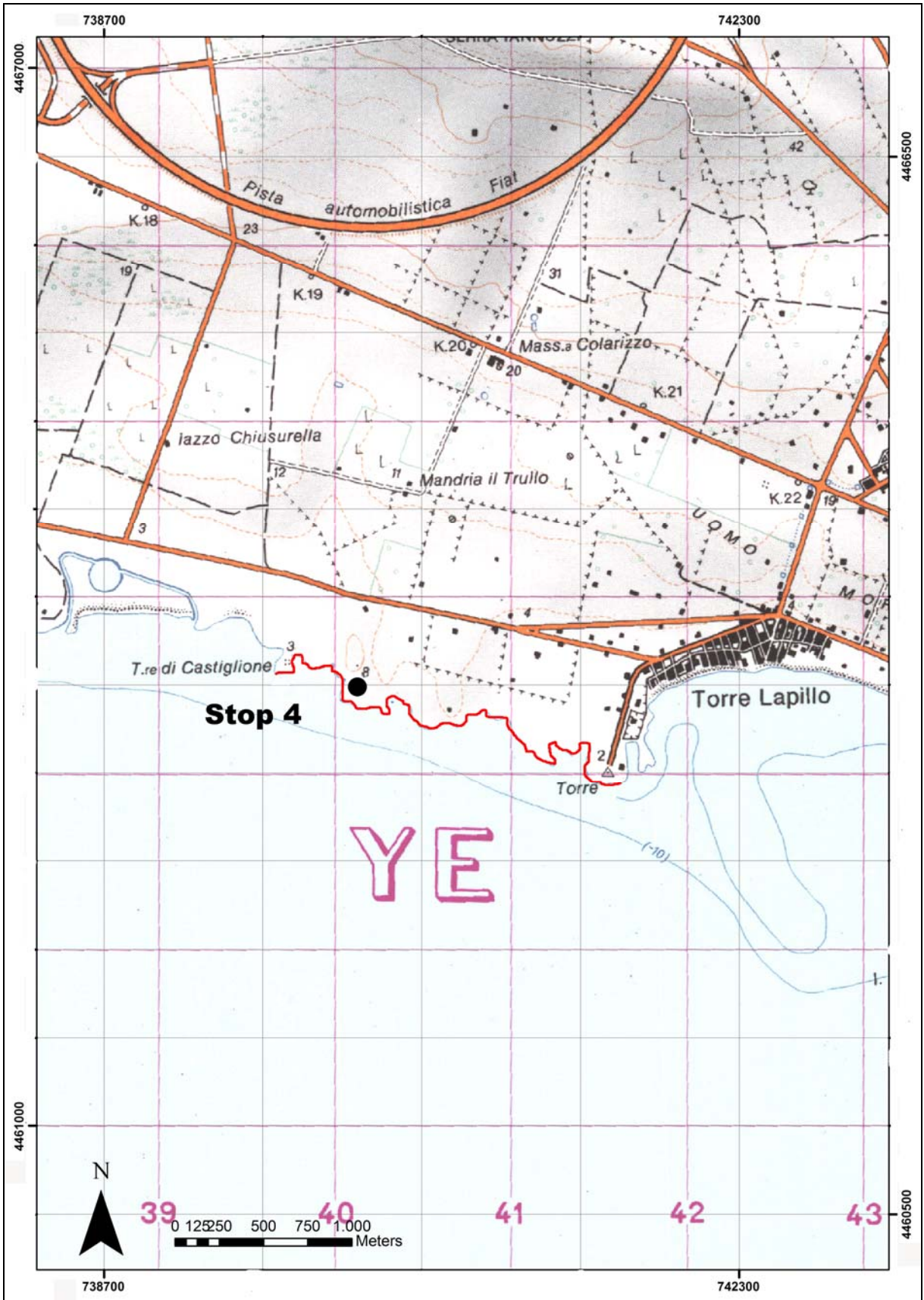
Finally, according to Vött et al (2006; 2008) a large tsunami struck the northern coast of the Ionian Islands about 3100 years BP.

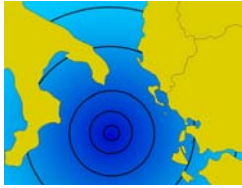
4.2.3. Conclusions

The collated data set suggests that the Costa Merlata deposit formed about 3300 years BP due to natural processes that were able to move hundred thousands of shells from the infralittoral area up to about six meters above past sea level. The archaeological analysis of coeval fireplaces at Torre Guaceto area allows an anthropic origin to be excluded. Present storm waves are not able to move onshore a large number of shells so that the Costa Merlata deposit could be the effect of catastrophic wave, may be connected to the Ionian Island tsunami occurred about 3.3 ky BP.

SECOND DAY
24 September 2008







CHAPTER 5	The Western Coast of Salento peninsula <i>Mastronuzzi G., Pignatelli C., Sansò P.</i>
----------------------------	-------------------------------------------------------------------------------------------------

5.1. The coast Between Taranto and Santa Maria di Leuca

Along the western coast of Apulia, several tracts of gently sloping rocky coasts are characterized by large boulders, up to 80 t in weight, scattered some meters above m.s.l.. (Fig. 5.1). Boulder accumulations have been recognized in several localities along the Ionian coast, generally where gently sloping rocky coasts are shaped on seaward dipping, stratified, jointed calcareous sandstones, since these conditions favour the detachment of rock slabs (Mastronuzzi & Sansò, 2000; Mastronuzzi et al., 2006).

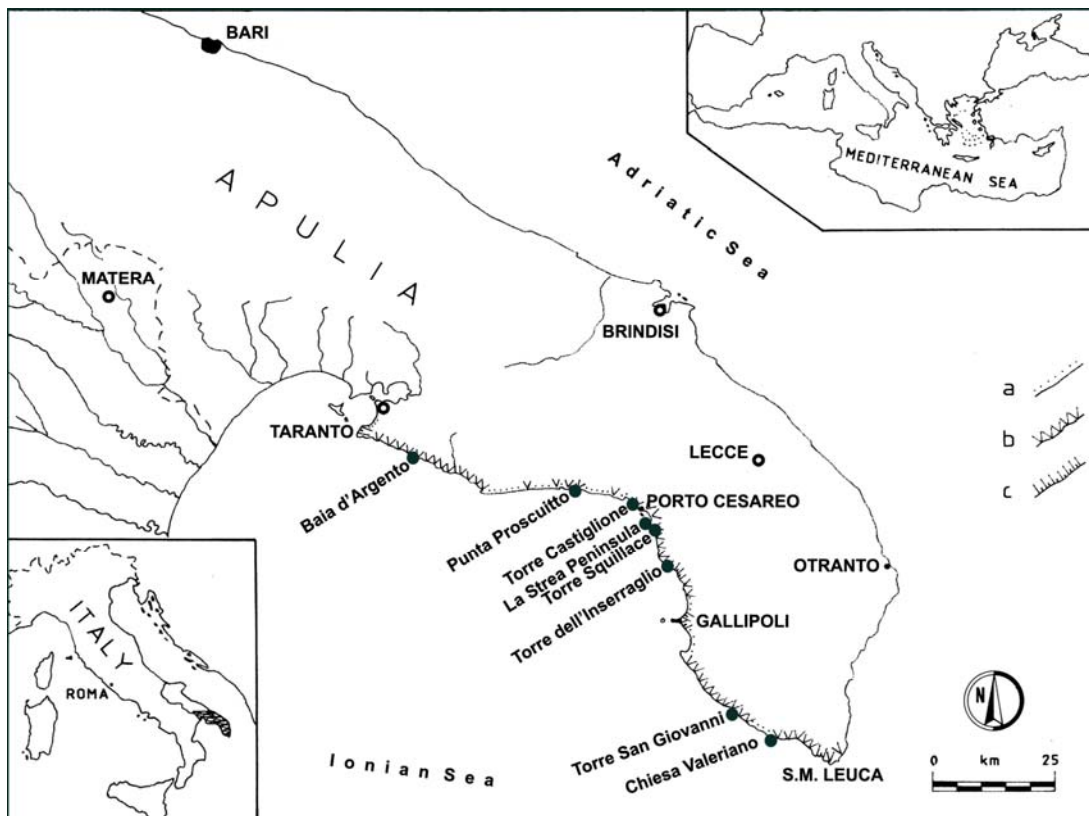


Figure 5.1 - Geographical position of studied area. The main morphological types of coasts are reported: (a) beaches; (b) gently sloping and convex rocky coasts; and (c) cliffs.

These last ones, in fact, were ripped generally from the lower part of the spray zone, as testified by solution features on their surface. More seldom, boulders were transported from below sea level as indicated by *Vermetus* encrustations, *Bryozoa* colonies and *Lithophaga* shells which affect their surface. Mega-boulders are sparse as for example in Torre Squillace locality where they are associated to soil strip areas and/or coarse sandy berms; more frequently they are arranged in field locally associated to sandy berms or abrasional surfaces (i.e. Torre Inserraglio (Fig. 5.2) and Torre Castiglione localities) or in well defined berms (Baia d'Argento locality).



Figure 5.2 – The hundred of boulders of Mesozoic limestone that constitute the boulders field of Torre Inserraglio (Le).

5.1.1. The deposit of Torre Squillace: STOP 3

In Torre Squillace locality, boulders lay directly on a bare rocky surface placed at about 2 m above m.s.l. and bordered seaward by a ramp sloping about 15%. Small karstic landforms, shaped on the sub-aerially exposed calcareous sandstones are represented mainly by potholes, which became increasingly deeper and wider toward the coastline. In the spray zone potholes are coalescent, giving place to pinnacle-like forms (*Spitzkarren*) separated by wide, flat depressions.

The boulders are generally represented by calcareous sandstone slabs ranging in size from 1x0.85x0.5 to 6.0x2.6x1.6 m³. Their volume ranges from less than 1 to 25 m³ and considering a specific weight of 2.35 g/m³, values less than 1 up to about 60 t in weight can be calculated (Fig. 5.3).

Boulders were ripped along strata and joints planes, generally from the lowest part of the ramp, very close to sea level. This evidence is pointed out by wide, relict solution potholes occurring on the upper surface of the biggest boulders. Similar features are at present forming only in the lowest part of the spray zone. The flat bottom of potholes is usually tilted landward by about 12-40° indicating that at least the biggest boulders slid on the rocky platform during the transport. Recent, sub-horizontal, smaller solution potholes, about 20 cm deep and 40 cm wide, developed after boulder transportation (Figs. 5.4 and 5.5).

The largest boulder, which broke during transport in four pieces (boulders 10, 11, 12 and 13), was about 80 t in weight and slid for about 40 m from the m.s.l. to about 1.8 m above sea level (Fig. 5.6). Since most of boulders are elongated, a detailed survey of their long axis orientation and distribution was carried out (Fig. 5.7).

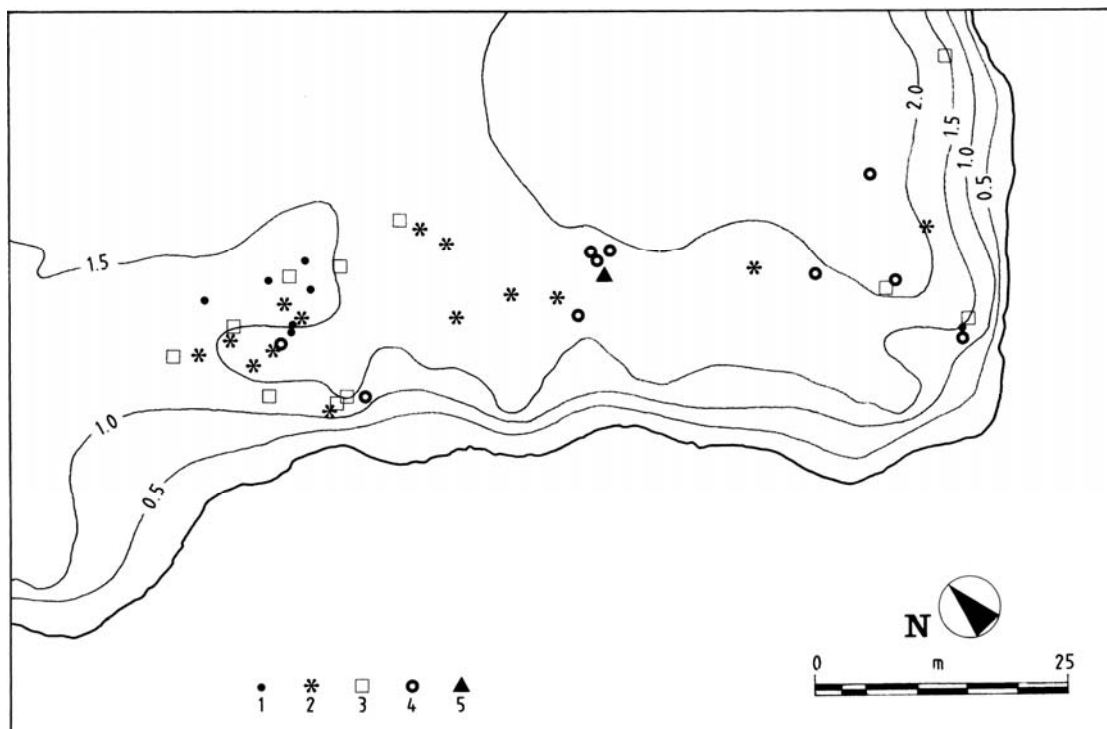


Figure 5.3 - Distribution of boulders on the rocky platform of Torre Squillace. Boulder weight classes: (1) $x < 1$ ton; (2) $1 < x < 2$ tons; (3) $2 < x < 5$ tons; (4) $5 < x < 20$ tons; and (5) $x > 20$ tons.

Results clearly show that elongated boulders rotated during transport, disposing their long axis tangent to the run-up fans induced by a single wave train approaching the NW-SE oriented coast (in this tract) from the South.

Two localities, Chiesa Valeriano (near Torre San Giovanni) and Punta Prosciutto (near Torre Colimena) are, in particular, characterized by a great number of boulders arranged in N-S oriented rows of imbricated elements (Fig. 5.8). The imbrication axis distribution is the same for these two localities and suggests that boulder quarrying and transport were produced by a single, catastrophic wave train approaching the coast from the South.



Figure 5.4 - Boulder no. 10. The tilted at potholes occurring on boulder surface suggest that boulder no. 10 was ripped by the seaward edge of the Torre Squillace platform and slid for about 40 m landward. New sub-horizontal solution features developed after the catastrophic event.



Figure 5.5 - T.S. Giovanni locality. Sub-horizontal solution pan formed after the catastrophic event on an embriated boulder inside a former, tilted pothole.



Figure 5.6 - The largest boulder broke during transport in four pieces (boulders 10, 11, 12 and 13). It is about 80 tons in weight and transported for about 40 m from the m.s.l. to about 1.8 m above sea level. In the background, Torre Squillace, built during the XV century.

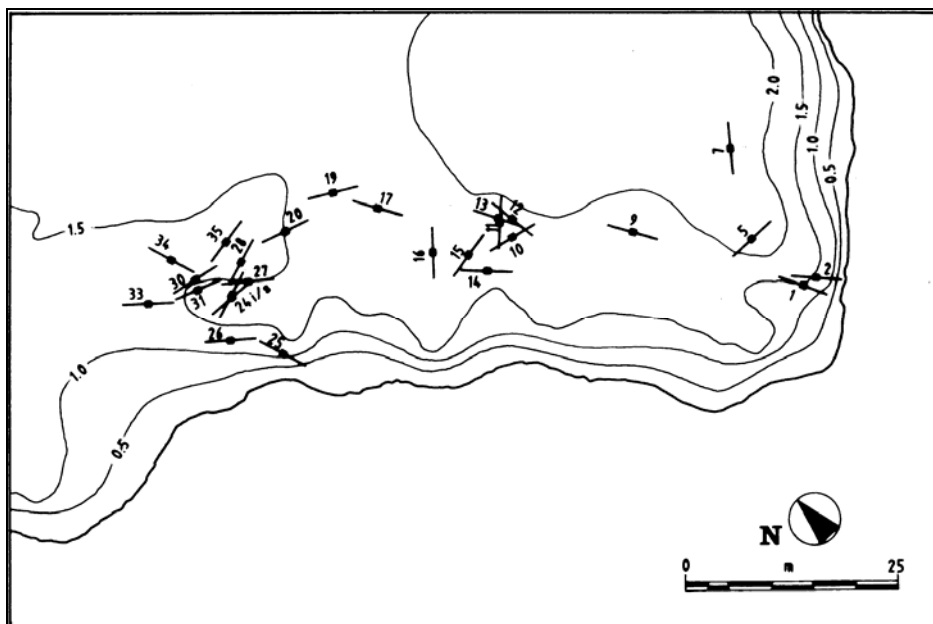


Figure 5.7 - Long axis orientation of elongated boulders on the rocky platform of Torre Squillace. The resulting pattern shows that elongated boulders rotated during transport disposing their long axis tangent to the run-up fans responsible for their deposition.

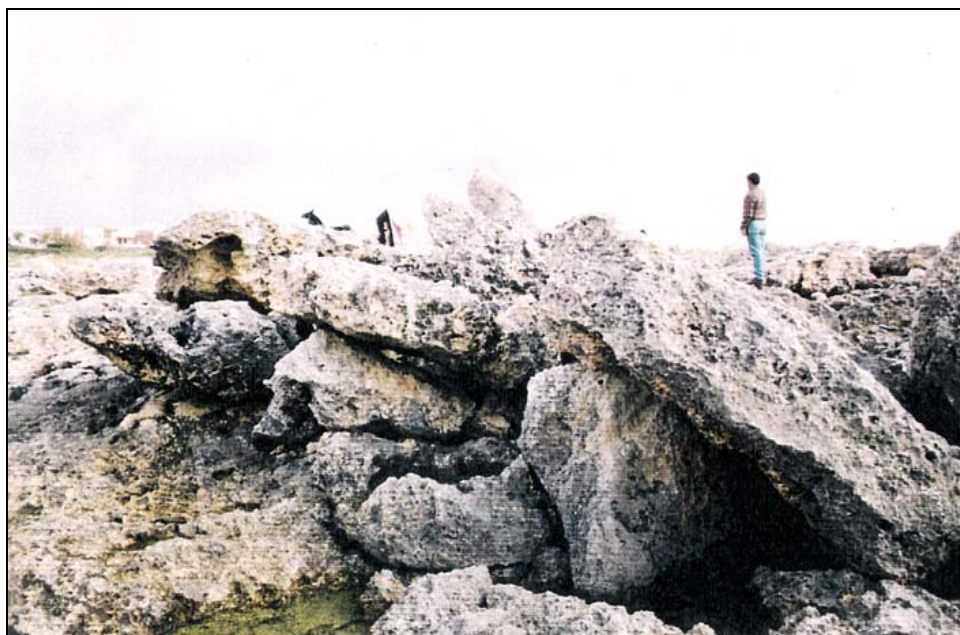


Figure 5.8 - N-S trending rows of imbricated boulders characterize some coastal tracts near Torre San Giovanni (Chiesa Valeriano locality).

5.1.2. The La Strea Peninsula

No far from Torre Squillace, few hundred meters northwestern to the biggest boulder, the La Strea Peninsula define the southernmost part of the Porto Cesareo bay. The peninsula is made by bioclastic calcarenites Late Pleistocene in age locally fractured and overlying the Mesozoic limestone local basement. The calcarenite top rarely exceed the 2 m above present sea level and is covered by a reddish-brown dark soil up to 1.0 m thick. All along the seaside the peninsula is characterised by an important swash zone on which present storm determine the abrasion of the calcarenite (Fig. 5.9); this area is about 40 m wide. It is limited landward by a 1.0 m cliff shaped on the soil. Locally the limit is represented by a bioclastic coarse sandy berm about 1.0 m thick partly

covered by discontinuous psammophile colonisation. It overlay directly the calcarenite and is characterised by the presence of frequent remains of *Columbella rustica*, *Patella* sp., *Conus* sp., *Arca* sp. and other mollusc fragments (Fig. 5.10).



Figure 5.9 - The vegetated berm placed at the beginning of the La Strea peninsula; in the background Torre Squillace is recognisable.

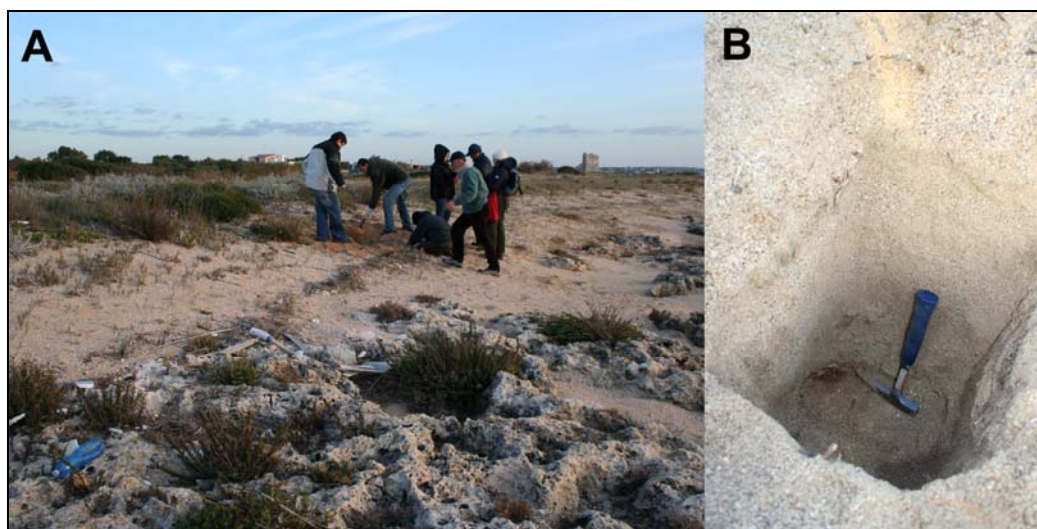


Figure 5.10 - **A**) Place of the coring of the sandy berm at La Strea Peninsula; **B**) The about 0.70 m of the corer, *Columbella rustica* samples have been collected from the deepest part of the hole.

5.1.3. Discussions

Boulder accumulations recognized and studied along the Ionian coast of Apulia formed clearly during one or more catastrophic events that occurred in recent times. However, the remarkably limited range of long axis and imbrication axis distributions suggests that boulder quarrying and transportation was produced by a single, catastrophic wave train, most likely a tsunami, approaching the coast from the South.

Morphological and historical data allow us to define the period in which this catastrophic event should have occurred. Moreover, horizontal solution features developed on boulder surfaces implied a not very recent age for

this event. On the other hand, the numerous coastal towers built all along this coast during the XV century have never experienced such a destructive event.

More precise age data have been obtained from rare boulders carved from below sea level and transported inland. At the Punta Prosciutto locality, one of them shows on the surface encrustations of *Vermetids* and Bryozoa colonies as well as very diffuse boreholes and shells of *Lithophaga*. Radiocarbon age determinations were performed both on a *Bryozoa* specimen and *Lithophaga* shells. An AMS radiocarbon age determination carried out on the former yielded a modern age (less than 100 years B.P.) which obviously does not fit the collected field data set. Conventional radiocarbon dating performed on *Lithophaga* shells supplied a non-calibrated age of 700±65 years B.P. Age calibration was kindly performed by Paula Reimer, Radiocarbon Lab, Queen's University of Belfast, according to the two measurements of ΔR (i.e. difference between the global mean reservoir age R and the local reservoir age) available for the Mediterranean area. One comes from shells collected in Algeria and dated AD 1954 (Broecker & Olson, 1961). The ΔR value for this sample was determined to be -133±83 years (Stuiver et al., 1986). Value of $\Delta R=149\pm30$ (Facorellis et al., 1998) was produced by determinations on charcoal/shells pairs collected in archaeological sites belonging to the 7th-8th millennium B.C. in the Aegean Sea, this last value of ΔR yielded an age between 1676 and 1878 AD. Not much different is the result adopting a ΔR value of 121±60 as suggested for the Adriatic Sea (1520-1870). In effect, the use of this value should permit to correlate the accumulation of the boulder to the tsunami generated by the strong earthquake occurred on the 24th of April, 1836; this attribution is in contrast with the presence of coastal towers at present very well preserved, and with historical chronicles.

More acceptable results have been obtained adopting the first ΔR value; the calibrated age ranges in this case between 1421 and 1568 A.D. However, historical chronicle studies do not report tsunamis along the coasts of southern Italy during this period (Tinti & Maramai, 1996). Furthermore, about the same calibrated age can be calculated using the ΔR value of -80.0±25.0 years which has been successfully used for the Aegean area by Stiros et al. (1992); in this last case the calibrated age ranges between 1472 and 1633 A.D. Others AMS age determinations have been performed on two shells of *Columbella rustica* sampled in the lowermost level of the sandy berm at the base of La Strea Peninsula. They suggest an age in accord to the available ¹⁴C age obtained for Punta Prosciutto locality. Unlikely, all the ΔR available don't have been obtained for this area: so each calibration is influenced by the ΔR adopted. The uncalibrated ages obtained for these samples seem to be in good agreement to that available (Tab. 5.1), even if the correct age is influenced by the choice of the ΔR value.

ID Sample	Description	$\delta^{13}C$	Radiocarbon Age	Age Uncertainty	ΔR	Calibrated Age	σ	2σ
Punta Prosciutto	<i>Lithophaga</i>	0,5‰	700	± 65 ¹⁴ C	121±60	1650 AD:1851 AD	1	
					121±60	1565 AD:1954 AD*	1	
					-133±83	1421 AD:1568 AD	1	
					149±30	1680 AD: 1854 AD	1	
					149±30	1647 AD: 1951 AD*	1	
					-80±25	1472 AD:1633 AD	1	
La Strea Peninsula BPS 1/A	<i>Columbella rustica</i>	-2,7‰	721	± 35 ¹⁴ C	121±60	1643 AD:1819 AD	1	
					121±60	1543 AD:1896 AD	0,99	
					121±60	1938 AD:1950 AD*	0,011	
La Strea Peninsula BPS 1/B	<i>Columbella rustica</i>	0,8‰	761	± 45 ¹⁴ C	121±60	1545 AD:1724 AD	0,96	
					121±60	1790 AD:1801 AD	0,03	
					121±60	1497 AD:1865 AD	1	

Table 5.1 - The AMS radiocarbon determination of some samples collected in Torre Squillace area. The calibrated ages have been obtained using Calib 5.01 software (Stuiver et al., 2005). Ranges marked with a (*) are suspect due to impingement on the end of the calibration data set.

Anyway, the strong attenuation of seismic sea waves in the Mediterranean (Soloviev, 1990) does not allow us to refer the examined catastrophic event recorded along the southern Apulia coasts with one of the numerous tsunamis which occurred in the same period along the Hellenic, Israeli and Lebanon coasts (Antonopoulos, 1979). However, Blandamura (1925) reports that the medieval village of Il Casale, placed at Punta Lo Scanno on the Cheradi islands, just few tens of kilometres to the north of the investigated area, was destroyed by an earthquake and flooded by high sea waves. This event occurred most likely during the very strong earthquake which hit southern Italy on December 5th, 1456 (Boschi et al., 1997; Marzo et al., 1998).

5.1.4. Conclusions

Boulder accumulations and the sandy berm of La Strea peninsula recognized along the Ionian coasts of southern Apulia could be the effects of a tsunami, which approached the coast from the South. Probably, it was generated by a submarine landslide, induced by the strong earthquake occurred on the December 5th, 1456. The recognition of this recent catastrophic event fills in part the lack of tsunami historical reports for this particular coastal area, which was deserted during the Middle Ages because of the occurrence of coastal swamps and the diffusion of malaria. Unfortunately, the growing urbanization of the coastal area poses new and alarming questions to coastal managers regarding the prevention and mitigation of the potential destructive effects of future, possible tsunamis in this region.

5.2. The Torre Castiglione coast: STOP 4

Torre Castiglione is a medieval tower facing the Gulf of Taranto, placed between Punta Prosciutto and Porto Cesareo localities (Fig. 5.11). The coastal landscape is marked by a staircase of abrasion platforms which have been recognized both above and below the present sea level.

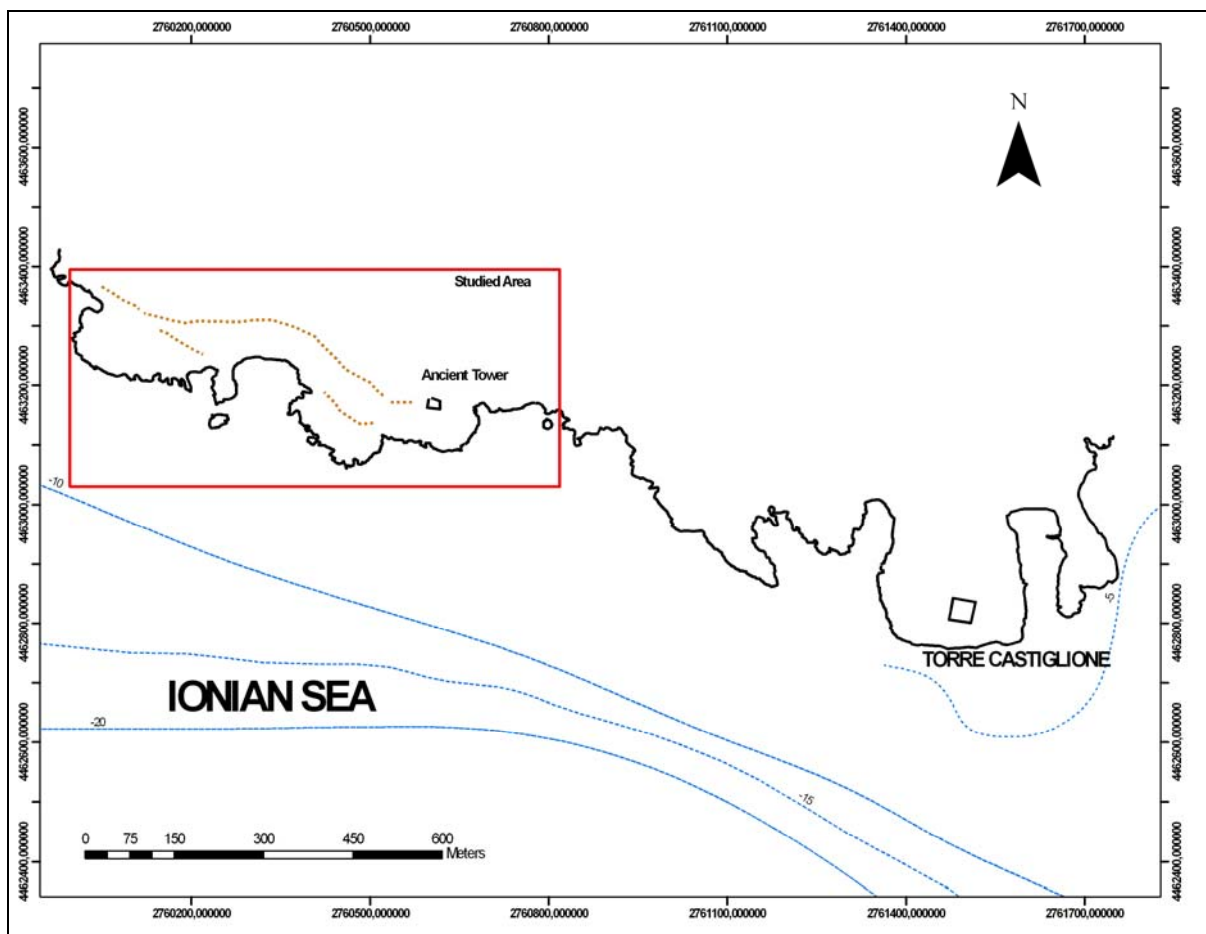


Figure 5.11 – Topographic and bathymetric sketch of Torre Castiglione area.

The submerged part of the coastal slope is marked by two discontinuous platforms, placed between 5 and 10 m of water depth. The emerged part is a gently sloping coast shaped on Pleistocene algal and bioclastic calcarenites, locally fractured, which constitute a marine terraced deposit referred to the last Interglacial period (MIS 5) (i.e.: Belluomini et al., 2002). They overlay the Mesozoic limestone of the local basement. In the inlet near the remains of the ancient tower the present shore platform reaches a width of 30-100 m; The heads that individuate the inlet are constituted by a gently sloping rocky coast elevated up to 3-10 m a.s.l. This indented area is characterised by a very intense corrosion that has produced extremely well developed potholes fringed by sharp ridges. These landforms can be put in relation to marine spray, leading to typical coastal karst phenomena, and to erosive effects of the sea storms along the coastline.

Sea storms erosion is responsible to the formation of soil-stripping zone along the coastline variously extended from coastline to landward; soil and sand stripping often affects Mid-Holocene dune system.

5.2.1. The deposits of Torre Castiglione

This coastal area is characterised by the presence of several morphological evidence of the impact of catastrophic waves. These imprints are concentrated along two promontory, separated by two small inlets on the west side of the Torre Castiglione (Fig. 5.11).

Here, the coast is represented by a very flat surface studded of calcarenite boulders, weighting up to 75 tons (Fig. 5.12); they are placed at about 45 m inland and between 3 and 5 m a.s.l..

Some boulders are covered by biogenic encrustations (*Vermetids*) and show morphological features (karstic pools, exposed joint surfaces) suggesting that they were detached and scattered from the mid-supralittoral zone. Biggest boulders are oriented in 300°-330° N direction and placed at the same distance from the coastline about 35 m (Fig. 5.13); other boulders are embriicated in groups of more elements and/or arranged in a ridge very close to adlittoral zone (Fig. 5.14). The boulders deposit ends inland at a distance of 80 m from the coastline; some small boulders often border seaward a sandy berm runnin about parallel to the coastline.



Figure 5.12 – The biggest boulders 3.2x2.8x1.8m placed at about 35 m inland of Torre Castiglione coastline.



Figure 5.13 – Isolated boulders with approx. same weight are aligned at about 35 m from coastline.

In the area at the foot of the ancient tower, boulders are arranged in a field marked by the presence of a continuous deposits of bioclastic sands, partially vegetated by psammophile and alophile plants (Fig. 5.15).

In the area placed to the west of the inlet, the coast is composed by a platform about 40 m wide up to 1.5 m above present mean sea level (Fig. 5.16). It is bordered landward by a well defined berm made by coarse bioclastic sands partially vegetated by psammophile and alophile assemblage (Fig. 5.17). The berm partially cover boulders scattered inland, occasionally embriacated or accumulated in rows.



Figure 5.14 – Field of embriacated boulders in the inlet westward of ancient tower near Torre Castiglione.



Figure 5.15 – The coarse bioclastic sandy berm and the boulders that constitute the vegetated berm at the foot of ancient tower near Torre Castiglione (in background).



Figure 5.16 – A recent detached boulder put in place in the adlittoral zone by sea storm action near the coastline of Torre Castiglione area.



Figure 5.17 – The partially vegetated berm constituted by coarse bioclastic sand and boulders placed to the west of the ancient tower near Torre Castiglione.

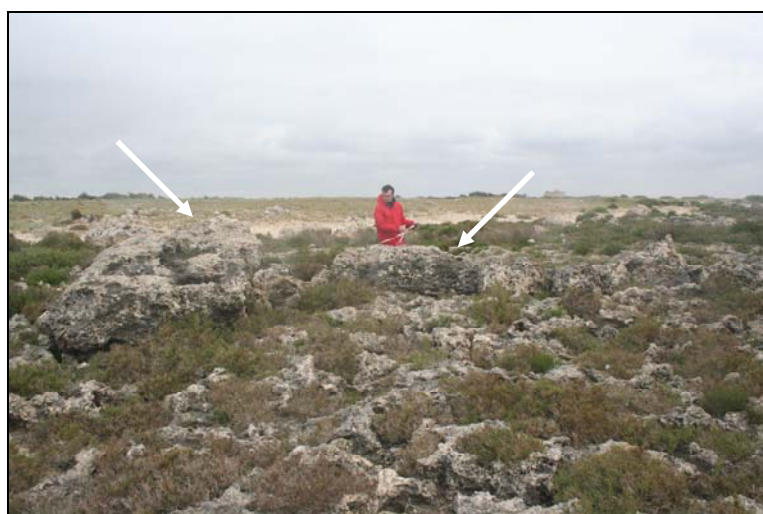


Figure 5.18 - Torre Castiglione locality: the boulders on which *Vermetids* samples TC1 and TC2 were collected.

5.2.2. Discussions

Vermetids encrusting the surface of sparse boulders (Fig. 5.18) have been sampled and dated by means of AMS technique. Samples were collected from two different boulders placed at about 30 m from the coastline at about 1 m above present sea level (Tab. 5.2).

ID Sample	Description	$\delta^{13}\text{C}$	Radiocarbon Age	Age Uncertainty	ΔR	Calibrated Age	σ	2σ
Torre Castiglione TC1	Vermetids	0,5‰	1242	$\pm 40 \text{ }^{14}\text{C}$	121±60	1202 AD:1331 AD	1	
						1126 AD:1412 AD		
Torre Castiglione TC2	Vermetids	1,9‰	608	$\pm 40 \text{ }^{14}\text{C}$	121±60	1764 AD:1785 AD	0,11	
						1804 AD:1950 AD*		0,89
						1697 AD:1951 AD*		1

Table 5.2 – The AMS radiocarbon determination of some samples collected in Torre Castiglione area. The calibrated ages have been obtained using Calib 5.01 software (Stuiver et al., 2005).

The obtained ages don't fit with previous analyses performed on bioencrustations sampled in nearby areas (i.e.: Punta Prosciutto and La Strea near this locality or Baia d'Argento some km to the north) (cfr. Tab. 5.1).

On the other hand, the data set available for this locality and the hydrodynamical consideration performed by Mastronuzzi et al. (2006) on the base of the Nott's equations (2006) exclude the possibility that boulders were scattered inland by extreme storm waves. In fact, eye witness indicate that storm waves inundate a belt about 20 m wide from the coastline as clearly indicated by the distribution of tar spots.

5.2.3. Conclusions

The collated data suggest that the coast in the surrounding of Torre Castiglione has been affected by the action of extreme waves. The huge size of boulders and hydrodynamic considerations would indicate the action of a tsunami.

The age obtained by AMS analysis on Vermetids collected on the surface of two sparse boulders indicate that the catastrophic event responsible for boulders carving, transportation and deposition at Torre Castiglione occur during the last millennium. However, further research is needed to refer this event to one of the tsunamis that historically struck the coasts of Ionian Salento and whose effects have been already detected along some other coastal tracts.

5.3. The Baia d'Argento (Silver Bay): STOP 5

Baia d'Argento is located on the Ionian side of Apulia, 20 Km south to Taranto (Fig. 5.19). The coastal area is characterized by a number of stair-case arranged marine terraces, stretching from an elevation of about 400 m toward to mean sea level (m.s.l.) results of the superimposition of regional uplift and of the glacio-eustatic sea level changes occurred from Middle Pleistocene to onward (Doglioni et al., 1994).

The area is marked by deep inlet corresponding to riverine erosive incision produced during the last glacial time with a sea level about 140/150 m lower than present (Mastronuzzi & Sansò, 1998; Lambeck et al., 2004).

Along the coastline the upper part of the Middle-Late Pleistocene sequence outcrops; it is synthetically represented by silty-clay capped by transgressive algal well cemented calcarenites (Belluomini et al., 2002 and references therein). The bay is limited by two rocky headlands shaped on this algal calcarenite.

The eastern one is characterized by a slightly undulating surface with a mean sloping of about 6-7%. (Fig. 5.20) that has maximum elevations of 11 m above biological sea level (a.b.s.l.).

Starting from coastline it is possible to divide them in three different zone: **1** – a terrace surface about 20 m wide; **2** – a boulder ridge leaning on a step placed between 2 and 5 meters (a.s.l.); **3** – a steeper terrace that reach the top approx 11 m (a.b.s.l.) (Fig. 5.21).

The lowernmost terrace is bare of vegetation, is quite flat and bordered seaward by a trottoir approx 3 m wide that marks the biological sea level (sensu Lalorel & Laborel Deguen, 1994) and a surf bench marked by rockpools. Adlitoral zone is characterised by a elevate roughness and a convex profile. Here, the micro-topography surface shows small karstic landforms, shaped on the sub-aerially exposed calcarenites and represented mainly by potholes, which became increasingly deeper and wider toward the coastline.

In the spray zone potholes are coalescent, giving place to pinnacle-like forms (*Spitzkarren*) separated by wide, flat depressions. Calcarenite bedrock presents very long fractures that become wider toward to the coastline. Several of these fractures are parallel to shoreline; some of these are also oriented to SE in relation with more frequent sea storm direction.

The analysis of the structural features of the rocks has evidenced the main orientation of the fractures: the first one is oriented on 142-190° N and the second one on 270-300° N (Fig. 5.22).

From this articulated surface numerous boulders have been carved and scattered inland; in fact isolated boulders are placed on this zone often not in equilibrium or imbricated in small groups. This seems to indicate the strong exposure to Ionian storm waves.

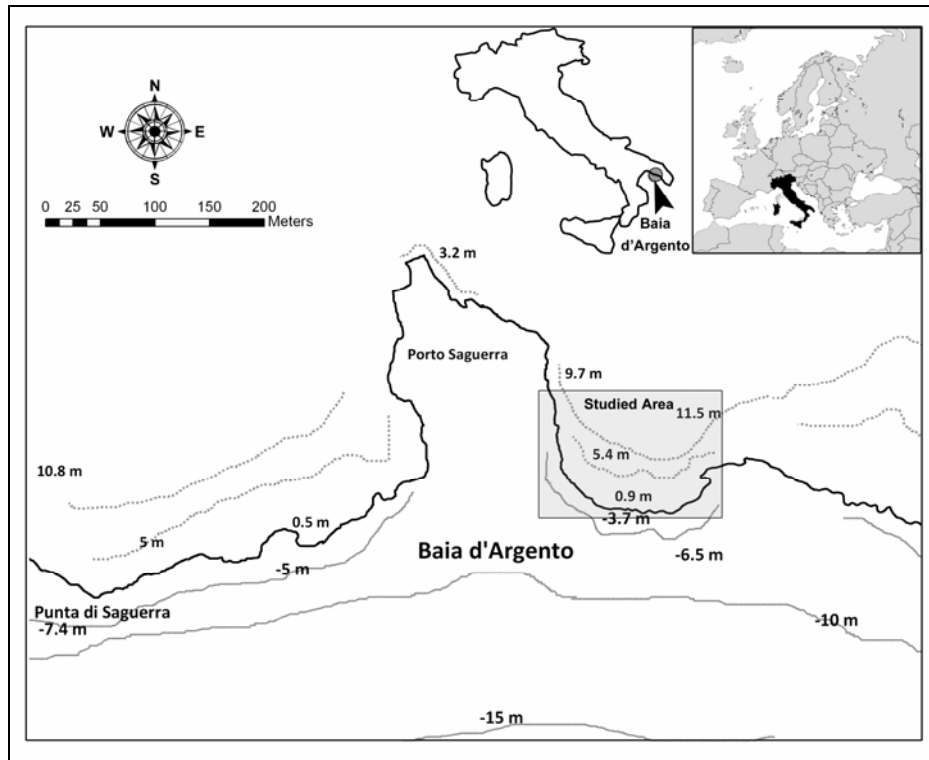


Figure 5.19 – Topographic and bathymetric sketch of the Baia d'Argento area.

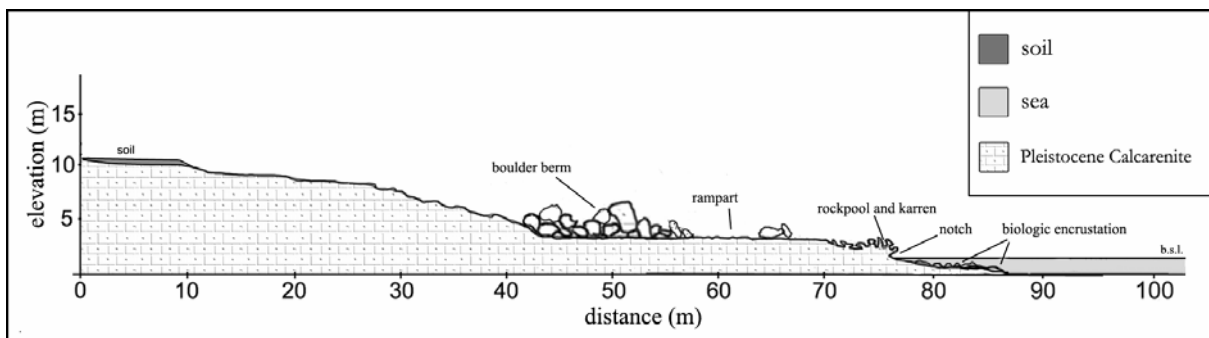


Figure 5.20 – Morphological profile of the studied area.

The second zone, about 100 m long, shows a boulders ridge that seems parallel to the present coastline at a distance ranging from 25 to 45 m.; the ridge leans on a low step shaped on the algal calcarenite. Boulders are generally constituted by algal calcarenite of various size between 1,5x0,4x0,8 m to 3,7x3,1x1,2m, adopting a specific weight of 2,2 g/m³; the mega-clasts volume ranges from about 2 to 30 tons. The biggest boulder is at 27 m inland at about 5 m above b.s.l. Most of the boulders have been carved out from an area close to the supratidal zone, as can be ascertained from the presence of wide, flat rock pools and of died barnacles on their surface. Often these boulders are overturned; due to the tilting rock pools have been subsequently modified by new, horizontal solution pools formed because of karstic processes. Moreover, some boulders were carved out from the mid-sublittoral zone, as confirmed by the presence of biogenic encrustations (*Vermetid sp.*). These well

preserved concretions indicate a very recent age of formation and limited reworking during the transport from the sublittoral to the adlittoral zone.

A DGPS survey has been performed in order to obtain the position of each boulders and to define the coastline (Fig. 5.23). Moreover, a morphological analysis has been performed by means of detailed topographical surveys, to define boulders volumes, imbrication and an axis azimuth. Both boulders spatial distribution and a-axis orientation seem indicate the inundation pattern and/or the behaviour of a catastrophic wave (Fig. 5.23).

The bedrock between the seaward surface and the boulders ridges, is marked by erosional s-forms similar to *sichelwanne* (Kor et al., 1991; Shaw, 1994; Bryant & Young 1996; Bryant, 2001). *Sichelwannen* can be described as smooth and polished surfaces, engraved by high energy plastic flow where the outcropping rock is not very resistant (Fig. 5.24); in general, the high pressure of the mixture water-debris due to catastrophic wave inundation, cause striation, channel mark, etc, on rocky promontory.



Figure 5.21 – The boulders berm of the Baia d’Argento area.

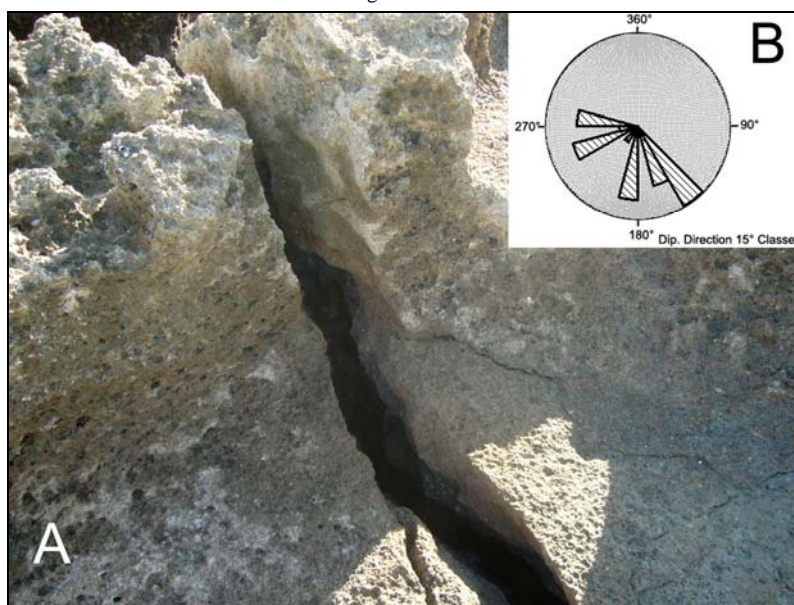


Figure 5.22 – A) A view of bedrock fracture near the coastline of Baia d’Argento. B) Polar diagram of main fracture analysed in the same area.

Supposing an extreme wave approaching perpendicular to coastline, *sichelwannen* could be classified as upslope form; in the studied area *sichelwannen* forms are placed at about 30-35 m landward and bound the base of the first step of the promontory at about 3 m (a.s.l.). Here, an undulating and smooth surface without soil coverage is developed from coastline to top of step where boulder deposit is arranged; these could be significant evidences of the impact of a tsunami (Kelletat & Schellmann, 2002, Whelan & Kelletat, 2003).

The third zone is a steeper terrace (about 7%) showing little rest of soil jointly to first halophyte vegetation; these pioneer plants live in the spray zone and are here represented essentially by *Salicornia* sp..

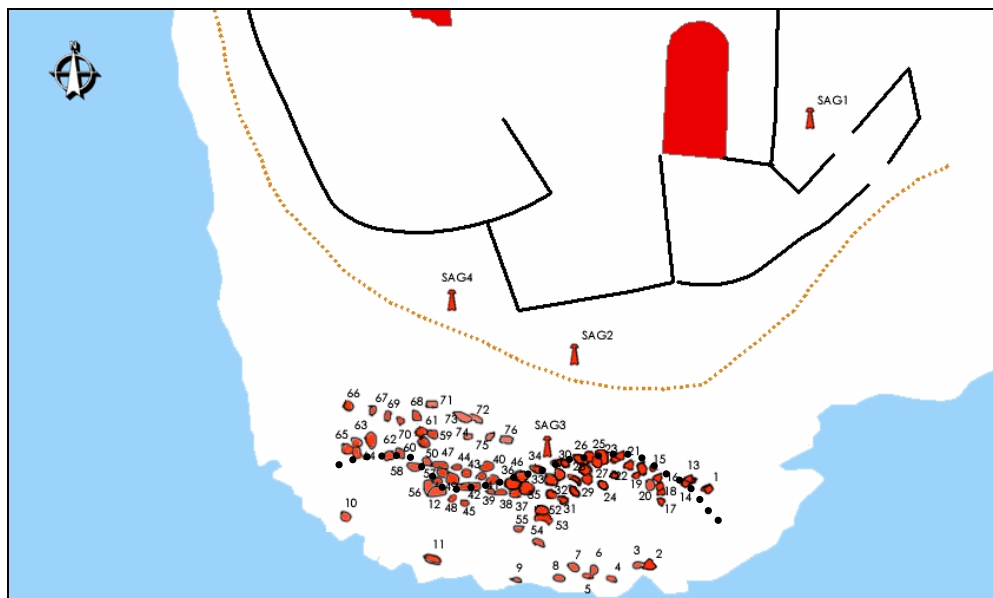


Figure 5.23 – Distribution of the boulders berm in Baia d'Argento locality measured with DGPS surveys. Grey dotted line shows the probable wave train direction responsible for the accumulation.

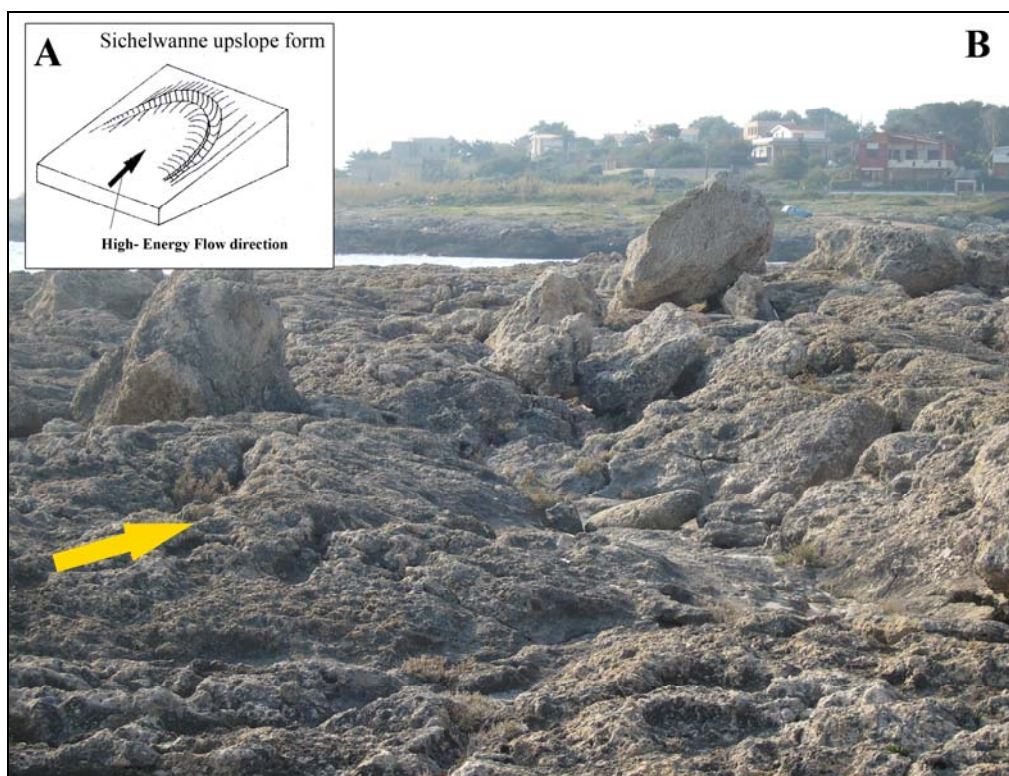


Figure 5.24 – An high energy erosional form recognised in Baia d'Argento locality. **A.** *Sichelwanne* upslope form described by Bryant (2001); **B.** Like-*sichelwanne* form near boulders berm in the studied area.

5.3.1. Discussions

The boulders that constitute the Baia d'Argento ridge are up to 30 tons heavy and are placed at a distance comprises between 25 and 45 m from the coastline. The disarticulation of the boulders and their transport inland was possible since the presence of horizontal (transgression surface and stratification in the calcarenite) and vertical discontinuities in the calcarenite body that wrote a rectangular pattern. These features seem indicate the "joint bounded boulders" scenario described by Nott (1997; 2003). Starting from the hydrodynamic equations suggested by Nott (2003) for tsunami and storm wave approaches, and applying these formulas to the biggest boulder recognizable in the ridge it is possible to characterize the minimum wave able to move it landward. So, to initiate the transport of the boulder 30 tons heavy, a storm wave of about 16,61 m high or a tsunami of about 4,15 m high was necessary. A storm wave with such characteristics is very unlikely in the Gulf of Taranto. In fact, here, the Crotona buoy, activated by RON – Rete Ondametrica Nazionale and RMN – Rete Mareografica nazionale, indicate in 6.2 m the maximum storm wave recorded in deep sea. Moreover applying the Gumbel treatment to available recorded data (1990 to 2006), a return time of 50 year for the maximum wave height of 7.01 m is obtained. Moreover, very important indications coming from the analysis of the bathymetry in front of the promontory - about - 5 m - jointly to the estimation of the bottom slope; experimental studies have been demonstrated that waves break if the ratio between wave height at breaking point and water depth, H_b/W_d , is approx 0.71–0.78 (Keulegan & Patterson, 1940). For a horizontal bottom, this ratio is smaller (0.44–0.6, Massel, 1997), while steeper bottom slopes show ratios ranging from 0.78 and 1.03 (Galvin, 1972). Assuming horizontal the bottom in front of Baia d'Argento, a storm wave of about 16,61 m has the breaking point at about 9 m depth. Considering the distance from this isobaths and the coastline (about 40 m) it is really hard to affirm that the wave responsible of the detachment and transport of the biggest boulder could be a sea storm wave. Besides, main boulders a-axis azimuth distribution of Baia d'Argento berm doesn't correspond completely to the approaching directions of the wave trains generated by known sea storms (Fig. 5.25); this seems to indicate a mixed depositional origin (sea-storm and tsunami) of the boulders, but this can be considered reliable for boulders that have weight lower than 1,5-2,5 tons (Mastronuzzi et al., 2006) (Tab. 5.3).

Baia d'Argento	Main Boulder	a-axis (m)	b-axis (m)	c-axis (m)	Weight (t)	Storm Wave height (m)	Tsunami height (m)
ps= 2,2 g/cm ³	BA01	3,00	1,10	0,70	4,967	19,55	4,89
	BA02	4,10	3,30	0,90	26,181	26,72	6,68
	BA04	3,30	1,63	0,87	10,061	21,51	5,38
	BA16	3,40	1,60	1,07	12,515	22,16	5,54
	BA35	3,70	3,10	1,20	29,593	24,11	6,03
	BA43	1,20	1,12	0,60	1,734	7,82	1,96
	BA55	0,90	0,64	0,60	0,743	5,87	1,47
	BA72	1,36	1,10	0,26	0,836	8,86	2,22

Table 5.3 – Features of more representative boulders from Baia d'Argento; they have been chosen in function of their weight, a-axis orientation, elevation and distance from the coastline. The wave heights able to move the largest boulders, compared to the return times of the maximum wave, suggests that the more probable wave able to move them is that of a tsunami.

Therefore, the estimated wave heights are indicative for possible impacting tsunami; it could well justify the detachment, the transport and the accumulation of entire berm.

On the other hand, the impact of catastrophic waves along this side of Apulia was reported in different time. The first one can be ascribed to the chronicle written by Tommaso Nicolo D'Aquino (XVII century) "... si ravvisano sopra di esse alcuni ruderi di antiche abitazioni: anzi dall'angolo dell'isola Maggiore, volto a ponente, si scorge a mar tranquillo nel fondo un aggesto di sprofondato edificio, e dicesi da' vecchi pescatori il Casale, da' quali si vuole che ivi anticamente fusse un villaggio, svelto già per forza d'un tremuoto da quel continente ed ingoiato dall'onde ... " (Carducci, 1771). This report just permitted to confirm geochronological data obtained from biogenic encrustations on boulders recognised in the southernmost part of the Apulia, near Torre Squillace (cfr. STOP 3 and STOP 4); the tsunami that hit this area was generated by a submarine landslide activated by the strong earthquakes occurred on the December 5th, 1456 (Mastronuzzi & Sansò, 2000).

The second report can be recognised in the chronicle written by Baffi (1929) "...dopo una primavera molto piovosa ed un'orribile tempesta accaduta il 17 aprile 1836 nel golfo tarentino seguirono pochi giorni sereni fino al 24 Aprile 1836 ... Verso mezzanotte dell'istesso giorno gli animali mostrarono soverchia inquietudine, il mare divenne grosso e tempestoso e sopra di esso fa' vista una meteora di color fuoco, in quel punto accompagnato da cupo rumore un terremoto durò 20 secondi e dopo 3 minuti replicò violentemente... ".

The results of the AMS age determinations performed on Baia d'Argento are well in agreement between them (Tab. 5.4).

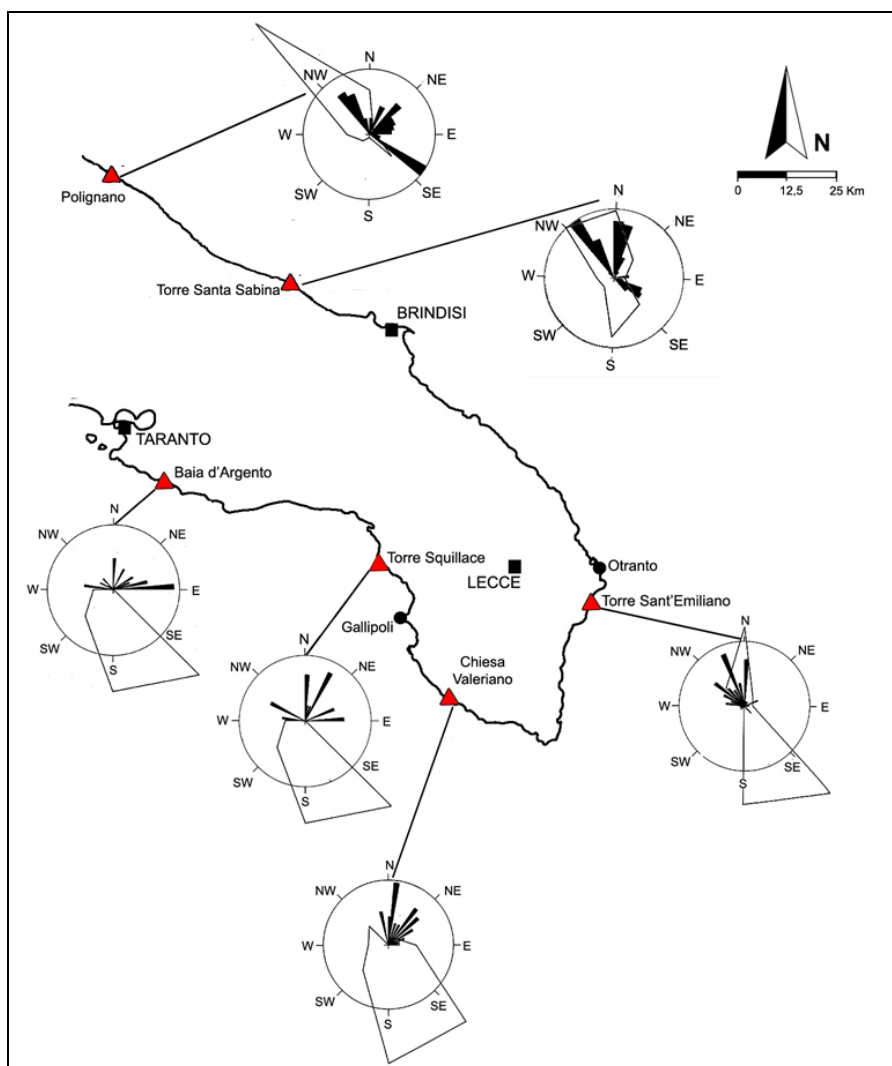


Figure 5.25 – Distribution of a-axis in relation to the extreme storm approach directions in the studied localities of Apulia.

ID Sample	Description	$\delta^{13}\text{C}$	Radiocarbon Age	Age Uncertainty	ΔR	Calibrated Age	σ	2σ
Baia d'Argento LTL1178A	Vermetids	0,5‰	413	± 40 ^{14}C	121 \pm 60	1889 AD:1947 AD	0,11	
					121 \pm 60	1813 AD:1955 AD*		1
Baia d'Argento LTL1179A	Vermetids	1,3‰	489	± 60 ^{14}C	121 \pm 60	1853 AD:1952 AD*		1
					121 \pm 60	1801 AD:1953 AD*		0,064
					121 \pm 60	1702 AD:1951 AD		0,904
Baia d'Argento LTL2209A	Vermetids	0,4‰	426	± 35 ^{14}C	121 \pm 60	1888 AD: 1954 AD*		1
					121 \pm 60	1811 AD: 1954 AD*		1

Table 5.4 -The AMS radiocarbon determination of some samples collected in Baia d'Argento. The calibrated ages have been obtained using Calib 5.01 software (Stuiver at al., 2005).

DAY	YEAR	ZONE	LOCALITIES	GEOGRAPHICAL COORDINATES		Earthquake Intensity (Mercalli Scale)	Tsunami Intensity (Ambraseys-Sieberg Scale)
				Lat	Long		
8 March	1832	Ionian Calabria	Crotone	39,00	17,00	10	3
24 April	1836	Ionian Calabria	Crosia, Marina di S., Angelo, Cropalati, Corigliano, Calopezzati Marina, Rossano, Golfo di Taranto	36,60	16,60	9	4
23 October	1907	Ionian Calabria	Capo Bruzzano	38,15	16,00	8.5	3

Table 5.5 – Tsunami events occurred in the Taranto Gulf in the 1801-1951 period (from CPTI, 2004; Tinti et al. 2004).

In fact, two ages are quite overlapping; the third one (LTL1179A) shows a little difference compensated by a major error bar. In substance they are very similar and the calibrated ages seem to indicate that one or more catastrophic events occurred in the time spanning from 1801 and 1951 (Tab. 5.3). Unluckily, the limits of the AMS on marine shells are time in time bigger for more recent time. The only data that can confirm radiocarbon ages derive from the Catalogo Parametrico dei Terremoti Italiani (Gruppo di Lavoro CPTI, 2004) and by the tsunami catalogue (Tinti et al., 2004) in which strong tsunami-generative earthquakes occurred on March 8, 1832 in the Crotone area (Central Calabria) and on April 24, 1836 along the coast of Rossano Calabro are reported (Tab. 5.5).

The distinction between the two events is really hard: reconstructed approaching wave direction comes from ESE and epicentres of both earthquakes are placed ESE respect to Punta Saguerra. Surely the 1836 tsunami was strongest (3rd degree of tsunami intensity scale) than 1832 one (2nd degree of tsunami intensity scale) (Gruppo di Lavoro CPTI, 2004). Moreover, this last one was generated by an earthquake which epicentre is more distant from Punta Saguerra.

About a third tsunami that hit the Apulian coast on 1907, few data are available: considering that at this time a lot of anthropic coastal activities were in act, it is so strange that no chronicle of its impact are available. Maybe, along the Ionian Apulian coasts this event was of small entity although it is classified as 3rd degree of tsunami intensity scale (Tinti et al., 2004).

The presence of erosional forms could be an indication of a huge wave like tsunami that impacted the coast promontory with high-energy flow; these landforms have been observed and attributed to the effect of tsunami flooding because plastic flow (water + debris) could take shape (Kor et al., 1991; Shaw, 1994). Only a similar flow can mark considerably the bedrock developing s-form. Moreover, in correspondence of *sichelwanne* a smooth surface without soil and vegetation is present. It could be considered as effect of the karstic solution below the soil cover; the tsunami flooding defined the soil stripping and the *sichelwanne* shaping.

5.3.2. Conclusions

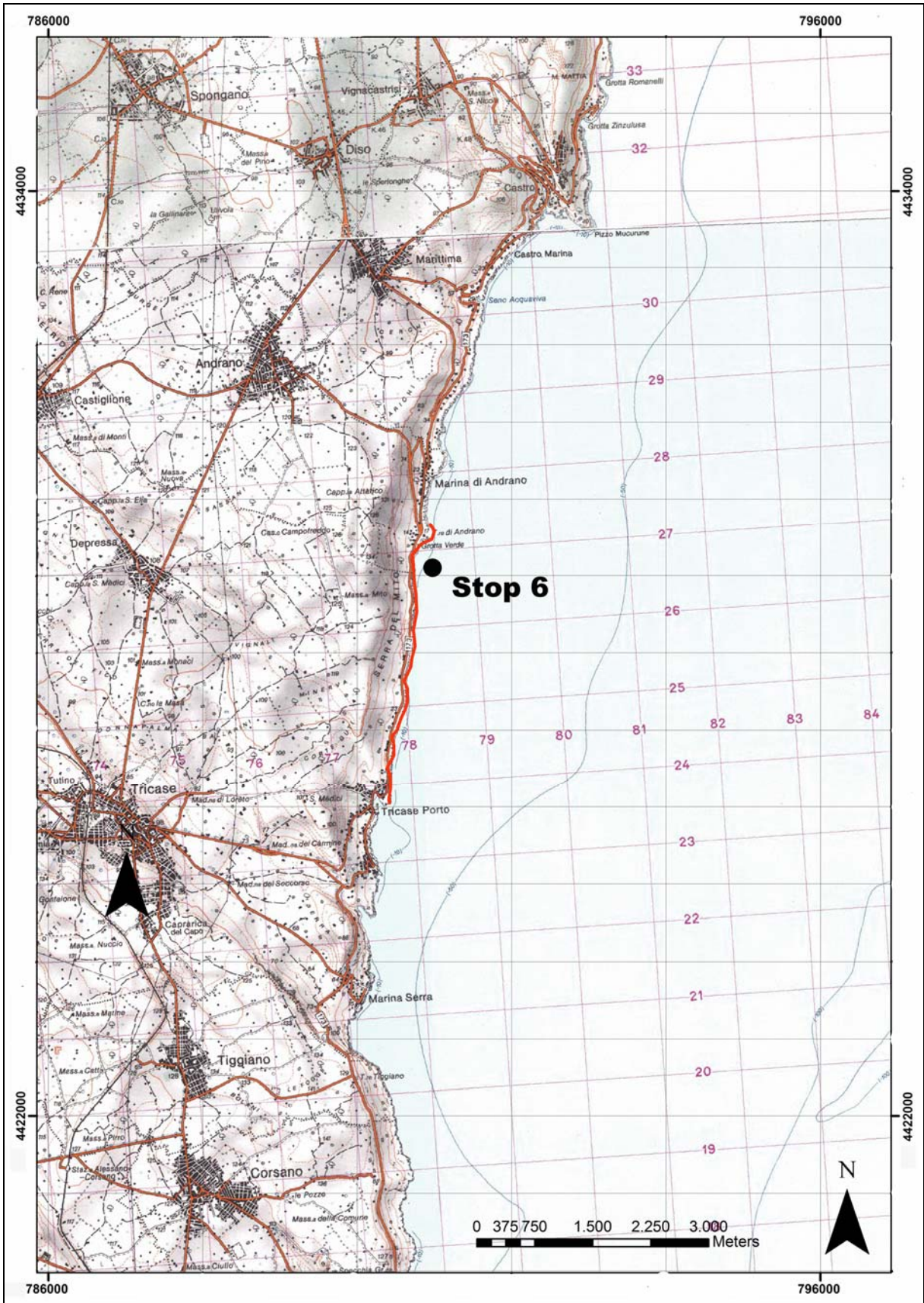
The integration of data derived by geomorphological and topographic surveys with geochronological and hydrodynamical ones permit to obtain an important conclusion about the boulder berm recognizable in Baia d'Argento – Punta Saguerra locality.

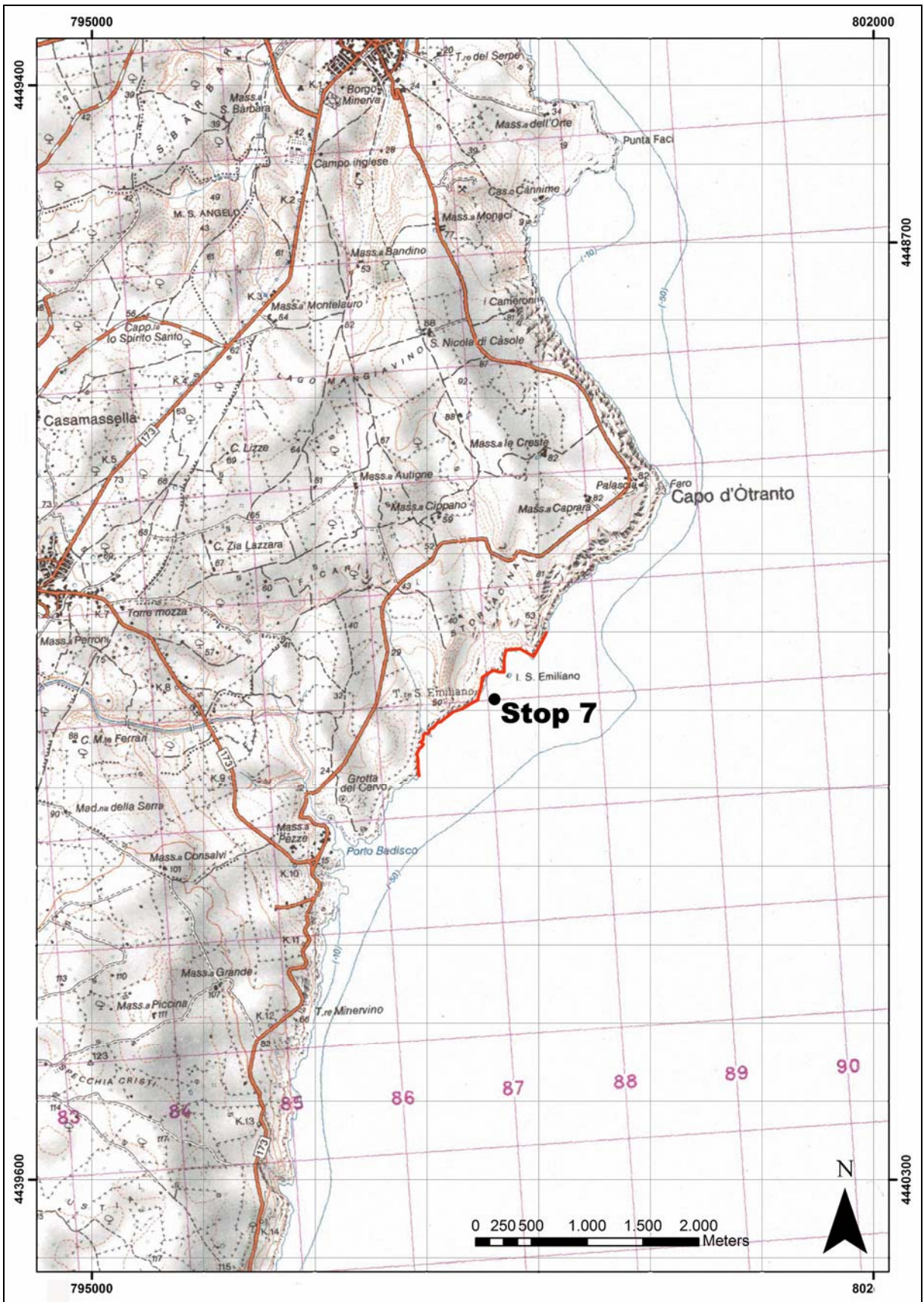
Reassessing and considering all the available data, it is more possible that the boulder berm was put in place by only one tsunami event generated by the earthquakes occurred April 24, 1836 near Rossano in Calabria. It is also possible that this strong event erased pre-existent evidence correlable to the known impact of the 1456 tsunami or to the more recent one dated on 1832.

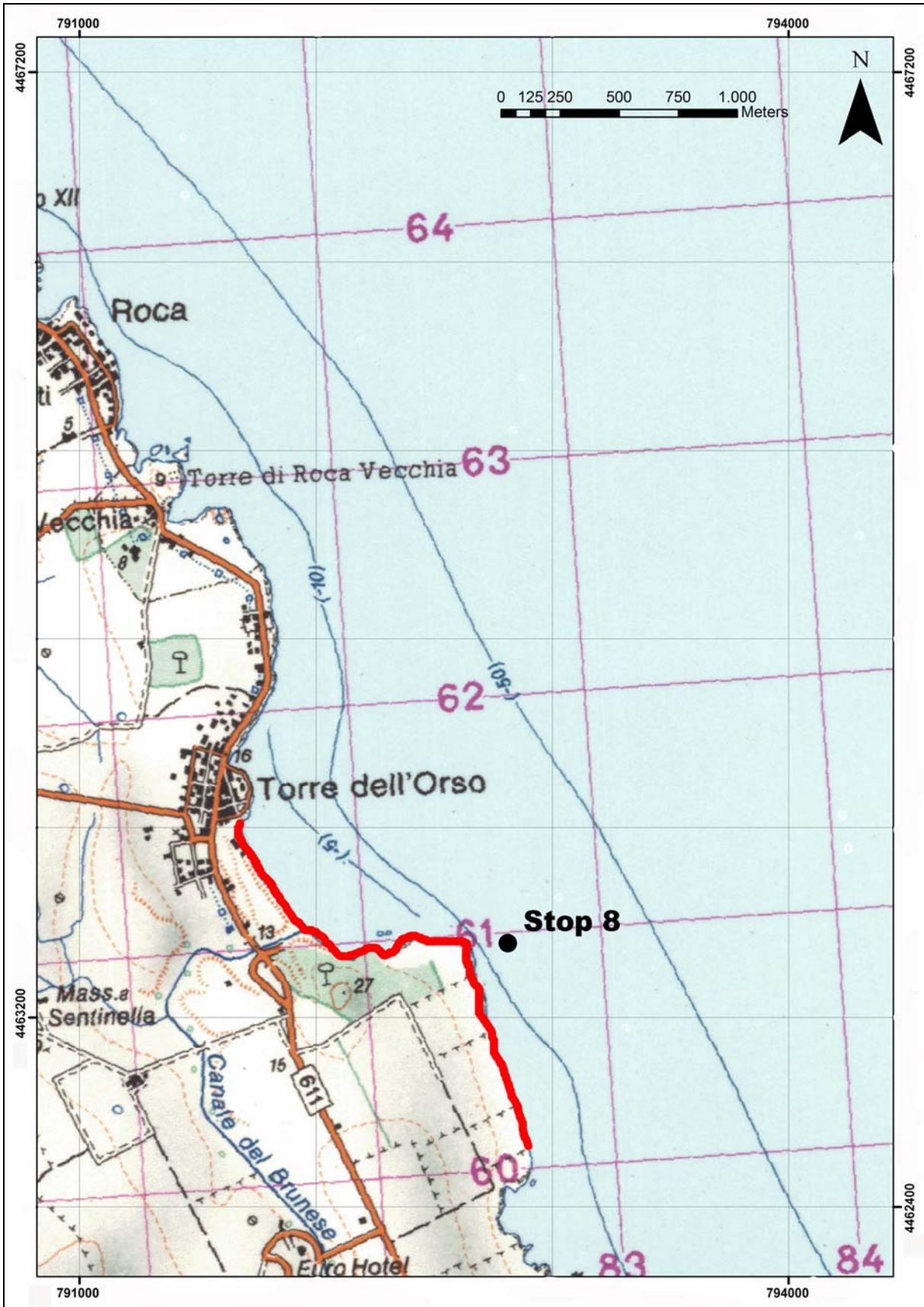
Moreover, it is also possible that more recent high energy flows destroyed and accumulated landward those boulders at present placed near to the coast line. They come generally from the adlittoral area and don't preserve any biological concretions that permit the chronological attribution of the events responsible of their put in place. These morphological features are perfectly compatible with a possible impact of one or more strong storms.

Last conclusion regards the erosional forms: phenomena of strip-soil are well evident at the base of the ridge where rounded smooth-surface deriving from covered karstic phenomena is recognizable. Unluckily it is not possible to evaluate if the stripping can be correlable to the 1907 events or was part of the more energetic 1836 events. The presence of s-shaped forms indicates that the events responsible of all these erosional landforms were really energetic but the chronological attribution of erosive landforms should be matter of debate for the next hundred years, the attribution of the biggest part of the present Punta Saguerra landscape to the April 24, 1836 tsunami is realistic.

THIRD DAY
25 September 2008









2nd International Tsunami Field Symposium

IGCP Project 495

Quaternary Land-Ocean Interactions:
Driving Mechanisms and Coastal Responses

Ostuni (Italy) and Ionian Islands (Greece) 22-28 September 2008



Project 495

CHAPTER 6

The Eastern Coast of Salento peninsula

Mastronuzzi G., Pignatelli C., Sansò P., Selleri G.

6.1. The Santa Maria di Leuca – Otranto coast

Two interesting areas characterized by boulder accumulations have been found along the southeastern Apulian coast, stretching from Otranto to Leuca, at Torre Sasso and Torre Sant’Emiliano locality (Fig. 6.1 A).

The landscape of this coastal area, placed in the southeastern Apulian region, is dominated by a steep slope extending from about 120 m above sea level to about 50 m below sea level. This surface has been generally interpreted by several authors as a high, degraded fault scarp. However, recent studies indicate it as a relict form inherited from pre-Quaternary times (Mastronuzzi et al., 2007). In fact, according to Bosellini & Parente (1995) and Bosellini et al. (1999) this regional slope roughly coincides with the Late Cretaceous margin of the Apulian platform. Along this margin several carbonate systems are laterally disposed and grafted one upon the other. Three of these systems are clinostratified and include well developed reef tracts from the Priabonian, early Chattian and early Messinian age. The cause of this unusual stratigraphic architecture is the relative tectonic stability of the Salento Peninsula that, since the late Cretaceous, has acted as an elevated area in the centre of the Mesozoic wider Apulia carbonate platform.

The coastal slope is affected by a number of normal faults with a NW-SE or NNW-SSE orientation, which in some cases cut Lower Pleistocene deposits (Bosellini et al., 1999), cropping up in some patches along the coast. They point out that the Apulian foreland is affected by several normal faults, some of them presently active since they displaced the sea floor by about 200-300 m (Merlini et al., 2000).



Figure 6.1 A - Geographical position of southern Apulia.

The coastal landscape is marked by a staircase of abrasion platforms which have been recognized both above and below the present sea level. The submerged part of the coastal slope is marked by two discontinuous platforms, placed at about 5 m and between 7 and 10 m of water depth, and by a wide plain stretching offshore below the 20 m depth (Parroni & Silenzi, 1997; Mastronuzzi & Sansò, 2003). The emerged part of the steep coastal slope is marked by five raised abrasion platforms placed between 60 and 50 m and at about 40 m, 20-15 m, 10-6 m and about 2 m above the sea level (Fig. 6.1 B).

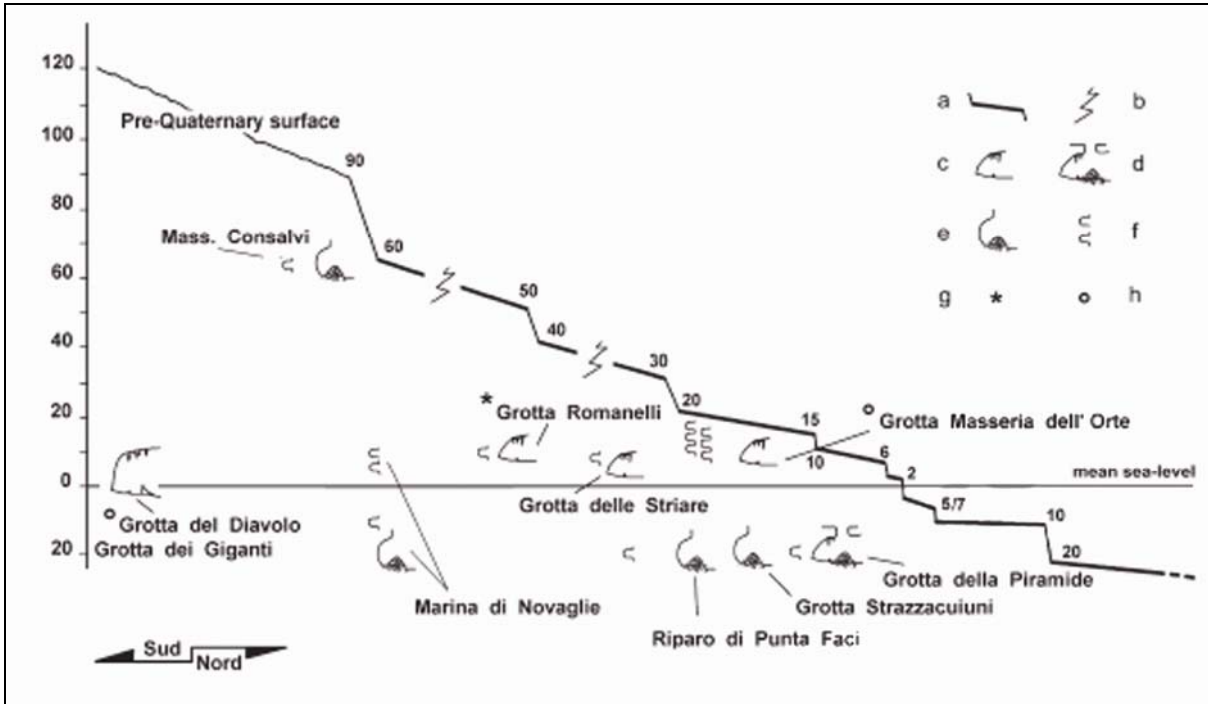


Figure 6.1 B - Schematic reconstruction of marine terraces sequence on the eastern coast of Salento Peninsula; a - marine terraces; b - morphological gap; c - karstic caves; d - karstic caves with collapse sinkhole; e - sea caves; f - notches; g - paleontological data; h - geochronological data.

6.2. Torre Sasso boulder accumulation: STOP 6

A remarkable accumulation of large boulders has been surveyed few kilometers to the north of the Marina di Tricase locality (Fig. 6.1). The accumulation is on a steep slope, which joins the outer margin of a 10 m marine terrace with the present sea level.

Boulders are placed from sea level to about 5 meters of elevation and clustered in groups made of several imbricated elements. In one case, boulders are arranged in a very unstable configuration (Fig. 6.2).



Figure 6.2 – A) The boulder accumulation at the Torre Sasso locality is marked by boulders emplaced in a very unstable assemblage; B) Three different zone are recognisable from coastline to landward: the first one is a ramp zone where boulders are detached, the second one marked by dotted line represents the crest of boulder accumulation, the third one is a steeper area where boulders aren't present.

A total number of 40 boulders have been surveyed. Most of them are calcareous sandstone slabs, from 0.5 to 1.0 m thick. The maximum volume of boulders is 13.5 m³, and considering the unit volume weight of the calcareous sandstone (2.27 g/cm³), a maximum weight of about 31 tons can be estimated (Fig. 6.3 A).

The analysis of imbrication axis azimuth and the A-axis elongated boulders also indicates the prevailing direction of the catastrophic wave responsible for their deposition to be from the SSE sector (Fig. 6.3 B).

Tilted solution potholes characteristically mark the boulder surface. They formed in the supratidal zone and were placed in the new position because of boulder detachment and transport; a new sub-horizontal generation of flat potholes developed after transport. An incipient alveolar weathering and, more rarely, boreholes of *Lithophaga* can also be detected.

Hydrodynamic calculations made on larger boulders surveyed at the Torre Sasso locality according to Nott (2003) relations indicate a tsunami wave height ranging from 3.7 to 7.7 m whereas wind wave breaking height comprise between 15 and 31 m.

Despite a detailed survey, Torre Sasso boulders accumulation did not supply elements useful for its chronological attribution.

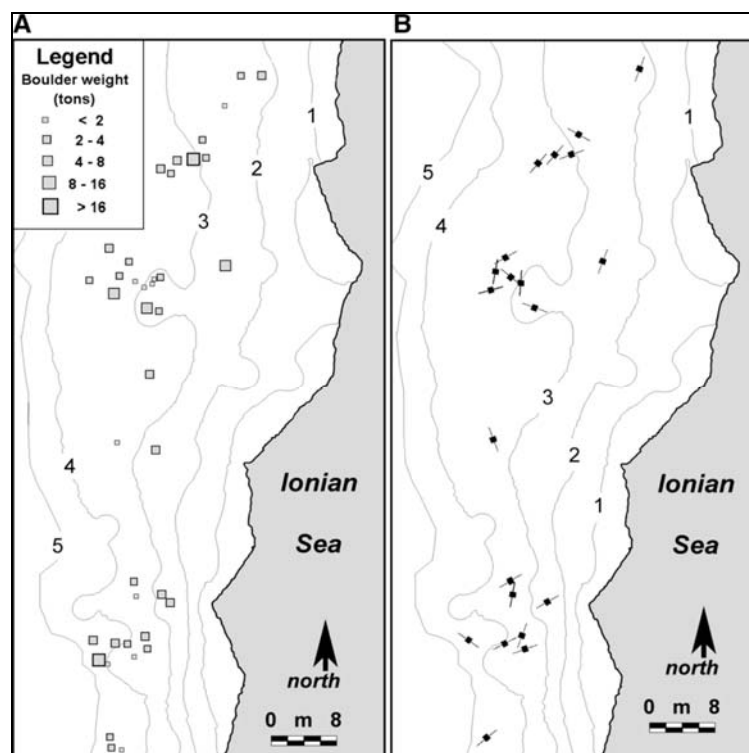


Figure 6.3 – A) Weight and distribution of some largest boulders at the Torre Sasso locality. B) A-axis of elongated boulders and perpendicular to imbricated boulders at the Torre Sasso locality.

6.3. Out-of-size coastal landform: the Torre S. Emiliano boulder accumulation: STOP 7

Another impressive accumulation of large boulders has been recognized between the Torre S. Emiliano and Porto Badisco localities (Fig. 6.4). The morphological analysis of this landform has been realized by means of detailed topographical and scuba surveys, by measuring boulder volumes and imbrication or elongation axis azimuth. The boulder accumulation rests on a wide marine terraced platform, about 150 m wide, and stretches from 10 m to about 4 m above sea level. A 13 m high paleocliff, with the base marked by the final course of small river cuts, borders the platform landward; the outer border is a steep cliff, deeply modified by coastal karstic features (pinnacles, grooves, and so on).

The marine terraced surface is mantled by a thin colluvial cover made of red clayey sands which thickens seaward. Geophysical survey reveals that this cover reaches the maximum thickness of about 2 m at a distance of about 100 m from the shoreline.

The boulder accumulation is about 40 m wide and stretches in a parallel way along the present coastline for about 2.5 km, with a variable distance from 15 to 40 m. Six detailed transverse profiles along the emerged tract of coast and three submarine morphological transects have been carried out (Figs. 6.5 A and 6.5 B). They reveal a wide submerged plain placed 20 m below p.s.l. which is joined to the coastline by a very steep surface. A cliff

marks the coastline, up to 4 meters high, followed landward by a rampart; at its back a ramp produced by the carving of boulders and extended from 20 to 60 m from the coastline can be recognized. The ramp is studded by some of the largest blocks, weighing up to 70 tons. The boulder accumulation starts at the inner margin of the ramp, represented by a small step covered by very large boulders emplaced in a near-vertical position.

The detailed morphological survey of the boulder accumulation shows that it is compound by two ridges. The ridge closest to the coastline shows seaward a very steep slope and the top placed at about 11.5 m above the mean sea level. The inner belt is about 1 m lower than the outer one and is generally compound by smaller imbricated boulders and, landward, by sparse boulders.

The two ridges are separated by a trough about 15-20 m wide and 2 m deep. The landward margin of the boulder accumulation partly covers the marine terrace colluvial cover (Fig. 6.6).

Boulder accumulation is made of limestone imbricated boulders, mostly coming from the supratidal zone, detached from the carved platform along joints and strata planes which locally dip seaward. However, some spheroidal boulders which can typically be found inside potholes in the wave breaking zone have been detected on the landward border of the accumulation. No significant differences in the morphological appearance of the boulder surfaces have been found between the two ridges.

The 18 largest boulders have been surveyed; they weigh up to 70 tons and are entrapped into fractures widened by storm waves and karst processes occurring along the carved surface or rest on the crest of the outer, higher ridge (Figs. 6.7 and 6.8).

A further analysis has been carried out on the A-axis orientation of the elongated boulders and on the imbrication axis. The collected data are comprised into the ESE – S sector with a slight prevalence in the SSE direction (Fig. 6.9).

The huge number of mobilized boulders, their great weight and anomalous position mark out this peculiar landform of the local coastal landscape. Hydrodynamic calculations made according to Nott (2003) relations indicate a tsunami wave height for the mobilization of the five largest boulders surveyed at the Torre S.Emiliano locality ranging from about 6.5 to more than 11 m (Tab. 6.1).

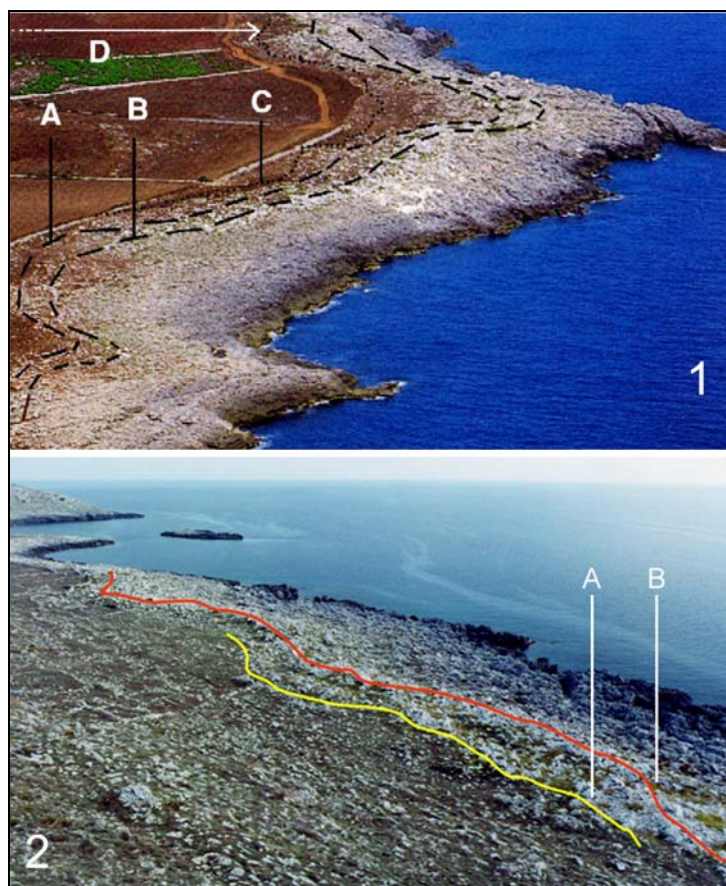


Figure 6.4 – 1) A view of the Torre S. Emiliano boulder accumulation. **Legend:** **A, B** — Crests of the two ridges that compound the boulder accumulation; **C** — landward margin of the boulder accumulation; **D** — marine terrace surface covered by reddish colluvial deposits; **2)** A view from the two crests, A and B, of Torre S. Emiliano area from hinterland.

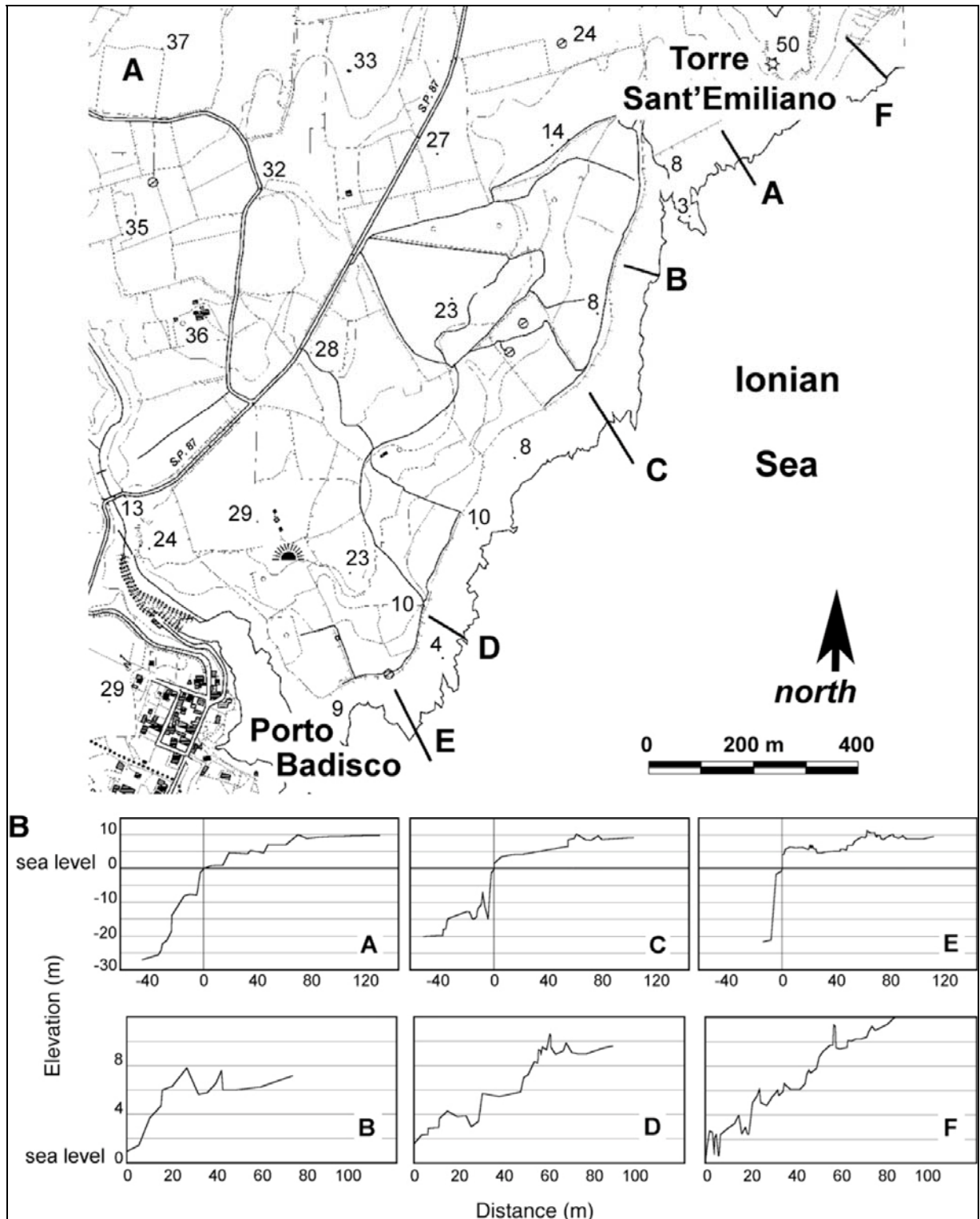


Figure 6.5 – A) Position of the detailed topographical profiles carried out at the Torre S. Emiliano locality. **B)** Detailed topographical profiles (A–F) carried out at the Torre S.Emiliano locality.

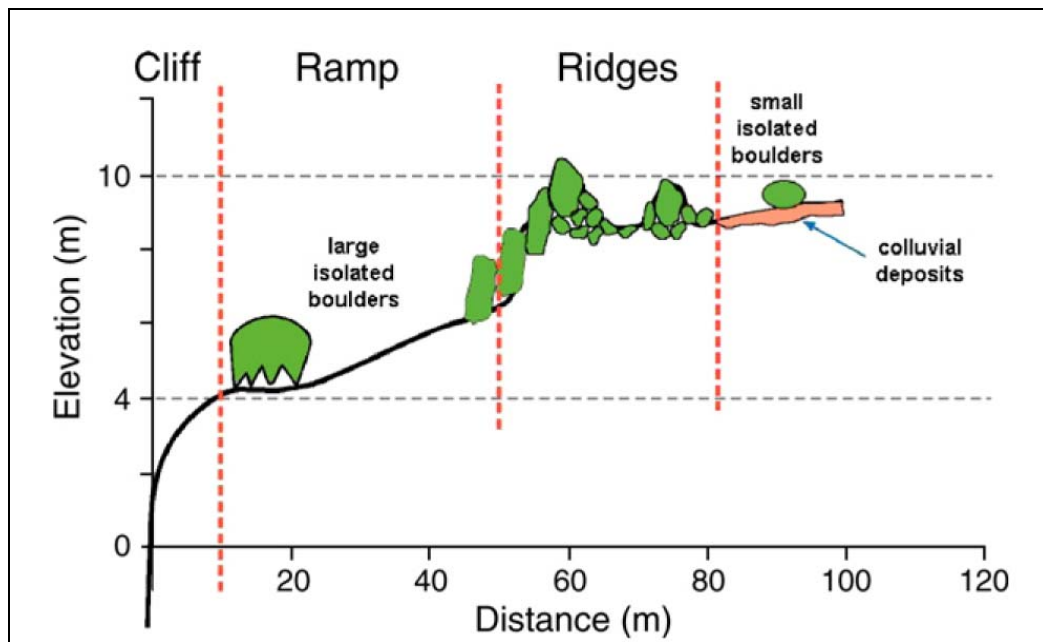


Figure 6.6 - Geomorphological scheme of the Torre S. Emiliano boulders accumulation.

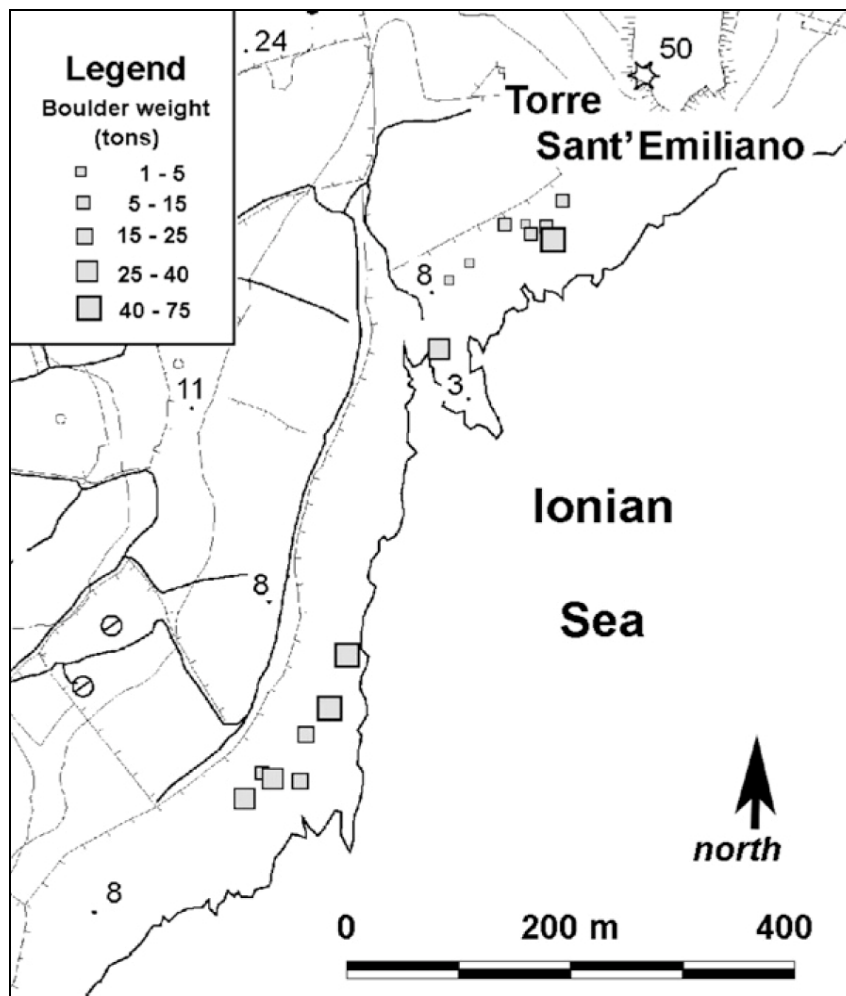


Figure 6.7 - Weight and distribution of some largest boulders at the Torre S. Emiliano locality.



Figure 6.8 – A view of the overturned largest boulder detected at the Torre S. Emiliano locality. It is 5.0×3.5×1.5 m large and weigh about 70 t. Note the coastal karstic features at the base.

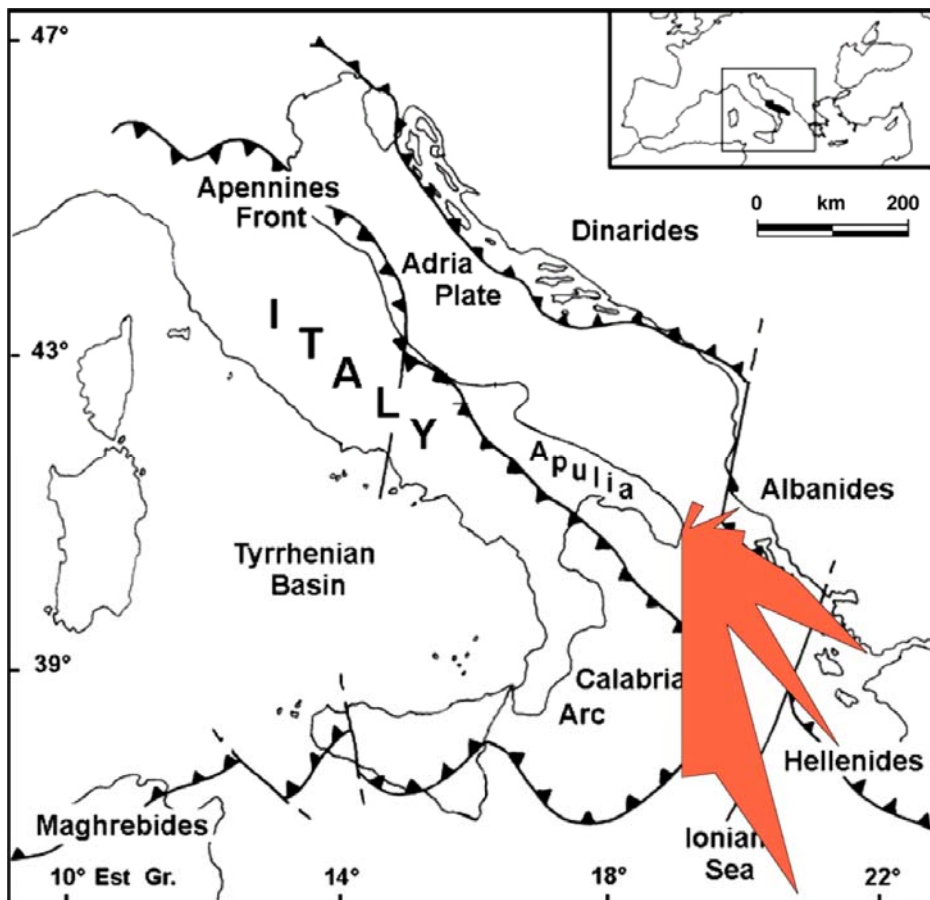


Figure 6.9 - Distribution of the perpendicular to the A-axis orientation of elongated boulders and embrication axes at the Torre S. Emiliano boulders accumulation.

By contrast, the removal of such large boulders requests wind breaking waves marked by heights ranging from 27 to 45 m.

Mastronuzzi & Sansò (2004) calculated by using Nott (1997) relations that along the Adriatic side of Apulia extreme storm waves can not transport boulders weighing more than 2.5 tons. So, the boulder accumulation of Torre S.Emiliano is clearly an out-of-size coastal landform in respect to local storm wave power.

Finally, calculations agree with boulders accumulation morphology that suggest a minimum run-up at Torre S. Emiliano of about 11 m. Moreover, the uniform morphological appearance of the boulders' surfaces suggests that the two ridges of the Torre S. Emiliano accumulation most likely formed as a consequence of two tsunami waves occurring during the same catastrophic event.

Torre S. Emiliano	Axis (m)			H_{storm}	H_{tsunami}
	<i>a</i>	<i>b</i>	<i>c</i>		
Boulder					
B084	2.40	2.20	2.00	21.82	5.45
B089	3.00	2.00	1.80	27.27	6.82
B098	3.50	2.10	1.60	31.82	7.95
B115	3.40	2.40	1.90	30.91	7.73
B077	3.80	2.60	2.30	34.55	8.64
B120	5.00	3.50	1.50	45.45	11.36
Torre Lupo					
Boulder					
215	2.20	1.80	0.90	15.06	3.76
210	2.50	1.40	1.30	17.11	4.28
220	2.70	0.90	0.90	18.48	4.62
204	2.30	1.50	4.10	15.74	3.94
234	4.50	1.50	2.00	30.80	7.70

Table 6.1 - Hydrodynamic calculations made according to Nott (2003) relations.

6.3.1. Inferred chronology of Torre S.Emiliano tsunami

The boulders accumulation of Torre S. Emiliano has been dated by using morphological, radiocarbon and archaeological data.

Some suggestions about the age of the Torre S.Emiliano boulders accumulation arise from the analysis of spheroidal boulders that have been carved from large potholes in the wave breaking zone. Some of these boulders have been found at the landward margin of the accumulation, partly covered by the colluvial cover. Some of them have been capsized aiming to detect some morphological differences between the aerial-exposed surface and the colluvium-covered one (Fig. 6.10).

In fact, the presence or absence of a cover is a very important factor, because karstic processes operate differently on exposed rock surfaces and at cover-rock surface interface (Jennings, 1985). On the bare rock surface small rainpits, solution flutes and bevels develop producing an irregular appearance of the surface. On the contrary, a smooth surface is produced on limestone below a cover surface because of solution promotion due to water retained in the soil cover that provides a biogenic CO₂ supply. The rock surface below the cover surface is smoothed and characteristically bleached white; a solution notch generally develops just below cover surface.

It would be expected that the greater the morphological difference between exposed and covered boulder surfaces the longer the time of boulder emplacement will be (Fig. 6.11).

The removal of some boulders occurring at the innermost margins of the accumulation has shown no morphological differences between exposed and covered rock surfaces. In conclusion, karstic features would indicate a very recent age for boulder depositions.

More precise data have been obtained by radiocarbon dating. Most of the boulders were carved by the supralittoral zone so that no biogenic encrustations able to supply a radiocarbon age for this tsunami event have been found on the boulder surface. However, numerous marine shells have been found inside the seaward boulder ridge, in correspondence with the outer slope (Fig. 6.12; Tab. 6.2).



Figure 6.10 - Torre S. Emiliano locality. Appearance of a spheroidal boulder surface capsized. Note the absence of morphological differences between the air-exposed (below, grey) and soil-covered (above, white) surface of the boulder.

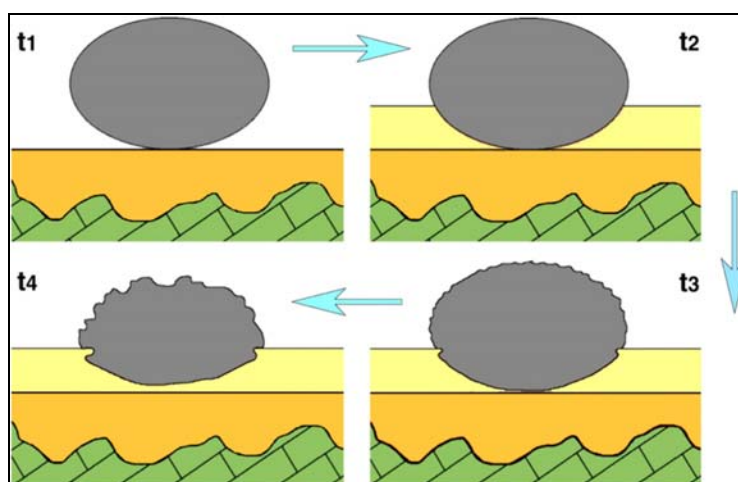


Figure 6.11 - Geomorphological model of a partly covered boulder. **t1** — a spheroidal boulder is transported from the wash zone inland, covering a colluvial cover. **t2**—Sheet superficial waters produce the partly covering of the boulder. **t3-t4**—the difference of karstic processes acting above and below soil surface determines a different morphological appearance of boulder surface; a solution notch forms at soil surface.



Figure 6.12 - Chronological data came from AMS analyses on marine samples and biogenic concretion-found inside the boulder accumulation.

Bivalves	Gastropods
<i>Arca noe</i> L.	<i>Columbella rustica</i> (L.)
<i>Arca tetragona</i> (Poli)	<i>Conus mediterraneus</i> Hwass
<i>Pteria hirundo</i> (L.)	<i>Murex brandaris</i> L.
<i>Modiolus barbatus</i> (L.)	<i>Calliostoma conulum</i> (L.)
<i>Venus</i> sp.	<i>Gibbula magus</i> (L.)
	<i>Haliotis lamellosa</i> Lamarek
	<i>Luria lurida</i> (L.)
	<i>Bittium reticulatum</i> (Da Costa)
	<i>Cerithium vulgatum</i> Bruguiere
	<i>Gibbula</i> sp.
	<i>Luria</i> sp.
	<i>Patella</i> sp.
	<i>Vermetus</i> sp.

Table 6.2 – List of marine shells from the Torre S. Emiliano boulder accumulation.

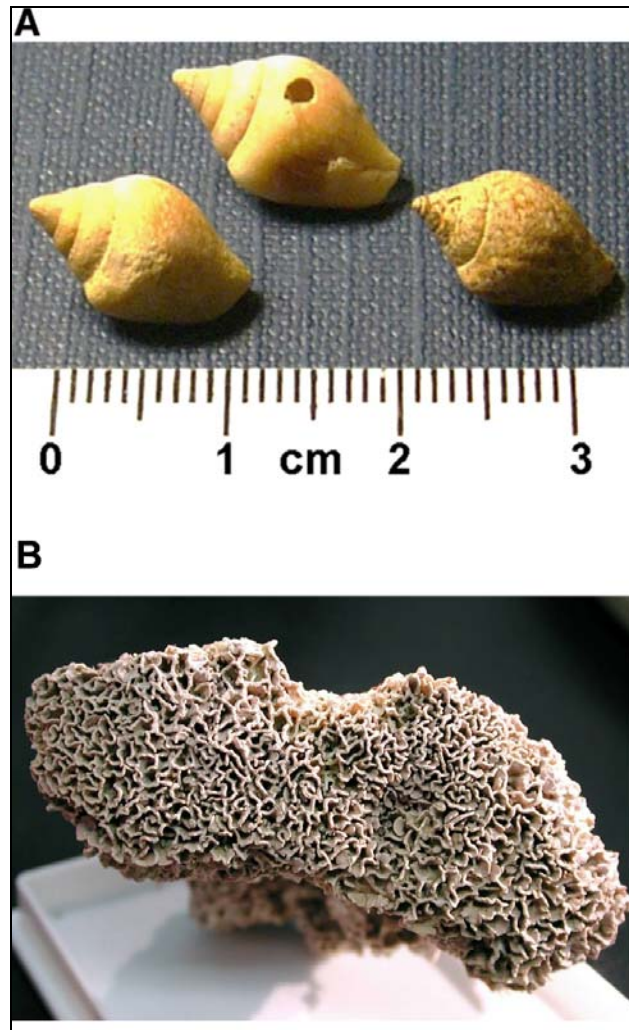


Figure 6.13 - (A) The three specimens of *Columbella rustica* dated by means of AMS radiocarbon determinations; **(B)** Samples of *Lythophyllum lichenoides* collected in the Torre S. Emiliano boulders accumulation.



Figure 6.14 - Pottery fragment found within the soil cover below a group of imbricated boulders at the landward margin of the accumulation. The pottery has been attributed to the 16th-17th centuries.

ID sample	Description	$\delta^{13}\text{C}\text{‰}$	Radiocarbon age	Age uncertainty	ΔR	Calibrated age	1 σ	2 σ	Lab.
Emilio X1 GX-31838-AMS	<i>Columbella rustica</i>	0,5	620	± 50	121 ± 60	1724 AD \pm 1745 AD	0,115		A
						1750 AD \pm 1790 AD	0,218		
						1801 AD \pm 1897 AD	0,581		
						1935 AD \pm 1951 AD	0,08		
						1685 AD \pm 1951 AD		1	
Emilio Y1 GX-31840-AMS	<i>Columbella rustica</i>	1,3	600	± 40	121 ± 60	1770 AD \pm 1775 AD	0,071		A
						1804 AD \pm 1951 AD	0,921		
						1702 AD \pm 1951 AD		1	
Emilio Y2 GX-31839-AMS	<i>Columbella rustica</i>	0,5	530	± 40	121 ± 60	1533 AD \pm 1599 AD	0,465		A
						1617 AD \pm 1671 AD	0,534		
						1739 AD \pm 1751 AD		0,009	
						1764 AD \pm 1802 AD		0,04	
						1533 AD \pm 1597 AD		0,38	
Emilio E1 LTL 1180 A	<i>Lithophilum licheinoides</i>	1.7 \pm 0.1	519	± 40	121 ± 60	1533 AD \pm 1597 AD	0,38		B
						1617 AD \pm 1682 AD	0,62		
						1495 AD \pm 1699 AD		0,88	
						1733 AD \pm 1806 AD		0,11	

Conventional ages have been calibrated using CALIB 5.0 software (Stuiver and Reimer, 2005). Legend: A = Geochron Laboratories, Cambridge, Massachusetts, USA; B = CEDAD, Università degli Studi Lecce, Mesagne, Brindisi Italy.

Table 6.3 – Radiocarbon age determinations performed on marine biogenic materials collected at the Torre S. Emiliano boulder accumulation.



Figure 6.15 - The 20th of February, 1743 earthquake. Circles size supplies an indication of MCS earthquake intensity at different localities. The dotted circle marks the estimated position of the epicentre (data from www.ingv.it).

Three AMS radiocarbon age determinations have been performed on *Columbella rustica* (L.) (Fig. 6.13 A); since this mollusk is not edible any possible accidental contamination due to the human and bird frequentation of the area can be excluded. The results of the AMS analyses have been calibrated by using the CALIB 5.0 software (Stuiver & Reimer, 2005) and adopting a ΔR value of 121 ± 60 (Tab. 6.3). Results indicate that the samples have a very recent age; their deposition would have occurred about two or three centuries ago. Unfortunately, radiocarbon analyses on recent marine samples do not allow us to obtain very precise age determinations (Stuiver & Polach, 1977).

However, the removing of one of the innermost groups of imbricated boulders allowed the finding of intertidal bioconcretions (*Lythophyllum lichenoides* Phil.) clasts and pebbles as well as some archeological remains and vertebrate bones within the top layers of the colluvial deposits covered by boulders (Fig. 6.13 B).

The AMS radiocarbon age determination of bioconcretions fits with the other available radiometric data (Tab. 6.3). Moreover, the occurrence of a pottery fragment allows the attribution of the archeological material to the 16th-17th centuries (Fig. 6.14).

The whole of this evidence indicates that the investigated boulder accumulations were produced about three centuries ago by at least two large tsunami waves propagating from the SSE, with a run-up of about 11 m.

Taking into account these data and the available strong earthquakes catalogue (Boschi et al., 2000) the best candidate for the generation of this tsunami is the strong earthquake that struck southern Apulia on the 20th of February, 1743. This strong earthquake reached its maximum intensity (IX grade of Mercalli scale) in the area of the Otranto Strait causing the most relevant damage to the villages of Nardò and Francavilla Fontana in southern Apulia and Amaxichi, on the Lefkada island, in Greece. The epicenter has been placed in the northern Ionian Sea, between the Greek Ionian Islands and southern Apulia (Fig. 6.15).

Chronicles report three main shocks which could justify the recorded occurrences of multiple tsunami waves and a withdrawal of the shoreline at the Brindisi harbour (Margottini, 1981). The absence of written records of this catastrophic event which severely struck the coast stretching from Otranto to S.Maria di Leuca could be explained by the lack of settlements along the coast, with the only exception of Otranto, placed in a sheltered position at the back of the Torre S.Emiliano area, and Castro, situated on a ridge at 90 m above sea level.

Morphological effects of the 1743 tsunami have also been reported by Mastronuzzi & Sansò (2004) along the coast of Torre Santa Sabina to the north of Brindisi (cfr. Chapter 4, STOP 1). In this locality, the tsunami impact produced large sparse boulders quarried from the intertidal zone and transported on a low elevated platform. Hydrodynamic calculations made on the largest boulders define a tsunami height of about 1.5 m.

6.3.2. Conclusions

Along the southeastern coast of the Apulian region, large boulder accumulations mark the coastal landscape. The detailed survey of these accumulations reveals that they are out-of-size landforms whose development has to be attributed to a tsunami event and not to the local much less powerful storm waves. In particular, the boulders' weight and arrangement suggest that this coastal tract has been struck by two consecutive large tsunami waves coming from the SSE and marked by a run-up of about 11 m. Numerous chronological data indicate a very recent age for this event which would have occurred about three centuries ago. Available earthquake catalogues indicate the 20th of February, 1743 earthquake to be the best candidate for the generation of this tsunami. It was responsible for severe damage to villages along the opposite coastal regions of the Otranto Strait. The epicentre was most likely placed in the Ionian Sea, some tens of kilometres to the SSE of the surveyed area. It is interesting to note that notwithstanding the effects of this tsunami which can be found up to the north of Brindisi, only a brief historical report is available. This is most likely due to the past-diffused presence of coastal swamps and malaria causing the coastal area to be practically deserted up through to the beginning of the last century. In conclusion, the collated data identify the presence of a tsunami-generative seismic structure offshore of the southeastern Salento coast and increase the need for studies that would define the tsunami vulnerability and risk along southern Apulian coast and for strategies devoted to tsunami risk mitigation.

6.4. Out-of-place landforms in a foreland stable area: the raised shore platforms of Otranto - Torre dell'Orso: STOP 8

The coastal area stretching from Torre dell'Orso to Otranto is marked by some shore platforms, both emerged and submerged. The altimetric position of the highest shore platform and its apparent Holocenic age pose a number of interesting considerations about relative sea level history in this area.

6.4.1. Geological and morphological setting of the area

The coastal landscape is shaped on calcareous - clayey sands, calcareous sandstones and marly calcarenites referred to Middle Pliocene - Lower Pleistocene which are transgressive on calcareous breccias and calcareous marls of Lower Pliocene age. These last ones crop out in the area of Otranto village where Miocene limestones and calcarenites can be also detected (Mastronuzzi et al., 1994).

The Mesozoic basement crops out extensively to the south of Otranto whereas northward it deepens in NE direction because of faulting. In the Alimini lakes area it is placed about 210 m below sea level; the Plio-Pleistocene units show in this area a great thickness, of about 100 m.

The coastal landscape of Otranto - Torre dell'Orso area is marked out by six flat surfaces very likely corresponding to remains of marine terraces placed between 103 m and a few meters above mean sea level (Fig. 6.16). The absence of sediments and/or significant fossil remains did not permit to attribute them to a clearly defined past sea level stands. Marine terraces are 2-3 kilometers wide and separated by degraded, low cliffs.

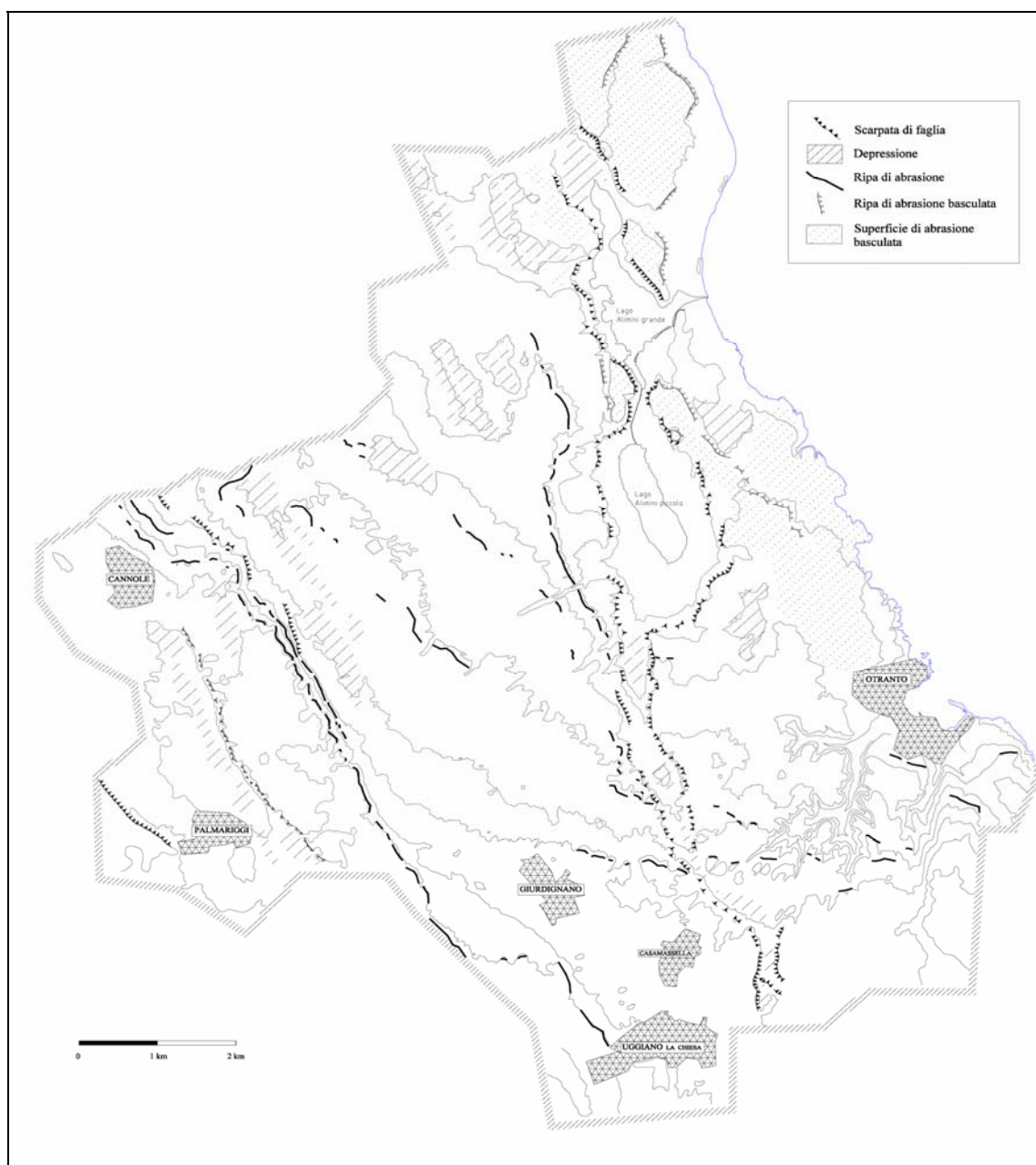


Figure 6.16 - Morphological sketch of the eastern Salento coastal area. **Legend** - scarpata di faglia: **fault scarp**; depression: **depression**; ripa di abrasione: **marine cliff**; ripa di abrasione basculata: **tilted marine cliff**; superficie di abrasione basculata: **tilted abrasion platform**.

The shaping of cliffs has been accomplished by the development of numerous, short river cuts which rarely affect more than one order of marine terraces. The drainage network is poorly developed with the exception of a drainage basin recognizable at the southernmost part of the area which is well organized and linked to a submerged shoreline.

A system of NNW-SSE elongated depressions running near the coastline breaks the stair-case of marine terraces. The depressions occurring to the northern sector of the area show a peculiar rhomboid shape and are bordered by straight, high scarps; two of these depressions are occupied by the Alimini lakes. In the southern part of the area, depressions are elliptic in shape and bordered by scarps that are cut by short river valleys.

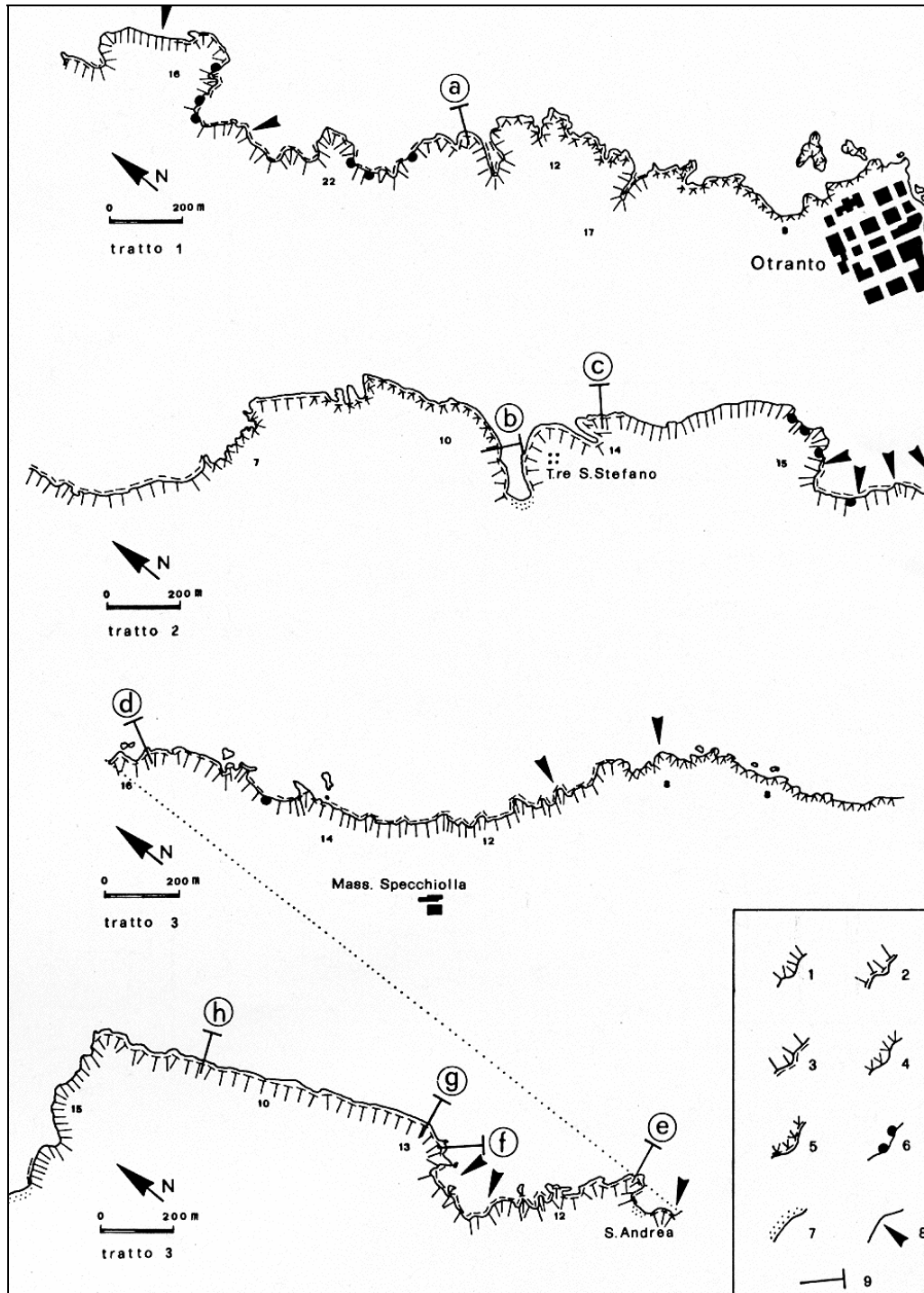


Figure 6.17 - Morphology of the coast between Torre dell'Orso and Otranto. **Legend:** 1) active cliff; 2) cliffs with emerged wave-cut platform at the foot; 3) cliffs with submerged wave-cut platform; 4) sloping coast; 5) sloping coast with emerged platform; 6) sea caves; 7) sandy inlet; 8) coastal tract in fast retreat; 9) position of profiles reported in Fig. 6.18.

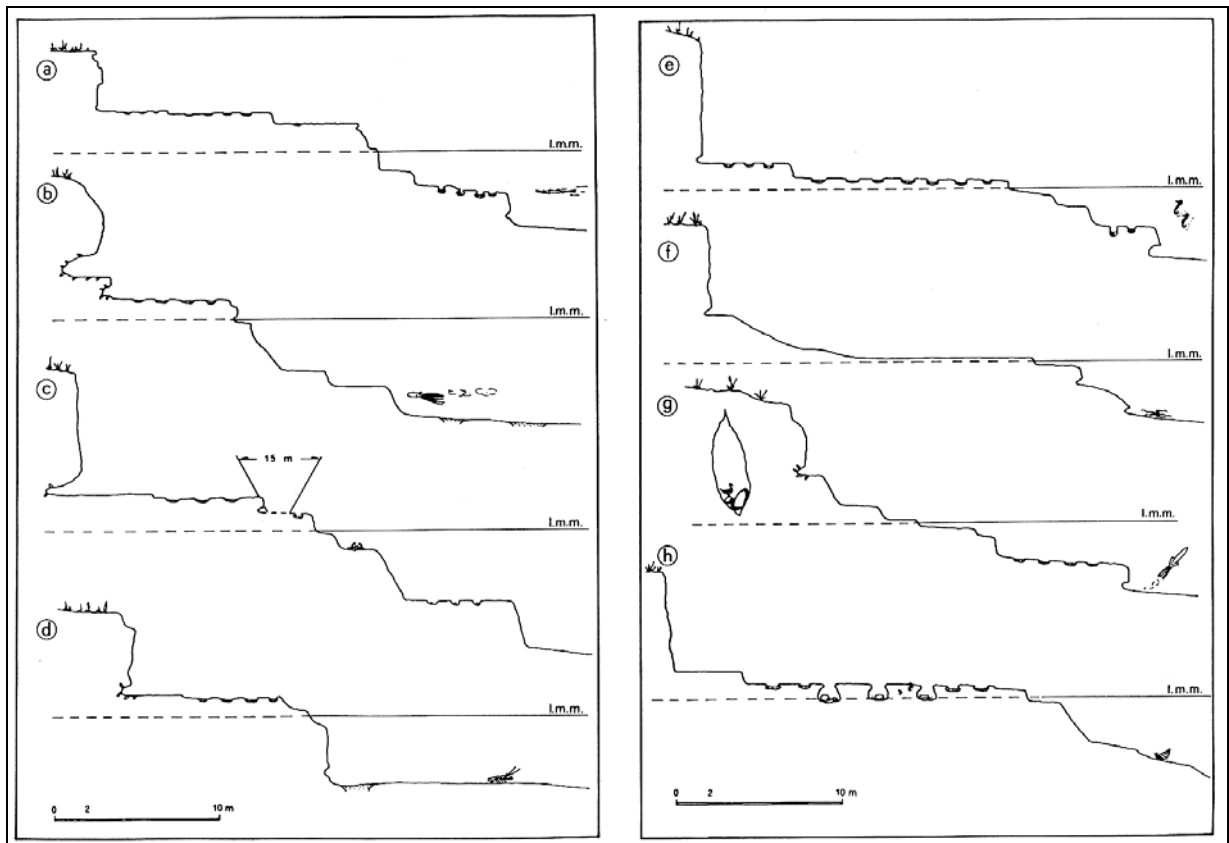


Figure 6.18 - Morphological profiles of raised shore platforms between Torre dell'Orso and Otranto. Vertical and horizontal scales are the same.

6.4.2. The raised shore platforms of Torre dell'Orso

The coast stretching from Torre dell'Orso to Otranto, on the eastern side of southern Apulia, is represented almost entirely by cliffed coasts (Mastronuzzi et al., 1994; Dini et al., 2000) (Fig. 6.17) composed of gently seaward sloping strata of fine fossiliferous calcarenites interbedded with clayey calcareous sands and somewhere with blue sandy clays.



Figure 6.19 - A view of the wave-cut platform placed at +3 m above p.s.l. placed to the south of Torre dell'Orso.

Numerous tracts of cliff coasts show a peculiar profile characterized by both submerged and subaerial platforms (Fig. 6.18). The lowest platform is 15 m below m.s.l. and is covered by terrigenous/bioclastic sands with *Cymodocea nodosa* (Ucaria) Areshoug and *Posidonia oceanica* Delile. It is in morphological continuity with the bottom of Torre Santo Stefano small inlet. A second platform is located between 11 and 6.5 m below m.s.l. and has a width ranging up to 80 m. The cliff which borders it landward shows blocks at its foot and the presence of marine grottos. A third platform is recognizable between 4 and 3 m below m.s.l.. It is bordered landward by a 3 m high cliff which in some places shows a notch about 0.3 m deep at its foot.

Furthermore, two wide platforms characterize the subaerial part of these cliffs (Fig. 6.19). They are not continuous with the present wave-cut shore platform. In fact, the lowest one is between 1.0 and 2.2 m above m.s.l.; the other one between 2.8 and 3 m above m.s.l.. Both of these last two platforms, up to 40 m wide, are bordered in some places - i.e. Torre Santo Stefano - by a more or less deep notch (Fig. 6.20). The cliff/platform junction is hidden by blocks from the bordering cliff and cemented by deposits of travertine which formed at their base. A sample of these deposits (Orso1 sample) yielded a radiocarbon age of 1358±80 years BP (Dini et al., 2000).

At Torre Stefano locality, storm deposits preserved at the inner margin of the highest raised platform yielded the radiocarbon age of 2060±50 years (TSS7 sample) and 1920±50 years (TS2 sample) (Figs. 6.21, 6.22 and 6.23) (Auriemma et al., 2004).

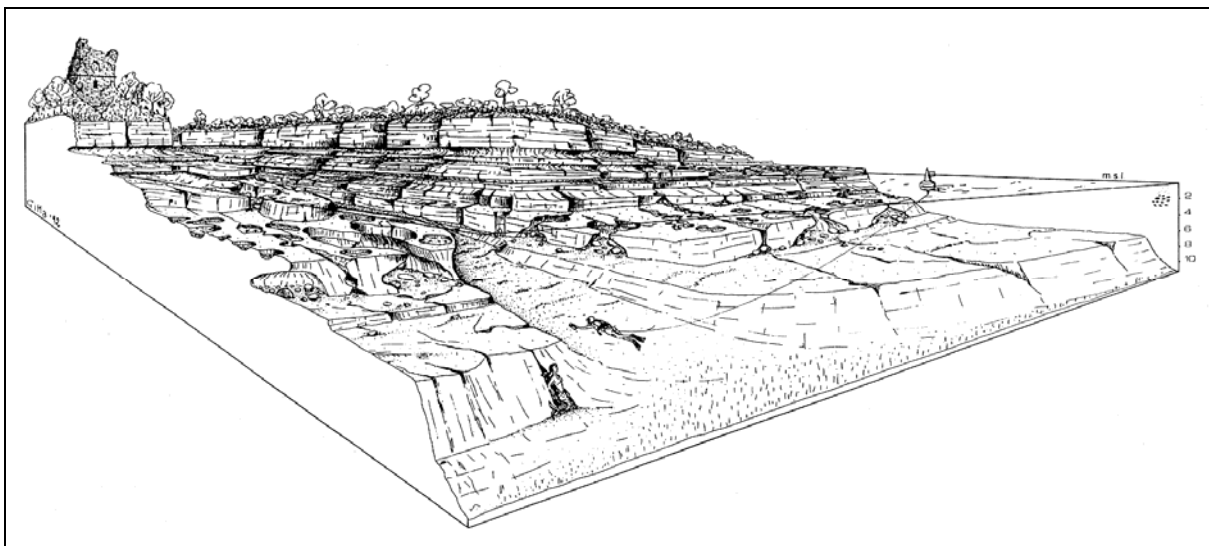


Figure 6.20 - Schematic block diagram of the Torre Santo Stefano coast.



Figure 6.21 - A view of the storm deposits preserved at the inner margin of the highest raised platform at Torre Santo Stefano localities



Figure 6.22 - A thick deposit of travertine cemented storm deposits at Torre Santo Stefano localities. On the foreground the present storm wave deposit can be recognized.



Figure 6.23 - A view of a boulder covered by Vermetids which has been carved and transported at the inner margin or raised shore platform by storm waves.

According to Mastronuzzi et al. (1994), the raised shore platforms of Torre dell'Orso may be of Middle-Late Holocene age because the good state of preservation of the cliff at their back notwithstanding the weakness of the outcropping rocks. Furthermore, the lack of slope deposits which would have been developed during last glacial period and the absence of sediments older than 2000 years BP would confirm this chronological attribution.

If the chronological attribution is correct, the shape of the widest platform should be referred to the mean Holocene sea stand, occurred during the Climatic Optimum about 6500 years B.P. (Auriemma et al, 2004). A relatively long period of stable sea level is in fact required for the development of a wide wave-cut platform.

Furthermore, a sudden uplift of the platform must be taken into account for its subsequent preservation since this is possible if the landform overcomes rapidly the area of maximum wave erosion, placed in correspondence of mean sea level. On the contrary, a slow relative lowering of sea level would have produced the strong erosion of the platform surface.

Sample	Locality	Material	Altitude (m)	$\delta^{13}\text{C}_{\text{PDB}}$ (‰)	$\delta^{18}\text{O}$ (‰)	Uncalibrated Age (years BP)	Calibrated Age (cal years BP)	Lab.	Reference
Orso 1	Torre Santo Stefano	Travertino	3.0	-	-	1358 ± 80	1280 ± 55	A	Dini et al., 2000
TS 2	Otranto Torre Sant'andrea	Marine shells	2.8	-0.4	-	1920 ± 50 AMS	1343 ± 75	B	Auriemma et al., 2004
TSS 7	Torre Santo Stefano	Vermetids boulder	2.5	-	-	2060 ± 50	1484 ± 90	A	Dini et al., 2000

Table 6.3 - Radiocarbon age determinations performed on continental and marine deposits occurring on the Torre dell'Orso wave-cut platforms. **A** - Laboratorio di Geochimica Isotopica, Università degli Studi, Trieste (Italia); **B** - Geochron Laboratoires Krueger Enterprises Inc. (Cambridge, Massachusetts, U.S.A.); calibration performed by Calibra 4.3 software by Stuiver et al. (1998) using $\Delta R=118\pm 60$.

6.4.3. The morphological evidences of recent tectonic activity

The geomorphological analysis of the entire coast stretching between Otranto and Torre dell'Orso has been carried out to understand the significance of Torre dell'Orso raised shore platform which would indicate an important, recent tectonic activity in the area.

The geomorphological analysis of the coastal landscape of eastern Salento revealed many other evidences of recent tectonic activity, mainly represented by the break of marine cliffs continuity and by the tilting of marine terraces top surfaces. These evidences are linked to a complex tectonic alignment NNW-SSE trending which has been active until very recent time. It affected the development of lowest marine terraces, related shorelines and drainage network, was responsible for the development of scarps and depressions, two of them occupied by Alimini lakes.

A system of depressions and scarps breaks the continuity of a relict marine cliff with foot at 30 m of altitude placed to the south of Alimini piccolo Lake. Another marine cliff and some river cuts linked to it are broken off by depressions near the SS16 road; in particular, river cuts show an evident bend at their final tract. A scarp breaks a marine cliff whose foot is at 70 m of altitude in the area between Otranto and Casamassella. The scarp is marked by a NNW-SSE orientation in its northern part and by a N-S direction in its southern one and it is in continuity with the system of depressions. Finally, relict marine cliffs placed to the west of the system of depressions show different altitude of those ones occurring to the east.

Tilted abrasion surfaces and marine cliffs occurred in the area stretching between the Alimini lakes depressions and the present coastline. The widest marine terraces have been recognized at Frassanito locality, tilted toward SE between 27 and 8 m of altitude, in the area between Alimini grande Lake and the S.Cataldo-Otranto road, tilted northeastward between 17 and 7 m of altitude, in the strip between Alimini piccolo Lake and the coastline, where two tilted abrasion surfaces separated by a low cliff have been recognized. In particular, the lowest of these two surfaces is tilted towards NE and stretches between 25 and 10 m of altitude.

Recent tectonic activity of faults occurring along the coast of Salento has been reported by some Authors (Martinis, 1962; Palmentola & Vignola, 1980). More recently, Marlini et al. (2000) point out offshore Capo S.Maria di Leuca a remarkable sea floor deformation due to normal active faulting.

Moreover, along the other side of Otranto channel, the Ionian Islands (Greece) show evidence of very recent coseismic uplift (Pirazzoli et al., 1994; Vött et al., 2006; 2007; 2008; Mastronuzzi et al., 2008). In particular along the southernmost part of the coast of Kerkira Island (Corfù) a very extended emerged shore platform is well preserved between Asprokavos and the Kanoula locality. It is some hundred meters long and about 50 m wide (Fig. 6.24). Point whereas about 1 km to the North it is represented by a smaller one in Kanoula harbour.

Here, the shore platform is shaped on a conglomeratic deposit, partially cemented by algal encrustation in formation at the foot of a very high cliff. The emerged part of the conglomerate, who top is at about 1 m above biological mean sea level (Fig. 6.25), is marked by encrustations of vermetids and serpulids (Fig. 6.26). AMS analyses indicated an age of about 3.0 ky BP (Tab. 6.4). The shore platform is limited to the North by an outcropping of well preserved beach rock placed at the same elevation on present biological sea level (Fig. 6.27).



Figure 6.24 - The 1.0 m uplifted platform between Asprokavos and the Kanoula locality (Kerkira, Ionian Islands, Greece).



Figure 6.25 - A particular of the same platform near the fisherman harbour of Kanoula (Kerkira, Ionian Islands, Greece); the top is at about 1.0 m above biological sea level.



Figure 6.26 - Encrustations of *Vermetus* on the algal encrustation of the platform of Fig. 6.24.



Figure 6.27 - The beach rock outcropping near the harbour of Kanoula; also the beach rock is about 1.0 m uplifted.

Sample	Laboratory ID	Specimen	Elevation m a.p.s.l.	Conventional age (yr BP +/- σ)	δC_{PDB} %	Calibrated age AD/BC Atmospheric (2 σ)
COR PIATT 1A	LTL2205A	Vermetid	1.1	3339 \pm 40	-12.6 \pm 0.3	1300 – 880 cal BC
COR PIATT 1B	LTL2206A	Vermetid	1.1	3137 \pm 40	-12.3 \pm 0.3	1050 – 700 cal BC
COR PIATT 1C	LTL2207A	Vermetid	1.1	2974 \pm 40	-11.3 \pm 0.3	800 – 420 cal BC

Table 6.4 – AMS age of the vermetids from the Kerkira Island performed by CEDAD – Università degli Studi del Salento, Lecce. Calibration was performed by mean of OxCal Ver. 3.10 software (Reimer et al., 2004) using $\Delta R=121\pm 60$ years.

6.4.4. Discussions

The morphological, sedimentological and geochronological data sets available for the wave cut platform of Otranto area seem indicate a their Late Holocene uplift. Unluckily, the marine sediment present of their top indicate an age *ante quem* the rose occurred. Moreover, the features of the concretions didn't permit to individuate a coseismic uplift but seem only suggest a very fast raising; this last was to fast so the waves were not able to destroy their flat morphology.

The modern bio-concretion of the corresponding present biocenosis is quite absent due to the character of the biological species (absence of any calcareous endo- or eso-skeleton) and to the rocky type. On the other hand, the very well preserved cliff shaped in soft rocks and the absence of every slope deposit confirm a recent age, surely not older than the Late Holocene.

The comparison of this landform to that existing in the Kerkira Island seem highlight their genesis and age. The presence on the top of this last shore platform of bioconcretions of Late Holocene age confirm that they are not of present shaping. Moreover, the presence of very fragile bioconcretions seem indicate a very fast emersion since a slow one should determine their total destroying by wave abrasion.

6.4.5. Conclusions

The wave cut platform of Otranto represent one of the few evidence of the existence of some isolated areas of recent uplift in Apulia. The available data set and the comparison to morphological similar evidence placed in the surroundings area confirm a very recent raising may be characterised by very fast uplift; in particular its coseismic origin is suggested by its flat morphology.

From the geodynamic point of view these conclusions need the presence of tectonic structures that justify this behaviour during the Late Holocene. In our mind the near tectonic structures that interest the seismically active areas of Albania and Greece need to be investigated offshore to better correlate the morphological consequence of their activity on the eastern side of Otranto Channel to the western ones. The individuation of the tectonic structures that was responsible for the February 20th, 1743 earthquake and the consequent tsunami in the area comprises between Capo Santa Maria di Leuca and Kerkira Island, in to the Otranto Channel, should be the key of lecture of all that.



2nd International Tsunami Field Symposium

IGCP Project 495

Quaternary Land-Ocean Interactions:
Driving Mechanisms and Coastal Responses

Ostuni (Italy) and Ionian Islands (Greece) 22-28 September 2008



Project 495

CHAPTER 7

Tsunami flooding and vulnerability

Mastronuzzi G., Milella M., Pignatelli C., Sansò P.

An effort has been made to define the main effects of tsunamis on different morphological types of coast as inferred from post-events reports, available for different regions of the world since 1992 (e.g., Baptista et al., 1993; Yeh et al., 1993; Shimamoto et al., 1995; Tsuji et al., 1995; Yeh et al., 1995; Imamura et al., 1995; Shuto & Matsutomi, 1995; Pelinovsky et al., 1997; Maramai & Tinti, 1997; McSaveney et al. 2000; Lavigne et al., 2006). Since the information about the modifications of coastal landscape due to tsunamis reported in these surveys are not generally very detailed, they have been integrated by data gained by the geological record. The adopted procedure allows to assess the vulnerability of different types of coast occurring along Apulia region (southern Italy) to tsunami events supplying a very important information to coastal planners and to define risk mitigation procedures.

7.1. The effects of tsunamis on coasts

The effects of a tsunami on coasts can be greatly influenced by coastal morphology. Since tsunami wave velocity is a function of water depth, sea bottom slope, bathymetry and morphology can determine different values of run-up and inundation along different coastal tracts. Several numerical models able to forecast these values along coast have been developed and validated (Mader, 1974; Synolakis, 1991; Tanioka & Satake, 1996; Hills & Mader, 1997; Titov & Gonzalez, 1997; Titov & Synolakis, 1998; Pelinovsky et al., 2002; Tinti & Armigliato, 2003; Asal, 2003; Weiss et al., 2006). In this following pages we will neglect this particular aspect, focusing only on effects of tsunami on different morphological types of coast. An evaluation of these effects has been carried out by means of the detailed analysis of available post-event reports, integrated by geological data on deposits and forms linked to recent and past tsunamis.

7.1.1. Cliffs and convex rocky coasts

Cliffs are subvertical slopes due to rockfalls promoted by an effective wave erosion at the cliff foot. Convex rocky coasts correspond to subaerial slopes shaped on resistant rocks which have been reached by sea level; coastal erosion is mainly due to biochemical processes. Post-event reports generally lack of a description of tsunami effects on cliffs and convex rocky coasts. Some effects of a tsunami wave impacting on a cliff face can be inferred from geomorphological studies. According to Young & Bryant (1993) tsunami would be responsible for some of the cliff morphology occurring along the coast of south-eastern Australia. In extreme cases tsunami waves swamped cliff lines ripping slabs of bedrock up to 6 m in diameter from cliff face as high as 40-50 m above sea level. Young et al. (1996) identified at Mermaid's inlet (Australia) a boulder measuring up to 4.0x2.3x0.4 m which was ripped from the cliff face and thrown upwards onto the sandstone top cliff surface. Catastrophic waves would have swept the entire cliff face, about 32 m high, overtopped it and produced



Figure 7.1 - The cliff of Roca locality (Adriatic coast) is affected by the development of numerous sea caves. No report exist on the effects of a tsunami wave on sandstone cliffs studded by large caves open to the sea.

extensive erosion on the cliff top surface. No data exist on the effects of a tsunami wave against limestone or sandstone cliffs studded by large caves open to the sea. It would be expected that in case of a rapid run-up, the incoming wave could induce diffuse rockfalls due to piston effect (Fig. 7.1).

7.1.2. Rocky gently sloping coasts



Figure 7.2 - A view of the characteristic shape of a low sloping rocky coast (Torre Santa Sabina locality, Adriatic coast). Note the sparse boulders carved and transported by the 6th April, 1667 and at the 20th of February, 1743.

Gently sloping rocky coasts are low elevated platforms shaped on resistant rocks which reach sea level without abrupt change of slope (Fig. 7.2). Main morphological effects of tsunamis hitting low sloping rocky coasts, always conditioned by the bottom features, are represented by the detachment of large boulders in the near-shore zone and their deposition farther inland (Dawson, 1994; 2000), and by the sculpturing of bedrock resulting in the production of both smooth, small scale forms and large scale features as well (Bryant & Young, 1996; Bryant, 2001). However, very few observations are dedicated in the post-event reports about the effects of the impact of the tsunami waves on this type of coast so that information are mostly inferred by geomorphological studies.

Bryant (2001) refers the shaping on the bedrock of small-scale landforms such as impact marks, drill holes, comma marks, sinuous grooves, throughs or cavettos and flutes to high velocity flows produced by tsunamis. Landforms greater than 1 m are vortex, whirlpools, canyons, drumlin-like and keel-like features.

7.1.3. Beaches

Beaches are the most vulnerable area due to their low slope and elevation and are those that underwent major damage because they usually border very populated or productive areas. Post-event reports point out generally the development of an erosional scarp into beach or foredune deposits; the eroded material is transported and deposited as a sheet of sand farther inland (cfr. Fig. 2.16).

Beach and foredune are the main source of sediments transported by tsunamis (Sato et al., 1995) well above extreme storm wave limits. These sediments can reach a thickness of about 30 m, can be transported up to 10 km inland and reach 130 m of altitude (Scheffers & Kelletat, 2003).

According to Minuora & Nakaya (1990) during the 1983 tsunami of the Japan Sea Earthquake incoming tsunami waves rapidly transported materials landward from beaches and dunes, together with man-made structures. Outgoing waves in turn carried land materials seaward. Removed materials accumulated in the shoreface region forming submarine bars. Pelinovsky et al. (1997) report that the 1996 Sulawesi tsunami waves eroded beach ridges higher than 70 cm by 30-50 cm.

The erosional scarps due to three different tsunamis occurred during the last 2500 years have been recognized on the Lesina Lake coastal barrier, along the northern coast of Puglia by Gravina et al. (2005). According to Nichol et al. (2003), a tsunami occurred during the late Holocene at Great Barrier Island (New Zealand) was responsible for the deposition of a gravel sheet extending from the toe of the foredune to 14.3 m above m.s.l. and 200 m landward from the beach.

7.1.4. Pocket beach

The most vulnerable coast is represented by pocket beaches, which are placed inside small bays bordered by high cliff (cfr. Fig. 2.16). In this case, cliffs determine the development of a reflected wave producing huge run-up values, up to 31.7 m during the 1993 Hokkaido Nansei-Oki tsunami according to Shuto & Matsutomi (1995). Moreover, rockfalls from cliffs behind prevent people to evacuate safely are often reported (Tsuji et al., 1995a).

7.1.5. Beach/lagoon system

A beach/lagoon system is linked to the formation of a coastal barrier which closes a more or less wide sound of sea from the open sea (cfr. Fig. 2.16). Narrow and low coastal barriers are particular vulnerable coastal landforms since they can be totally overwashed by tsunami waves. Tsunami waves can break a spit closing seaward a coastal lagoon or lake, whose fresh water became salty due to the inundation (Tsuji et al., 1995b). The rise of water level in the lagoon can impede the escape of people inland.

Known evidence of the impact of tsunami on beach/lagoon systems are largely diffuse in all the world. For instance, Minoura & Nakaya (1991) point out that the 1983 tsunami of the Japan Sea Earthquake invaded intertidal lagoonal lakes and deeply eroded subsurface deposits. Molluscs and their shells were sorted out from the deposits by sediment agitation and were then transported to shallower environments. Moreover, seismic shock cracked beaches and dunes separating some ponds from the Japan Sea. Tsunami wave rushed into ponds through these cracks depositing a sand layer eroded by beaches and dunes. Sea water remained for a long period at a deeper layer of the pond. A similar process produced most likely four wide wash-over fans recognized along the sandy coastal barrier which divides the Lesina Lake from the Adriatic sea (northern Apulia, Italy) (Gianfreda et al., 2001) (Fig. 7.2). These landforms would be formed by three tsunamis which struck the coastal barrier at 2500 years BP, 493 AD and 1627 AD.

Andrade (1992) studied some overwash features which mark the barrier islands located in front of the Algarve in southern Portugal and attributed them to the Lisboa Tsunami of 1755.

Goff et al. (2000) studied catastrophic saltwater inundations recorded in the sediments of the Okupe Lagoon (New Zealand). Some of these events have been correlated to the action of strong tsunamis which struck this coastal lagoon during the last 5000 years. Chagué-Goff et al. (2002) identify a short-lived catastrophic saltwater inundation at northern Hawke's Bay (New Zealand) which may suggest the occurrence of a tsunami at about 6300 years BP.

McSaveney et al. (2000) surveyed along the spit fronting the Sissano Lagoon (Papua New Guinea) struck by the 17 July 1998 tsunami the occurrence of sand deposition exceeding 1 m on the seaward beach ridges along with scour holes up to 2 m deep.

7.1.6. River mouth

Another coastal area of high vulnerability is represented by river mouths and river banks (i.e.: Shimamoto et al., 1995). If a tsunami hits the mouth mainly parallel to the coast, much of the tsunami would run-up along the river. But if it hits the mouth of a river at an angle to the coast, tsunami will invade from the mouth and deluge the river bank. Also in this case, the flooding of backshore area can impede people from escaping inland. Erosion at river mouth has been reported by Tsuji et al. (1995) during the 1992 Flores Island tsunami. On the other hand, the 1994 Miraduro Island Tsunami (Philippine) produced the closing of a river mouth due to the redeposition of marine sands.

7.1.7. Discussions

Field data indicate that Apulian coast has been struck by several large tsunamis during the last 500 years. In particular, Tinti et al. (1995) detected 4 historical tsunamis along the Apulian coasts of Gargano and Tavoliere. The 30th of July, 1627 tsunami was particularly violent along the northern coast of Gargano; chronicles report the withdrawal of shoreline for about 3.5 km followed by seismic waves with catastrophic effects. Recent geomorphological and sedimentological research on the Lesina coastal barrier and in the Fortore Coastal plain point out the effects of three tsunamis occurred during the last 2500 years (Gianfreda et al., 2001; De Martini et al., 2003; Gravina et al., 2005; cfr. Chapter 3).

The presence of large boulders transported and deposited above the limit of storm waves suggests the occurrence of two other catastrophic events along the Ionian coasts of Apulia. The oldest event was most likely generated by a submarine landslide triggered by the 5th of December, 1456 earthquake and struck the Ionian coast of Salento peninsula (Mastronuzzi & Sansò, 2000; cfr. Chapter 6, STOP 6). The most recent one is likely connected to the strong earthquakes that occurred on 24 of April, 1836, whose epicenter is located near Rossano, in Calabria (cfr. Chapter 6, STOP 7).

A detailed geomorphological study of boulder accumulations occurring along the coast from Bari to Capo Santa Maria di Leuca individuates two other distinct tsunamis triggered most likely by the strong earthquakes occurred at Ragusa (present day Dubrovnik) the 6th April, 1667 and at the Ionian Sea the 20th February, 1743 (Mastronuzzi & Sansò, 2004; Mastronuzzi et al., 2007; cfr. Chapter, STOP 3 and STOP 5; cfr. Chapter 6, STOP 7). Soloviev (1990) reports along the Albanian and Greek coasts several tsunamis of great intensity, from II to V

grade of Sieberg-Ambrasey scale. These events cluster in correspondence of the Ionian islands (Zante, Giacintos, Corfù) and of the Corinth Gulf; Recent studies performed on Ionian Island individuated coseismic vertical movements and morphological evidence of the impact of several tsunami (Pirazzoli et al., 1994; Mastronuzzi et al., in prep.; Vött et al., 2006; 2007; 2008a; 2008b). This available data set seem indicate for the eastern coasts of Italy a recurrence period of tsunamis of about 50 years and maximum intensity of III-VI grade of Sieberg-Ambrasey scale. On the eastern Adriatic coast, tsunamis show similar intensity and recurrence period of 25 years.

The coast of Apulia region is composed by four principle morphological types: beaches, low sloping rocky coasts, convex rocky coasts, cliffs. Beaches are generally less than 40 m wide and 8 km long, and are generally bordered by a dune belt, often covering a former mid-Holocene cemented dune, and by reclaimed and urbanised swamps (Caldara et al., 1998; Mastronuzzi et al., 2002). Beaches are separated by long tracts made of low sloping rocky coasts. These last ones are constituted by an even plain sloping gently seaward cut through well-cemented Plio-Pleistocene calcareous sandstones (Fig. 7.2).

Convex rocky coast are mostly subaerial slopes shaped on limestones which have been partly submerged by sea; wave action has produced more or less high cliffs at sea level. Cliffs developed along coastal tracts composed either of clays, or calcareous sandstones, or intensely dissected and karstified limestones which are greatly affected by wave erosion; they are usually backed by a tabular landscape (Fig. 7.1).

Vulnerability is defined as being an estimate of the degree of loss resulting from a potentially damaging phenomenon (UN-DHA, 1992 Russo & Valletta, 1995; Crichton, 1999; Granger et al., 1999).

The analysis of available post-event surveys as well as the geological data on recent and past tsunami points out that the vulnerability of a coastal area to tsunami can vary greatly in function of coastal morphology (Table 7.1).

Morphological type of coast	Post-event reports	Geomorphological record	Vulnerability Class
Convex rocky coast	-	Detachment of boulders	I
Retreating cliff	-	-	II
Gently sloping rocky coast	-	Detachment of boulders Deposition of sandy sheets	II
Beach	Erosional scarp	Erosional scarp Marine sand layers into foredune	III
Beach/lagoon system	Washover fan Salt water inundation Sand sheet	Washover fan Salt water inundation Sand sheet	IV
Beach at river mouth	Erosion Deposition Inundation	Erosional scarp Marine sand layers into lagune/swamp	III
Pocket beach	Highest run-up values Rockfall from the backing cliff	Marine sand layers into foredune	V

Table 7.1 - Vulnerability class of different types of coasts.

The most vulnerable coastal type comprises pocket beaches bordered landward by high cliffs which produce very high run-up values; rockfalls from the cliff face impede people to move inland. Beaches are effectively overwashed by tsunami waves, with intense erosion of beach and dune materials which are brought farther inland; erosional scarps form on beaches and foredunes and some distinct sandy layers can be deposited. Where a coastal barrier divides a lagoon by the open sea, washover fans can form at its landward border; the lagoon is inundated by salt water preventing people to escape inland.

River mouths represent a fairly large entrance for tsunamis; extensive damage on river banks is produced by tsunami hitting at an angle to the coast. Finally, rocky platforms placed close to sea level are strongly affected by tsunamis which determine the reshaping of these landforms, with extensive carving and deposition of large boulders. Tsunami effects on unstable cliffs have not been investigated, even if some retreat due to mass movements could be expected.

This data set allows the vulnerability of Apulian coasts to tsunamis to be assessed (Fig. 7.3). The most vulnerable coasts (*Vulnerability Class: Very high*) are those made of a narrow beach bordered inland by high cliffs.

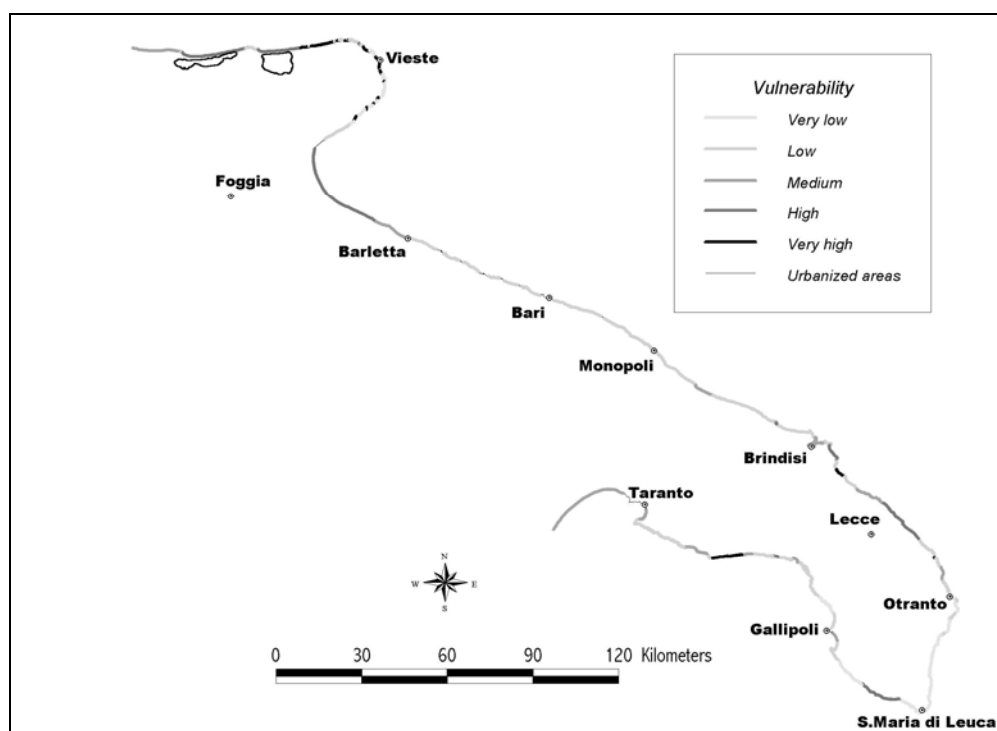


Figure 7.3 - The vulnerability of the Apulian coasts to tsunami action.

They characterize about 6 % of the coast and are placed mainly at the Gargano Promontory (Foce Romandato, Baia delle Zagare, Mattinatella, etc.) and in Salento Peninsula (Torre S. Gennaro, Torre dell'Orso, etc). Very vulnerable coastal tracts (*Vulnerability Class: High*) are those made of a beach dune/lagoon system such as Lesina and Varano Lakes, Siponto-Margherita di Savoia, Cesine, etc. along the Adriatic coast of Apulia. The Ionian coast is studded by small beach/dune/backdune swamp systems which are also very vulnerable to tsunamis. High vulnerable coasts represent about 15 % of the entire coastal perimeter.

Coastal area prone to the effects of tsunamis (*Vulnerability Class: Medium*) are represented, by the mouths of main rivers, i.e. Fortore River, at the north westernmost part of the region, and the Ofanto River. However, a number of relict valleys showing at the present their mouth below present sea level and at present constituting small inlets must be also taken into account (Brindisi inlet, Otranto inlet). This class comprises also main beaches attached directly to mainland; it covers about 16 % of the Apulian coastal perimeter. Furthermore, coastal tracts made by low gentle platforms sensible to tsunami action (*Vulnerability Class: Low*) are very diffuse along the Adriatic coast of Apulia, from Barletta to Otranto, and on the Ionian one, from Leuca to Taranto. In the same vulnerability class are retreating cliffs which mark some spots of Gargano Promontory, Bari province and Salento Peninsula. This class of vulnerability is the most diffuse since it covers about 42 % of the Apulian coast. Finally, convex rocky coasts, potentially prone to tsunami action (*Vulnerability Class: Very low*), are diffuse along the coast of Gargano Promontory and in the Salento Peninsula for about 15 % of the Apulian coastal perimeter.

7.1.8. Conclusions

The definition of the tsunami risk along a coast prone to this low frequency-high magnitude events is based on the assessment of hazard, linked to the frequency and intensity of tsunami events, of coastal vulnerability to tsunami and of demographic and

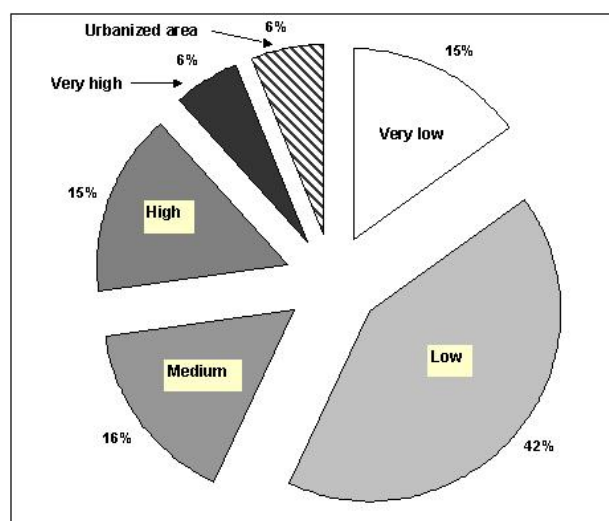


Figure 7.4 - The frequency distribution of tsunami vulnerability classes along the Apulian coast

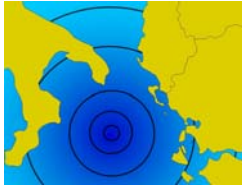
land value distribution as well. Most of research is at present focused on the definition of tsunami hazard whereas study about the vulnerability are still very few.

The shown methodology define the vulnerability of different coastal morphological types which compound the Apulian coastal landscape basing on the analysis of available post-event reports integrated with the geological data about the modifications produced by recent and past tsunami in the coastal landscape. In summary, the analysis of vulnerability class distribution along the Apulian coast (Fig. 7.4) shows that more than half of the Apulian coastal perimeter is marked by a very low or low vulnerability to tsunami action (57 %) whereas about a quarter (21 %) shows a high or very high vulnerability.

This study should represent a step towards the risk assessment of the Apulian coast which is not negligible. In fact, notwithstanding this region has been struck several times by destructive tsunamis in historical times, it is extensively urbanized and densely populated. Notwithstanding, no early warning systems exist, no evacuation plans have been realized, no first aid intervention has been planned but mainly any educational activity toward the population on tsunami event has never been realised.

IONIAN ISLAND FIELD TRIP

26-27 September 2008



**CHAPTER
8**

**Geomorphological, sedimentological and
geoarchaeological traces of Holocene tsunami impact
between Lefkada and Lake Voulkaria (NW Greece)**

Vött A., Brückner H., May S.M.

8.1. Around the Sound of Lefkada

The Lefkada-Preveza coastal zone is directly exposed to the northern part of the Hellenic Trench, especially to the Cefalonia (CF) and Lefkada (LF) transform faults (Fig. 8.1). The Hellenic Trench represents the border between the African Plate in the southwest and the Aegean Microplate as part of the Eurasian Plate in the northeast. Due to the westward pressure of the Anatolian Plate, the Aegean Plate is being forced to move in a southwestward direction by up to 35 mm/a, hereby overriding the African Plate along the Hellenic Trench subduction zone (Haslinger et al., 1999; McClusky et al., 2000; Doutsos & Kokkalas, 2001). The Hellenic Trench, together with major fault systems in the Aegean and western Anatolian regions, represents the seismotectonically most active structure in the Mediterranean (Fig. 8.2, see Papazachos & Papazachou, 1997). As an example, during the month of February 2008, the Institute of Geodynamics of the National Observatory of Athens, registered some 991 earthquakes stronger than M 1.5 most of which occurred along the Hellenic Trench between the Island of Corfu (Kerkyra), the Peloponnese and Crete (Fig. 8.3). A major earthquake of M 6.7 occurred on February 12, 2008 only a few kilometers off the coast near Methoni (USGS 2008).

Based on the geotectonic and seismological constellations, the shores of the eastern Ionian Sea are subject to strong tsunami hazard (Fig. 8.4). Tsunami catalogues for the Mediterranean basin show the highest numbers of tsunami landfalls for this region (Papazachos and Dimitriu, 1991). Based on statistical analyses, the west coast of Greece between the Ionian Islands and the southern Peloponnese is characterized by a re-occurrence interval for tsunami events of 8 to 11 years only (Soloviev et al., 2000; Vött et al., 2006a; Schielein et al., 2008).

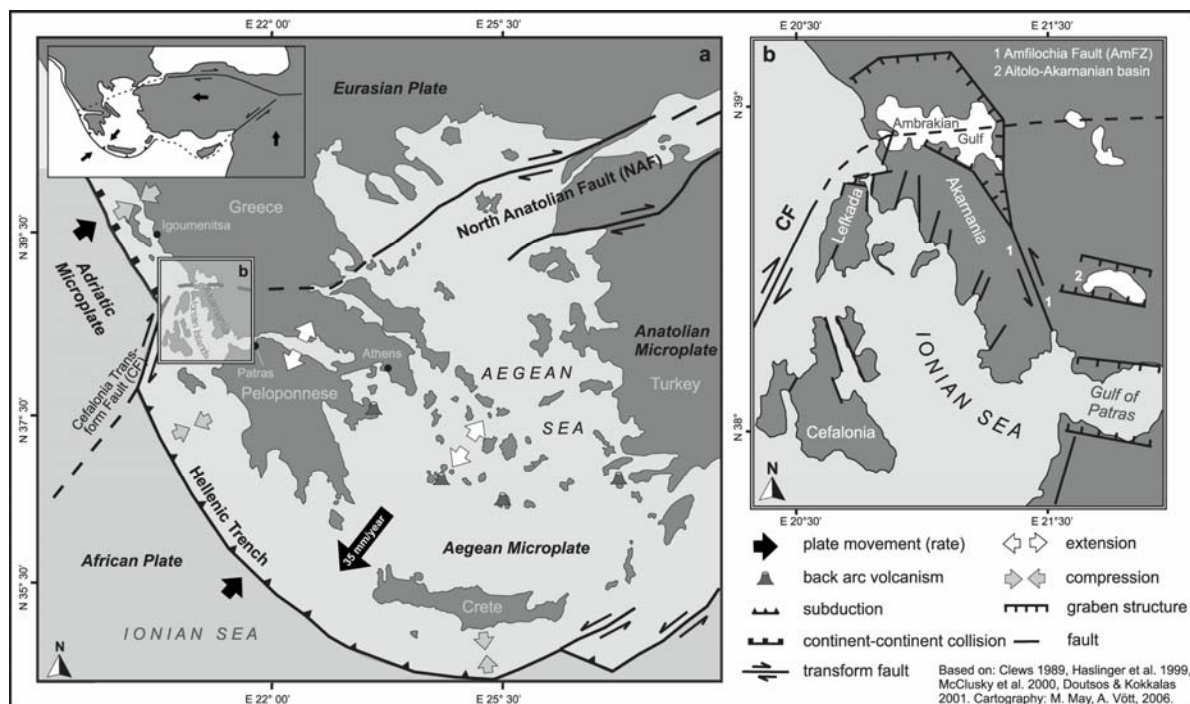


Figure 8.1 - The Hellenic Trench – predominant factor in the geotectonic constellation of the eastern Mediterranean.

The last major earthquake which affected the Lefkada-Preveza coastal zone took place on August 14, 2003 reaching a magnitude of M 6.3. The earthquake was due to an activation of the Lefkada transform fault (Karakostas et al., 2004; Papadopoulos et al., 2003; Papathanassiou et al., 2005; Papadimitriou et al., 2006). A small 0.5 m tsunami was observed in the Bay of Vlychos south of Nidri (EERI, 2003).

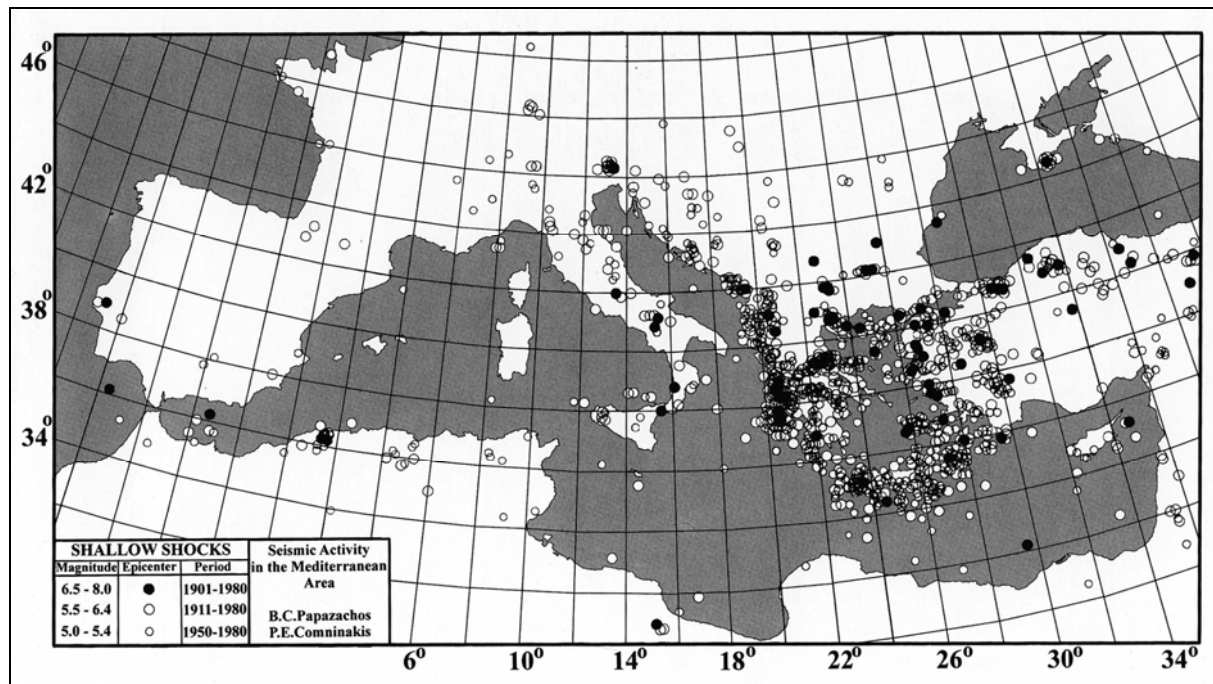


Figure 8.2 - Geographical distribution of 20th century shallow earthquakes in the Mediterranean region. From Papazachos & Papazachou, 1997.

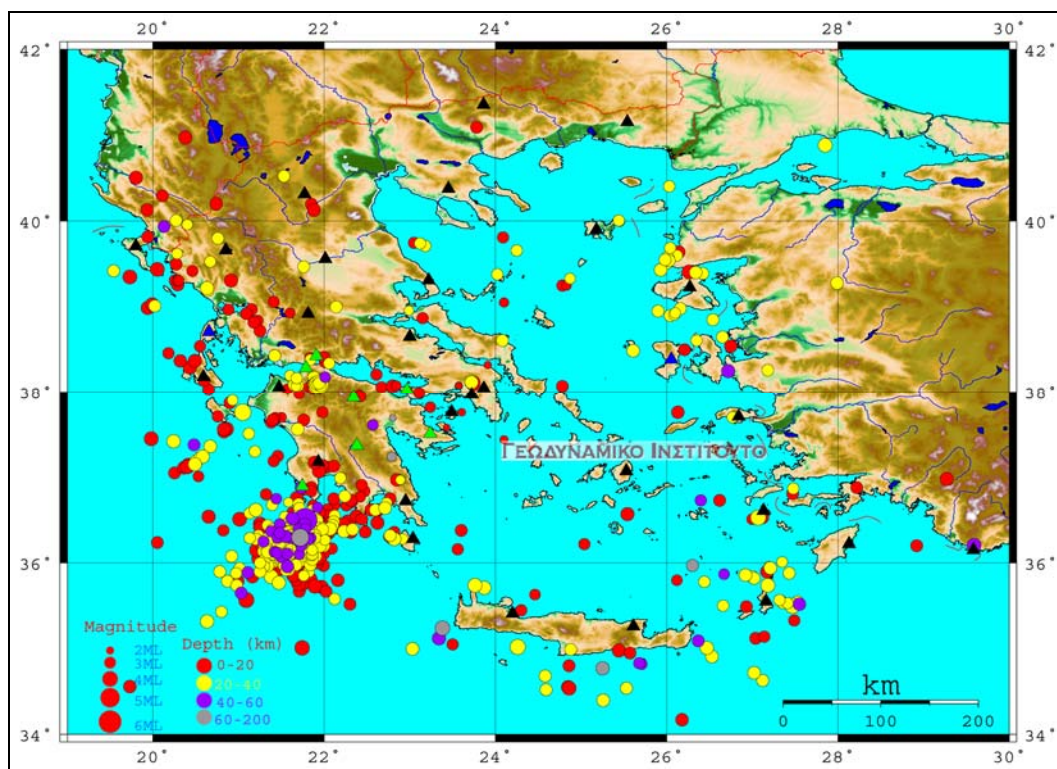


Figure 8.3 - February 2008 earthquakes in the Ionian and Aegean Seas registered by Greek seismological stations (N = 991 > M 1.5). Please note the M 6.7 earthquake from February 14, 2008 and accompanying shocks offshore Methoni, southern Peloponnese. From National Observatory of Athens, Institute of Geodynamics, 2008 and USGS, 2008.

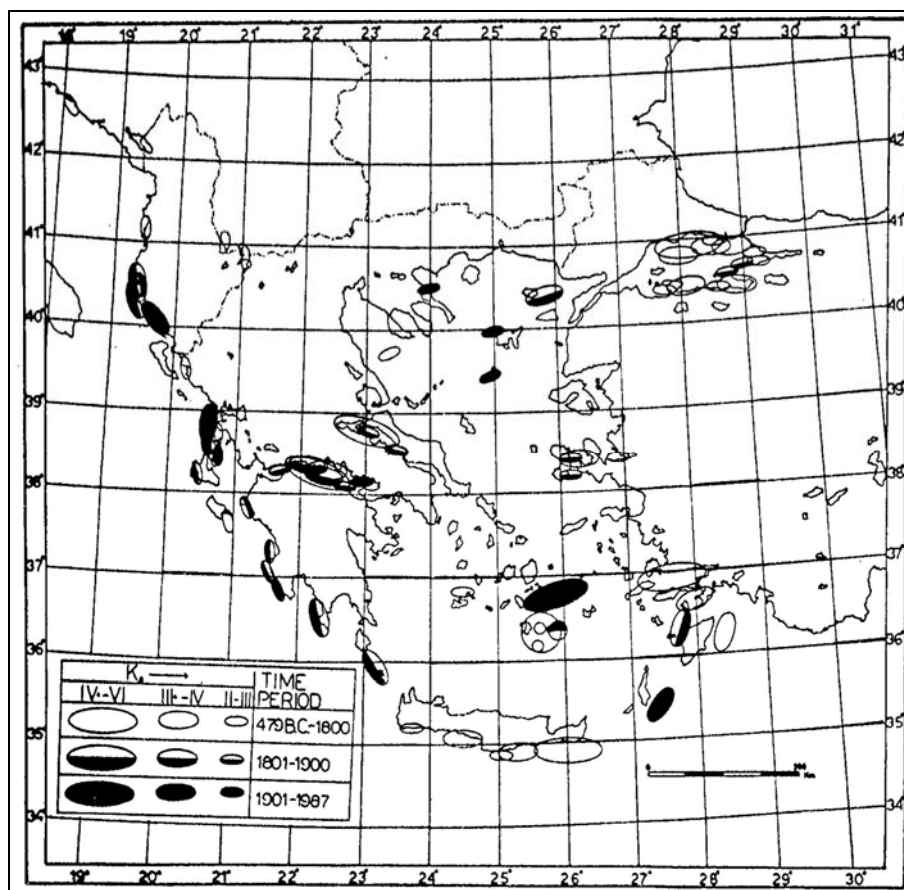


Figure 8.4 - Tsunamigenic zones along the Greek and Turkish coasts of the Ionian and Aegean Seas based on tsunami catalogues and inferred estimation of tsunami hazard. K_0 is the estimated maximum tsunami intensity on the 6-degree Sieberg-Ambraseys scale. From Papazachos & Dimitriou, 1991.

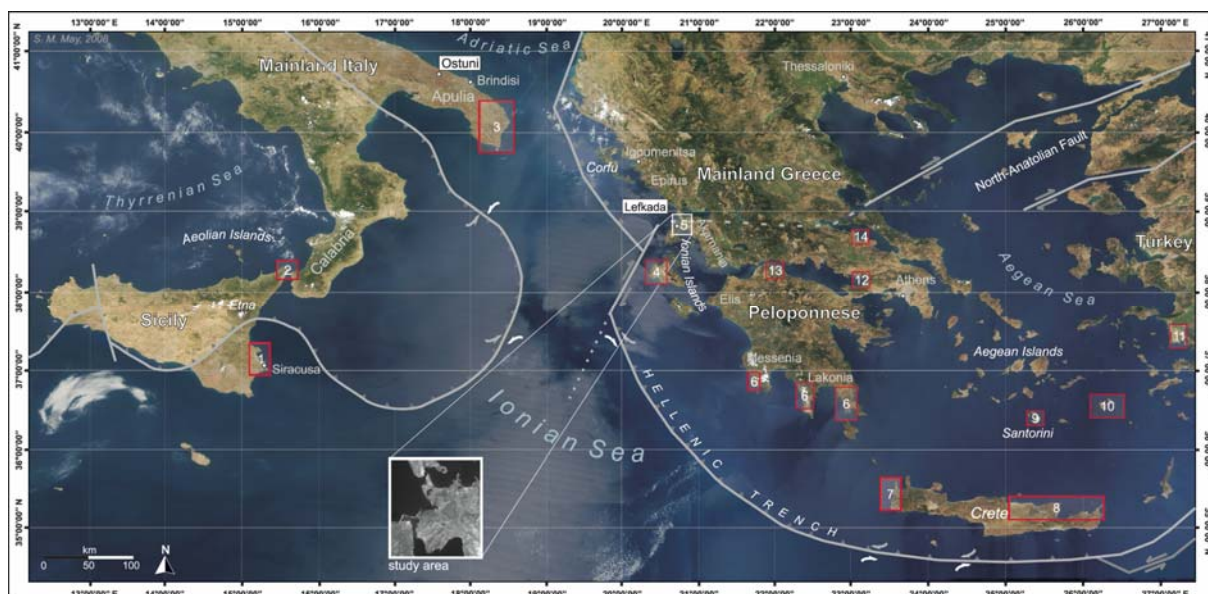


Figure 8.5 - Topographic overview of the region around the Adriatic and Ionian Seas showing the conference venue of Ostuni, the field trip areas in southern Italy (Apulia) and northwestern Greece (Ionian Islands, Lefkada-Preveza coastal zone). The map also summarizes selected publications on tsunami landfalls during the Holocene along the coasts of southern Italy and Greece and western Turkey.

Site indices: 1 – Scicchitano et al., 2007; 2 – Pantosti et al., 2008; 3 – Mastronuzzi & Sansò, 2000, Mastronuzzi et al., 2007; 4 – Vött et al., unpubl.; 5 – Vött et al., 2008a, 2008b; May et al., 2007; 6 – Scheffers et al., 2008; 7 – Scheffers & Scheffers, 2007; 8 – Bruins et al., 2008; 9 – McCoy & Heiken, 2000; 10 – Dominey-Howes et al., 2002; 11 – Minoura et al., 2000; 12 – Kortekaas, 2002; 13 – Kontopoulos & Avramidis, 2003; 14 – Cundy et al., 2000.

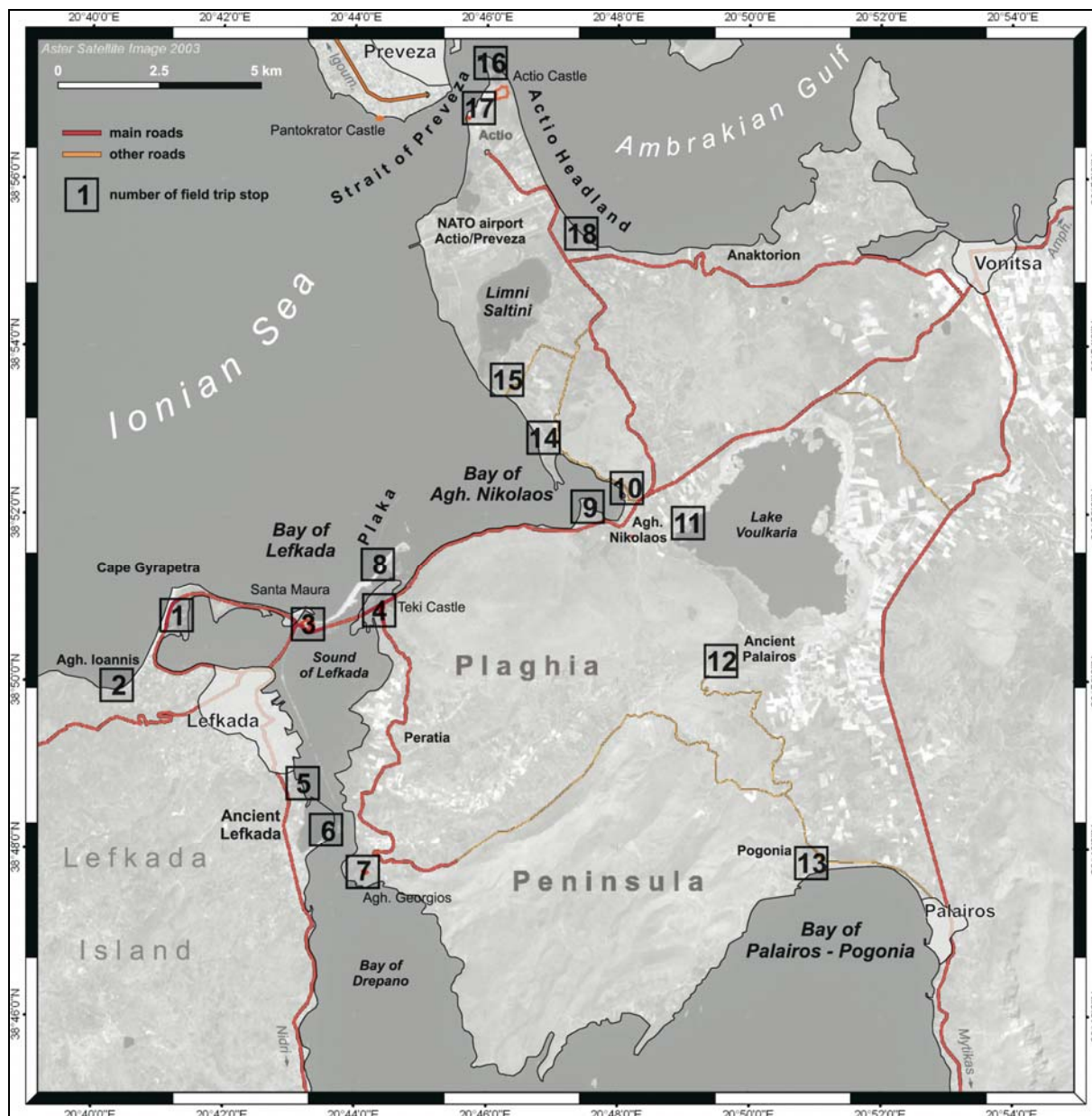


Figure 8.6 - Topographical overview of the Lefkada-Preveza coastal zone (Ionian Islands, NW Greece) and location of stops during the field trip.

Sedimentological, geomorphological and geoarchaeological evidence of (palaeo-) tsunami landfall along the Greek shores of the eastern Ionian Sea was first described by Vött et al. (2006a, 2007a, 2007b, 2008a, 2008b) for some 25 km of coastline between the cities of Preveza and Lefkada as well as for the Sound of Lefkada (Figs. 8.5 and 8.6).

8.1.1. The Gyrapetra chevron: STOP 1

The Gyrapetra chevron is located in the northwestern part of the Sound of Lefkada. The sound is closed off from the open Ionian Sea by a beach ridge system which evolved along major SSW-NNE and ESE-WNW running fault lines. The lagoonal waters of this part of the sound are extremely shallow with water depths < 30 cm. The longitudinal axis of the chevron trends in a NNW-SSE direction. The subaerial part of the triangle-shaped washover fan is up to 1.2 km long and continues for some hundreds of meters under water (Fig. 8.7). Vibracores drilled on top of the chevron (LEF 1, LEF 22) show sandy to gravelly deposits, up to 1.5 m thick and full of shell debris, covering homogeneous lagoonal mud. Core LEF 22 gives additional evidence of an older extreme event represented by a sandy intercalation, 50 cm thick, in the lower part of the core. In each core, the base of the sequence is made up of beachrock.



Figure 8.7 - The Gyrapetra tsunami chevron near Lefkada (NW Greece) as seen from the road to Tsoukalades near the Faneromenis Monastery. Photo by A. Vött, 2006.

Sea weed remains from the lower part of the tsunamigenic sequence at LEF 1 were dated to 387-472 cal AD rendering a terminus ad or post quem for the youngest tsunami landfall (Vött et al., 2006a). Towards the east, several smaller chevrons as well as the large Canali Stretti washover plain indicate further tsunamigenic influence.

Best view of the Gyrapetra chevron is given from the Faneromenis Monastery and the road to Tsoukalades.

8.1.2. The Bay of Aghios Ioannis: STOP 2

In the eastern part of the Bay of Aghios Ioannis, a notch is developed in the outcropping limestone bedrock at present sea level. The roof of the notch reaches up to approximately 1 m above sea level (m a.s.l.). Pirazzoli et al. (1994) interpreted the notch therefore as indicator for a phase of Holocene sea level slightly higher than the present one.

A similar notch can be observed in the neighbouring Bay of Skala Gialou to the north of Tsoukalades. In both cases, the notch is fully exposed to open marine wave dynamics and associated to pebbly deposits. It is therefore suggested that the notch is rather due to littoral erosion by cobbles and pebbles than to bio-erosive activity, and that the notch can be completely explained by the currently prevailing mid-to high-energy processes especially during winter storms. We thus refrain from using the notch as reliable sea level indicator.

At Cape Aghios Ioannis, however, we found *Lithophaga* sp. boreholes and corals up to 12.55 m a.s.l., dated by electron spin resonance technique (ESR) to $113,000 \pm 9,000$ BP (ESR-laboratory at the Department of Geography, Universität zu Köln). These findings document considerable uplift since the last interglacial sea level highstand (Fig. 8.8).

There is no reliable evidence that relative sea level during the Holocene has ever been higher than at present. In contrast, vibracore data and submerged archaeological remains such as the mole of the Corinthians, the necropolis of ancient Lefkada, a Hellenistic to Roman bridge across the sound as well as several submerged brick-kilns indicate that there is no general difference in sea level evolution between the Lefkada-Preveza coastal zone and coastal Akarnania (see Vött, 2007). Relic signs of gley-related oxidation found in sedimentary sequences fairly below present sea level also suggest a former sea level lowstand; their good conservation further indicates that the corresponding sites may have come into their present position by co-seismic submergence.



Figure 8.8 - MIS 5.5 corals and boreholes of boring mussels at Cape Aghios Ioannis some 3.5 km to the west of Lefkada city. The palaeo sea level indicators reach up to 12.55 m a.s.l. thus indicating considerable coastal uplift during the 120,000 or so years.

8.1.3. Santa Maura Castle and the mouth of the modern channel: STOP 3

The Castle of Santa Maura is located at the present mouth of the navigable channel across the Sound of Lefkada and on top of the beach ridge facing the open Ionian Sea. A first navigable channel across the lagoonal waters is reported to have been excavated by Corinthian settlers in the 7th century BC (Murray, 1982). In antiquity and at least until medieval times, the sound was entered via the Bay of Aghios Nikolaos and the Canali Stretti (Fig. 8.6). In 1844, the British administration of Lefkada Island dredged a new channel between the city of Lefkada and the artificial breakthrough near the Castle of Santa Maura. Later, in 1902/03, the Greek authorities restored the British channel and excavated a second one from the city towards the south where a breakthrough across the spit of Alexandros was realized (Partsch, 1889; von Marées, 1907; Naval Intelligence Division, 1944; Papadatou-Giannopoulou, 1999).



Figure 8.9 - Detail of historic map showing the Battle of Lefkada between the Venetian forces under Francesco Morosini and the Turkish occupying forces between July 23 and August 7, 1684. Please note parts of the Canali Stretti tsunamigenic washover plain to the east of the castle of Santa Maura. The coastline configuration shown to the west of the fortress considerably differs from the present situation. The Gyrapetra chevron is not depicted in the map; this may be due to the more simplistic illustration of the topography of this lateral part of the Sound of Lefkada.

Several vibracores were drilled to the immediate east of the fortification walls of Santa Maura and revealed similar sequences as observed in the landward position of Cape Gyrapetra: up to 2 m-thick layers of gravel lie on top of homogeneous clayey silt which was deposited under lagoonal conditions. Along the southern fringe of the beach ridge, these gravel deposits are covered by a thin layer of silty lagoonal or marsh deposits.

The gravelly high-energy deposits go hand in hand with geomorphological washover structures and thus indicate a sudden and temporary change of sedimentary conditions. In general, radiocarbon-dating of tsunami deposits is difficult as they may comprise reworked material. In this case, we know that the Castle of Santa Maura was built by the Venetian family of Orsini around 1300 AD. This date gives the most reliable terminus ante quem for the tsunami event because the fort was erected on top of the corresponding tsunami deposits (Fig. 8.9).

8.1.4. Teki Castle and the Canali Stretti washover plain: STOP 4

The Teki castle was built by the Turkish occupying force between the 15th and 17th centuries AD at the eastern shore of the Sound of Lefkada. From its walls there is a great view of the beach ridge and the washover fans entering into the shallow lagoonal waters of the Sound. A large washover fan lies approximately 1 km to the north of the castle showing a NW-SE trending longitudinal axis and a total length of approximately 500 m. Smaller fans, each of them almost 300 m long, can be observed to the NW and W of the castle.

A series of vibracores along the narrow waterway behind the present beach ridge revealed that the marshy grounds, which extend into the sound towards the south some 700-1000 m distant from the present shore, are based on a sheet of sandy deposits which discordantly overlie thick lagoonal sediments. These sandy deposits include remains of micro- and macrofaunal associations adapted to open water conditions. We thus interpret this sand sheet as part of a large washover plain running behind the present beach ridge from NE to SW with a total length of 2.2 km (Vött et al., 2008b). Articulated specimens of *Dosinia exoleta* found at the base or in between tsunami deposits from cores LEF 2 and 4 as well as roof tile fragments cemented in dislocated beachrock plates date to Classical-Hellenistic times. The Canali Stretti represents an artificial channel which was excavated across the plain during some time after the 3rd century BC (Vött et al., 2008b) and which served as entrance to the sound until the 19th century AD (Figs. 8.9 and 8.10).

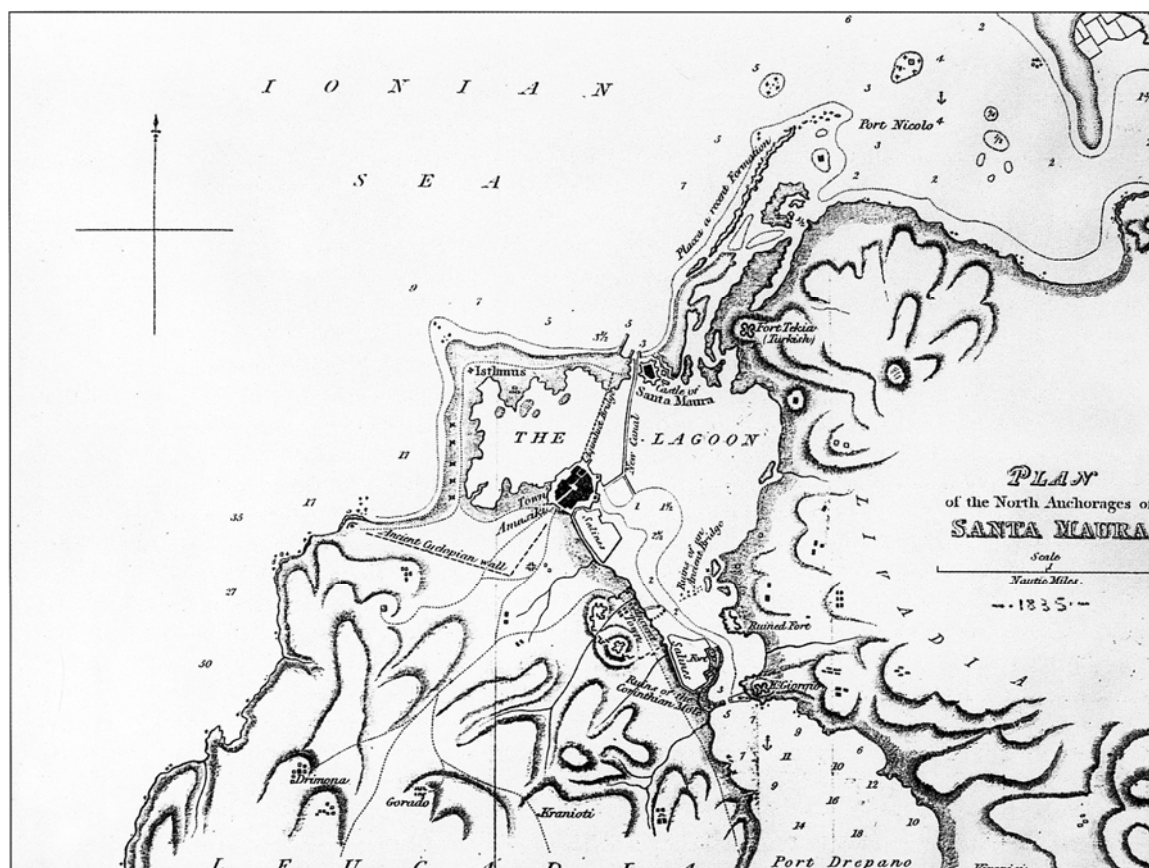


Figure 8.10 - Historic map of the Sound of Lefkada showing the topography in 1835. The map was drawn by the British Captain R.N. Smyth. From Papadatou-Giannopoulou, 1999.

8.1.5. The central Sound of Lefkada near the ancient bridgehead: STOP 5

In antiquity, the central Sound of Lefkada was spanned by a bridge, approximately 750 m long, which connected Lefkada Island with the Plaghia Peninsula in Akarnania. Only few archaeological remains of this bridge are still visible, such as parts of a west and an east tower (Fig. 8.10). Dredging for the Greek canal across the sound in 1902/03, however, revealed vault stones dating to Hellenistic to Roman times. The fact that large parts of the bridge are nowadays submerged and, at the same time, covered by sediments proves that the relative sea level at the time of its use was considerably lower than at present. Négris (1903, 1904) reconstructed the corresponding palaeo sea level at 2.80-3 m b.s.l. Moreover, during the same dredging works numerous tombstones, well preserved in between lagoonal mud, were found to the east of ancient Lefkada (Kolbe, 1902). It thus seems as if at least parts of the central sound around the discovered ancient necropolis were dry land before they got submerged by the lagoonal waters of the sound (Brockmüller et al., 2007).

Around 50 vibracores were drilled at both sides of the sound as well as on top of a dam out of excavated material along the eastern side of the Greek channel of 1902/03 (also in our days, the latter is dredged regularly to maintain its navigability). Sediment cores from the central inner sound show the following stratigraphic sequence: the base is made up of terrestrial (palaeosol) or stiff limnic deposits. In some places, the latter show slight influences of saltwater in their upper part. Subsequently follow, on top of a subsequent sharp erosional disconformity, mostly coarse sandy to fine gravelly deposits including marine shell debris and, from time to time, ceramic fragments. The coarse layer is then covered by clayey to silty lagoonal mud. This mud layer may be interrupted another 3 to 4 times by layers of coarse-grained marine material.

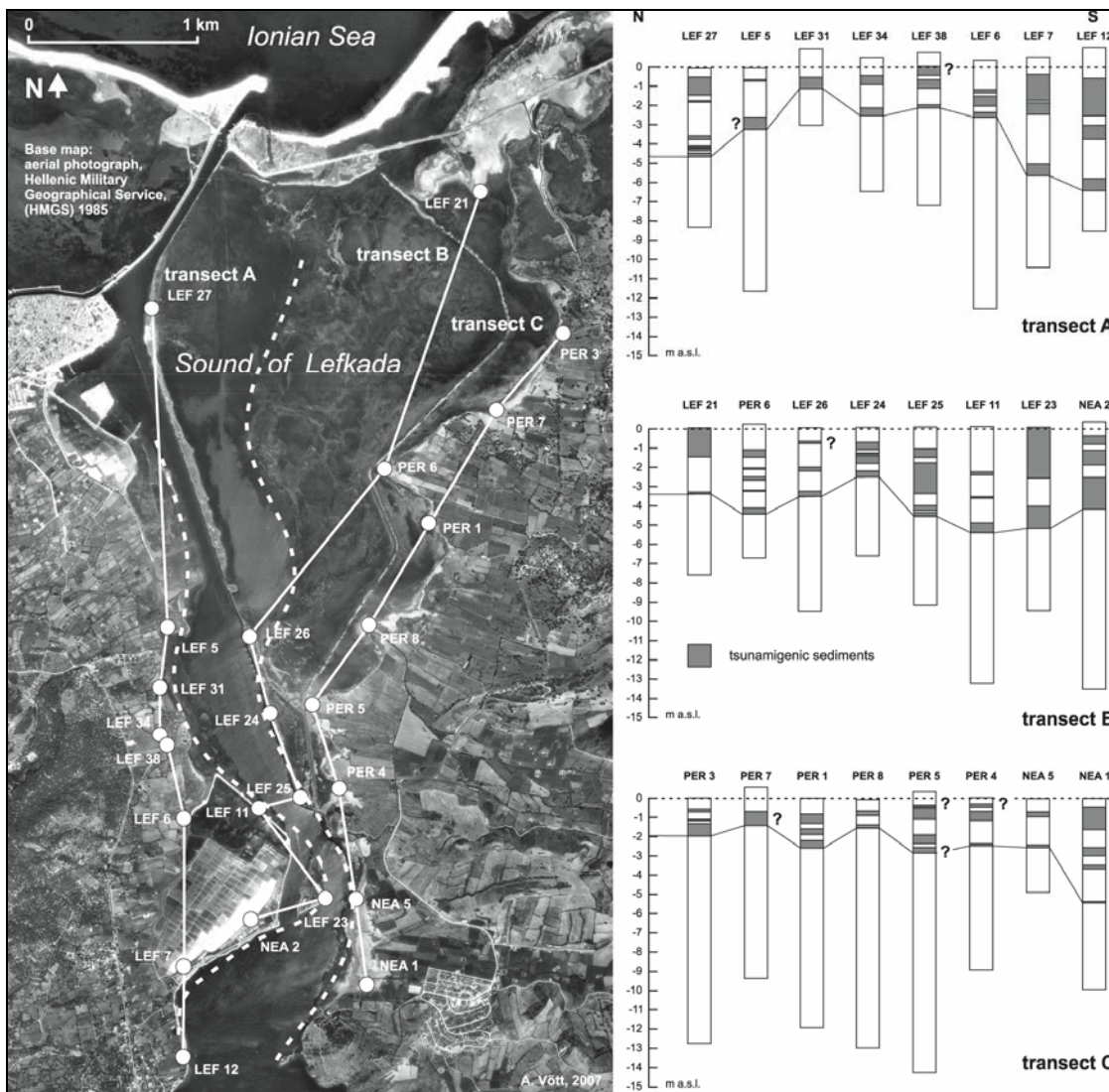


Figure 8.11 - Simplified logs for 24 selected vibracores from the Sound of Lefkada showing tsunami deposits (shaded in grey). Vibracoring was realized in three N-S-trending transects. From Vött et al., 2008b.

The uppermost layer is in turn made up of clayey silt and corresponds to the present sedimentary conditions in the shallow waters of the sound. Besides the artificial channel, water depth in the inner sound does not exceed 0.3 to 0.7 m (von Marées, 1907). Based on micro- and macrofaunal and geochemical studies as well as on the analyses of thin sections, the mentioned coarse-clastic intercalations in between the autochthonous lagoonal mud deposits are interpreted as allochthonous tsunami deposits (Vött et al., 2008b) indicating that tsunami waters hit the the area from the north and partly flowed through the sound. These deposits may neither be explained by the present sedimentary conditions in the sound, nor by anthropogenic impact, nor by the influence of storms as storm are not able to reach inner sound areas some 3 and more kilometers away from the open sea. Geochronological studies showed that tsunami influence on the Sound of Lefkada started at least around 2800 cal BC, eventually already in the 6th millennium BC (Vött et al, 2008b). The stratigraphic sequences from the inner sound reveal at least 4 different major tsunami events, one of which corresponds to the impact during Classical-Hellenistic times (Fig. 8.11). Geoarchaeological analyses of vibracores from the shores of the sound indicate that at least parts of the ancient city of Lefkada were flooded and destroyed by this event; contemporaneous co-seismic or subsequent continuous submergence may further explain the abandonment of the ancient necropolis.

8.1.6. The southern Sound of Lefkada near Alexandros spit: STOP 6

In the south, the Sound of Lefkada is closed off from the Bay of Drepano by the spit of Alexandros (Fig. 8.12). This spit is approximately 1.1 km long and extends into the sound in a SW-NE direction. It was cut into two pieces during the excavation of the Greek channel in 1902/03. Before that time, a natural meander-like channel formed a narrow, 250 m-wide water strait between the Alexandros spit and the Plaghia Peninsula. This meandering channel started in the inner sound at the southern outskirts of the modern city of Lefkada and is recognizable in historic topographic maps (Parsch, 1889; von Marées, 1907) and aerial photographs. The old saltworks of Lefkada, used until the beginning of the 20th century, were located to the immediate north of the spit.

Several vibracores along the spit of Alexandros and at the eastern fringe of the former saltworks revealed stratigraphies similar to the ones discovered in the inner sound. Terrigenous deposits and a basal palaeosol are covered by a thick layer of sediments accumulated under limnic to slightly brackish, quiescent conditions. Then follows, on top of a sharp erosional unconformity, a thick layer of allochthonous coarse-grained deposits including marine shell debris.



Figure 8.12 - View into the Sound of Lefkada from the Castle of Aghios Georgios. The left middleground shows the Alexandros spit which is cut through by the Greek channel excavated in 1902/03. Also note the transgressive character of the waters of the sound, for instance along the shores of Nea Plaghia in the right middleground. Photo by A. Vött, 2005.

Subsequently established shallow marine conditions towards the south and lagoonal conditions towards the north. We thus interpret the present Alexandros spit to be formed out of littorally reworked tsunami deposits which were transported across the sound from northern direction (Vött et al., 2008b). Our vibracores revealed multiple passage of high-energy water masses across the sound which is expected to have strongly affected the navigability of the water strait during historic times (Vött et al., 2008c).

8.1.7. The castle of Aghios Georgios at Nea Plaghia: STOP 7

The large castle of Aghios Georgios is located at the southern end of the sound at the eastern shore of the Sound of Lefkada and to the southeast of the spit of Alexandros. Early fortification facilities date to Classical times (Lang et al., 2007). The fortress in its present form was erected by the Venetians in late Medieval times and re-used by Turkish, British, French and Russian occupying forces. From its walls, there is an intriguing view of the sound (Fig. 8.12). Looking at the shore near Nea Plaghia, it can be discerned that sea level is currently rising and slowly intruding landwards. In the inner sound, there are tidal differences of 20-40 cm; northern winds may enhance these differences by blowing out the water towards the south.

The village of Nea Plaghia was founded at the southeastern shore of the sound in the 1950s, after the preceding village of (old) Plaghia, situated at the foot of a large thrust fault scarp some 4 km to the NE, was almost completely destroyed by an earthquake in 1953.

8.2. The Bay of Aghios Nikolaos and the Lake Voulkaria

8.2.1. The Plaka beach ridge ruin: STOP 8

The beach ridge which separates the Sound of Lefkada from the open Ionian Sea shows some outstanding geomorphological features. Approximately 1.5 km to the NE of the castle of Santa Maura, the present beach ridge makes a sharp curve to the east before re-adjusting to the general SSW-NNE direction. At this point, the overall base of the beach ridge, made out of thick layers of beachrock, directly continues towards the NNE but is completely void of any loose beach material (Fig. 8.13).

Obviously, the beachrock structure of the so called Plaka is the ruin of a former beach ridge. This palaeo strandline can be traced some 7.5 km further towards the NNE where it approximates Actio Headland.



Figure 8.13 - The beach ridge some 1.5 km to the NE of Santa Maura Castle where the present shoreline separates from the Plaka beachrock. The Plaka represents a palaeo shoreline and is characterized by dislocated beachrock slabs and blocks lying on top of its surface. These blocks are partly imbricated. Corresponding block accumulations and rubble ridges were also found during geomorphological underwater surveys to the east of the Plaka. Photo by A. Vött, 2007.

The southeastern, best preserved subaerial part of the Plaka is almost 2.2 km long; further towards the NNE, the Plaka lies partly under water and is in some places interrupted. The surface of the Plaka is characterized by many dislocated blocks out of beachrock, partly turned upside down (with bio-erosion features facing towards the bottom) and partly imbricated (Vött et al., 2006a). Underwater geomorphological surveys immediately east of the Plaka revealed similar block associations under water as well as ridges out of beachrock plates, the plates showing diameters up to 1 meter (Vött et al., 2007a, 2008a). Dislocated mega blocks are up to 15 m³ large, some of them broken into pieces and/or lying surrounded by and on top of fine sand deposits.

Block dislocations along the Plaka, both above and under the present water level, are due to repeated tsunami influence. Multiple tsunami wave action has destroyed the palaeo beach ridge, blew the loose beach ridge material into the Bay of Aghios Nikolaos, tore out parts of the beachrock base and catapulted blocks and plates towards the east. Shallow test corings in the profundal zone of the adjacent Bay of Aghios Nikolaos revealed silty to clayey lagoonal deposits interrupted by a thick sand layer including large amounts of shell debris (Vött et al., 2008a). Dating of the dislocated blocks themselves is problematic and will be approached by surface exposure dating techniques. Dating of tsunami-borne facies changes in nearby cores yielded strong tsunami influence to the Plaka at least during the late Bronze Age, during Classical-Hellenistic times, around 840 cal AD and 1000-1300 cal AD (Vött et al., 2006a, 2007a, 2008a).

8.2.2. The Cheladivaron Promontory: STOP 9

The Cheladivaron Promontory closes off the quiescent and, during summertime often stinky (H₂S), waters of the Bay of Cheladivaron from the outer Bay of Aghios Nikolaos. The surface of the promontory is irregularly scattered by numerous blocks and stones out of limestone. Most of the blocks, up to 1 m large, are characterized by boreholes and other bio-erosion features indicating that the material originates from the littoral zone. Even the highest parts of the promontory, up to 14.80 m a.s.l., are densely covered by allochthonous blocks and stones (Fig. 8.14). The remains of a boring mussel encountered in a dislocated stone at 14.80 m a.s.l. were dated to 947-1021 cal AD and present a terminus ad or post quem for the corresponding tsunamigenic extreme wave event. Unfortunately, the terrain surface was bulldozered during recent construction works for a holiday resort; many geomorphological findings are thus destroyed.

A series of 13 vibracores were drilled at the western and eastern shores of the promontory. We found the following general stratigraphic sequence: terrestrial deposits plus palaeosol show an erosional disconformity and are abruptly covered by a thick layer of marine deposits.

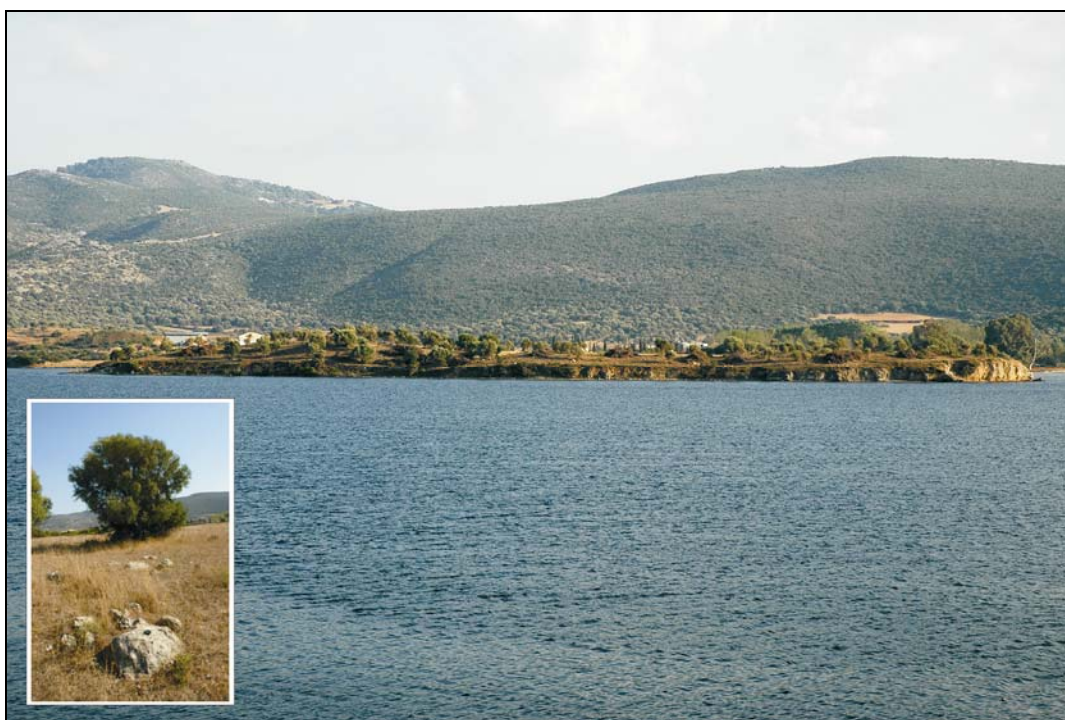


Figure 8.14 - The Cheladivaron Promontory in the Bay of Aghios Nikolaos. In contrast to the present situation characterized by low-energy littoral dynamics, the promontory shows a steep cliff at its western and northern sides. Its surface, up to 14.8 m a.s.l., is covered by scattered stones and blocks. Due to bio-erosive features this material was dislocated from the littoral zone. Photo by A. Vött, 2007.

The latter are characterized by an upward increase in sorting and a clear fining upward sequence; moreover, they are thinning in a landward direction (see Vött et al., 2008 for further sedimentological criteria typical of tsunami deposits). We thus interpret these deposits as of allochthonous nature. The uppermost part of the marine deposits are subaerially weathered and bear well developed soils. Diagnostic ceramic fragments encountered at the base of the high-energy marine deposits date to Classical-Hellenistic time. A nearby earthen cistern revealed a twofold high energy input; the first one is associated with the mentioned erosional unconformity and shows a distinct layer of imbricated ceramic fragments dating to Classical-Hellenistic times; the second one – separated from the lower generation by a palaeosol unit – corresponds to the superficial findings of dislocated blocks and stones and is dated to late medieval times (Vött et al., 2008a). Along the western shore of the promontory, a bedrock outcrop at approximately 5 m a.s.l. is superficially covered by a carbonate crust which contains numerous shell fragments and marine clasts. In lower positions but still some decimeters above sea level, the lower part of the crust is made up of a thick sand unit which seems to correspond to the allochthonous sand layer encountered in adjacent vibracores; the upper part of the crust also contains angular stones of terrigenous origin. The cementation of the tsunami-borne material by calcium carbonate was initiated by subaerial weathering and, at least partly, under a soil cover.

8.2.3. The inner Bay of Cheladivaron and the ancient watchtower at Vigla: STOP 10

Present day sedimentary conditions in the inner Bay of Cheladivaron are characterized by the deposition of silty clay in a quiescent water body.

This water body is almost completely sheltered from wave dynamics by the Plaka beach ridge ruin, the Cheladivaron Promontory, and the Phoukias sand spit which extends into the Bay of Aghios Nikolaos from a northern direction. A nice view of the inner bay area is possible from the ancient Vigla watchtower just above Aghios Nikolaos (Fig. 8.15). During periods of hot summer temperatures, the Bay of Cheladivaron sometimes shows anoxic conditions resulting in the formation of hydrogen sulfide (H₂S) by sulfur bacteria. Close to the present harbour mole of Aghios Nikolaos and at the northern shore of the bay, we encountered several sequences of coarse-grained, allochthonous marine sediments deposited on top of an erosional disconformity developed in terrestrial material (palaeosol). The oldest extreme event was dated to around 1000 cal BC (Vött et al., 2006a); at least two major events, separated by a younger palaeosol, occurred during the last 1000 or so years (around 1000 cal AD and around 1400 cal AD, Vött et al., 2007a and unpublished data). The allochthonous marine deposits show an upward increase in sorting and a laminated structure and also include rip-up clasts of the underlying terrigenous material. They are interpreted as tsunamigenic runup and/or backwash deposits.



Figure 8.15 - View to the NW to the inner Bay of Aghios Nikolaos (= Bay of Cheladivaron) from the ancient watchtower at Vigla. The left middleground shows the Cheladivaron Promontory and, opposite to it, the Phoukias sand spit. Photo by A. Vött, 2007.

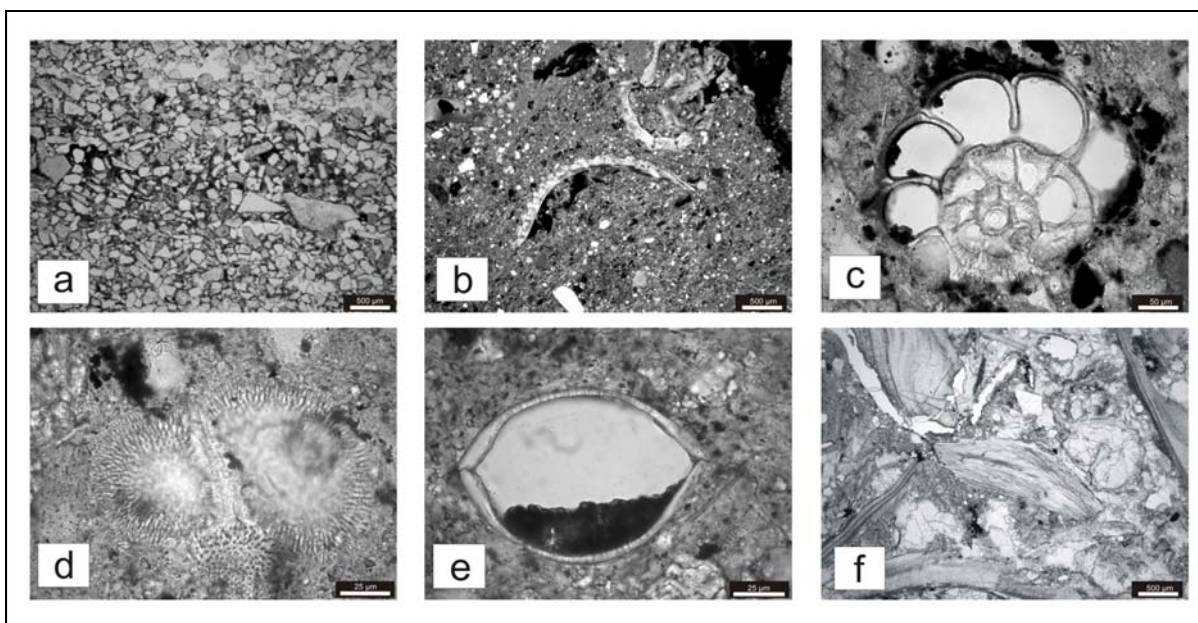


Figure 8.16 - Thin section photographs of samples from trench ANI NBU L2 excavated approximately 80 m inland from the northern shore of the Bay of Cheladivaros at 7.06 m a.s.l. (a) angular components in the upper part of the profile (ANI NBU L2/1 DS, 0.10-0.15 m b.s.), (b) fragments of marine molluscs (ANI NBU L2/2 DS, 0.18-0.23 m b.s.), (c) specimen of a benthic foraminifera (order: Rotaliina, ANI NBU L2/2 DS, 0.18-0.23 m b.s.), (d) specimen of a planctonic foraminifera (*Globigerina* sp., ANI NBU L2/2 DS, 0.18-0.23 m b.s.), (e) specimen of an undetermined ostracod (ANI NBU L2/3 DS, 0.25-0.28 m b.s.) and (f) carbonate crust with fragments of marine molluscs (ANI NBU L2/4 DS, 0.30-0.33 m b.s.). From May et al., 2007.

Tsunami sediments, partly encrusted, were also found intercalating terrestrial sediments and palaeosols in landward positions up to 7.06 m a.s.l. including shell debris and remains of foraminifers (Fig. 8.16, May et al., 2007). Thick layers of coarse-grained sediment clasts were also retrieved by shallow coring from the inner Bay of Cheladivaros. These allochthonous deposits discordantly cover autochthonous clayey to silty mud, the latter corresponding to the modern sedimentary environment of the bay.

8.2.4. The Cleopatra Canal and the Lake Voulkaria: STOP 11

The Bay of Cheladivaros is separated from the Lake Voulkaria by a bedrock sill reaching 5-18 m a.s.l. Jahns (2005) and Vött (2007b) showed that the Lake Voulkaria has developed as a freshwater environment in a polje-like tectonic graben situation since the early Holocene. An artificial channel, the so called Cleopatra Canal, connects the bay with the lake and is reported to have been built during Hellenistic to Roman times (Lang, 2007, pers.comm.). Vibracore studies at the western shore of the lake revealed an up to 2 m-thick package of sand and gravel including marine shell fragments on top of homogeneous lake-deposits (Vött et al., 2006a). In some cores, the coarse-grained layer is covered again by sediments of a swampy to limnic environment. Composition, texture and thickness of the encountered material indicate that it was washed into the lake from the seaside during a high-energy event. The thickness of the allochthonous deposits is highest where the bedrock sill shows lowest elevations around 5 m a.s.l. Here, associated breakthrough fan deposits were also encountered. By means of microfaunal and thin section studies, the so called "Brown Layer" which was first described by Jahns (2005) from a core from the central Lake Voulkaria turned out to be a tsunamigenic suspension deposit related to the formation of this breakthrough fan (Vött et al., 2006a).

In detail, vibracore ANI 7 from the western shore of the lake as well as core VOUL 1 recovered by Jahns (2005) show at least twofold tsunami influence on the lake around 1000 cal BC and between 400-233 cal BC (Classical-Hellenistic times). We assume that after the second event, the Cleopatra Canal could be easily excavated along the naturally eroded tsunami breakthrough channel to connect the lake harbour of ancient Palairos with the open sea (Vött et al., 2006a; 2008c, unpublished data). Ex-situ marine deposits were also recovered from vibracores drilled at the eastern shore of the lake some 5 km to the east of the shore at Aghios Nikolaos.



2nd International Tsunami Field Symposium

IGCP Project 495

Quaternary Land-Ocean Interactions:
Driving Mechanisms and Coastal Responses

Ostuni (Italy) and Ionian Islands (Greece) 22-28 September 2008



Project 495

CHAPTER 9

Geomorphological, sedimentological and geoarchaeological traces of Holocene tsunami impact between Palairos and Preveza (NW Greece)

Vött A., Brückner H., May S.M.

9.1. The Bay of Palairos-Pogonia

9.1.1. The ancient polis of Palairos: STOP 12

The ancient polis of Palairos is located on top of the spur of Kechropoula which extends into the northern part of the Palairos coastal plain. The city was founded in the 6th century BC; after the defeat of the Akarnanian allies of Cleopatra in the Battle of Actium in 31 BC, most of the people from Palairos were resettled to Nikopolis near Preveza. The city is said to have had a lake harbour in the adjacent Lake Voulkaria and, since 431 BC, also a seaport, probably close to the modern village of Pogonia (Lang et al., 2007). For a long time, it was suggested that ancient Palairos was once situated directly at the open sea and that the Lake Voulkaria thus may represent the remains of a former marine embayment. Palynological studies of Jahns (2005) and palaeogeographical investigations by Vött et al. (2006b; 2007b) however showed that, during the Holocene, the Ionian Sea has never reached further inland than around 1 km distant from the present shore near Pogonia and Palairos.

9.1.2. The submerged mole and geoarchaeological cliff deposits at Pogonia: STOP 13

Geoarchaeological investigations were also carried out along a natural cliff in the Bay of Palairos-Pogonia in the southern part of the Palairos coastal plain. The cliff near Pogonia, almost 100 m long and up to 2 m high, reveals a homogeneous colluvial deposit including isolated ceramic fragments predominantly dating to the Byzantine epoch.

The colluvial deposit covers an up to 2 m-thick stratum with plenty of diagnostic ceramic fragments, well adjusted, partly imbricated, and mixed up with beach gravel and sand as well as with numerous remains of marine macrofossils.

Due to its texture and contents, this mixed geoarchaeological layer may neither be interpreted as (i) colluvial deposit, nor as (ii) landslide deposit, nor as (iii) (supra-)littoral deposit. In its upper part, it shows a well developed palaeosol. Supplementary vibracoring revealed that the layer overlies, on top of an unconformity, fine-grained foreshore sand deposits. Within the mixed layer, we also encountered rip-up clasts out of the underlying marly bedrock. Microscopic analyses revealed that the matrix of the ceramic-rich stratum contains further marine indicators such as shell debris of marine macro- and microfauna and marine foraminifers. The larger part of the matrix, however, seems to be made out of weathered and reworked bedrock material as indicated by mostly angularly shaped mineral grains.

Based on these distinct sedimentological and palaeontological features, it is concluded that the mixed geoarchaeological layer is of tsunamigenic origin. The chaotic and wide-spread spatial distribution of archaeological remains of a nearby ancient mole, today submerged (Murray, 1985), may also be caused by destructive tsunami landfall in conjunction with co-seismic subsidence (Fig. 9.1). Former palaeogeographical studies in the Palairos coastal plain already suggested that the area was subject to considerable tsunami impact (Vött et al., 2007b).

Diagnostic ceramic fragments from the destructive layer are up to 20 cm large. We found both rounded and angular fragments. Preliminary archaeological studies show that they all date to Classical/Hellenistic to (early) Roman times. This is consistent with Murray (1985) who found a homogeneous group of pottery wedged in the submerged mole dating to the late 4th to 2nd centuries BC. Further studies will have to clarify possible relations to the strong tsunami which hit the nearby Lefkada coastal zone between 395 and 247 cal BC (Vött et al., 2008a).

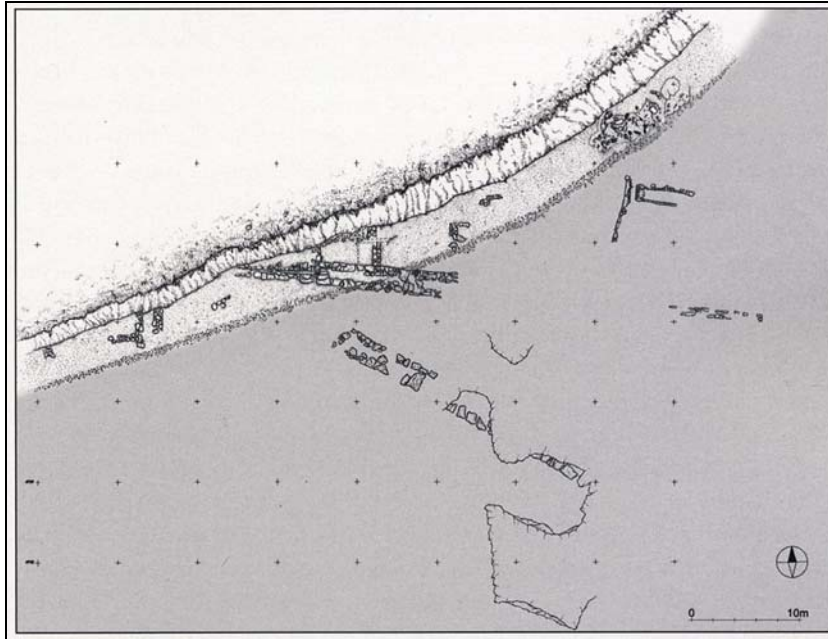


Figure 9.1 - Topographic plan showing submerged remains of the ancient mole near Pogonia. Associated ceramic fragments date to the Hellenistic epoch. The site is covered by up to 2.5 m of sea water. From Lang et al., 2007.

9.2. Actio Headland

9.2.1. The Phoukias tsunami sequence and the Phoukias sand spit: STOP 14

The Phoukias sand spit extends into the Bay of Aghios Nikolaos and, together with the Cheladivaron Promontory, seals off the Bay of Cheladivaron from the outer Bay of Aghios Nikolaos. In its northern part, around 1 km north of the present tip of the spit, we drilled a vibracore transect perpendicular to the present coastline. Similar to the findings from the inner Bay of Cheladivaron, the cores revealed terrestrial deposits covered by thick marine sediments accumulated on top of a clear erosional disconformity. At their base, the marine deposits are fairly unsorted and contain large amounts of shell debris. Their upper part is slightly laminated and consists of finer-grained deposits. Among others, these sedimentological features are typical of tsunami impact. In higher places, brown soils have developed out of the strongly weathered ex-situ marine deposits. Geochronological studies of different cores yielded a consistent age of around 2800 cal BC for the first high-energy impact on the former near-coast terrestrial sites (vibracores AKT 2 and AKT 35, Vött et al., 2007a). In most cases, the upper part of the profiles is made up of younger shallow marine deposits accumulated by longshore drift and obviously related to the Phoukias spit itself.

Based on a vibracore transect across the central part of the Phoukias sand spit some 600 m to the NNW of the tip of the present spit (vibracores ANI 2 and ANI 14), it was possible to detect at least three more younger high-energy events. In addition to the results mentioned above, it was found that the formation of the present spit did not start before around 840 cal AD when a major tsunami landfall occurred (Vött et al., 2007a, unpublished data for core AKT 35). The 840 cal AD event strongly altered sedimentary conditions in the inner Bay of Aghios Nikolaos from quiescent lagoonal to higher-energetic shallow marine conditions which enabled mats of seaweed to grow up with the rising sea level. This change of the environmental conditions was most probably connected to severe damage to the Plaka beach ridge ruin; at that time, the Plaka definitely lost its function as barrier separating the Lagoon of Aghios Nikolaos from the open sea. Since the 840 cal AD event, it represents a mere wave breaker which is overflowed by marine waters (Vött et al., 2007a).

9.2.2. The tsunami ripples at Paliokoulio: STOP 15

Some 2.6 km to the NNW of the Phoukias spit, we encountered several series of ripples along two geomorphological transects across Paliokoulio (Fig. 9.2). In each case the ripples are separated from each other by depressions partly filled with saltwater and characterized by swampy conditions. As to the oldest ripple

generation, the ripple which is located farthest inland shows small lobes of up to 90 m length extending into the fringing marshes of Limni Saltini in the form of a sand sheet.

Based on our results, the ripples have to be considered as tsunamigenic features rather than as palaeo beach ridges because: (i) the marine deposits are always deposited on top of a sharp erosional contact; (ii) every ripple shows the same stratigraphic sequence, the base of the marine deposits lying on a slightly landward increasing depth level; (iii) the lower part of the marine deposits are strongly unsorted and contain abundant marine shell debris as well as numerous articulated specimens of bivalves. The latter was found to be characteristic for tsunami deposits encountered in the Sur Lagoon, Oman, by Donato et al. (2008). (iv) Furthermore, the upper part of the marine deposits show well developed brown soils; the basal shell debris layer, as revealed by excavated trenches across the ripples, is strongly cemented in the form of a crust. Both findings indicate subaerial weathering and carbonate dissolution in the upper horizons as well as carbonate cementation in the lower horizons subsequent to the deposition of the material. Thus, the marine deposits are assumed to have been deposited by extreme events on land way above the sea level at that time (see Vött et al., 2007a).



Figure 9.2 - Aerial photograph from the southwestern part of Actio Headland showing several generations of tsunamigenic ripples between Paliokoulio and Phoukias. From Hellenic Military Geographical Service, 1985.

9.2.3. The spit of Actio and Actio Castle: STOP 16

The northern tip of Actio Headland is the triangle-shaped spit of Actio. The spit marks the entrance to the tectonic basin of the Ambrakian Gulf which is connected to the Ionian Sea by the only 620 m-wide Strait of Actio or Strait of Preveza. Strong fortifications such as Actio Castle on the southern as well as Pantokrator Castle and the fortress of Preveza on the northern side of the strait were erected by the Venetians and continued to be of strategic importance during the time of Ottoman occupation.

The spit of Actio, starting from Actio Castle and extending some 800 m into the Strait of Preveza, is made up of comparatively young marine deposits and looks like formed due to alongshore sediment transport. From Actio Castle towards the south, this kind of lowland is accompanied by a higher terrace-like unit reaching up to approximately 3.5 m a.s.l. The transition between these two geomorphological units is a clear erosional edge (Fig. 9.3). Two W-E trending vibracore transects across the spit south of Actio Castle were realized. The bases of the vibracores are made up of limnic, terrestrial (palaeosol) or aeolian deposits. Going down the erosional edge, the basal units are all abruptly covered by up to 3.5 m-thick marine deposits. The contact between the two core sections is always represented by an erosional contact. The marine deposits, in their upper parts, are strongly weathered and bear well developed brown to reddish-brown soils; therefore, the marine layer is suggested to have been accumulated fairly well above the sea level at the time of deposition. The lower part of the marine deposits is made up of gravelly to sandy, unsorted deposits including abundant marine shell debris. We interpret this basal unit as representing tsunamigenic runup deposits. The middle and upper parts of the marine section consist of fairly laminated and well sorted sand layers showing fining-upward and thinning landward features (for instance AKT 45-48, AKT 20 and 21) and seem to represent tsunami deposits which were accumulated while the spit was completely inundated by overflowing water masses (Vött et al., 2007a). Some of the profiles indicate multiple impact of high-energy events. Vibracore AKT 45, for instance, contains sediments of at least two tsunami impacts. The age of the older tsunami landfall seems to be consistent with the 2800 cal BC event which hit the neighbouring Phoukias area.

Vibracores drilled to the north of Actio Castle show thick sequences of homogeneous fine to middle sand at their base which were deposited in a littoral environment. In contrast, the upper parts of the profiles show up to 2.5-4 m-thick, strongly unsorted gravel and sand (AKT 49). In some cases, the upper sequence is fining upward (AKT 16, AKT 17). Well developed brown soils document that the upper marine deposits have not been subject to mid- to short-term reworking by littoral processes. Moreover, the upper approximately 50 cm of the profiles are strongly decalcified and re-precipitation of calcium carbonate in deeper horizons has formed a carbonate crust, up to 20 cm thick. Radiocarbon dating of a large wood fragment encountered at the very border between autochthonous fine sand and allochthonous unsorted gravelly deposits at the very tip of the spit of Actio (AKT 49) rendered 1030-1152 cal AD as age for a younger extreme event.



Figure 9.3 - Erosional edge at Actio Headland near Actio Castle. Vibracore transects across the two geomorphological units revealed thick marine deposits on top of an erosional unconformity formed in older limnic, terrestrial (palaeosol) or aeolian sediments. The flat surface of the upper unit is characterized by scattered blocks and stones as well as by ceramic fragments from different epochs and of different states of conservation (a – roof tile, Roman; b – pithos fragment, undetermined age; c – roof tile, Hellenistic to Roman; d and e – jar bottom, 4th cent. BC; f – roof tile, Laconian style, Hellenistic to Roman). Abundant dislocated ceramic fragments and stone material were also found underwater to the immediate east of the northern part of the headland. The ancient Sanctuary of Apollo which is located near Actio Castle is suggested to have been repeatedly hit by tsunami waves flushing most of the archaeological remains into the Ambrakian Gulf.

This age is consistent with geoarchaeological findings of dislocated blocks, stones (partly beachrock originating from the Plaka beach ridge ruin some 2 km to the west) and ceramic fragments scattered on the terrain surface south of Actio Castle which indicate a tsunami event that took place at or after the Byzantine epoch (Vött et al., 2007a).

Snorkeling surveys conducted along the eastern shore of Actio Headland revealed abundant ceramic fragments and dislocated blocks and stones which do not correspond to the recent littoral dynamics and seem to have been flushed into the Ambrakian Gulf by an extreme event. Multiple tsunami landfall and inundation at Actio Headland seems the reason for the fact that there are almost no archaeological remains left from the famous Sanctuary of Apollo which was used by the Akarnanian League as a national sanctuary until Roman times (Fig. 9.3). For detailed discussion and arguments against interpreting our results as caused by storms or as sea level highstand deposits please see Vött et al. (2007a, cfr. Chapter 11).

9.2.4. The Strait of Preveza: STOP 17

Additionally, sub-bottom profiling was carried out by the Hellenic Center of Marine Research, Dr. D. Sakellariou and team (August 20-28, 2007). Acoustic profiles along the Strait of Preveza depict a system of two narrow channels which run in an approximate SW-NE direction down to a maximum depth of 35 m below present sea level (m b.s.l.) and which are flanked by up to 20 m-thick deposits with a quasi horizontal layering (Fig. 9.4). These deposits lie on top of an erosional unconformity and, due to their position in the stratigraphical sequence, seem to be of Holocene age. This age is also suggested by Tziavos (1997) who reports on thick sandy deposits retrieved by commercial corings in preparation of the modern Preveza tunnel. Unfortunately, this core material was not archived so that repeated analyses and radiocarbon datings are impossible.

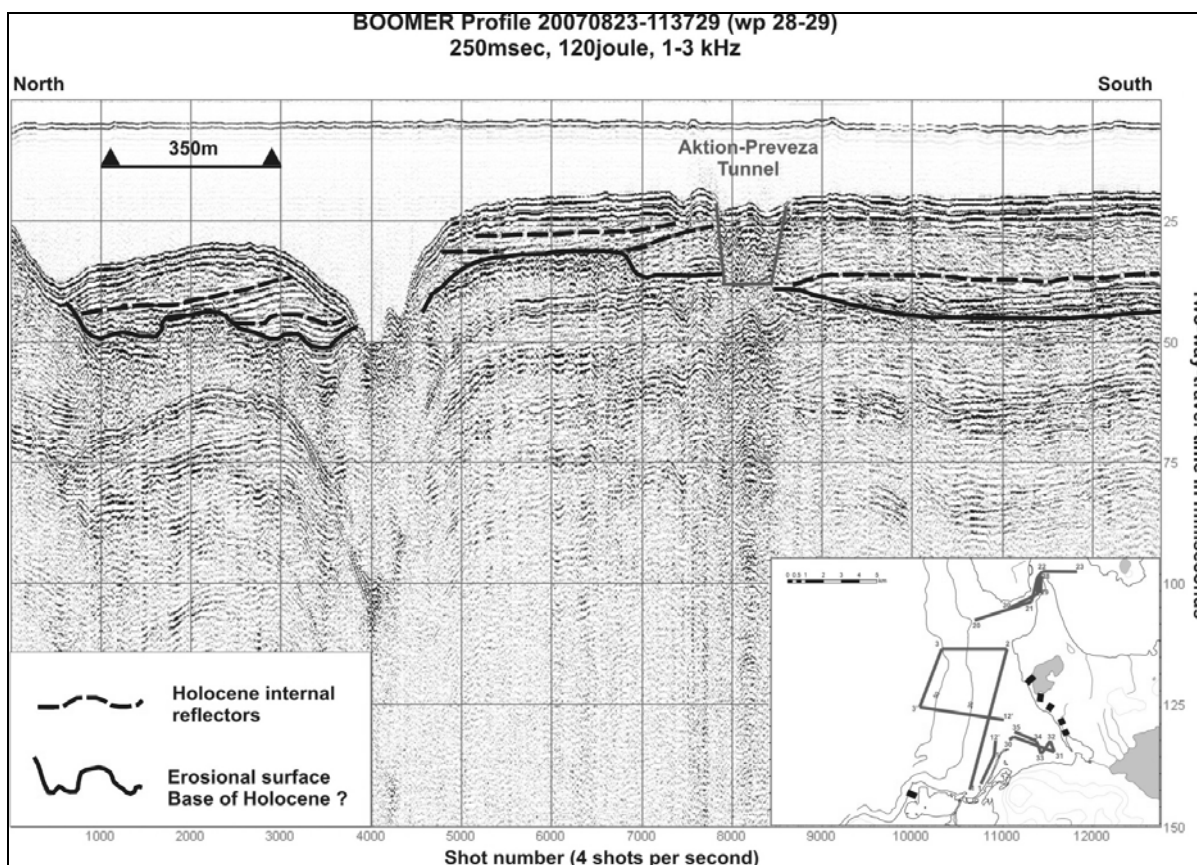


Figure 9.4 - Sub-bottom profile along the Strait of Preveza measured during geophysical investigations by the Hellenic Center of Marine Research, Dr. D. Sakellariou and team (August 20-28, 2007). A steep channel goes down to approximately 35 m b.s.l. in a northeastern direction. It is incised into older, probably Pleistocene deposits and ends up in a pothole-like setting. The channel system as well as the accompanying thick deposits are interpreted to be of tsunamigenic origin and of Holocene age. The sandy underwater deposits (Tziavos, 1997) seem to be tsunamigenically dislocated beach ridge material which formerly covered the Plaka beachrock. This is also suggested by tsunami-borne sand sheets encountered on land around Preveza and Actio Headland. There are no alternative sources for the huge amounts of Holocene sediments found in the environs of the Strait of Preveza.

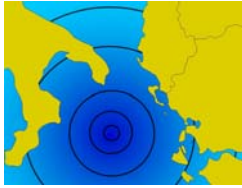
Against the background of geomorphological, geoarchaeological and sedimentological evidence of multiple tsunami landfall at Actio Headland (Vött et al., 2007a) and of tsunami traces found in vibracores drilled to the northeast of Preveza, the channel system as well as the flanking deposits are most probably of tsunamigenic origin.

This idea is also supported by the facts that (i) the sandy deposits of the inner strait are not connected to the sandy Louros and Arachthos River deltafront areas in the inner Ambrakian Gulf and (ii) that there is no longshore drift of sandy material along the present coastline. It further seems as if tsunami wave action may have played a major role in the opening of the Ambrakian Gulf: It is still unclear how and when this happened during the Holocene (Poulos et al., 1995; Tziavos, 1997; Jing & Rapp, 2003; Brockmüller et al., 2007; Kapsimalis et al., 2005; Poulos et al., 2005). Therefore, the Strait of Preveza is also a key site for the understanding of tsunami influence on the long-term coastal evolution in northwestern Greece. Marine coring in the central Strait of Preveza would be the first-choice method to check the hypothesis of strong tsunamigenic imprint on the opening of the Ambrakian Gulf.

9.2.5. The eastern shore of Actio Headland: STOP 18

Vibracore studies were also realized at the eastern shore of Actio Headland approximately 500 m to the east of the NATO airport of Actio/Preveza. We found a clear temporary change in the stratigraphic sequences documenting that limnic or even swampy conditions were temporarily interrupted by strong saltwater influence. Saltwater input went hand in hand with the deposition of shell debris. After this disturbance, limnic to swampy environmental conditions were quickly re-established. At vibracoring site AKT 14, a wood fragment encountered at the very base of the marine shell debris layer yielded 2858-2623 cal BC, an age which is perfectly consistent with the tsunami event which hit the Phoukias area (AKT 2, AKT 35) and the spit of Actio (AKT 45) around 2800 cal BC. These results document that, at that time, Actio Headland as a whole must have been inundated by tsunami waters (Vött et al., 2007a).

Some of the vibracore profiles give even evidence of a younger event which must have affected the area. Autochthonous and homogeneous, silty to clayey sediments – accumulated under quiescent conditions – are abruptly covered by a layer of unsorted gravel with diameters of up to 20 cm and including numerous marine shell fragments. This high-energy event may correspond to the younger tsunami-generation which hit the spit of Actio (AKT 49, Section 1.5.3) around 1000 AD some 4 km further to the NNW. Corresponding findings were made all across Actio Headland and let us suggest that the shallow-water lagoon of Limni Saltini is the result of tsunamigenic erosion and inundation during late-medieval times (Vött et al., 2007a, Section 3.2).



2nd International Tsunami Field Symposium

IGCP Project 495

Quaternary Land-Ocean Interactions:
Driving Mechanisms and Coastal Responses

Ostuni (Italy) and Ionian Islands (Greece) 22-28 September 2008



Project 495

CHAPTER 10

Strong tsunami impact on the Bay of Aghios Nikolaos and its environs (NW Greece) during Classical–Hellenistic times*

Vött A., Brückner H., May S.M., Lang F., Herd R., Brockmüller S.

**Totally reprinted from Quaternary International 181 (2008), 105–122*

10.1. Introduction

As opposed to many other oceans worldwide showing a high tsunamigenic potential, the Mediterranean is characterized by an irregular shape, a limited spatial extent and only small and unconnected deep sea basins with more than 5000 m water depth. Nevertheless, tsunami deposits known from all over the region document a high tsunami risk. As to the eastern Mediterranean, this is obviously due to the seismo-tectonic activity pattern of the Hellenic Arc where oceanic crust of the African plate is being subducted by the overriding Eurasian plate. Strong submarine earthquakes, seismically induced submarine mass movements, and volcanic eruptions occur with high frequency and high magnitude and implicate a high tsunami potential dangerous for the coasts of southeastern Europe, northern Africa, and the Near East.

In the course of the past two decades, a variety of tsunami deposits has been discovered in the eastern Mediterranean. In Italy, Gianfreda et al. (2001) report on sandy washover fans from the Gargano coast. Mastronuzzi and Sanso` (2004) found tsunamigenically dislocated mega blocks in southern Apulia, and from Stromboli Island, Maramai et al. (2005) described similar blocks accumulated by the December 2002 tsunami which was induced by land slide masses. On Cyprus, Kelletat and Schellmann (2001, 2002) and Whelan and Kelletat (2002) studied imbricated mega blocks, bimodal sandy to gravelly sediments, and fields of scattered stones which they assigned to tsunamigenic influence. Fields of tsunamigenically scattered stones are also known from the southern Turkish coast (Kelletat, 2005). In Greece, research on tsunami deposits has mainly concentrated on the Aegean Sea (Dominey-Howes, 2002). According to Minoura et al. (2000), thin sand layers found on Crete reflect a tsunami caused by the Minoan eruption of the Santorini volcano (cf. Dominey-Howes et al., 2000a; McCoy and Heiken, 2000).

Recently, even tsunamigenically dislocated boulders were detected in several coastal areas of the island indicating strong and repeated tsunami events (Scheffers, 2006a). Runup sediments were reported from the 1956 tsunami which hit the island of Astypalaea (Dominey-Howes et al., 2000b) and from the area around ancient Kynos in Lokris, where a sandy tsunami layer could be assigned to the earthquake of 426 BC (Gaki-Papanastassiou et al., 2001). In the Gulf of Corinth — although the tsunami potential is considerably high (Stefatos et al., 2006) — findings of tsunami deposits are restricted to a few thin-layered sand sheets found near Aegio and Itea (Kontopoulos and Avramidis, 2003; Kortekaas et al., 2005).

A series of interrelated tsunami deposits—unique for the eastern Mediterranean—were found between Lefkada Island and the adjacent Plaghia Peninsula within the framework of an international and interdisciplinary project on the coastal evolution of Akarnania (Vött et al., 2006b, c, d). Lefkada tsunami deposits comprise washover fans (chevrons), dislocated mega blocks, fields of scattered stones, sandy to gravelly runup and breakthrough sediments as well as suspension deposits found in the nearcoast Lake Voukaria. Based on radiocarbon datings, tsunami impacts were dated to around 1000 cal BC, 300 cal BC, 430 cal AD and 1000–1400 cal AD (Vött et al., 2006a).

This paper presents new geomorphological, geoarchaeological, geophysical and geochronological data for tsunamigenic influence during the Classical–Hellenistic period in and around the Bay of Aghios Nikolaos between Lefkada city and the Plaghia Peninsula (Fig. 10.1). The main objectives of the study were (i) to detect and describe sedimentary evidence of tsunami impacts at different sites based on geomorphological and geoarchaeological indicators, (ii) to compare and interrelate tsunami deposits, and (iii) to reconstruct tsunami influences on coastal environments during Classical–Hellenistic times and to assess their consequences for human activities.



Figure 10.1 - Topographic overview of the coastal zone between Preveza and Lefkada. Locations of study sites in and around the Bay of Aghios Nikolaos.

10.2. Topography and geotectonic setting

The Bay of Aghios Nikolaos is located between the Santa Maura beach ridge complex and the Plaghia Peninsula to the south and the hills of Stoupas and the Actio headland to the north (Fig. 10.1). The Santa Maura beach ridge complex is part of the Lefkada spit system which closes off the shallow waters of the Sound of Lefkada from the open Ionian Sea (Fig. 10.2). The complex starts at the fort of Santa Maura and runs in a ESE–WNW, then in a NNE–SSW direction. Its base is made up of a thick beachrock unit.

In the north, at the so-called Plaka, this beachrock unit is completely uncovered from loose littoral deposits. Additionally, the Plaka beachrock is broken into pieces which are partly heaped up to at least 1 m above present mean sea level (a.s.l.). Several blocks even show clear imbrication (Vött et al., 2006a, Fig. 10.5).

In the past, parts of the Plaka were used as a quarry because blocks could be easily removed and used as building material (von Seidlitz, 1927, p. 366f.). Due to a relative rise in sea level, some of the former working sites are slightly submerged at present. The northern part of the Santa Maura beach ridge describes a sharp bend towards the east (Figs. 10.2 and 10.3) while the Plaka, representing a former strandline, runs almost straight towards Actio headland.

As a wavebreaker, the Plaka protects the Bay of Aghios Nikolaos from open sea wave dynamics. The Cheladivaron promontory as well as the opposite lying Phoukias sand spit induce quiescent water conditions in the eastern part of the bay, the Cheladivaron embayment. During summer, hydrochemical conditions in the Bay of Cheladivaron are even often anoxic and characterized by the production of hydrosulphide (H₂S). The overall coastal topography is characterized by a funnel-like contour which considerably enlarges tsunami signals approaching the coast from the western quadrant (Vött et al., 2006a).

The tectonic evolution of Lefkada Island, the Plaghia Peninsula, and Actio headland is closely related to a multiple plate junction in the northern part of the Ionian Sea which marks the northwestern end of the Hellenic Arc. Not far offshore the Ionian Islands, Africa, the Adriatic, and the Aegean form different types of plate boundaries by collision, subduction, transform faulting, and spreading (Sachpazi et al., 2000, p. 303). Some 25km west of Lefkada Island, the SSW–NNE running right-lateral strike slip Cefalonia transform fault (CF) represents the most important tectonic feature of the region. Its direct prolongation, the highly active Lefkada fault, defines the western flank of Lefkada Island. To the north and to the west of the CF, crustal motion is negligible whereas areas to the south and to the east show rates of crustal motion up to 40 mm/a (Kahle et al., 1993, 1995, 2000; Cocard et al., 1999). Additionally, van Hinsbergen et al. (2005, p. 30) showed by palaeomagnetic studies that northwestern Greece has undertaken an average 40° clockwise rotation during 15–8 Ma and a second phase of 10° clockwise rotation after 4 Ma. For northern Akarnania, Broadley et al. (2004) even found a 90° clockwise rotation since Oligo–Miocene times.

On August 14, 2003, Lefkada Island experienced a 6.2Mw earthquake shock which caused extensive damage to the infrastructure of the island (Papadopoulos, 2003; Karakostas et al., 2004). However, due to the behaviour of the CF, earthquakes mostly occur in shallow depths and with high frequency (Galanopoulos, 1952, 1954; Papazachos and Papazachou, 1997). Lefkada Island belongs to the areas with the highest seismic hazard in the whole Mediterranean (Scordilis et al., 1985; Hatzfeld et al., 1995; Louvari et al., 1999; Laigle et al., 2002, 2004).



Figure 10.2 - The Lefkada spit system closing off the shallow lagoonal waters of the Sound of Lefkada (left side) from the open Ionian Sea (right side). The foreground shows the Santa Maura beach ridge complex and the washover plain east of the Canali Stretti with locations of vibrocorings and transects of earth resistivity measurements. View to the west. Photo taken by F. Lang, 2006.

Thus, it is also characterized by a high tsunami risk (Papazachos & Dimitriu, 1991, Fig. 10.4) documented by numerous reports on historical tsunami events in the region (regional tsunami catalogue, see Vött et al., 2006a, Table 2).

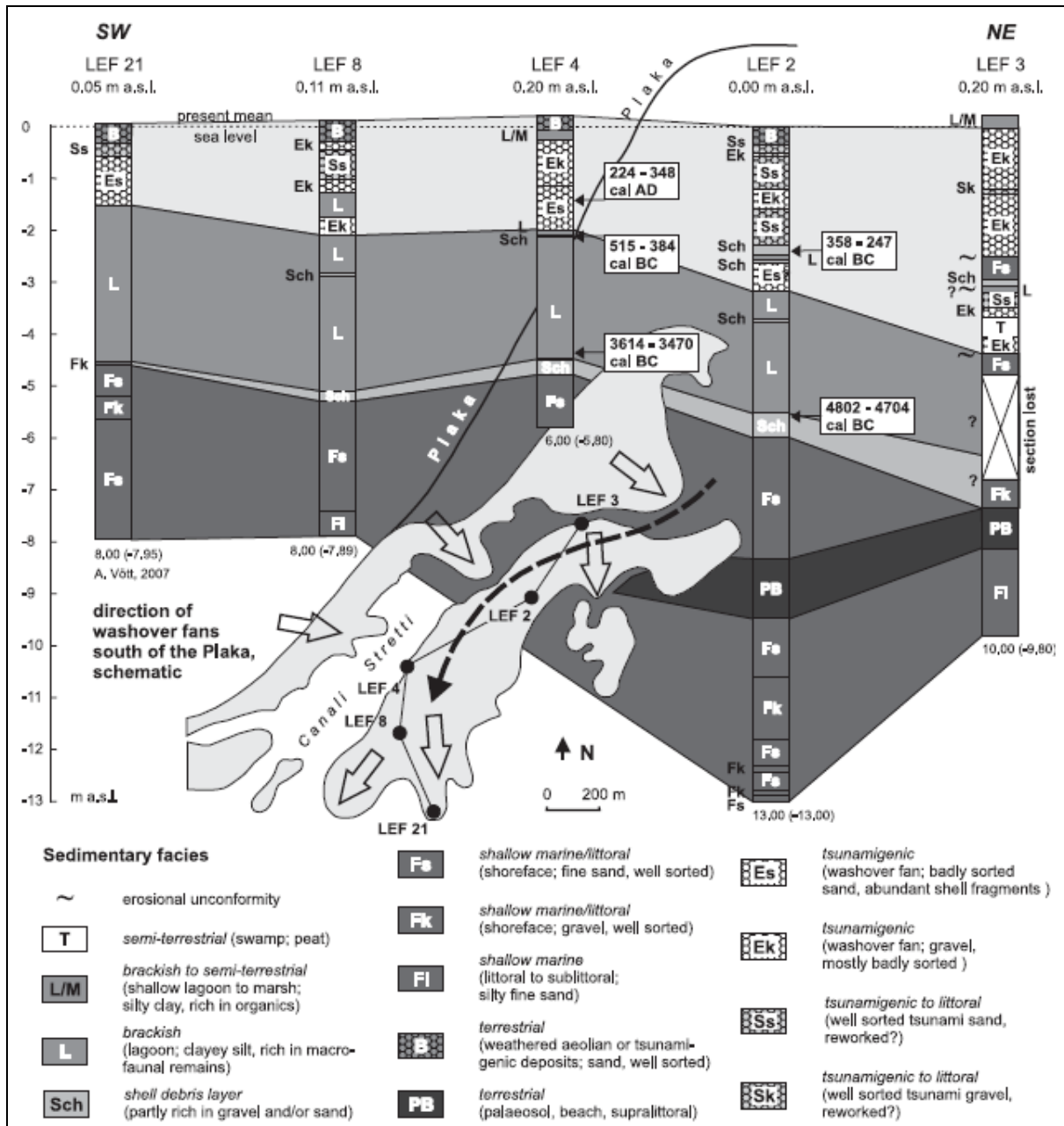


Figure 10.3 - Stratigraphic sequences of vibracores east of the Canali Stretti revealing coarse-grained tsunami deposits and schematic map of the tsunamigenic washover plain.

10.3. Materials and methods

(Palaeo-) tsunami research was accomplished within an interdisciplinary and international project. We carried out intense geomorphological surveys, drilled numerous vibracores, and studied outcrops of sediment layers in artificial trenches, for example in loutsas (Greek for agricultural cisterns, mostly dug out of alluvial deposits). An Atlas Copco mk1 device with core diameters of 6 and 5 cm was used for vibracoring. The maximum recovery depth was 13 m below surface (m b.s.). Vibracores and profiles were studied sedimentologically and geomorphologically and sampled for further analyses. In the laboratory, geochemical parameters of sediment samples such as electrical conductivity, pH-value, carbonate content, orthophosphate, loss on ignition, concentrations of heavy metal, alkaline and earth alkaline metal ions were determined. Together

with statistical analyses of geochemical data, macrofaunal and macrofloral remains allowed to determine the sedimentary environment (Vött et al., 2002, 2003).

We carried out earth resistivity measurements by means of a multi-electrode Syscal R1 plus-instrument in order to detect the thickness of coarse grained sediment layers and of subsurface structures. Further, we realized detailed geomorphological and geomorphometric studies within two zones of the Santa Maura beach ridge complex measuring the size, the strike direction of the longitudinal axis, the direction of dip and the inclination of dislocated beachrock slabs. Differential GPS measurements were carried out along earth resistivity transects, of vibracoring sites, and artificial trenches. Additional topographic surveys were made across and along the Santa Maura beach ridge complex. We interpreted remote sensing data such as Corona satellite photos and mid-to high-resolution Aster and GoogleEarth satellite pictures in search of spatial structures of tsunamigenic origin.

In the Bay of Aghios Nikolaos, scuba-divers realized geomorphological survey and sampling of dislocated beachrock slabs under water. Several underwater sediment cores were drilled by hand down to 1 m below sediment surface. The geochronological frame of the study is based on (i) ¹⁴C-AMS datings of organic material or biogenetically produced carbonate and (ii) the age determination of diagnostic ceramic fragments encountered in vibracores and trenches. Radiocarbon ages of marine samples were corrected for a mean marine reservoir effect of 402 years (Reimer and McCormac, 2002). However, we assume that there is considerable fluctuation of the (palaeo-)reservoir effects through time, depending on the local (palaeo-) environmental conditions (see also Geyh, 2005, pp. 69ff.).

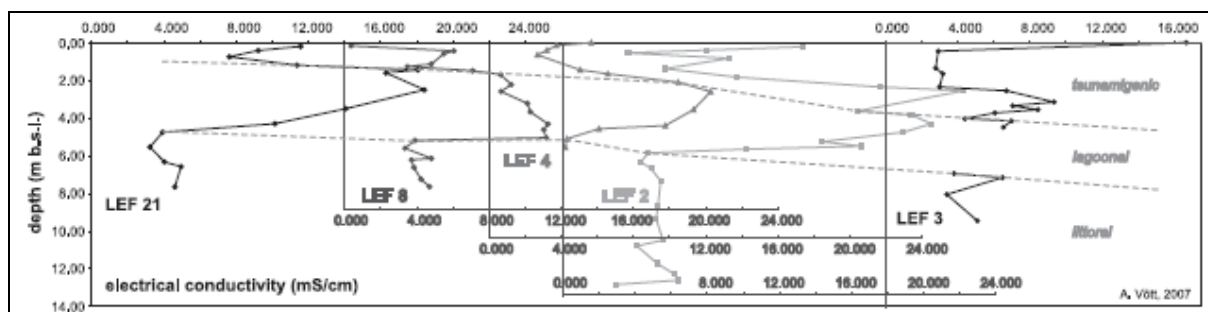


Figure 10.4 - Vertical profiles of electrical conductivity values measured in sediment samples from vibracores drilled at the washover plain east of the Canali Stretti. Curves and corresponding x-axes are shifted to the right. Distances between the curves/axes do not correspond to real distances between vibracoring sites.

10.4. Geomorphological and geoarchaeological records of extreme events and geochronological data

We present evidence of strong extreme events which hit the Bay of Aghios Nikolaos and its environs (Fig. 10.1). This evidence comprises sedimentological, geomorphological, geochemical and geoarchaeological findings both on land and under water.

10.4.1. Washover deposits east of the Canali Stretti

A series of vibracores were drilled east of the Canali Stretti on top of a wide and comparatively flat geomorphological unit (Fig. 10.2). The schematic contour of this tongue-shaped coastal plain is depicted in Fig. 10.3. The Canali Stretti are the remains of a formerly navigable channel which allowed small ships to cross the Sound of Lefkada (Parsch, 1889, p. 6). Vibracores were carried out along a SSW–NNE running transect over a distance of about 1.3 km. LEF 8 lies close to the modern national road which crosses the channel on top of an artificial dam. LEF 21 is located at the southern edge of the plain which is accessible from the road only during times of low water level in the sound. LEF 3 and 4 are situated at the western fringe of the plain facing the Canali Stretti whereas LEF 2 was drilled in a more central and eastern position (Fig. 10.2).

The stratigraphic sequences of vibracores LEF 21, 8 and 3 are almost identical (Fig. 10.3). The lower parts of the profiles are made up of sandy to gravelly littoral deposits. They are covered by thick packages of homogeneous lagoonal mud. The beginning of the lagoonal unit marks the time when a new coastline had formed to the west of the transect probably close to the modern Santa Maura beach ridge. A ¹⁴C-AMS age from LEF 4 indicates that lagoonal conditions at this site started in the 4th millennium BC (3614–3470 cal BC, Fig. 10.3, Table 10.1). The upper parts of the profiles show a sudden change towards coarse material originating from the littoral zone such as sand and gravel, mostly badly sorted, with bimodal grain size distribution and numerous fragments of marine macrofauna. At LEF 8, three different phases of highenergy input can be distinguished.

They are separated by lagoonal mud or by well-sorted coarse deposits which probably correspond to reworked tsunami deposits. At LEF 4, a shell debris layer marks the end of undisturbed lagoonal conditions and dates to Classical-Hellenistic times (515–384 cal BC, Fig. 10.3, Table 10.1). A second event occurred after a short lagoonal phase and brought almost 2 m of sand and gravel to the site. At LEF 21, 8 and 4, a brown soil developed out of coarse material. At LEF 4, however, the material might be of anthropogenic origin, formerly dredged from the Canali Stretti in order to guarantee the navigability of the channel. Today's sedimentary conditions in the area are characterized by shallow lagoonal waters with water depths between 20 and 70 cm and the exclusive deposition of silt and clay.

The bottom section of LEF 2 shows littoral deposits including a palaeosol in a supralittoral position. Lagoonal conditions set in during the 5th millennium BC (4802–4704 cal BC, Fig. 10.3 and Table 10.1), i.e. a little earlier than at LEF 4, and lasted for several thousands of years. The system was first disturbed by high-energy input of sand at 3.17 m b.s.l. Subsequent to a short period when quiescent lagoonal conditions were re-established, a second event occurred and left a thick shell debris layer covered by well-sorted sand. The shell layer dates to the Classical–Hellenistic epoch (358–247 cal BC, Fig. 10.3 and Table 10.1). Another two layers of unsorted gravel and sand seem to have been caused by further high-energy impacts. The top of LEF 2 is made up of weathered sandy littoral to aeolian deposits.

Sample name	Depth (m b.s.)	Depth (m b.s.l.)	Sample description	Lab. no.	$\delta^{13}\text{C}$ (ppm)	^{14}C Age (BP)	1 σ max; min (cal BP)	1 σ max; min (cal BC)
ANI KW BM 1	0.00	0.80 m a.s.l.	Rock-boring mussel, artic. specimen	Erl 9050	-6.0	2737 \pm 45	2506–2344	557–395
ANI 12/2+PR	0.23	7.63	Unidentified plant remains, sea wood?	Erl 9798	-13.2	585 \pm 37	277; 147	1673; 1803 AD
ANI 12/5M	0.44	7.84	<i>Dosinia exoleta</i> , artic. specimen	Erl 9797	-1.6	2353 \pm 50	2041–1904	92 BC–46 AD
LEF 2/7+M	2.41	2.41	<i>Dosinia exoleta</i> , artic. specimen	UtC	0.3	2574 \pm 37	2308–2197	358–247
LEF 2/14+M	5.59	5.59	<i>Dosinia exoleta</i> , artic. specimen	UtC	0.0	6257 \pm 37	6752–6654	4802–4704
LEF 4/5PR	1.62	1.42	Sea weed remains	Erl 9053	-18.7	2093 \pm 41	1726–1602	224–348 AD
LEF 4/7M	2.30	2.10	<i>Dosinia exoleta</i> , artic. specimen	Erl 9054	-1.8	2709 \pm 45	2464–2333	515–384
LEF 4/10M2	4.60	4.40	<i>Macoma</i> sp., artic. specimen	Erl 9799	0.0	5104 \pm 55	5563–5419	3614–3470

Table 10.1 - ^{14}C -AMS dating results for samples from the Bay of Aghios Nikolaos and its environs. Note: b.s. – below ground/sediment surface; b.s.l. – below sea level; a.s.l. – above sea level; artic. specimen - articulated specimen; 1s max; min cal BP/BC (AD) – calibrated ages, 1s range; “;” – there are several possible age intervals because of multiple intersections with the calibration curve; Lab. no. – laboratory number, University of Utrecht (UtC), University of Erlangen (Erl); calibration was carried out using the calibration software Calib from Stuiver et al. (2006); for all samples the marine reservoir effect was corrected by 402 years of reservoir age.

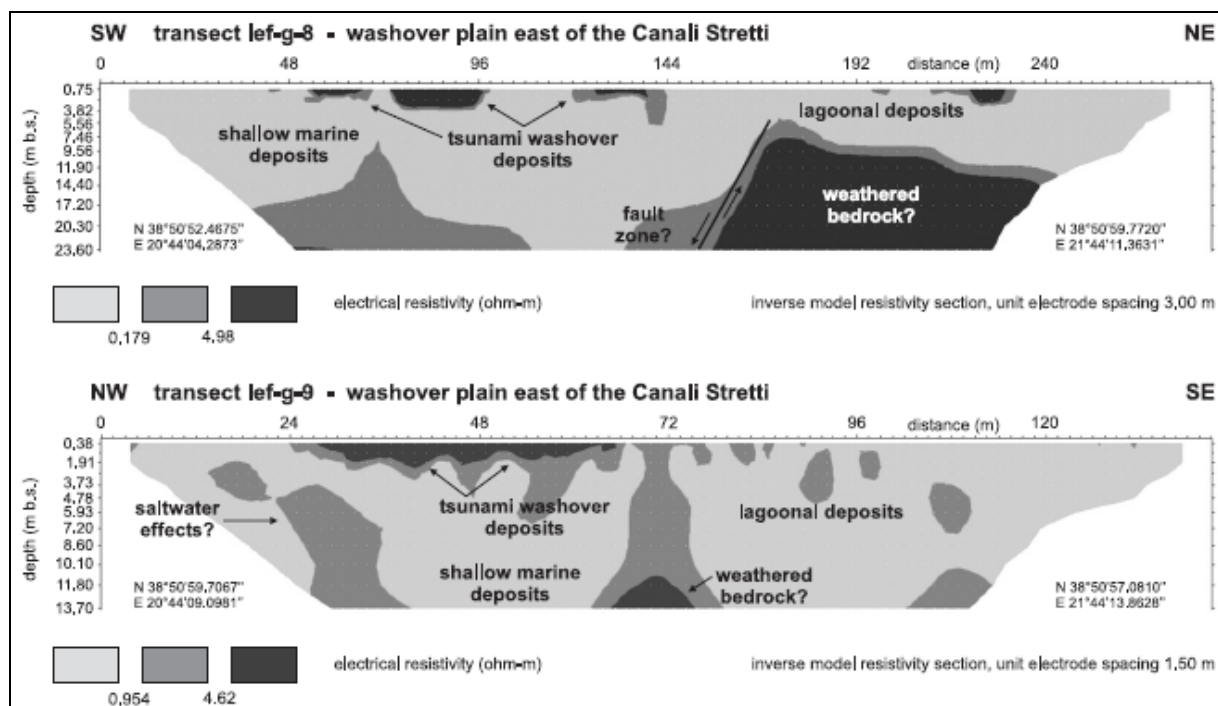


Figure 10.5 - Simplified inverse model sections of earth resistivity measurements along and across the washover plain east of the Canali Stretti.

The lower part of vibracore LEF 3 is similar to LEF 2 showing partly weathered littoral deposits. Lagoonal sediments were not found. High-energy coarse clasts, however, already appear at 4.57 m b.s.l. Similar to LEF 2, profile LEF 3 indicates four different events each reflecting the input of coarse material and thus a sudden increase of energy flowing into the system. LEF 3 shows the thickest event layers and the highest portion of coarse clasts of all vibracore profiles. Therefore, it seems probable that lagoonal deposits were completely eroded by highenergy events.

Sharp bends in the vertical profiles of geochemical parameters such as electrical conductivity (Fig. 10.4) also reflect the event-like character of the coarse grained deposits. Additionally, earth resistivity measurements along two transects lef-g-8 and -9 across the plain east of the Canali Stretti (Figs. 10.2 and 10.5) revealed that the coarse material is floating on top of autochthonous shallow marine or lagoonal sediments.

10.4.2. Dislocated beachrock slabs at the Santa Maura beach ridge complex

Detailed topographic DGPS measurements were carried out along 46 transects across the Santa Maura beach ridge complex. Moreover, geomorphometric analyses were accomplished in two case study zones in the southwestern part of the beach ridge (Figs. 10.6 and 10.7).

At the seaward side of case study zone A, numerous beachrock slabs were encountered in the recent littoral zone. Some slabs were imbricated, some tilted and partly covered by sediment, and some were turned upside down as documented by bio-erosive features now facing towards the ground (Fig. 10.6a). The largest slabs or blocks are more than 3 m in length and 2 m in width (Fig. 10.6b). Obviously, the slabs were torn out of the original beachrock unit which, probably, was already broken into pieces by seismic events. *In situ* beachrock, partly weathered and eroded, can be seen to the immediate south and north of zone A (Fig. 10.6c).

Numerous beachrock slabs were also found on top of the beach ridge. On land, the largest slabs concentrate on elevations ≤ 0.5 m a.s.l. showing volumes of ≤ 1 m³. Numerous slabs up to a volume of 0.1 m³ were, however, encountered on the very crest of the beach ridge up to around 2.30 m a.s.l. in zone A and 3.60 m in zone B. Many tubeworms which still adhere to the surface of the slabs testify to the previously marine environment (Fig. 10.6d). Morphometric analyses revealed that beachrock slabs and fragments ≤ 0.2 m³ concentrate on the landward side of the beach ridge. Most of these beachrock fragments are characterized by numerous boreholes from marine boring mussels. It is thus concluded that, during inundation by an extreme event, the largest blocks were dumped at the crest of the ridge where water masses diverge and loose most of their transport energy whereas smaller beachrock fragments were transported further landwards on the leeward side of the ridge (Fig. 10.7e).

In zone B, a set of three imbricated slabs which were partly embedded in beach ridge deposits was found some 30 m distant from the present strandline. The uppermost beachrock plate at 3.52 m a.s.l. is made up of gravelly beachrock into which a large ceramic fragment was cemented (Figs. 10.6e to g, 10.7f and g). The fragment was determined as part of a well preserved and barely moved roof tile dating to Classical–Hellenistic times. Beachrock formation was thus still in process during or shortly after the 5th to 3rd centuries BC. Then, the beachrock was broken into plates and dislocated by marine water masses. Hence, the tile fragment gives a terminus post quem for the extreme event which moved the hosting beachrock slab on top of the beach ridge.

Dislocated beachrock slabs concentrate on the southwestern section of the beach ridge complex. Strike and direction of dip of beachrock slabs and fragments found in zones A and B indicate that the main flow direction of the high-energy event was almost perpendicular to the modern coast (Fig. 10.7a and b). Fig. 10.7c depicts five selected cross sections of the Santa Maura beach ridge complex. Highest elevations, up to almost 4 m a.s.l., were encountered between Sections 2 and 4 and lowest elevations, around 2 m a.s.l., to the north of Section 4 (Figs. 10.2, 10.7c and d).

10.4.3. Sublittoral disturbances in the Bay of Aghios Nikolaos

Nikolaos in order to survey the underwater morphology. Fig. 10.8 illustrates geomorphological features encountered along two selected transects located at the landward side of the northern Plaka heading towards Actio headland. One transect is located at the northernmost tip of the Plaka close to an obelisk which marks the navigable route towards Aghios Nikolaos (Figs. 10.1, 10.8a and b). The other transect lies to the east of a partly submerged section of the Plaka called Skoupeloi Achilleos some 1.3km to the north of the tip (Figs. 10.1, 10.8c and d).

Unfar the obelisk, we found an underwater ridge made up of beachrock slabs. The slabs, up to 2 m long, lie in water depths of 3–5 m and thus far beyond the range of the modern wave regime. The ridge is about 20–30 m long and several metres wide. Its structure is partly chaotic. However, in some parts there is clear imbrication. All the beachrock plates are covered by marine algae and other marine organisms indicating that they have not been moved since they were deposited at the site. Some slabs are partly embedded in the underlying substrate

(Figs. 10.8a and b). Closer to the Plaka remains, numerous dislocated, tilted and even partly imbricated mega blocks, up to at least 15 m³ large, were found in water depths between 2 and 5 m. Around 40 m east of Skoupeloi Achilleos a ridge composed of dislocated beachrock fragments was encountered in 2.5–3.2 m water depth. The diameter of the fragments shows a maximum of 1 m, and the material is better sorted than around the obelisk (Fig. 10.8c). Immediately to the east of the *in situ* beachrock ruin of Skoupeloi Achilleos, we also found isolated beachrock mega blocks up to 4 m long, 3 m wide and 2 m high in 2–5 m water depth. Similar to the obelisk site, most of the mega blocks were tilted, some even imbricated. One block was obviously broken into two pieces when it hit the ground (Fig. 10.8d).

Two sediment cores ANI 12 and 13 were drilled by hand in the profundal zone of the Aghios Nikolaos Bay at 7.40 m water depth (Figs. 10.1 and 10.8e). The distance between the coring sites is approximately 20 m. Both cores show a thick homogeneous layer of undisturbed clayey silt from a shallow marine to lagoonal environment which is abruptly covered by a stratum, 10–20 cm thick, consisting of fine sandy silt and abundant shell debris. The sandy layer is in turn overlain by clayey to silty sublittoral deposits. An articulated specimen of *Dosinia exoleta* taken 1 cm below the base of the intersecting event layer yielded an age of 92 cal BC–46 cal AD. Plant remains encountered 1 cm above the top of the layer date to 1673–1803 cal AD (Fig. 10.8e, Table 10.1).



Figure 10.6 – Beachrock slabs at the Santa Maura beach ridge complex dislocated by tsunami impact. (a, b) detached and dislocated slabs and blocks in the littoral zone with blocks up to 3 m long; length of rule is 2 m; (c) *in situ* beachrock eroded by littoral processes; (d) dislocated beachrock slab on top of the beach ridge; (e, f) imbricated beachrock slabs at the crest of the beach ridge. The uppermost slab, found at 3.52 m a.s.l., shows a cemented roof tile fragment from Classical–Hellenistic times; (g) comparison of the cemented roof tile fragment (top) with two roof tile fragments from reference material (bottom). Photos taken by A. Vött & S. Brockmüller, 2005.

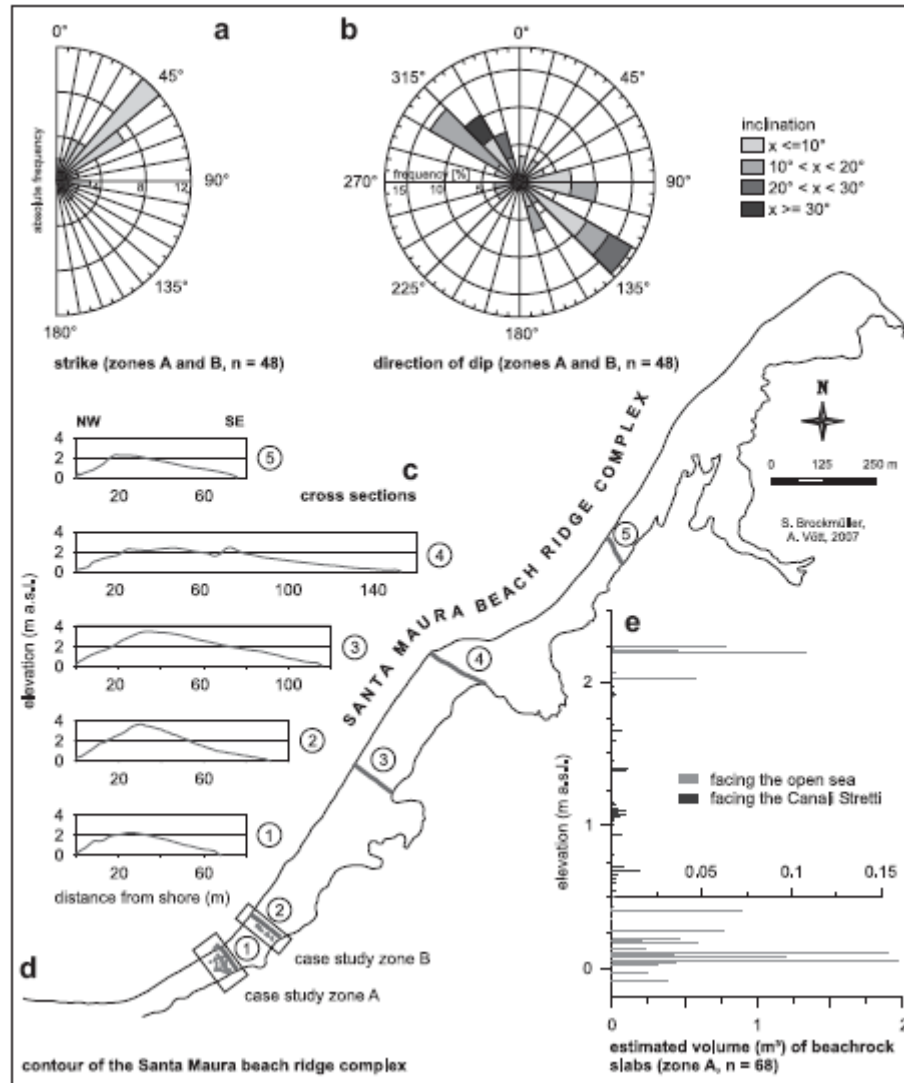


Figure 10.7 - Geomorphometric and topographic studies at the Santa Maura beach ridge complex: (a) strike direction of the longitudinal axes of dislocated beachrock slabs found in case study zones A and B; (b) direction of dip and inclination of dislocated beachrock slabs found in case study zones A and B; (c) selected topographic cross sections measured by differential GPS; (d) contour of the Santa Maura beach ridge complex measured by differential GPS and location of cross sections and case study zones A and B; (e) estimated volume (length x width x height x correction factor 0.8) and elevation of dislocated beachrock slabs found in case study zone A.

10.4.4. Evidence of strong landfall

10.4.4.1. Cheladivaron promontory

At the western fringe of the Cheladivaron promontory, some 20 m distant from the present shore, profile LOU 8 (ground surface at 1.30 m a.s.l.) was studied at the eastern side of an earthen cistern. At its base, LOU 8 shows a deeply weathered palaeosol. The palaeosol is followed by a layer, almost 20 cm thick, which includes abundant ceramic fragments within a loamy matrix (Figs. 10.1 and 10.9). Most of the ceramic fragments, up to 10 cm long, were adjusted parallel to the surface of the underlying palaeosol, some fragments were even partly pressed into it. Other ceramic fragments showed slight imbrication (Fig. 10.9a, left). The sherds are characterized by different grades of conservation. Some are slightly rounded, some are sharp edged and were broken into pieces shortly before deposition. Many ceramic fragments have a thick crust of iron and manganese oxides and hydroxides indicating strong weathering in a wet environment since the time of their deposition. Diagnostic ceramic fragments were dated to Classical–Hellenistic times. The layer also contains numerous well-rounded pieces of gravel, which partly show signs of a former cementation. Together with a 12 cm long gravelly

beachrock fragment—made up of similar pieces of gravel—these findings document a strong marine impact which transported beachrock fragments to the site (Figs. 10.9b and e). Considering that the large clasts of ceramic and beachrock fragments were embedded in a loamy substrate, the general grain size distribution of the event layer is bimodal.

Subsequent to the ceramic stratum follow two layers of colluvial deposits (Fig. 10.9a). They are, in turn, covered by a thin band of grus associated with a large block. The upper part of the profile is again made up of colluvial sediments. The whole profile is strongly weathered and void of carbonate.

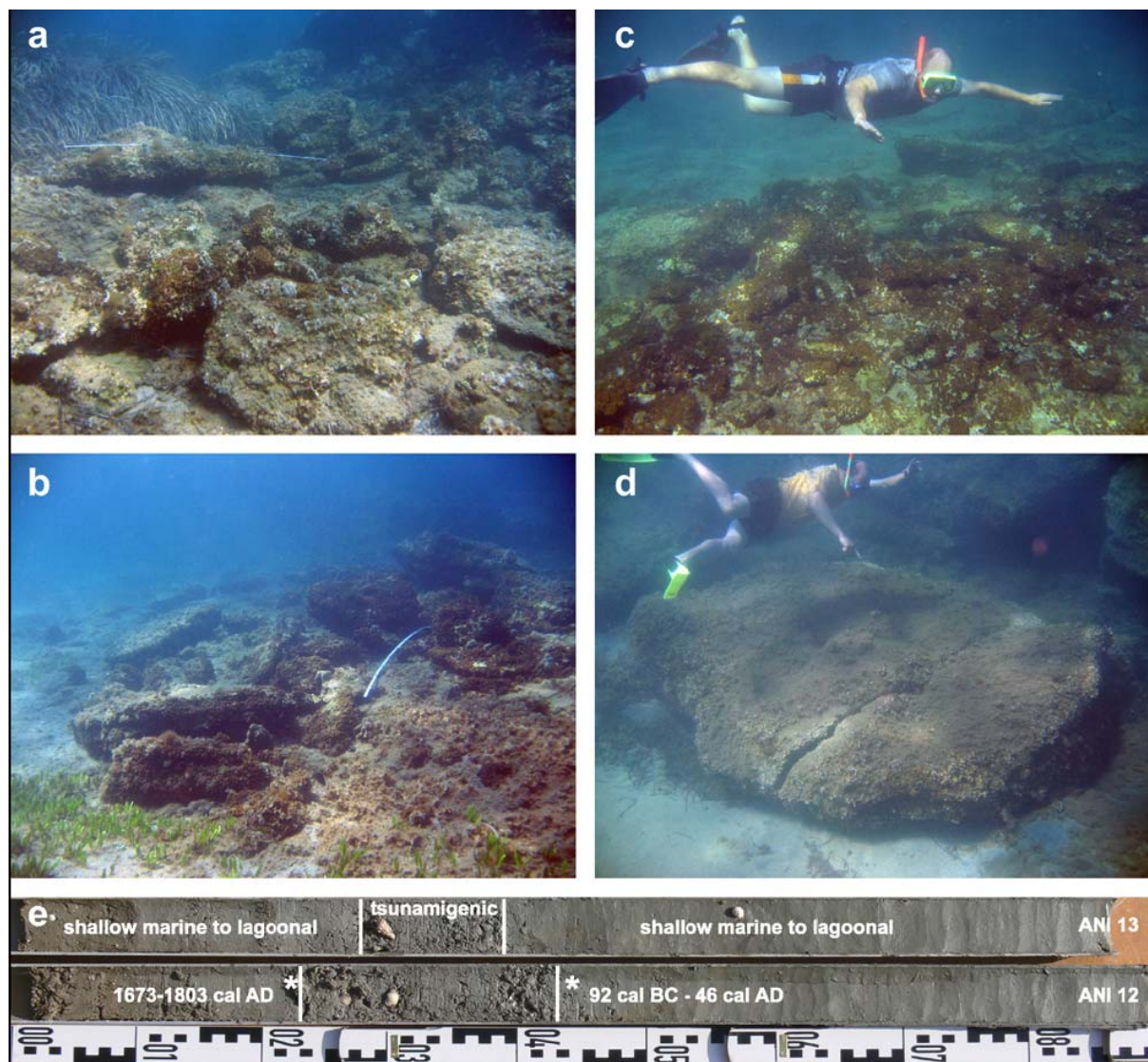


Figure 10.8 - Selected photos from geomorphological underwater studies along the Plaka and in the Bay of Aghios Nikolaos: (a, b) ridge out of dislocated beachrock slabs and blocks east of the Plaka close to the obelisk; (c, d) ridge out of dislocated beachrock slabs and dislocated mega block east of Skoupeloi Achilleos; water depth for (a–d) about 2–5 m; length of rule is 2 m, size of snorkellers is 1.90 m; (e) underwater cores ANI 12 and 13 retrieved from the profundal zone of the Bay of Aghios Nikolaos at 7.40 m water depth. Photos taken by R. Grapmayer and M. May, 2006.

10.4.4.2. Pine forest beach

Pine forest beach is located at the northern shore of the Bay of Cheladivaron just opposite to the Cheladivaron promontory. This coastal section, almost 150 m long, is the only one which is exposed to the west (Fig. 10.1). The supralittoral zone forms a flat surface at about 1.20–1.50 m a.s.l. which extends around 150 m inland and is covered with a pine forest. As the Cheladivaron promontory and the Phoukias sand spit essentially reduce wave action from the open sea, the littoral zone at Pine forest beach is limited to a narrow band below 0.40 m a.s.l. even during winter (Fig. 10.10).

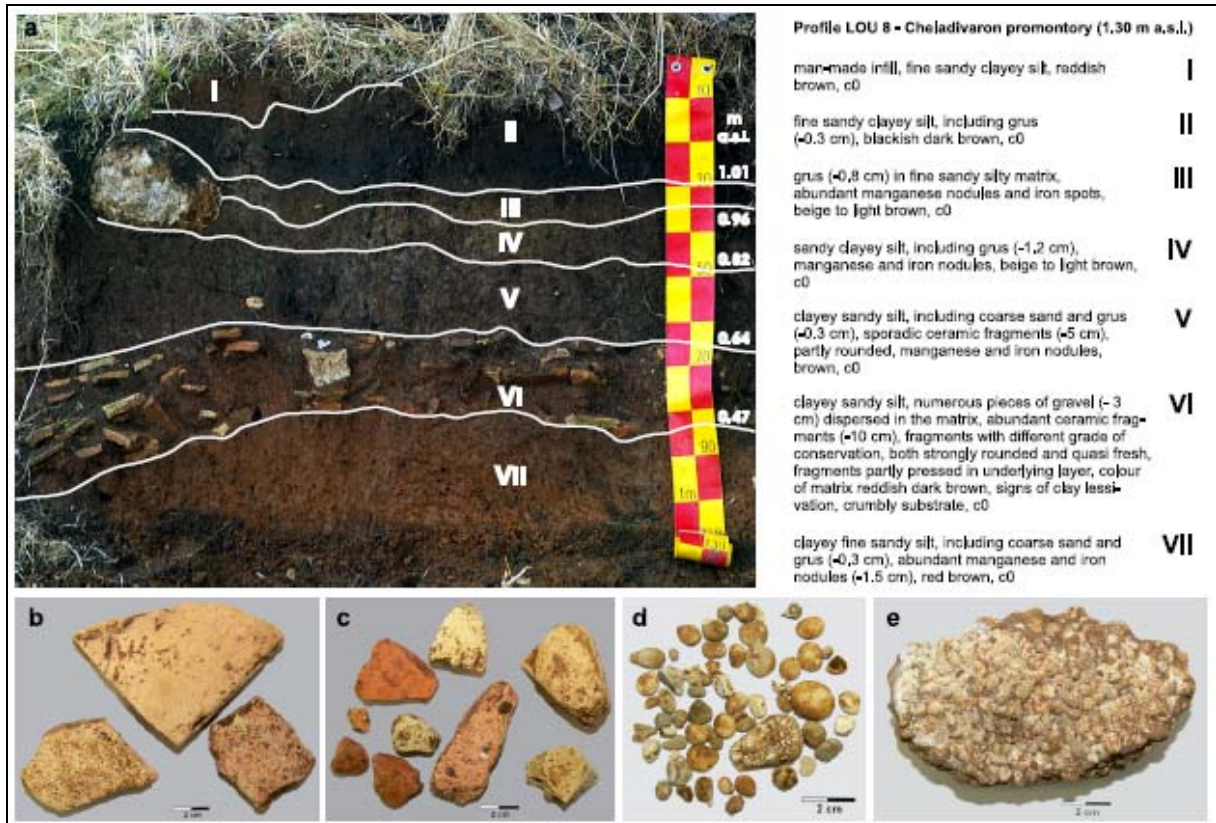


Figure 10.9 - Tsunamigenic event layer found in profile LOU 8 near the western coast of the Cheladivaron promontory. Carbonate contents: c0 = minimum (null), c5 = maximum; (b-e) ceramic fragments, beach gravel and piece of beachrock found in layer VI. Photos taken by S. Brockmüller and M. May, 2006.



Figure 10.10 - Coarse tsunami deposits at Pine forest beach at the northern shore of the Bay of Cheladivaron. Photo taken by A. Vött, 2005.

Uncovered by erosion, coarse marine deposits crop out at elevations higher than 0.80 m a.s.l. at the edge of the pine forest. The sediments show a bimodal grain size distribution as they mainly consist of middle to coarse sand and gravel up to 12 cm in length. The pebbles are well rounded and characterized by numerous boreholes made by marine boring mussels such as *Lithophaga* sp. In some pebbles, articulated specimens of *in situ* mussels are conserved. Singular pebbles are also spread on top of the supralittoral platform under the pine trees as well as between the maximum (sub-)recent strandline and the described outcrop at 0.80–1.20 m a.s.l. For these reasons, we assume that the bimodal deposits form a thick layer which extends far inland. An articulated specimen of a boring mussel found in a pebble at the northern end of Pine forest beach was ¹⁴C-AMS dated to 557–395 cal BC (Fig. 10.10).

The occurrence of well-rounded large lithoclasts with signs of bio-erosion at Pine forest beach above present mean sea level (0.8–1.2 m a.s.l.) can be explained as follows. (i) Bedrock fragments were abraded and well rounded in the littoral zone. (ii) Then, the beach gravel came out of range of littoral dynamics and under the influence of more quiescent conditions—maybe due to a change of the relative sea level, maybe due to a shift of the shoreline—so that the pebbles were no longer moved and polished. (iii) The material was subsequently colonized by bio-erosive organisms such as rock-boring mussels before it was (iv) mixed with finer material and transported on land. We interpret this last step to have been caused by an extreme event which hit the coastal zone.

10.4.4.3. Paliokoulio on Actio headland

At the southern shore of the Lagoon of Saltini, six vibracores were drilled at the eastern side of the modern outlet around 400 m distant from the modern coastline (Fig. 10.1). Fig. 10.11 exemplarily illustrates vibracore profile AKT 9 (ground surface at 1.09 m a.s.l.). The base of the profile is made up of a gleyic palaeosol showing two distinct fossil horizons. The lower horizon (fGor; symbols according to Ad-hoc-Arbeitsgruppe Boden, 2005) is dominated by bleaching spots and contains plant remains both of which indicates reduction during soil formation. The upper horizon (fG(k)so) was strongly oxidized and shows abundant nodules of manganese and iron oxides and hydroxides. Both horizons are strongly weathered and void of any carbonate.

The palaeosol is covered by badly sorted sand mixed with gravel and *grus*. The sand layer includes, at its base, numerous fragments of marine mollusks which document the marine origin of the material. The upper part of the stratum shows a similar texture but appears to be strongly weathered and does not contain any micro- or macrofaunal fragments made out of carbonate. We also encountered several ceramics fragments in this layer some of which could be used for age determination. Fragments found at 0.55 m b.s. (0.54 m a.s.l.) are definitely older than the Byzantine epoch. Potsherds found at 0.82 m b.s. (0.27 m a.s.l.) were dated to Archaic to Hellenistic times (7th–3rd century BC, Fig. 10.11).

Most of the vibracorings carried out at Paliokoulio around AKT 9 revealed a clear erosional unconformity at the base of the badly sorted sand unit. We thus assume that this part of the profiles reflects a sedimentary event.

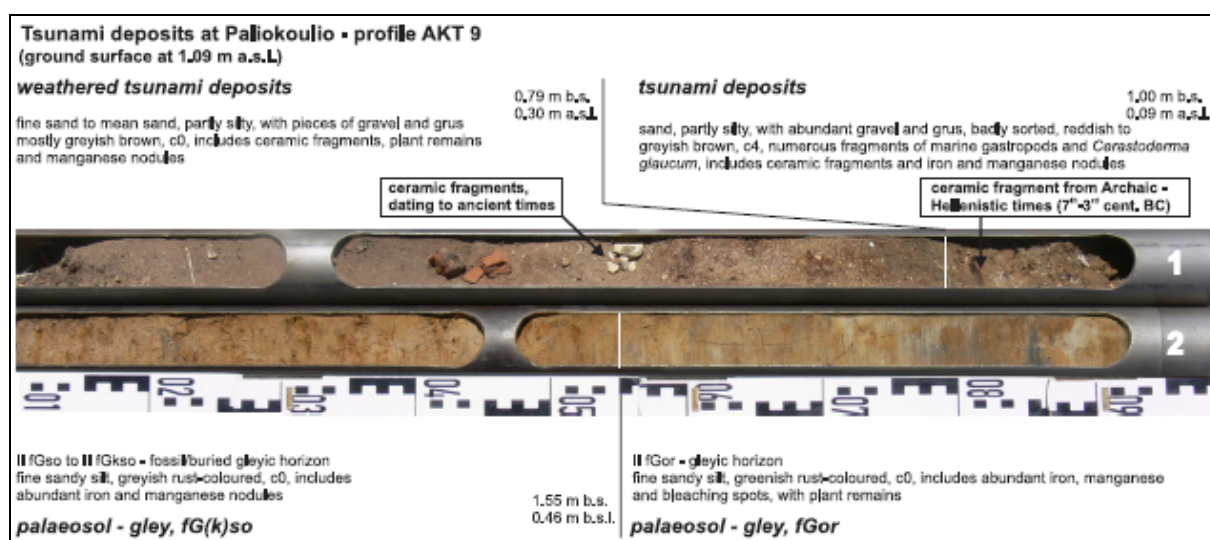


Figure 10.11 - Tsunami sediments on top of a palaeosol in a (semi-) terrestrial environment at Paliokoulio found in vibracore AKT 9. Carbonate contents: c0 = minimum (null), c5 = maximum. Photo taken by M. May, 2006.

10.5. Discussion

10.5.1. Tsunami versus storm or sea level high stand deposits

10.5.1.1. Environs of the Canali Stretti

Comparing the vibracore profiles from the washover plain east of the Canali Stretti with each other, it is remarkable that, towards the SSW, (i) the number of sedimentary events as reflected by layers of unsorted coarse material decreases, (ii) the thickness of the event layers gets smaller, and (iii) gravel is gradually replaced by sand (Fig. 10.3). We further conclude that the intensity of the highenergy events decreased towards the SSW.

Based on the stratigraphic sequences presented in Section 4.1 we interpret these event layers as tsunamigenic washover deposits. Our main argument against classifying them as storm deposits is that mid- to late-Holocene lagoonal conditions encountered between LEF 21 and LEF 2 do not show any interferences by storm wave action over a period of several millennia (Fig. 10.3). Due to their more or less regular appearance, storm events should have left thin layers of sand and gravel repeatedly intersecting the lagoonal deposits. This is not the case. Moreover, bimodal deposits as encountered in the coarse grained event layers east of the Canali Stretti are a common feature of tsunami sediments (Scheffers & Kelletat, 2003, 2004; Scheffers, 2006b). Similar tsunamigenic washover fans were detected by Gianfreda et al. (2001) at the coast of northern Gargano (Italy).

Geochemical data also reflect the tsunamigenic nature of the encountered event layers. Fig. 10.4 exemplarily depicts the electrical conductivity of sediment samples from vibracores LEF 21, 8, 4, 2 and 3. Conductivity is low for basal littoral deposits. The curves indicate that lagoonal conditions were established during a short period of time by the activation of a new coastline further seawards. It is still unclear whether tsunamigenic influence affected the coastal evolution already at this stage. However, lagoonal sediments are characterized by high conductivity values with negligible oscillations showing that the sites were not interfered by storm activity. The top sections of the profiles are characterized by an abrupt decrease of the conductivity values which reflects a sudden change in the energy household of the system as it may be caused by tsunamis. Fig. 10.4 also illustrates that the intensity of tsunamigenic impact decreases towards the SSW.

Earth resistivity measurements along transects lef-g-8 and -9 across the washover plain (Figs. 10.2 and 10.5) revealed that the coarse grained event deposits are floating on top of fine grained lagoonal and shallow marine deposits. The latter are characterized by low resistivity values. Thus, it can be excluded that the coarse units belong to an older beach ridge generation which, in former times, might have developed further landwards. If this was the case the unit should be in contact with the deeper subground. Further, inverse model resistivity sections illustrate that the event deposits do not form a singular morphological unit but are rather composed of several channel-like structures. These structures show, by the depth of their bases, different grades of erosion of the underlying sediments. As to size and direction, some of the structures correspond well to the washover fans which can be seen at the landward side of the Santa Maura beach ridge complex (Fig. 10.2) and may therefore be interpreted as their landward prolongation. Fig. 10.5 also shows that resistivity values of transects lef-g-8 and -9 are affected by saltwater effects.

Both Partsch (1907, p. 276) and von Seidlitz (1927, p. 368) suggest that the sandy area east of the Canali Stretti has been formed by aeolian processes. In fact, sandy aeolian deposits were found, but only in the uppermost parts of vibracore LEF 2 and of some smaller trenches. However, thick packages of badly sorted sand and gravel as shown in Fig. 10.3 cannot be explained by aeolian dynamics. We assume that the aeolian deposits were blown out of the large tsunamigenic washover flats and the littoral zone.

In summary, based on vibracoring, geochemical analyses, geophysical studies, and the interpretation of remote sensing data, the morphological unit east of the Canali Stretti is interpreted as a large tsunamigenic washover plain. The plain is partly submerged due to ongoing sea level rise (Vött, 2007). However, it consists of several washover fans and associated channels of different sizes (Fig. 10.5). The fact that these fans converge to one plain may be due to the nearby (palaeo-) cliff line which let the tsunami surge pile up and forced it to dump its sediments on a wider area (Figs. 10.2 and 10.3). Backwash flow may have initiated a first cut through the plain along which tsunami deposits were reworked. Later, this cut may have been deepened and dredged by man in order to use it as the navigable Canali Stretti (cf. von Seidlitz, 1927, p. 368).

10.5.1.2. Santa Maura beach ridge complex

Geomorphometric data presented in Section 4.2 indicate that the numerous beachrock slabs encountered on top of the Santa Maura beach ridge complex were dislocated by tsunami impact. The sizes of the dislocated beachrock plates lying at the present strandline, up to 2 m³ large, the high number of associated beachrock slabs deposited at the crest and the leeward side of the beach ridge over a distance of up to 150 m, and imbrication

features are our main arguments against considering these geomorphological records as caused by storms (see also Scheffers, 2006b).

Moreover, topographic cross sections show that the tsunami inundation between Sections 2 and 4 dumped large beachrock slabs at the maximum elevation of the ridge due to the divergence of the water masses overflowing the crest. However, around Section 4, the beach ridge was washed over by much thicker water masses. This is shown by the facts that the maximum elevation of the ridge is almost 1.5 m lower than further south and that large beachrock slabs are missing on top of this part of the ridge (Fig. 10.7). Starting from the point where today's beach ridge is detached from the Plaka, parts of the Santa Maura beach ridge seem to have been taken up by the tsunami surge, transported and re-deposited further landwards (Section 4.2). Younger tsunamis then caused secondary washover fans across the dislocated beach ridge unit as can be seen in Fig. 10.2. Indicators of tsunamigenic washover dynamics found at the Santa Maura beach ridge complex correspond well with tsunami deposits encountered east of the Canali Stretti.

10.5.1.3. Bay of Aghios Nikolaos

There is a lot of geomorphological evidence along the Plaka that one or several catastrophic tsunamis struck the former strandline and threw large parts of the beachrock into the Bay of Aghios Nikolaos (Vött et al., 2006a). Based on the formulae given by Nott (1997, 2003b), blocks of 6 m³ and 14 t need wave heights of around 30 m to be dislocated by storm action. However, storm waves of these dimensions are not known from the Mediterranean Sea. On the contrary, these blocks can be moved by an 11 m high tsunami surge (Bartel & Kelletat, 2003).

The fact that the Plaka beachrock was severely destroyed by an extreme event implies that the once overlying (palaeo-)beach deposits of the Plaka (cf. von Seidlitz, 1927, p. 368) were also completely flushed towards the east. The stratigraphic sequences of underwater cores ANI 12 and 13, drilled at 7.40 m b.s.l., clearly show a thick fine sand and shell debris layer intersecting shallow marine to lagoonal mud (Section 4.3). There are two arguments for which it can be excluded that this layer was accumulated by storm wave action. (i) The waters are too deep for being affected by storm wave dynamics, especially in a leeward position behind the Plaka wavebreaker, and (ii) the nearest potential sediment source is the palaeo-shoreline of the Plaka where sandy littoral deposits existed before its destruction. However, the Plaka lies some 1.7 km further west, a distance too far to span for even the largest storm. Thus, underwater findings prove strong tsunamigenic influence to the Bay of Aghios Nikolaos and fit well with the sedimentary evidence of tsunami impacts detected at the eastern shore of the bay (Vött et al., 2006a).

10.5.1.4. Cheladivaron promontory

Profile LOU 8 described from the Cheladivaron promontory also reflects strong tsunamigenic impact (Section 4.4.1). The numerous ceramic fragments found in the event layer show different grades of roundness and destruction and are embedded in a loamy matrix. Moreover, the event layer is characterized by a bimodal grain size distribution. From an archaeological point of view, it can be excluded that the ceramic layer represents a local destruction horizon such as an (*in situ*) accumulation of roof tiles from a collapsed house, for example. In this case, the ceramic fragments are supposed to be packed denser and characterized by the same grade of conservation with edges rather sharp than rounded because post-depositional transportation is missing. Moreover, the ceramic fragments found at LOU 8 are pressed into the underlying stratum and show clear lamination and, in part, even slight imbrication which is a strong argument for tsunami imprint (Scheffers, 2006b). Beachrock fragments and pebbles encountered in the event deposits testify to a strong marine influence to the site. Hereby, it has to be kept in mind that the nearest sediment source is the Plaka beachrock lying 3 km to the west of the promontory. Due to the position well above mean sea level, the sediments, the sherds as well as the beachrock fragments are deeply weathered and thus completely void of carbonate. This explains the lack of any fossil contents.

The ceramic fragments found at LOU 8 date to Classical–Hellenistic times and represent a terminus ad or post quem for a tsunami impact. As the site is not affected by torrential river systems, the *grus* layer in the upper part of the profile and the associated block may even document another tsunami. This younger tsunami possibly corresponds to the event described by Vött et al. (2006a) from the northern part of the Cheladivaron promontory around 400 m north of LOU 8. There, a field of scattered blocks and stones from the littoral zone found up to 14.80 m a.s.l. gives evidence of strong tsunami influence which—based on the ¹⁴C-AMS dating of an *in situ* boring mussel from a dislocated block—was dated to 947–1021 cal AD (Vött et al., 2006a, Fig. 10.4, Table 10.1).

10.5.1.5. Pine forest beach

There are several arguments which underline that the marine deposits encountered at Pine forest beach were not accumulated due to changes of the relative sea level but by tsunamigenic wave action (Section 4.4.2). (i) The sediments show a bimodal grain size distribution typical of tsunami deposits (Scheffers & Kelletat, 2003, 2004). (ii) Boring mussels do not colonize rocks where, at the same time, sand is being moved, suspended and deposited in the littoral zone. These organisms are used to filter their food out of comparatively clear water (Poppe and Goto, 2000). (iii) Along the adjacent coasts of Akarnania, there is no evidence of (sub-)recent or fossil beach deposits with bimodal grain size distribution (Vött et al., 2006b, c, d). (iv) We encountered sandy to partly gravely deposits in similar elevations at the harbour of Aghios Nikolaos (Vött et al., 2006a, pp. 151ff., Figs. 10.6 and 10.7) as well as around Paliokoulio. In most cases, these deposits are characterized by a clear erosional unconformity towards the underlying sediments. This indicates a sudden change from low energy to extremely highenergy conditions and the additional input of large amounts of sediments to the system. Slow gradual or even sudden coseismic submergence of the coast, however, cannot explain both the strong increase in transport energy and the increase of sediment masses; they do not cause a strong water current towards the coast. Moreover, subsequent coastal uplift would be required to explain today's high position of the deposits.

Von Seidlitz (1927, p. 368f.) suggested a sequence of coastal uplift and submergence for the Lefkada coastal zone. In his opinion, the formation of the Plaka was initiated by coastal uplift probably during the mid- Holocene. He further assumed that then, since the 7th century BC, the area has experienced a phase of coastal submergence by several metres. In fact, recent studies along the Akarnanian coast and the southern entrance to the Sound of Lefkada brought to light a considerable rise of the relative sea level since the mid-Holocene (Vött, 2007). However, the present position of the deposits at Pine forest beach well above sea level cannot be explained by coastal submergence since the time of their deposition.

Pirazzoli et al. (1994a) studied large beachrock blocks at Cape Gyrapetra (Fig. 10.1) and assumed that they document co-seismic uplift. However, these blocks are, similar to those found at the Plaka, tsunamigenically dislocated from the original beachrock unit and additionally associated to large washover fans (chevrons) across the northern shore of the Lefkada spit system (Vött et al., 2006d).

We conclude that, according to the age of the dislocated boring mussel (Section 4.4.2), the event layer at Pine forest beach was accumulated by a tsunami landfall after Archaic to Classical times and represents a runup deposit. The layer corresponds well with the younger generation of runup deposits which were encountered at the harbour of Aghios Nikolaos by Vött et al. (2006d, Fig. 10.6).

In antiquity, the Phoukias sand spit was no obstacle for a tsunami landfall at Pine forest beach. According to radiocarbon dates from a vibracore which was drilled in its centre, the spit has only been formed during the past 1000 or so years (Vött et al., 2006d, Fig. 10.4). We assume that it is made up of reworked tsunami deposits originating from the former Plaka strandline. Possibly, the formation of the spit is related to another tsunami event which occurred between 1000 and 1400 cal AD or even to a younger impact (Vött et al., 2006d, p. 159f.).

10.5.1.6. Paliokoulio

In addition to the arguments discussed for the Pine forest beach site, the Paliokoulio event layer (Section 4.4.3) may not be interpreted as sea level high stand deposit because it was accumulated inland and well above sea level so that soil formation and weathering could start immediately after deposition. Before and after the event, the site has never again been affected by influences from the seaside during the Holocene. The diagnostic ceramic fragments found at AKT 9 thus allow to conclude that a strong tsunami landfall occurred at or after Archaic to Hellenistic times (*terminus ad or post quem* for the tsunami event).

10.5.2. Strong tsunami impact during Classical–Hellenistic times

The data presented in this paper give evidence of multiple tsunami impact on the Bay of Aghios Nikolaos and its environs (Sections 4 and 5.1). In some cases it is difficult to distinguish between different tsunami events in the sedimentological record. Older tsunami deposits may have been eroded or partly reworked by a younger inundation. Depending on the direction of the tsunami landfall, the height of the tsunami surge, and the availability of sediments, some areas may even not have been affected by the deposition of tsunami sediments at all. Modern tsunami research on the 2004 southeast Asian event has shown that there are enormous local differences in the thickness and the texture of tsunami deposits (Kelletat & Scheffers, 2005; Lavigne et al., 2006; Richmond et al., 2006; Scheffers & Kelletat, 2006).

However, the Lefkada and Aghios Nikolaos coastal zones are excellent sediment traps, unique for the Mediterranean, for high frequency and mid to high magnitude tsunami events. The high sensitivity of the area is

mostly due to its direct exposure towards the open Ionian Sea and to the funnel effect caused by the contour of the coastline which amplifies tsunami waves and passes them on towards the coastal zone. Vött et al. (2006d) described sedimentological signals of four different tsunami events which occurred around 1000 cal BC, 300 cal BC, 430 cal AD and 1000–1400 cal AD.

The interpretation of radiocarbon dates received from samples out of tsunami sediments is problematic. Tsunami deposits usually represent a mixture of sediments of different age so that the resulting date can only be considered as maximum value. Sandwich dating of tsunami deposits by sampling both the underlying and the covering units is a more promising approach. However, sandwich dating is difficult to realize in cases when (i) the availability of datable material is limited, (ii) the underlying deposits were eroded by tsunami wave action, or (iii) tsunami deposits became subject to soil formation and weathering immediately after deposition because they were accumulated in terrestrial environments and were not covered again by other deposits. Future approaches will thus require the use of alternative dating techniques such as optical stimulated dating (OSL), electron spin resonance (ESR), and surface exposure dating (SED).

In this study, however, we cross-checked radiocarbon data reflecting tsunami events with the age of ceramic fragments which were found in a geoarchaeological context of strong tsunami impact. Vibracorings east of the Canali Stretti revealed at least four different tsunami events (Section 4.1, Fig. 10.3). At LEF 2, an articulated specimen of *Dosinia exoleta* from a shell debris layer associated to thick sandy deposits of tsunamigenic origin was dated to 358–247 cal BC. There is at least one older tsunami generation recorded in the profile, possibly corresponding to the 1000 cal BC event detected by Vött et al. (2006d) in the environs of the Lake Voukaria. At LEF 4, an articulated *Dosinia exoleta* specimen, also encountered in a shell debris layer, yielded an age of 515–384 cal BC. We suggest that both dates describe the same tsunami event. On the one hand, the difference in age may be explained by different (palaeo-)reservoir effects. On the other hand, both samples were taken from shell debris layers and may therefore be reworked. We thus prefer the younger age of LEF 2 as a time marker for the tsunami event.

A cemented roof tile fragment of Classical–Hellenistic age (5th–3rd century BC) associated to tsunamigenically dislocated beachrock slabs at the Santa Maura beach ridge complex gives a terminus ad or post quem for a strong tsunami event (Section 4.2). The time range given for this event overlaps with the two radiocarbon dates presented for LEF 2 and 4. It is remarkable that we did not find any younger ceramic fragments along the Santa Maura beach ridge complex which were associated to tsunami deposits.

At the Cheladivaron promontory, geoarchaeological findings give evidence of a tsunami event which occurred at or after Classical–Hellenistic times and possibly of a younger event which corresponds to a nearby tsunamigenic field of scattered blocks and stones dating to around 1000 cal AD (Vött et al., 2006d). Data collected at Pine forest beach suggest a tsunami impact shortly after 557–395 cal BC which is the time period during which a dislocated boring mussel was alive. The 395 cal BC date thus represents a *terminus post quem* for the tsunami. However, it may be a little too old because the boring mussel is supposed to have taken up old carbon from the hosting carbonate rock. At Paliokoulio, ceramic fragments incorporated into tsunami deposits yielded a terminus ad or post quem; considering that (i) soil formation and weathering of the upper part of the tsunami deposits took a considerable period of time and (ii) the event layer did not contain any younger ceramic fragments, we assume that the tsunami occurred during or only a short time after Archaic to Hellenistic times (7th–3rd century BC).

According to the radiocarbon dates available for underwater core ANI 12, a strong tsunami event hit the Bay of Aghios Nikolaos shortly after 92 cal BC–46 cal AD (Section 4.3). This means an age difference of around 300 years compared to the tsunami event detected at the Santa Maura beach ridge and the area east of the Canali Stretti. However, it has to be taken into account that the articulated specimen of *Dosinia exoleta* from ANI 12 lived in the profundal zone. Satellite pictures and bathymetric data show that the latter is a small circular kettle-like basin surrounded by areas of shallower water depths. Its formation is possibly related to strong karstification of Triassic limestone or gypsum layers. Outcrop of gypsum is known from many sites of coastal Akarnania (Underhill, 1988) and is supposed to play a considerable role in the seismic behaviour of the region (Galanopoulos and Ekonomides, 1973). The (palaeo-)reservoir effect around ANI 12 may therefore be lower than in adjacent areas due to increased freshwater input by submarine springs what might explain the 300 years difference in age. Therefore, it seems probable that the tsunami deposits encountered at ANI 12 and 13 still correspond to the same tsunami impact which affected the Santa Maura beach ridge complex and the Canali Stretti during Classical–Hellenistic times. Another point should be mentioned: the region was controlled by the Romans since the 2nd century BC (Murray, 1982). If the 92 cal BC–46 cal AD age of ANI 12 was correct, we would therefore expect some Roman sherds to be associated with the kind of tsunami deposits and event layers encountered at the Santa Maura beach ridge complex, the Cheladivaron promontory, and at Paliokoulio. It is barely conceivable that the ANI 12 event did not affect the adjacent coasts at all. The 1673–1803 cal AD age of plant remains found near the top of the tsunami layer at ANI 12 may indicate that the deposits were (i) reworked by a younger tsunami event and/or (ii) affected by bioturbation.

In summary, radiocarbon dates and archaeological ages from five different sites where evidences of strong tsunami impact were found clearly overlap and indicate a major tsunami during Classical–Hellenistic times. Based on the given ages, it is concluded that the event occurred after 395 cal BC, most probably during 358–247 cal BC.

Remarkably, there are no accounts by ancient writers that a tsunami or unusual event ever hit the coastal region around Lefkada and Aghios Nikolaos. Nevertheless, there is detailed information on the navigability of the Sound of Lefkada which, from time to time, is reported to have been choked with sediments and thus was impassable for ships (Partsch, 1889, 1907; Murray, 1982). Against the background of multiple tsunami impact as shown by Vött et al. (2006d) and in this paper, it is therefore suggested that the sound was repeatedly affected by tsunami runup and runthrough dynamics. This includes the tsunamigenic accumulation of allochthonous deposits in the shallow water lagoonal environment or tsunamigenic flush-through effects creating or renewing navigable channels (see also Vött et al., 2008c). Further research is though required to improve our knowledge on (palaeo-) tsunami landfalls in this area and their implications for human societies and man-made infrastructure.

10.6. Conclusions

Based on geomorphological, sedimentological, geochemical and geophysical analyses, the study of this paper revealed repeated tsunami impact on the Bay of Aghios Nikolaos and its environs. Geochronological data from five sites show that a strong tsunami event happened during the Classical–Hellenistic period. Evaluating the available radiocarbon ages against the background of various geoarchaeological findings the tsunami occurred after 395 cal BC and most probably before 247 cal BC. By comparing and combining tsunami traces, it was possible to set up the following scenario.

(i) Geomorphometric data indicate that the Classical– Hellenistic tsunami hit the Santa Maura beach ridge complex from a northwestern direction (Fig. 10.7). At the southern part of the ridge, up to almost 4 m a.s.l., dislocated beachrock slabs were dumped by the tsunami surge (Fig. 10.6) which additionally produced a washover plain and associated washover fans into the landward lying lagoon (Figs. 10.2 and 10.3). The northern part of the ridge was pushed in a more landward position. Geomorphological data reflect a minimum height of the tsunami wave train of 4–6 m a.s.l.

(ii) The central and northern parts of the former Plaka strandline were completely destroyed by tsunami wave action (Fig. 10.8). Loose beach deposits were flushed into the Bay of Aghios Nikolaos and also affected the adjacent coast. The Plaka beachrock structure, broken into pieces, was partly dislocated landwards. Further geochronological data are, however, necessary to clarify the extent of destruction during the Classical–Hellenistic event.

(iii) Due to tsunamigenic inflow into the Bay of Aghios Nikolaos, a sandy shell debris layer was deposited in the profundal zone of the bay some 1.7km east of the Plaka. Large parts of the backwash obviously flowed in a southwestern direction and affected the washover plain east of the Canali Stretti (Figs. 10.2, 10.3 and 10.8).

(iv) As reflected by a thick tsunamigenic destruction layer found at LOU 8 between 0.47 and 0.64 m a.s.l. the tsunami surge hit the Cheladivaron promontory (Fig. 10.9). At Pine forest beach, a thick package of dislocated beach deposits, possibly originating from the former Plaka coast around Skoupeloi Achilleos some 3.6km further west, was accumulated up to 1.20 m a.s.l. (Fig. 10.10). The tsunami landfall at Paliokoulio caused considerable erosion of preexisting semi-terrestrial palaeosol units, and tsunami sediments, up to 1 m thick, were deposited (Fig. 10.11). The findings suggest that the tsunamigenic inundation reached at least 2–3 m a.s.l.

It is further concluded that the Classical–Hellenistic tsunami event, though it is not mentioned by ancient sources, had considerable effects on the local population and infrastructure, especially on the navigability of the Sound of Lefkada.



2nd International Tsunami Field Symposium

IGCP Project 495

Quaternary Land-Ocean Interactions:
Driving Mechanisms and Coastal Responses

Ostuni (Italy) and Ionian Islands (Greece) 22-28 September 2008



Project 495

CHAPTER 11

Late Holocene tsunami imprint at the entrance of the Ambrakian gulf (NW Greece)

Vött A., Brückner H., May S.M., Lang F., Brockmüller S.

**Totally reprinted from Méditerranée 108 (2007), 43–57*

11.1. Introduction

The Ionian Sea and its coasts belong to the seismically most active regions of the Mediterranean and has been affected by many earthquakes and associated tsunamis. The high tsunami risk has decisively been revealed by the increasing number of tsunami studies which have been carried out during the last two decades. By these studies, a variety of event deposits have been identified and used to reconstruct tsunami landfall history during the Holocene (for instance Dominey-Howes, 2002; Dominey-Howes et al., 2000b; Kelletat & Schellmann, 2002; Mastronuzzi & Sansò, 2004; Minoura et al., 2000; Morhange et al., 2006; Reinhardt et al., 2006; Scheffers, 2006a; Stefatos et al., 2006).

Geological records for multiple tsunami impacts on the coast near Lefkada were encountered during the course of interdisciplinary investigations on the Holocene evolution of coastal Akarnania in northwestern Greece (Vött et al., 2006b, 2006c, 2006d). Different types of interrelated tsunami deposits were identified. They are part of a system of tsunami sediment traps which seem to be unique for the eastern Mediterranean (Vött et al., 2006a, 2008c).

This paper gives evidence for tsunami landfall at Aktio headland at the entrance to the Ambrakian Gulf (NW Greece). The main objectives of our study are (i) to present geomorphological, sedimentological and geoarchaeological records of tsunamigenic activity, (ii) to establish a tsunami geochronology, and (iii) to reconstruct the flow direction and the flow intensity of palaeo tsunami waves in order to assess the present tsunami risk of the area.

11.2. Topography and geotectonic setting

Aktio headland, almost 7 km long and 4 km wide, is located in the coastal zone between Preveza and Lefkada (Fig. 11.1). It is bordered by the Ionian Sea to the west, by the Ambrakian Gulf to the east, and by the Strait of Aktio/Preveza, only 600 m wide and 8 m deep, to the north. The headland is a low lying coastal area with maximum elevations of 6 m above present sea level (m a.s.l.) and has a slightly undulating surface. The Phoukias sand spit which extends into the Bay of Aghios Nikolaos and the Plaka are the most striking geomorphological features of the present-day coast. The Plaka represents the partly submerged ruins of a former strandline and is entirely made up of beachrock (von Seidlitz, 1927), up to 6-10 m thick.

The formation of the Plaka beachrock started in the 5th millennium BC at the latest closing off the lagoons of Lefkada and Aghios Nikolaos from the open Ionian Sea (Vött et al., 2006a). The shallow waters of the Lagoon of Saltini cover the central parts of the Aktio lowlands. In the north, the spit of Aktio bears the sparse archaeological remains of the ancient sanctuary of Apollo which was used by the Akarnanian people at least during Hellenistic times (Murray, 1982).

According to Paschos et al. (1991) and IGME (1996), the Aktio headland is largely made up of Holocene coastal sediments and swamp deposits. The Preveza area and parts of the hills of Stoupas (Fig. 11.1) consist of Pleistocene sand units and Pliocene to Pleistocene marls, sandstones and conglomerates of a Flyschlike facies. In contrast, the Plaghia Peninsula, the hills between Aghios Nikolaos and Vonitsa as well as the hills east of Aghios Thomas near Preveza are composed of limestone, partly brecciated, and dolomite of Triassic to Cretaceous age. Parts of the underground are characterized by thick Triassic evaporitic units which have considerable influence on tectonodynamic (Galonopoulos & Ekonomides, 1973; Laigle et al., 2004) and coastal evolution (Underhill, 1988).



Figure 11.1 - Topographic overview of the coastal zone between Preveza and Lefkada and detailed map of the Aktio headland showing vibracoring sites and location of underwater studies.

The Ambrakian Gulf is a tectonic basin which has been formed by NE-SW directed crustal compression and NNW-SSE trending extension (Clews, 1989). The main triggering factors are pull-apart dynamics caused by the rapid southwestward movement of the Aegean microplate (Doutsos & Kokkalas, 2001). Moreover, northwestern Greece underwent a 40° clockwise rotation during 15-8 Ma and a 20° clockwise rotation after 4 Ma (van Hinsbergen et al., 2005). Northern Akarnania even shows a 90° clockwise rotation since Oligo- Miocene times (Broadley et al., 2004). Both rifting and rotation are responsible for the opening and spreading of the Ambrakian Gulf.

The northernmost section of the Hellenic Arc lies not far offshore Aktio headland. As part of a multiple plate junction, the right-lateral strike slip Cefalonia transform fault (CF) and the Lefkada fault (LF) induce the high

seismo-tectonic activity of the area (Cocard et al., 1999; Louvari et al., 1999). Rates of crustal motion south of the CF and LF reach up to 40 mm/a whereas north of the CF, they are negligible (Kahle et al., 2000; Peter et al., 1998).

The study area experienced a $M_w = 6.2$ earthquake shock on August 14, 2003, which was induced by the Lefkada fault (Karakostas et al., 2004) and triggered a small tsunami of 0.5 m south of Nidri on Lefkada Island (EERI, 2003). The Preveza-Lefkada coastal zone is strongly affected by high frequency and mid to high magnitude earthquakes (Papazachos & Papazachou, 1997) and is thus characterized by a high tsunami risk (Papazachos and Dimitriu, 1991). It is known to have been repeatedly hit by tsunami events. A regional tsunami catalogue, mainly based on historical sources analyzed by several authors, has been compiled by Vött et al. (2006a).

11.3. Materials and methods

A series of 28 vibracores was drilled at Aktio headland in search of tsunamigenic deposits. Vibracoring was carried out by means of an Atlas Copco mk1 corer using core diameters of 6 cm and 5 cm. The maximum recovery depth in the study area was 18 m below ground surface (m b.s.). Vibracores were analyzed in the field using geomorphological and sedimentological methods. Colour, grain size, texture, macrofossil fragments and carbonate content were determined for each sediment layer. Macrofaunal remains were used to elucidate the sedimentary environment.

Sediment samples were taken for geochemical analyses of parameters such as electrical conductivity, pH-value, loss on ignition, content of orthophosphate, as well as of the concentration of (earth-) alkaline and heavy metals. Geochemical values were helpful to detect facies changes (Vött et al., 2003).

Detailed geomorphological surveys were conducted on land and under water by means of scuba diving along transects across the submerged Plaka beachrock remains. Underwater findings of dislocated beachrock blocks and rubble ridges were measured, photographed, and sampled. A high-resolution differential GPS system (Leica SR 530) was used to determine the position and elevation of vibracoring sites.

The geochronological framework of the study is based on (i) ^{14}C -AMS analyses of organic material and shells made out of marine carbonate as well as on (ii) the age determination of diagnostic ceramic fragments encountered in vibracore profiles and during field surveys. Concerning samples from marine environments, the palaeo-reservoir effect may differ from the modern one and has possibly been variable through time and space (Geyh, 2005). This is why we refrained from determining the modern reservoir effect and corrected all marine samples for a mean marine reservoir age of 402 years ($\Delta R = 0$; Reimer and McCormac, 2002). Calibration was carried out using the Calib 5.0.2 software.

11.4. Event deposits at Aktio headland

We present sedimentological and geomorphological evidence of multiple tsunami impacts encountered in 15 selected vibracores from the Aktio headland and during underwater studies around Skoupeloi Achilleos (Figs. 11.2 to 11.6).

11.4.1. Phoukias and the Phoukias sand spit – transect A

Vibracore transect A shows a general SSE-NNW direction (Fig. 11.1). The transect starts at the Phoukias sand spit and, in its greatest part, runs almost parallel to the modern coastline some 200-400 m inland. Facies distribution for transect A is illustrated in Fig. 11.2.

The base of vibracore ANI 2 is made up of clayey silt which was deposited in the sublittoral zone of a quiescent shallow marine to lagoonal environment. These deposits are abruptly covered by fine sand (11.11-10.17 m below sea level (= m b.s.l.)). The medium to high energy influence subsequently led to a complete change of the sedimentary environment and a thick package of clearly laminated silty to fine sandy deposits with abundant sea weed remains was deposited. The latter document upgrowing generations of sea weed mats. Although wave dynamics seem to have been restricted, conditions were much more energetic compared to the preceding quiescent phase. An intersecting layer of homogeneous fine sand (6.16-5.72 m b.s.l.) may indicate another temporary shift towards higher energy conditions. Quiescent sedimentary conditions at the base of ANI 14 were interrupted by the input of a thick sequence of badly sorted middle sand including marine shell debris and fragments of *Echinoidea* and *Bryozoa* (9.65-7.77 m b.s.l.). Afterwards, lagoonal conditions were re-established. Intersecting layers of shell debris embedded in a silty to sandy matrix and partly rich in organic material (7.08-4.87 m b.s.l.) document, once more, abrupt high energy interferences of the quiescent environment. In the uppermost parts of profiles ANI 2 and ANI 14, silt-dominated lagoonal units are abruptly

topped by coarse to middle sand reflecting another sudden increase of energetic input to the system (ANI 2: 3.27-1.22 m, ANI 14: 2.88-0.36 m b.s.l.). Hereafter, ANI 2 came under shallow marine influence and sandy littoral sediments were deposited. Meanwhile, at ANI 14, a soil was formed. Lagoonal conditions were then neither re-established at ANI 2 nor at ANI 14. However, a layer of gravel in a silty to sandy matrix, 6 cm thick, which was found at ANI 14 on top of the subrecent soil (0.33-0.39 m a.s.l.), documents short-term influence from the littoral zone.

Vibracores AKT 1-3 largely differ from the stratigraphic sequences of cores ANI 2 and ANI 14. The base of profile AKT 1 consists of weathered silty to clayey sediments. They are covered by strongly weathered silty lagoonal and fine to middle sandy littoral deposits. The upper part of the sand unit shows a brownish palaeosol the top of which is clearly eroded and overlain by grey coloured and badly sorted sand with abundant fragments of marine mollusks and pieces of gravel (1.90-1.65 m b.s.l.). Subsequently, a layer of well sorted sand follows (1.65-0.58 m b.s.l.) which, in turn, is covered by another thick stratum of badly sorted middle sand including shell fragments and gravel (0.58 m b.s.l. – 0.84 m a.s.l.). This stratum is of a brownish colour and obviously underwent weathering after it had been deposited. The following stratum of well sorted sand (0.84-1.42 m a.s.l.) is covered by aeolian deposits. Vibracore AKT 1 clearly documents the high energy input of marine sediments into a terrestrial environment and the partial erosion of the underlying pre- to mid-Holocene palaeosol. The intersecting upper palaeosol documents that the site must have been affected twice by sudden wave activity from the seaside. The total thickness of the event deposits at AKT 1 is 3.32 m.

Vibracore profile AKT 2 is similar to AKT 1. The erosional unconformity at the base of the sandy event layer (1.59 m b.s.l. – 0.50 m a.s.l.), however, is formed on top of strongly weathered silty lagoonal deposits. At vibracoring site AKT 3, the older generation of event deposits (0.43 m b.s.l. – 0.40 m a.s.l.), including numerous shell fragments, is partly weathered. The younger generation is characterized by shell debris and badly sorted sand which was deposited well above sea level (0.40-0.83 m a.s.l.). The uppermost part of AKT 3 is made up of aeolian fine sand.

11.4.2. Underwater geomorphology at Skoupeloi Achilleos

Skoupeloi Achilleos belongs to the northern section of the partly submerged Plaka palaeo coastline. It is located some 2.3 km to the west of Phoukias and some 2.2 km to the north of the outermost tip of the Santa Maura beach ridge (Fig. 11.1). Underwater studies were conducted along a WNW-ESE running transect.

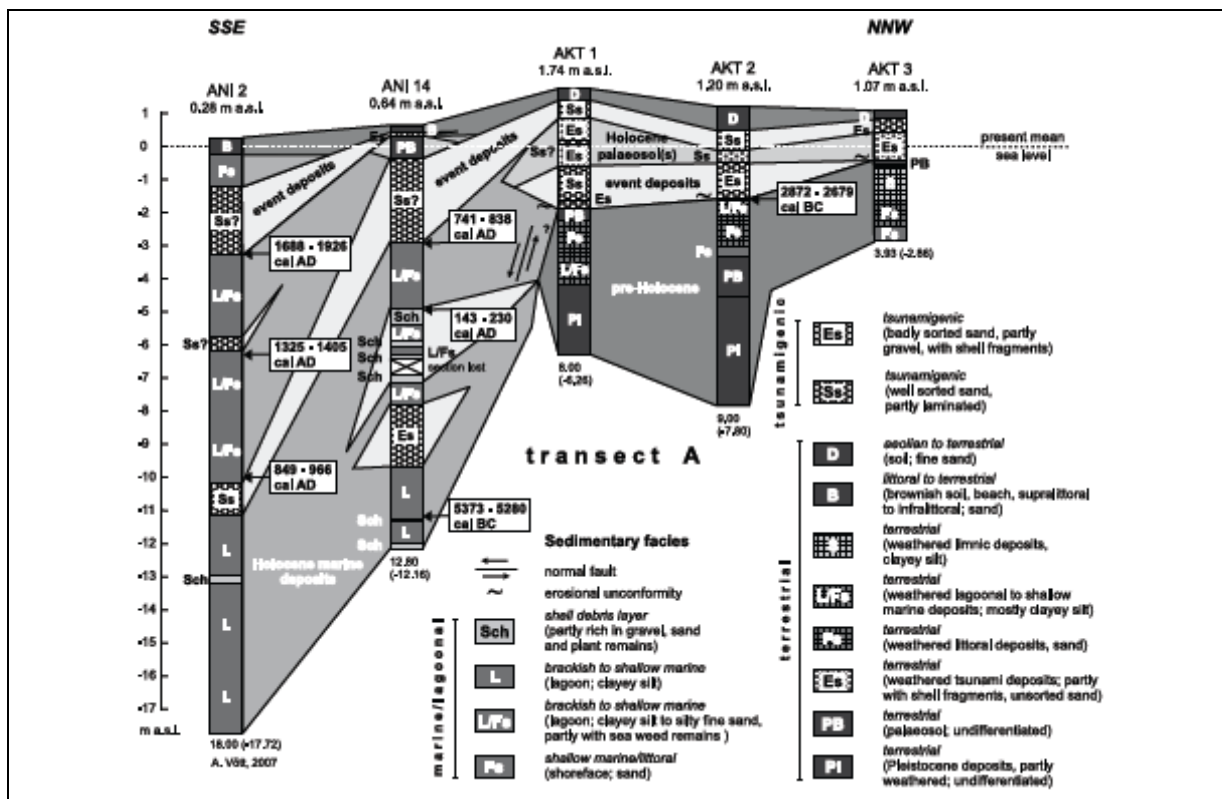


Figure 11.2 - Facies distribution and tsunami deposits found in vibracores from the Phoukias sand spit and Phoukias (transect A).

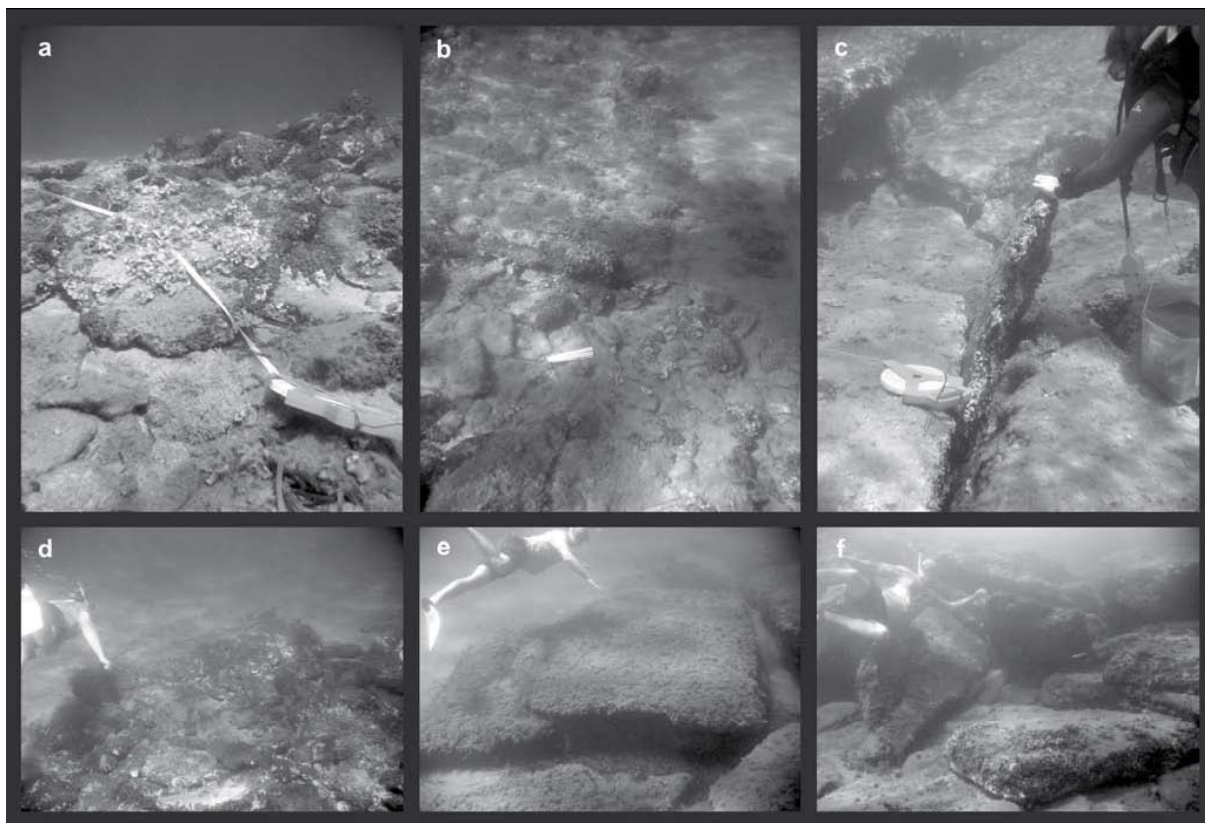


Figure 11.3 - Geomorphological underwater studies at Skoupeloi Achilleos to the west of the Phoukias sand spit. (a), (b), (d): Isolated rubble ridge made up of beachrock fragments. Beachrock stones and slabs originate from the partly submerged Plaka ruin. They were dislocated by tsunamigenic wave action and moved over a distance of 40 m. Beachrock fragments are partly embedded in or lie on top of sandy deposits. (c), (e), (f): Beachrock slabs and blocks some 15-20 m east of the in-situ Plaka beachrock. One slab sticks vertically between dislocated blocks. Some of the blocks show imbrication. All slabs and blocks are detached from the in-situ beachrock and partly embedded in a sandy substrate. Body length of snorkeler is around 1.90 m. Photos taken by R. Grapmayer, 2006.

Around 40 m east of the in-situ beachrock ruin of the Plaka, we found a ridge made out of isolated beachrock fragments at 2.5-3.2 m water depth. The rubble ridge is up to 0.9 m thick. The dislocated beachrock slabs along the transect show a maximum diameter of 1.0 m and a maximum volume of 0.3 m^3 (Fig. 11.3a). Close-by the transect, we encountered individual slabs up to 2 m long (Fig. 11.3d). The ridge structure is completely separated from the Plaka and its components lie on top of or are partly embedded in sandy deposits. Approaching the Plaka, numerous large beachrock blocks lie in extraordinarily disordered positions completely detached from the in-situ beachrock ruin at 2.9-4.6 m water depth. Some of the blocks were obviously broken into pieces when they hit the ground. Along the scuba dive transect, the largest dislocated blocks show a maximum volume of $\approx 3 \text{ m}^3$. However, not far off the transect, we measured blocks up to $\approx 25 \text{ m}^3$. Many blocks are piled up to block clusters. In some places, we found clear imbrication (Figs. 11.3e and f). Isolated beachrock blocks larger than 1 m^3 were encountered up to 15-20 m to the east of the Plaka.

Both rubble ridge and dislocated blocks are densely overgrown by marine algae and other marine organisms. This documents that the deposits are not affected by recent wave activity even during storms. Bio-erosion and bio-construction features found at the bottom sides of slabs and blocks prove dislocation of the material from its original position.

From a palaeogeographical point of view, the lagoonal deposits encountered at the base of vibracore ANI 2 (Fig. 11.2) prove that the formation of the Plaka beachrock had already started and induced quiescent hydrodynamic conditions east of it. The Plaka beachrock was part of a beach ridge system which separated the lagoonal Bay of Aghios Nikolaos from the Ionian Sea. Geomorphological underwater evidence found at Skoupeloi Achilleos clearly documents high energy impact to the former coastline. The impact destroyed the beach ridge and the Plaka beachrock throwing stones, slabs and blocks in an easterly direction. We assume that the beachrock had already been broken into pieces by previous earthquake influences along the Lefkada fault. The adjacent lagoon of Aghios Nikolaos, deprived of its natural barrier, subsequently experienced increasing sea water influence and wave activity. The findings at Skoupeloi Achilleos correspond well to dislocated beachrock units described from the Santa Maura beach ridge system and the southern part of the Plaka by Vött et al. (2006a, 2008c).

11.4.3. Paliokoulio and Koumaros – transect B

Transect B trends in a SSE-NNW direction across the southern outlet of the Lagoon of Saltini (Fig. 11.1). Vibracores AKT 9-12 were drilled within a distance of 30 m along a line running from the top of a natural ridge-like topographic unit across its northern flank towards the southern shore of the Saltini channel. Vibracores AKT 23 and AKT 24 are located on the opposite shore of the lagoon.

The lower part of profile AKT 9 is a gleyic palaeosol comprising fine sandy to predominantly silty deposits and is characterized by iron oxide spots down to 0.66 m b.s.l. (Fig. 11.4). On top of an erosional unconformity, we found a layer of badly sorted sand rich in fragments of a marine macrofauna and gravel (0.09-0.61 m a.s.l.) which also includes ceramic fragments. The subsequent stratum has a similar texture (0.30- 0.61 m a.s.l.) and contains gravel and potsherds. However, it is strongly weathered and thus void of carbonate. The top of the core is made up of weathered aeolian fine sand.

The facies pattern encountered at site AKT 10 is almost identical to the one described for AKT 9. However, the lower unweathered unit of coarse grained deposits (0.08-0.17 m a.s.l.) mainly consists of gravel and includes fragments of beachrock, up to 6 cm large. The erosional discordance is even clearer than at AKT 9. The upper coarse grained unit is almost 30 cm thick (0.17-0.46 m a.s.l.). We found ceramic fragments in these two units (Fig. 11.4). The top of profile AKT 10 is made up of weathered dune sand.

At AKT 11, the sandy layer (0.23-0.12 m b.s.l.) on top of the palaeosol is entirely weathered and void of fossil remains out of carbonate. It is covered by clayey silt which was deposited under limnic to brackish conditions and which, at its top, forms a dark palaeosol. The palaeosol, in turn, is abruptly covered by another sand stratum (0.16-0.29 m a.s.l.) which includes ceramic fragments.

The basal palaeosol of vibracore AKT 12 shows spots of iron oxide down to 0.55 m b.s.l. The subsequent layer consists of coarse sand and gravel (0.54-0.43 m b.s.l.) with embedded remains of a marine macrofauna. Another layer of marine sand, laminated and comparatively well sorted, appears on top of intersecting lagoonal mud and is also rich in marine fossils (0.38-0.10 m b.s.l.). The upper part of the profile is made up of clayey to silty marsh deposits.

Vibracores AKT 9-12 clearly document that sediments from marine environments were thrown onto near-coast terrestrial sites by high energy impact. The depositional event caused an erosional unconformity. The event deposits, according to their unsorted nature and the included fragments of marine fossils, seem to be mixed up and consist of material from different marine environments. According to their weathered appearance, most of the event layers were deposited above sea level at the time of deposition. Profiles AKT 11 and AKT 12 were affected twice by a sedimentary event.

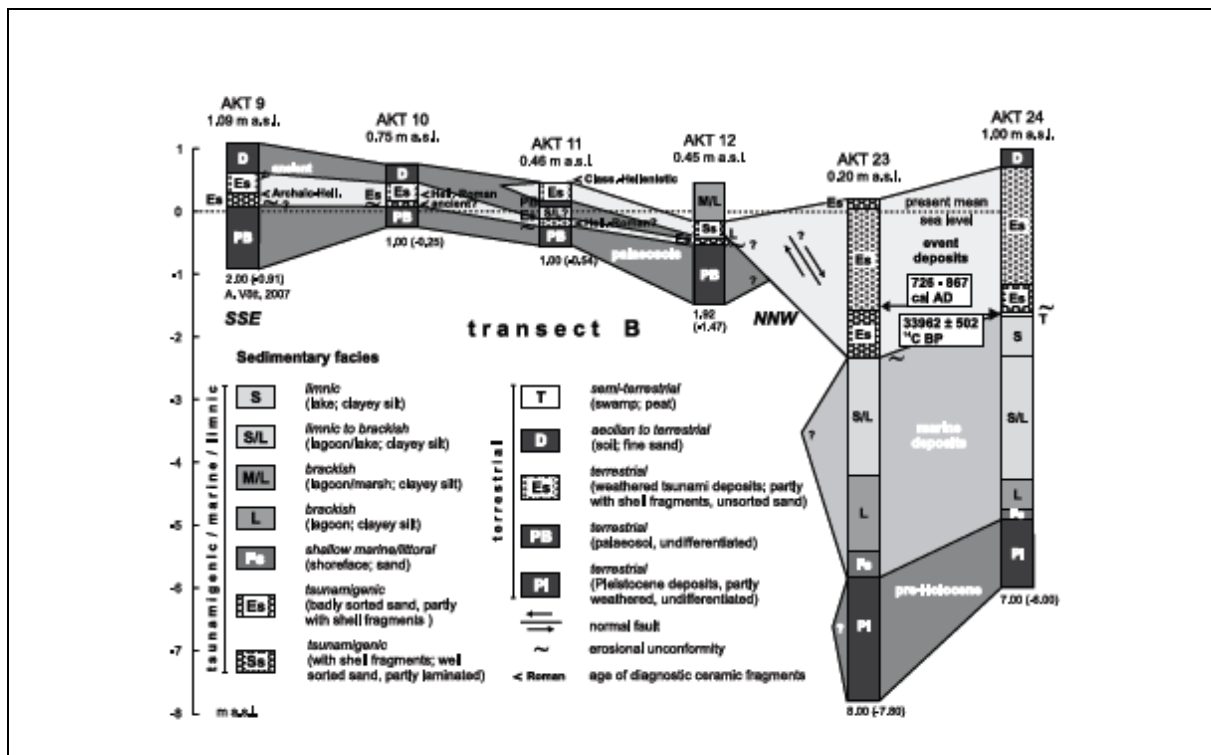


Figure 11.4 - Facies distribution and tsunami deposits found in vibracores from Paliokoulio and Koumaros (transect B).

The base of vibracore AKT 23 is made up of cemented fine sand possibly identical to the aeolianite of Pleistocene age described by Paschos et al. (1991) from the Preveza area. It is covered by littoral sand and subsequent lagoonal mud. In its upper part, the mud, according to the decreasing content of marine macrofossils, reflects increasing influence by freshwater. The following limnic sediments were cut by an erosional unconformity and covered by mean sand (2.73-1.98 m b.s.l.) which, partly weathered (1.98-0.05 m b.s.l.), documents sudden and abrupt high energy influence at the site. On top of it, we found coarse sand (0.05 m b.s.l. – 0.20 m a.s.l.), including fragments of *Cerastoderma glaucum* and *Pecten sp.*, which is suggested to corresponds to a younger event generation.

The facies pattern encountered at AKT 24, drilled some 50 m inland, is almost identical to the one of AKT 23. However, the erosional unconformity was formed in a peat layer rich in gastropod fragments. Moreover, the overlying stratum of coarse sand (1.61-1.15 m b.s.l.) includes fragments of a marine macrofauna. Young generation event deposits were not found at AKT 24. In contrast, the top of the profile is made up of weathered aeolian sand.

Vibracores AKT 23 and AKT 24 confirm the twofold landfall of strong wave events. The comparatively deep position of the coarse grained event deposits however indicate that the area (i) has been affected by coastal subsidence along NE-SW running faults (Paschos et al., 1991), (ii) represents a pre-existing topographic low and/or (iii) reflects a deep erosion channel. We found spots of iron oxide down to 1.20 m b.s.l. at AKT 23 and 1.60 m b.s.l. at AKT 24 which indicates that subaerial weathering of the event deposits took place for a certain time period after deposition.

11.4.4. Northeastern shore of the Lagoon of Saltini

Several vibracores were drilled at the northeastern shore of the Lagoon of Saltini east of the road between Vonitsa and Preveza (Fig. 11.1). In this area, the lagoon has almost completely desiccated. Fig. 11.5 exemplarily illustrates vibracore AKT 14 (ground surface at 0.20 m a.s.l.) which was drilled some 30 m from the shore of the Ambrakian Gulf (Fig. 11.1). The lower part of the profile shows brownish grey, clayey to silty deposits (4.80-3.20 m b.s.l.) which – due to numerous spots of iron oxide – were accumulated in an ephemeral shallow lake. Several indeterminable ceramic fragments found at 3.37 m b.s.l. indicate a mid- to late Holocene age. The following deposits are of similar grain size and texture (3.20-1.44 m b.s.l.). Their grey colour, however, reflects a permanent limnic environment. An intersecting peat layer documents temporary semi-terrestrial conditions (2.43-2.30 m b.s.l.).

Numerous fragments of marine shells, partly in the form of shell debris layers, abruptly appear in the subsequent layer (1.44-0.96 m b.s.l.) which consists of clayey silt and was accumulated on top of a slight erosional unconformity. The deposits also include wood remains and a lot of organic matter. However, subsequent brownish silty clay void of marine shell fragments (1.09-0.70 m b.s.l.) documents that the water body came again under prevailing freshwater influence and partly dried up. The uppermost part of the profile is made up of similar deposits including some fragments of *Cerastoderma glaucum* which indicate slight saltwater influence.

Vibracore AKT 14 documents the sudden and temporary influence of saltwater on a near-coast limnic environment typical of an extreme marine event.

11.4.5. Vasiliko – transect C

Vibracores AKT 20-22 were drilled in the northern part of Aktio headland (Fig. 11.1). They are arranged in the W-E running transect C (Fig. 11.6) across an erosional terrace facing the low lying coastal plain.

The base of profile AKT 20 is made up of clay deposited in a limnic environment. An intersecting shell debris layer (1.81- 1.61 m b.s.l.) indicates temporary influence from the seaside. The top of the limnic deposits is a clear erosional surface followed by a thick stratum of middle and coarse sand (0.92-0.12 m b.s.l.). The sand layer includes gravel and abundant marine shell fragments such as from *Cerastoderma glaucum*, *Cerithium sp.*, *Pecten sp.*, *Tellina sp.*, and *Echinoidea*. It is covered by well sorted middle to fine sand (0.12 m b.s.l. – 0.22 m a.s.l.). The uppermost part of profile AKT 20 is a strongly weathered soil (0.22-0.74 m a.s.l.) out of the same substrate. The sandy units encountered at AKT 20 contain some indeterminable ceramic fragments.

Basal lake deposits found at AKT 21 are abruptly covered by strongly weathered middle and coarse sand (1.75-1.20 m b.s.l.) including pieces of gravel and a chert artefact. Provided that the material is of marine origin, it may have been deposited during an extreme event. The subsequent thick stratum of well sorted brown to light brown fine sand probably represents weathered aeolian deposits. This dune palaeosol shows an erosional discordance on top of which strongly unsorted sand and gravels were deposited (0.10-0.65 m a.s.l.). The upper section of the core consists of deeply weathered and comparatively well sorted sand (0.65-1.50 m a.s.l.). Several indefinable ceramic fragments were found in the sand unit on top of the erosional surface.

The base of vibracore AKT 22 shows weathered sand and gravel followed by a thick brownish red palaeosol. Another palaeosol comprising deeply weathered reddish brown silty to clayey sand (2.34-2.68 m a.s.l.) follows. It is covered by a thin sand stratum rich in carbonate and beachrock fragments (2.68-2.73 m a.s.l.) which is partly weathered (2.73-3.15 m a.s.l.). Above 2.19 m a.s.l., we found a lot of ceramic fragments and, on top of the terrain surface, abundant stones and blocks out of beachrock, associated with numerous large potsherds in different states of conservation and roundness. The beachrock fragments presumably originate from the submerged Plaka several kilometers to the west.

Vibracores AKT 20-22 document the sudden input of marine deposits in both limnic and terrestrial environments. The presence of erosional unconformities as well as the composition, the grain size distribution, and the degree of sorting of the overlying sand and gravel units indicate that an extreme event hit the former shoreline. Vibracore transect C shows that the coast at that time lay to the west of AKT 20 (Figs. 11.1 and 11.6).

We also conducted geomorphological surveys in the southern part of Vasiliko. Along the shore of the Ambrakian Gulf, some 0.9 km to the southeast of transect C, we found pebbles, up to 10-15 cm in diameter, with boreholes and living in-situ specimens of marine boring mussels. Some of the pebbles were covered by barnacles (Figs. 11.7a and b). Recent marine bioerosion and bio-construction demonstrate that the pebbles are barely moved by modern wave activity. We thus suggest that the coarse beach material is allochthonous and was dumped by a sedimentary event. Colonization by marine organisms occurred post-depositionally.

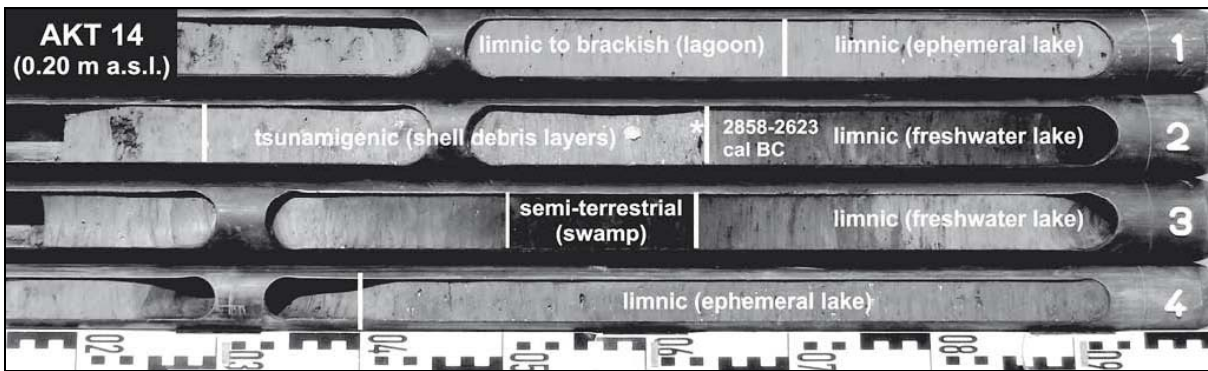


Figure 11.5 - Facies distribution of vibracore AKT 14 from the northeastern shore of the Lagoon of Saltini. The autochthonous limnic environment was abruptly affected by tsunami waves which left several shell debris layers. Gaps are due to rodding processes. The top-up direction for the core segments is to the left. Photo taken by M. May, 2006.

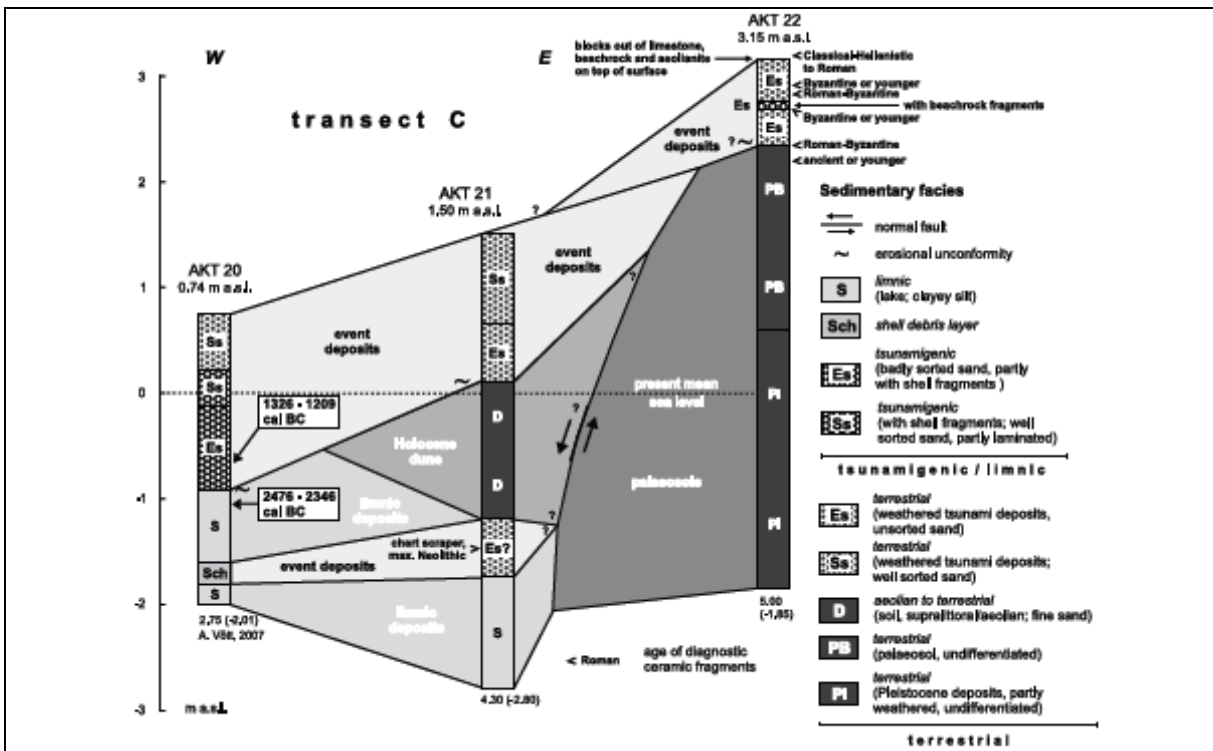


Figure 11.6 - Facies distribution and tsunami deposits found in vibracores from Vasiliko (transect C).

Further inland – some 0.6 km to the south of transect C, around 1 km east of the open sea and 2.5 km east of the nearest in-situ beachrock off cape Skilla – the terrain surface is strewn with large stones and blocks. These stones and blocks are also of allochthonous origin. We found (i) breccias including chert fragments and beach pebbles (Fig. 11.7c), (ii) calcareous sandstones, possibly sandy beachrock, with boreholes from marine boring organisms (Fig. 11.7d), and (iii) beachrock slabs, up to 60 cm in diameter, comprising gravel, with signs of bioerosion (Figs. 11.7e and f). These findings support the idea of a high energy impact on the Aktio headland by a strong marine event approaching from a westerly direction.



Figure 11.7 - Geomorphological indicators of a tsunami imprint found at Vasiliko. (a), (b): recent shore of the Ambrakian Gulf. Large pebbles colonized by boring mussels and barnacles indicate that the beach material is not moved by modern wave action. (c)-(f): Findings of large stones and blocks scattered on top of the terrain surface in the southern part of Vasiliko including a breccia with cemented beach gravel (c), a limestone block with boreholes from marine boring organisms (d), and dislocated beachrock slabs (e, f). Photos taken by A. Vött, 2006.

11.5. Ages derived from ceramic findings and radiocarbon data

Ceramic fragments were found in a number of vibracores. In most cases, age determination was difficult due to the small sizes of the fragments or because they were strongly weathered. Diagnostic ceramic fragments used for relative dating are depicted in Figs. 11.4 and 11.6 within the stratigraphic context.

Radiocarbon dating of samples taken from event deposits is problematic as they may be reworked. ¹⁴C-dating thus results in a maximum age or a simple *terminus ad* or *post quem* for the wave impact. Provided that sufficient and appropriate material for dating was found, we preferred sampling the underlying and/or covering sedimentary units (sandwich dating). However, an erosional unconformity at the base of an event layer may represent a considerable hiatus. Moreover, datable material is missing in cases where event deposits were accumulated above sea level and weathering started immediately after deposition. Altogether, 14 samples from

vibracores from Aktio headland were ¹⁴C-AMS analysed (Table 11.1). Samples AKT 10/4+ PR and AKT 12/3 PR yielded modern ages and were not considered for further interpretation. It is assumed that the samples were parts of (sub-)recent plant roots.

11.6. Discussion

11.6.1. Tsunami sediments versus storm or sea level high stand deposits

Based on sedimentological characteristics of vibracores, on the geomorphological underwater findings at Skoupeloi Achilleos and on geoarchaeological records at Paliokoulio and Vasiliko, we assume that the high energy event deposits encountered at Aktio headland represent tsunamigenic sediments. This interpretation goes well with historical accounts and tsunami catalogues which document that the region has been repeatedly affected by tsunamis. Moreover, the data presented fit with the scenario of multiple tsunami imprints on the Lefkada coastal zone and the Lake of Voulkaria reported by Vött et al. (2006a, 2008c).

At Aktio headland, tsunami deposits were encountered between several meters below and up to 3.15 m above present sea level (Fig. 11.6). In some cases, they were completely weathered, in other cases they were intersected by a palaeosol. The latter indicates that the headland experienced at least two different tsunami landfalls. The maximum thickness of tsunami deposits was found at AKT 1 measuring 3.32 m (Fig. 11.2).

Considerable parts of the tsunamigenic sediments at Aktio headland lie well above present sea level (Figs. 11.2, 11.4 and 11.6). The following arguments contradict their interpretation as storm or sea level high stand deposits.

(i) Two different types of tsunami deposits were found. One type consists of poorly sorted middle and coarse sand and includes gravel as well as abundant shell fragments. It corresponds perfectly with deposits accumulated by the 1992 tsunami in Indonesia described by Shi et al. (1995). The second type is made up of well sorted sand which is, in part, clearly laminated and may also contain fragments of marine fossils. The first type represents bi- or even multi-modal deposits and documents turbulent transportation and more or less chaotic sediment accumulation possibly induced by runup or backwash vortices. Bimodal deposits are regarded, by some researchers, as typical of tsunami deposits (Scheffers & Kelletat, 2004; Scheffers, 2005, 2006b). The second type, due to its more homogeneous texture and lamination, is the result of a laminar water flow. Laminar flow dynamics occur both during runup and backwash of tsunami waters as reported, for instance, from the December 26, 2004 tsunami in southeast Asia (Richmond et al., 2006). Both types of event deposits found at Aktio headland therefore show characteristic features of tsunami events. The fact that they can be found in one and the same sedimentary sequences indicates that the site was affected by both turbulent and laminar flow probably during the same event. Storm deposits, however, produce more or less well sorted sand or gravel sheets fining landwards (Schäfer, 2005).

Sample Name	Depth (m b.s.)	Depth (m b.s.l.)	Sample Description	Lab. No.	$\delta^{13}\text{C}$ (ppm)	¹⁴ C Age (BP)	1 σ max; min (cal BP)	1 σ max; min (cal BC)
AKT 2/9 PR	2.80	1.60	unidentified plant remains	Kia 31674	-5.2	4160 ± 31	4821; 4628	2872; 2679
AKT 10/4+ PR	0.70	0.05 a.s.l.	unidentified plant remains	Kia 31673	-23.7	modern	–	–
AKT 12/3 PR	0.60	0.15	unidentified plant remains	Kia 31672	-27.8	modern	–	–
AKT 14/4+ PR	1.64	1.44	wood fragment	Kia 31671	-23.8	4122 ± 32	4807; 4572	2858; 2623
AKT 20/7 M	1.48	0.74	Tellina planata, artic. spec.	Kia 31668	-3.1	3350 ± 35	3275 - 3158	1326 - 1209*
AKT 20/10 PR	1.91	1.17	unidentified plant remains	Kia 31669	-27.0	3930 ± 38	4425; 4295	2476; 2346
AKT 23/6+ PR	1.72	1.52	unidentified plant remains	Kia 31667	-19.3	1222 ± 27	1224; 1083	726; 867 AD
AKT 24/9 PR	2.64	1.64	peat, organic material	Kia 31666	-23.6	33962 ± 502	–	–
ANI 2/7+ PR	3.53	3.25	wood fragment	UtC 13679	-24.8	113 ± 41	262; 24	1688; 1926 AD*
ANI 2/12+ PR	6.53	6.25	sea weed remains	UtC 13678	-18.0	1003 ± 46	625 - 545	1325 - 1405 AD*
ANI 2/16++ PR	10.28	10.00	sea weed remains	Eri 9794	-14.4	1499 ± 40	1101 - 984	849 - 966 AD*
ANI 14/7+ PR	3.53	2.89	sea weed remains	Kia 31664	-13.8	1590 ± 29	1209 - 1112	741 - 838 AD*
ANI 14/11+ PR	5.52	4.88	sea weed remains	Kia 31665	-12.9	2170 ± 27	1807 - 1720	143 - 230 AD*
ANI 14/25 M	11.80	11.16	Mytilus gall., artic. spec.	Kia 31676	-6.8	6745 ± 40	7322 - 7229	5373 - 5280*

Table 11.1 - Radiocarbon dating results for selected samples from Aktio headland. Note: a.s.l. – above sea level; b.s. – below ground surface; b.s.l. – below sea level; artic. spec. – articulated specimen; Mytilus gall. – Mytilus galloprovincialis; * – marine reservoir correction with 402 years of reservoir age; 1 σ max; min cal BP/BC (AD) – calibrated ages, 1 σ -range; “;” – there are several possible age intervals because of multiple intersections with the calibration curve; Lab. No. – laboratory number, University of Erlangen-Nürnberg (Erl), University of Kiel (Kia), University of Utrecht (UtC).

(ii) Most of the event deposits encountered at Aktio headland lie on top of an erosional surface (Fig. 11.8). Vibracore transects A, B and C reveal that the elevations of erosional discordances are different and partly even lie above present sea level (AKT 9, AKT 10, AKT 21). Moreover, they seem to increase in a landward direction (Figs. 11.2, 11.4 and 11.6). Similar unconformities at the base of tsunami deposits are described by Shi et al. (1995) from Flores Island and by Lavigne et al. (2006) from Banda Aceh, both in Indonesia (see also Dawson & Shi, 2000). Storm-borne sand sheets which reach further inland, in most cases concordantly overlie the pre-existing topography (Schäfer, 2005).

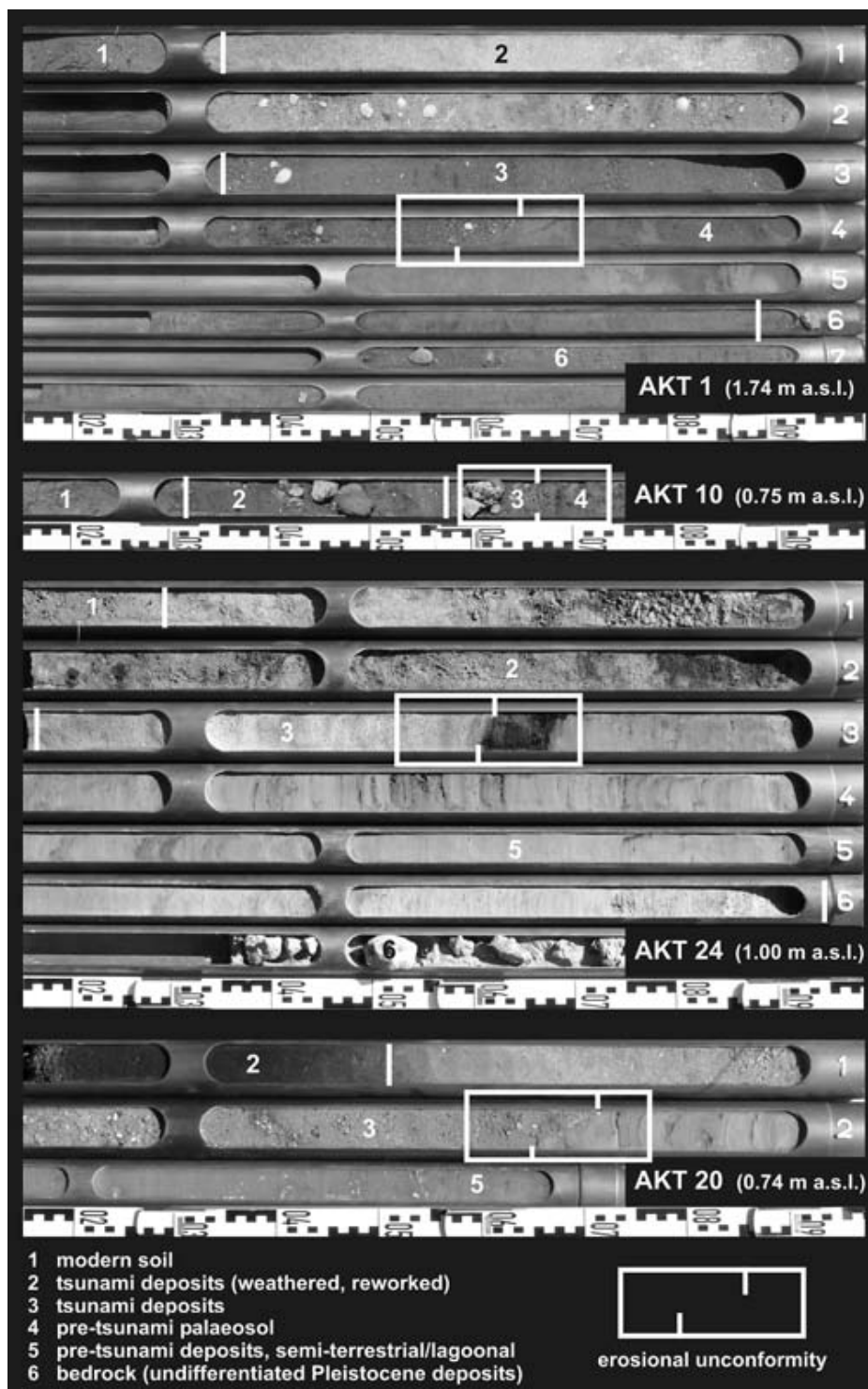


Figure 11.8 - Examples of erosional unconformities due to tsunamigenic impact encountered in vibracores from Phoukias (AKT 1), Paliokoulio (AKT 10), Koumaros (AKT 24), and Vasiliko (AKT 20). Photos taken by M. May, 2006.

(iii) Event deposits at Aktio headland were either thrown onto terrestrial sites and lie on top of a palaeosol (Figs. 11.2, 11.4 and 11.6) or into shallow limnic or lagoonal water bodies (Figs. 11.4 and 11.6). Both types of environment do not show any signs of earlier, pre-event as well as later, post-event influence from the seaside. Onshore and near-shore environments are usually affected repeatedly by storm activity (Reineck & Singh, 1980; Einsle, 2000).

(iv) Pirazzoli et al. (1994b) radiocarbon dated emerged beachrock near Cape Gyrapetra and deduced a 0.5-1.0 m a.s.l. relative sea level high stand during the 4th and 3rd millennia BC. Considering the well-known mole of the Corinthians at the southern entrance to the Lagoon of Lefkada which has been submerged by around 2.5 m since the 5th century BC, the authors concluded that the Lefkada area has experienced tectonic up- and down movements during the Holocene. Similar yo-yo dynamics were already suggested by von Seidlitz (1927). However, according to recent findings of tsunamigenically uplifted and dislocated beachrock mega blocks along the northern coast of Lefkada (Vött et al., 2006a, 2008c), we assume that the beachrock unit sampled by Pirazzoli et al. (1994b) and the beachrock to which von Seidlitz (1927) refers is not in-situ but probably relocated and uplifted by tsunamigenic influence. Moreover, it cannot be excluded that the tsunami events which hit the coast at different times during the Holocene went hand in hand with co-seismic displacements of the coastal zone.

Recent sea level studies along the Akarnanian coast, including the Palairos area (Fig. 11.1), revealed that during the Holocene relative sea level has never been higher than today (Vött, 2008c). Further research is required to check if the relative sea level evolution between Preveza and Lefkada shows a different pattern. However, the fact that tsunami deposits at Aktio headland bear signs of relic subaerial weathering – such as spots of iron oxide – down to a minimum depth of 1 m b.s.l. indicates that the relative sea level must have been considerably lower at or shortly after the time of their deposition and that the area has subsequently experienced a considerable sea level rise. Weathering of the event deposits and soil formation seem to have begun immediately after deposition and the sites have never been affected again by sediment input from the seaside.

(v) It is impossible to explain the Aktio headland event deposits by abrupt co-seismic submergence even if it occurred in the order of several meters. Firstly, co-seismic subsidence is not known to cause strong water currents towards the coast. Secondly, it is not able to activate large sediment masses and transport them in a landward direction. The elevation of the event layers above present sea level would furthermore require subsequent coastal uplift.

(vi) Both subaerial (Vött et al., 2006a) and underwater findings of dislocated mega blocks along the Plaka prove tsunamigenic impact on the coast. Hydrodynamic calculations show that a block of 6 m³ requires storm waves higher than 30 m to be transported. The same block may be dislocated by tsunami surge, only 11 m high (Nott, 2003b; Bartel & Kelletat, 2003).

We conclude that Aktio headland experienced at least two strong tsunami landfalls approaching from the west. Tsunami waves caused strong erosion at the western coast of the headland as well as in its northern part and left thick sequences of coarse grained deposits. Geological findings from the eastern part of the headland around Vasiliko and the Lagoon of Saltini, however, prove that the Aktio headland was entirely inundated by tsunami waters which then flowed into the Ambrakian Gulf. Furthermore, vibracore profiles of transect B (Fig. 11.4) show that the Lagoon of Saltini has not been created by longshore sand transport and related beach accretion but seems to be the result of strong tsunamigenic erosion in a SSW-NNE direction. The resulting basin was probably submerged due to ongoing relative sea level rise by tectonic subsidence along active faults.

At vibracoring site AKT 22, tsunami deposits were found up to 3.15 m a.s.l. (Fig. 11.6). Considering the large blocks found at Vasiliko, it is assumed that the tsunami surge reached at least 5 m above present sea level. If we take into account that the relative sea level at the time of deposition of the tsunami sediments was at least 1 m lower than today, this results in a minimum height of inundation of 6 m.

11.6.2. Geochronology of tsunami landfalls at Aktio headland

Aktio headland plays a key role in understanding the Holocene evolution of the Ambrakian Gulf. Previous studies conducted in the area concentrated on the analysis of underwater sediments by means of seismic reflection profiles (Poulos et al., 1995; Kapsimalis et al., 2005) or on the reconstruction of Holocene palaeoenvironments and the progradation history of the Louros and Arachthos River deltas based on sediment cores (Jing & Rapp, 2003; Poulos et al., 2005). Tsunamigenic deposits were not identified within the framework of these studies. However, Piper et al. (1982, 1988) found isolated sandy deposits at the sea bottom in the Strait of Aktio and Tziavos (1997) reports on a sequence of “recent terrigenous silty sand”, 11-28 m thick, which he encountered in underwater cores from the same area. Considering that, to the west of Preveza, the longshore drift is limited due to prevailing rocky coasts and that there is no significant fluvial input of sand, it is difficult to explain these deposits merely by outflow dynamics in the Strait of Aktio. We suggest that they represent

tsunamigenic sediments, partly reworked, which probably correlate to the event deposits encountered at the Aktio headland.

The geochronology of Holocene tsunami landfalls presented in this paper is based on ten radiocarbon dates. At least two distinctive clusters of ¹⁴C-AMS ages were recognized, one around 2870-2350 cal BC and another around 840 cal AD (Table 11.1).

11.6.2.1. The mid-Holocene environment and the 2870-2350 cal BC tsunami event

An articulated specimen of *Mytilus galloprovincialis* taken from lagoonal deposits at the base of vibracore ANI 14 shows an age of 5373-5280 cal BC (ANI 14/25 M, 11.16 m b.s.l.). This documents that the formation of the Plaka beach ridge and beachrock west of Phoukias, which induced quiescent hydrodynamic conditions in the Bay of Aghios Nikolaos around ANI 14, had already started in the 6th millennium BC, i.e. some 550 years earlier than further south around the Santa Maura beach ridge (Vött et al., 2006a).

The oldest dated tsunami which affected the Lagoon of Aghios Nikolaos and its shores occurred in the 3rd millennium BC. Indeterminable plant remains found below the base of the tsunami deposits at vibracore AKT 2 date to 2872-2679 cal BC (AKT 2/9 PR, 1.60 m b.s.l.). As vibracores AKT 1-3 show almost identical stratigraphies (Fig. 11.2) and are drilled within a short distance (Fig. 11.1), the event layers encountered at AKT 1 and AKT 3 seem to be of the same age. The underlying deposits experienced strong weathering before they were affected by tsunamigenic influence. They presumably date to Eemian/ Tyrrhenian times. At AKT 2 and AKT 3, seawater influenced sediments of Eemian/Tyrrhenian age are in a slightly higher position than those found at AKT 23 and AKT 24 (Fig. 11.4) which indicates post-sedimentary subsidence of the Koumaros area relative to Paliokoulio and Phoukias (Figs. 11.1 and 11.2) possibly along a SW-NE running fault system (Paschos et al., 1991). However, vibracores AKT 1-3 prove that around 2872-2679 cal BC, a tsunami impact eroded palaeosols and covered them by thick event layers (Section 4.1).

A wood fragment from the very base of the tsunami deposits at AKT 14 at the northeastern shore of the Lagoon of Saltini yielded an age of 2858-2623 cal BC (AKT 14/4+ PR, 1.44 m b.s.l.), which is almost identical to the age found for the event layer at site AKT 2. This suggests that, around that time, tsunamigenic inundation affected the entire Aktio headland between Koumaros and the shore of the Ambrakian Gulf. Unidentified plant remains from vibracore AKT 20 at Vasiliko – possibly roots from plants growing on a higher surface – were dated to 2476-2346 cal BC (AKT 20/10 PR, 1.17 m b.s.l.). The sample was taken out of slightly weathered limnic sediments shortly below an erosional unconformity and a subsequent event layer (Section 4.5). It seems that the erosional surfaces at AKT 20 and AKT 21 were produced by the same tsunami impact which influenced AKT 1-3 and AKT 14 in the 3rd millennium BC. Further datings will have to clarify the difference in age. Sedimentological and geochronological data from Phoukias, Vasiliko, and the northeastern shore of the Lagoon of Saltini thus indicate a major tsunami landfall at 2870-2350 cal BC which caused considerable erosion along the western flank of the Aktio headland.

11.6.2.2. Intermediary events

An articulated specimen of *Tellina planata* taken from the lower part of the badly sorted tsunami sediments of vibracore AKT 20 revealed an age of 1326-1209 cal BC (AKT 20/7 M, 0.74 m b.s.l.). This is a mere *terminus ad* or *post quem* which documents that the area was also affected by a younger extreme event, possibly by the one which hit the Bay of Aghios Nikolaos around 1000 cal BC and which brought marine sediments into the Lake Voukaria freshwater environment (Vött et al., 2006a).

Further ages were obtained for samples from the Phoukias sand spit. A sequence of shell debris layers (7.08-4.87 m b.s.l.) encountered in the middle section of vibracore ANI 14 is probably of tsunamigenic origin. Radiocarbon sample ANI 14/11+ PR (4.88 m b.s.l.) yielded an age of 143-230 cal AD and post-dates tsunami-borne influences at the site. Vött et al. (2006a) detected tsunamigenic impact on the nearby Lefkada coastal zone around 300 cal BC documented by tsunamigenic washover fans east of the Santa Maura beach ridge. One of the mentioned shell debris layers of core ANI 14 therefore may be attributed to the 300 cal BC or even to an unknown younger event.

There are no usable radiocarbon dates to estimate the age of tsunami sediments at Paliokoulio. However, the youngest ceramic fragments found in vibracores AKT 9 and AKT 10 date to ancient times (7th century BC to 4th century AD) resulting in a *terminus ad* or *post quem* for the event. At site AKT 11, potsherds associated with the older generation of tsunami deposits yield a Hellenistic to Roman age (1st century BC to 4th century AD) as another *terminus ad* or *post quem*. Deposits of the younger tsunami generation are related to fragments dating to Classical-Hellenistic times (5th to 1st centuries BC). Obviously, these fragments were reworked by tsunami wave action. We assume that Paliokoulio was affected by the 300 cal BC event detected by Vött et al. (2006a) in

the area east of Santa Maura (Fig. 11.1). Younger tsunami deposits are probably associated to the 840 cal AD event.

11.6.2.3. The 840 cal AD and (sub-) recent events

The lower section of vibracore ANI 2 documents tsunamigenic interference of a lagoonal environment by the abrupt input of fine sand including marine shells and plant remains (11.11-10.17 m b.s.l., Section 4.1, Fig. 11.2). The tsunami impact induced a severe facies change from quiescent lagoonal to higher energy shallow marine conditions characterized by gradually upgrowing mats of sea weed. Sea weed remains from shortly above the event layer post-date the tsunami to 849-966 cal AD (ANI 2/16++ PR, 10.00 m b.s.l.). At almost the same time, the lagoonal environment at site ANI 14 experienced the sudden input of a thick package of well sorted middle to coarse sand. Sea weed remains from the uppermost part of the lagoonal unit pre-date the impact to 741-838 cal AD (ANI 14/7+ PR, 2.89 m b.s.l.). It is concluded that a major tsunami affected the Phoukias sand spit area between 741-838 cal AD and 849-966 cal AD and induced a general change of sedimentary conditions in the area east of the former Plaka strandline. The Plaka beach ridge system which, up till then, closed off the Aghios Nikolaos lagoon from the open Ionian Sea obviously sustained severe damage by the tsunami impact around 840 cal AD. It is concluded that previous tsunami events only partly affected the palaeo beach along the Plaka. Based on sedimentological and geochronological data found for ANI 2, the 840 cal AD event, however, seemed to have completely flushed westwards the loose Plaka beach material and destroyed the solid beachrock base of the system. Rubble ridges and dislocated mega blocks studied at Skoupeloi Achilleos (Fig. 11.3) as well as dislocated beachrock material encountered along the southern part of the Plaka (Vött et al., 2006a) are most probably due to the same tsunami event.

Undetermined plant remains from the base of weathered tsunami deposits found at AKT 23 yielded an age of 726-867 cal AD (AKT 23/6+ PR, 1.52 m b.s.l.). In fact, this is a mere maximum age or *terminus ad* or *post quem* for the tsunami as the event may have reworked older material. However, sedimentological and geochronological evidence of the 840 cal AD impact from the nearby Phoukias sand spit suggests that the thick tsunami deposits at AKT 23 and AKT 24 were accumulated by the same event.

Ceramic findings in vibracore AKT 22 document that the coast around Vasiliko was hit by a tsunami during or after Byzantine times (7th to 15th centuries AD, Fig. 11.6). This event may possibly also correspond to the 840 cal AD impact. Multiple impacts of Vasiliko by tsunami waves at 2870-2350 cal BC, around 1000 cal BC and probably at 840 cal AD possibly explains why there are almost no remains left of the ancient sanctuary of Apollo (Murray, 1982). Collignon (1886) reports on multiple destruction of the sanctuary by unknown invaders. Based on our results, we instead suggest that these destructions are, at least partly, due to repeated tsunamigenic influences.

At Phoukias, samples from vibracore ANI 2 indicate that younger tsunami events occurred shortly after 1325-1405 cal AD (ANI 2/12+ PR, 6.25 m b.s.l.) and around 1688-1926 cal AD (ANI 2/7+ PR, 6.25 m b.s.l., Fig. 11.2). The tsunamigenic gravel layer encountered in the uppermost part of vibracore ANI 14 (0.39-0.50 m a.s.l.) seems to have been deposited during one of these younger events. The age of the younger generation of tsunami deposits found at sites AKT 1-3 remains unclear. The degree of weathering and the thickness of the overlying dune sands, however, indicate that the event layers are possibly related to the tsunami landfall at 840 cal AD.

11.7. Conclusions

Detailed geomorphological, sedimentological and geochemical analyses of vibracores, geoarchaeological studies and geomorphological underwater surveys give evidence of strong tsunamigenic impact on Aktio headland. Based on ¹⁴C-AMS dates and archaeological age determination of ceramic fragments our results reveal multiple tsunamis which hit the coast between Preveza and the Bay of Aghios Nikolaos during the late Holocene. The following conclusions can be made.

(i) Around 2870-2350 cal BC, a major tsunami hit and inundated the entire Aktio headland between Phoukias and Vasiliko. The tsunami water flow seem to have eroded a SW-NE running wide channel-like basin east of Koumaros which, due to subsequent relative sea level rise, was filled by the lagoonal waters of the Lagoon of Saltini. Strong erosional unconformities induced by the 2870-2350 cal BC event were found both in the southern- and in the northernmost parts of the headland at Phoukias and Vasiliko.

(ii) Parts of the Aktio headland were affected by tsunamis which struck the coast northeast of Lefkada and which were identified in a former study (Vött et al., 2006a, 2008c). The northernmost part of the Aktio headland around Vasiliko was possibly hit by the tsunami which intruded into the Lake Voulkaria around 1000 cal BC. The areas around Phoukias and Paliokoulío were probably influenced by a tsunami around 300 cal BC which produced large washover fans northeast of Lefkada.

(iii) A strong tsunami landfall occurred around 840 cal AD and hit the entire Aktio headland. At Koumaros, the tsunami caused considerable erosion and left thick layers of event deposits. Sedimentological and geochronological data indicate that the 840 cal AD event destroyed the former Plaka beach ridge and its beachrock base and thus exposed the former lagoonal environment of the Bay of Aghios Nikolaos to open sea wave dynamics. It is further assumed that it was the 840 cal AD tsunami which (a) formed underwater rubble ridges and dislocated mega blocks at Skoupeloi Achilleos and all along the Plaka and (b) scattered beachrock blocks and material from the littoral zone on top of the terrain surface at Vasiliko up to 3.15 m a.s.l. We estimate the distance of transport of this material at minimum 2.5 km and the minimum elevation of the tsunami surge at 6 m.

(iv) Further tsunami impacts have occurred during the past 700 or so years but further field data and alternative dating techniques are needed to reconstruct and precisely date these events.

(v) Multiple tsunamigenic influences during the late Holocene show that Aktio headland is exposed to a high tsunami risk. The adjacent NATO airport and nearby centres of mass tourism indicate the high vulnerability of the area. The sensitivity of the Preveza-Lefkada coastal zone to tsunami events is due to (a) the funnel-like shape of the shoreline which amplifies tsunami waves approaching the coast and (b) the availability of excellent tsunami sediment traps.

References

- Ad-hoc-Arbeitsgruppe Boden der Staatlichen Geologischen Dienste und der Bundesanstalt für Geowissenschaften und Rohstoffe (2005). *Bodenkundliche Kartieranleitung*, fifth ed. Schweizerbart, Stuttgart, p. 438.
- Aiello G., Bravi S., Budillon F., Cristofalo G.C., D'Argenio B., De Lauro M., Ferraro L., Marsella E., Molisso F., Pelosi N., Sacchi M., Tramontano M.A. (1995). *Marine Geology of the Salento shelf (Apulia, south Italy). Preliminary results of a multidisciplinary study*. *Giornale di Geologia*, ser. 3", vol. 57/1-2, 1995, 17-40.
- Ambraseys N. N. (1962). *Data for the investigation of the seismic sea waves in the Eastern Mediterranean*. *Bulletin of the Seismological Society of America*, 52, 895-913.
- Ambraseys N.N. (1965). *Data for the investigation of seismic sea waves in Europe*. UGGI, Monographie 29, Paris, 78-80.
- Amore C., D'Alessandro L., Di Geronimo S., Giuffrida E., Lo Iudice A., Zanini A. (1988). *Dinamica litorale del Golfo di Taranto tra Capo Spulico e Punta Rondinella*. *Bollettino Accademia Gioenia Scienze Naturali*, 21, 39-74.
- Anderson H., Jackson J. (1997). *Active tectonics of the Adriatic region*. *Geophysical Journal Royal Astronomical Society*, 91, 937-983.
- Andrade C. (1992). *Tsunami generated forms in the Algarve barrier island (South Portugal)*. In: Dawson, A.G. (Ed.), *European Geophysical Society 1992 Tsunami Meeting*. *Science of Tsunami Hazards*, 10 (1), 21-34.
- Antonoli F., Deino A., Ferranti L., Keller J., Marabini S., Mastronuzzi G., Negri A., Piva A., Vai G.B., Vigliotti L. (2008). *Lo studio della sezione "Il Fronte" per la definizione del piano Tarantino (Puglia, Italy)*. *Il Quaternario, Italian Journal of Quaternary Sciences*, 20(2), 31-34.
- Antonopoulos J. (1979). *Catalogue of tsunamis in the eastern Mediterranean from antiquity to present times*. *Annali di Geofisica*, 32, 113-130.
- Arena F. (1999). *Il rischio ondoso nei mari italiani*. Ed. BIOS, Cosenza, 136 pp.
- Argnani A., Bonazzi C. (2005). *Malta Escarpment fault zone offshore eastern Sicily: Pliocene-Quaternary tectonic evolution based on new multichannel seismic data*. *Tectonics* 24 (4).
- Asal F. F. F. (2003). *Airborne remote sensing for landscape modelling*. Ph.d. Thesis, The University of Nottingham, UK, pp. 317.
- Atwater B.F. (1987). *Evidence for great Holocene earthquakes along the outer coast of Washington State*. *Science*, 236, 942-944.
- Auriemma R., Mastronuzzi G., Sansò P. (2004). *Relative sea-level changes during the Holocene along the Coast of Southern Apulia (Italia)*. *Géomorphologie*, 1, 19-34.
- Auroux C., Mascle J., Campredon R., Mascle G., Rossi S. (1985). *Cadre géodynamique et évolution récent de la dorsale apulienne et des ses bordures*. *Giornale di Geologia*, 47, 101-127.
- Baffi E. (1929). *Saggio di effemeridi tarantine*. In: *Bollettino della Provincia Ionica (Taras)*, Anno IV, n°1-2, pp. 47-61.
- Baptista A.M., Priest G.R., Murty T.S. (1993). *Field survey of the 1992 Nicaragua tsunami*. *Marine Geodesy*, 16, 169-203.
- Barbano M.S., Pantosti D., De Martini P.M., Smedile A., Gerardi F., Pirrotta C. (2007). *Historical, archaeological and geological records of strong earthquakes at Capo Peloro (southern Italy)*. XXVI Convegno GNGTS. Extended Abstract Volume, pp. 211-215.
- Bartel P., Kelletat D. (2003). *Erster Nachweis holozäner Tsunamis im westlichen Mittelmeergebiet (Mallorca, Spanien) mit einem Vergleich von Tsunami- und Sturmwellenwirkung auf Festgesteinsküsten*. *Berichte Forschungen - und Technologiezentrum Westküste der Universität Kiel, Büsum*, 28, 93-107.
- Beck C., de Lépinay B.M., Schneider J.-L., Cremer M., Çağatay N., Wendenbaum E., Boutareaud S., Ménot G., Schmidt S., Weber O., Eris K., Armijo R., Meyer B., Pondard N., Gutscher M.A., MARMACORE Cruise Party, Turon J.-L., Labeyrie L., Cortijo E., Galle Y., Bouquerel H., Gorur N., Gervais A., Castera M.-H., Londeix L., de Rességuier A., Jaouen A. (2007). *Late Quaternary co-seismic sedimentation in the Sea of Marmara's deep basins*. *Sedimentary Geology*, 199, 65-89.
- Bedosti B., Caputo M. (1987). *Primo aggiornamento del catalogo dei maremoti delle coste italiane*. *Atti dell'accademia Nazionale dei Lincei, Rendiconti Classe di Scienze Fisiche, Matematiche e Naturali*, ser.8, vol. LXXX(7-12), 570-584.
- Belluomini G., Caldara M., Casini C., Cerasoli M., Manfra L., Mastronuzzi G., Palmentola G., Sansò P., Tuccimei P., Vesica P.L. (2002). *Age of Late Pleistocene shorelines, morphological evolution and tectonic history of Taranto area, Southern Italy*. *Quaternary Science Reviews*, 21, 4-6, 427-454.
- Bianca M., Monaco C., Tortorici L., Cernobori L. (1999). *Quaternary normal faulting in southeastern Sicily (Italy): a seismic source for the 1693 large earthquake*. *Geophysics Journal International*, 139, 370-394.

- Bigazzi G., Laurenzi M.A., Principe C., Brocchini D. (1996). *New geochronological data on igneous rocks and evaporites of the Pietre Nere point (Gargano peninsula, southern Italy)*. Bollettino Società Geologica Italiana, 115, 439-448.
- Blandamura G. (1925). *Choerades Insulae. Le Cheradi del Jonio*. Stabilimento Tipografico Arcivescovile, Taranto, 288 pp.
- Boenzi F., Caldara M., Pennetta L. (1985). *La Trasgressione Tirreniana nei dintorni di Castellaneta (Taranto)*. Geologia Applicata e Idrogeologia, 20, 163-175.
- Boenzi F., Caldara M., Pennetta L. (2000). *L'influenza delle variazioni climatiche e dei processi storico sociali sull'evoluzione delle forme del rilievo del Mezzogiorno*. Territorio e Società nelle Aree Meridionali, Laterza Editore, Bari, 5-29.
- Boncio P., Mancini T., Lavecchia G., Selvaggi G. (2007). *Seismotectonics of strike-slip earthquakes within the deep crust of southern Italy: geometry, kinematics, stress field and crustal reology of the Potenza 1990-1991 seismic sequences*. Tectonophysics, doi: 10.1016/j.tecto.2007.08.016.
- Bondevik S., Svendsen J.I., Mangerud J. (1997a). *Tsunami sedimentare deposited by the Storegga tsunami in shallow marine basins and coastal lakes, western Norway*. Sedimentology, 44, 1115-1131.
- Bondevik S., Svendsen J.I., Johnsen G., Mangerud J., Kaland P.E. (1997b). *The Storegga tsunami along the Norwegian coast, its age and runup*. Boreas, 26, 29-53.
- Bordoni P., Valensise G. (1998). *Deformation of the 125 ks marine terrace in Italy: tectonic implications*. In: Stewart I.S., Vita Finzi C., eds., Coastal Tectonics. Geological Society, London, Special Publications, 146, 71-110.
- Boschi E., Guidoboni E., Ferrari G., Mariotti D., Valensise G., Gasperini P. (2000). *Catalogue of strong Italian earthquakes from 461 B.C. to 1997*. Annali di Geofisica, 43, 1-868.
- Boschi E., Guidoboni E., Ferrari G., Valensise G., Gasperini P. (1997). *Catalogo dei Forti Terremoti in Italia dal 461 a.C. Al 1990*. ING-SGA Eds., Bologna, 644 pp.
- Bosellini A., Bosellini F.R., Colalongo L., Parente M., Russo A., Vescogni A. (1999). *Stratigraphic architecture of the Salento coast from Capo d'Otranto to S. Maria di Leuca (Apulia, Southern Italy)*. Rivista Italiana di Paleontologia e Stratigrafia, 105 (3), 397-416.
- Bosellini A., Parente M. (1995). *The Apulian Platform margin in the Salento Peninsula (southern Italy)*. Giornale di Geologia 56 (2), 167-177.
- Bossio A., Mazzei R., Monteforti B., Salvatorini G. (1991). *Note geologiche e stratigrafiche sull'area di Palmariaggi (Lecce, Puglia)*. Rivista Italiana di Paleontologia Stratigrafica, 97(2), 175-234.
- Bourgeois J., Hansen T.A., Wiberg P.L., Kauffman E.G. (1988). *A Tsunami deposit at the Cretaceous-Tertiary Boundary in Texas*. Science, 241, 567-570.
- Bourrouilh-Le Jan F.G., Beck C., Gorsline D.S. (2007). *Catastrophic events (hurricanes, next term tsunami and others) and their sedimentary records: Introductory notes and new concepts for shallow water deposits*. Sedimentary Geology, 199, 1-2, 1-11.
- Bourrouilh-Le Jan F.G., Talandier J. (1985). *Sédimentation et fracturation de haute énergie en milieu récifal: Tsunamis, ouragans et cyclones et leurs effets sur la sédimentologie et la géomorphologie d'un atoll: motu et hoa, à Rangiroa (Tuamotu, SE Pacific)*. Marine Geology, 67, 263-333.
- Broadley L., Platzman E., Platt J., Matthews S. (2004). *Palaeomagnetism and tectonic evolution of the Ionian thrust belt, NW Greece*. In: Chatzipetros, A., Pavlides, S. (Eds.), Proceedings of the Fifth International Symposium on Eastern Mediterranean Geology, 14-20 April 2004, Thessaloniki. Extended Abstracts Volume plus CD-ROM, Vol. II, Thessaloniki, pp. 973-976.
- Broecker W.S., Olson I.A. (1961). *Lamont Radiocarbon Measurements VIII*. Radiocarbon, 3, 176-204.
- Brockmüller S., Vött A., Brückner H., Handl M., Schriever A. (2005). *Die holozäne Entwicklung der Küstenebene von Boukka am Ambrakischen Golf (Nordwestgriechenland)*. In: Beck N. (Ed.). *Neue Ergebnisse der Meeres- und Küstenforschung*. Schriften des Arbeitskreises Landes- und Volkskunde Koblenz, 4, 34-50.
- Brockmüller S., Vött A., May S.M., Brückner H. (2007). *Palaeoenvironmental changes of the Lefkada Sound (NW Greece) and their archaeological relevance*. In: Gönnert G., Pflüger B., Bremer J.-A. (Hrsg.): *Von der Geoarchäologie über die Küstendynamik zum Küstenzonenmanagement*. Coastline Reports, 9, 127-138.
- Brückner H. (1980). *Marine terrassen in Suditalien. Eine Quartar-morphologische Studie über das Küstentiefland von Metapont*. Dusseldorfer Geographische Schriften, 14, 235.
- Bruins H.J., Macgillivray J.A., Synolakis C.E., Benjamini C., Keller, J., Kisch H.J., Klügel A., van der Plicht J. (2008). *Geoarchaeological tsunami deposits at Palaiokastro (Crete) and the Late Minoan eruption of Santorini*. Journal of Archaeological Science, 35, 191-212.
- Bryant E. A., Young R. W., Price D. M. (1996). *Tsunami as a major control on coastal evolution, Southeastern Australia*, J. Coast. Res., 12, 831-840.

- Bryant E.A. (2001). *Tsunami. The Underrated Hazard*. Cambridge University Press, Cambridge, UK, 320 pp.
- Bryant E.A., Nott J. (2001). *Geological Indicators of Large Tsunami in Australia*. *Natural Hazards*, 24(3), 231-249.
- Bryant E.A., Young R.W. (1996). *Bedrock-Sculpturing by Tsunami, South Coast New South Wales, Australia*. *Journal of Geology*, 104, 565-582.
- Butler R.W.H., Mazzoli S., Corrado S., De Donatis M., Scrocca D., Di Bucci D., Gambini R., Naso G., Nicolai C., Shiner P., Zucconi V. (2004). *Applying thick-skinned tectonic models to the Apennine thrust belt of Italy - Limitations and implications*. In: McClay K.R., ed., *Thrust tectonics and hydrocarbon systems*. American Association Petroleum Geology Memoir, 82, 647-667.
- Cabanes C., Cazenave A., Provost C. L. (2001). *Sea Level Change from Topex-Poseidon Altimetry for 1993-1999 and Possible Warming of the Southern Oceans*. *Geophysical Research Letters*, 28(1), 9-12.
- Caldara M. (1987). *La sezione tirreniana di Ponte del re (Castellaneta Marina, Taranto): analisi paleoecologica*. *Atti della Società Toscana Scienze Naturali, Mem. A XCIII*, 129-163.
- Caldara M. (1996). *Aspetti di Geologia ambientale e di morfologia costiera in alcuni tratti del litorale nord-barese*. In: *Atti Convegno «Cave e coste nel territorio del nord-barese*. *Geologia, Suppl. 2*, 39-61.
- Caldara M., Centenaro E., Mastronuzzi G., Sansò P., Sergio A. (1998). *Features and present evolution of Apulian Coast (Southern Italy)*. *Journal of Coastal Research, Supplement Issue*, 26, 55-64.
- Capaldi G., Civetta L., Lirer L., Munno R. (1979). *Caratteri Petrografici ed età K/Ar delle cineriti intercalate nelle formazioni argillose pleistoceniche della Fossa Bradanica*. *Geologia Applicata ed Idrogeologia, XIV (III)*, 493-501.
- Caputo M., Faita G. (1984). *Primo catalogo dei maremoti delle coste italiane*. *Atti dell'Accademia Nazionale dei Lincei, Memorie Classe di Scienze Fisiche, Matematiche e Naturali, ser.8, vol.XVII(7)*, 211-356.
- Caputo R., Di Bucci D., Mastronuzzi G., Fracassi U., Sansò P., Selli G. (2008). *Late Quaternary extension of the southern Adriatic foreland (Italy): evidence from joint analysis*. *Rendiconti online Società Geologica Italiana, 1, Note Brevi*, www.socgeol.it, 62-67.
- Carducci C.A. (1771). *Delle delizie tarentine di Tommaso Nicolò D'Aquino*. Stamperia Raimondiana, Napoli.
- Castello B., Selvaggi G., Chiarabba C., Amato A. (2005). *CSI, Catalogo della sismicità italiana 1981-2002, versione 1.0*. INGV-CNT, Roma. Available online: <http://www.ingv.it/CSI/>.
- Chaguè-Goff C., Dawson S., Goff J.R., Zachariasen J., Berryman K.R., Garnett D.L., Waldron H.M., Mildenhall D.C. (2002). *A tsunami (ca. 6300 years BP) and other Holocene environmental changes, northern Hawke's Bay, New Zealand*. *Sedimentary Geology*, 150, 89-102.
- Channel J.E.T., D'Argenio B., Horvath F. (1979). *Adria. The African Promontory, in Mesozoic Mediterranean*. *Paleogeography. Earth Sciences Reviews*, 15, 213-272.
- Ciaranfi N., Ghisetti F., Guida M., Iaccarino G., Lambiase S., Pieri P., Rapisardi L., Ricchetti G., Torre M., Tortorici L., Vezzani L. (1983). *Carta Neotettonica dell'Italia Meridionale*. Progetto Finalizzato Geodinamica CNR, 515, 1-62.
- Ciaranfi N., Pasini G., Rio D. (2001). *The meeting on the Plio-Pleistocene boundary and the Lower/Middle Pleistocene transition: type areas and sections (Bari, 25-29 September 2000)*. *Memorie di Scienze Geologiche*, 53, 1-123 pp.
- Ciaranfi N., Pieri P., Ricchetti G. (1988). *Note alla carta geologica delle Murge e del Salento (Puglia centro-meridionale), 1:250.000*. *Memorie della Società Geologica Italiana*, 42, 449-460.
- Cinque A., Patacca E., Scandone P., Tozzi M. (1993). *Quaternary kinematic evolution of the southern Apennines. Relationship between surface geological features and deep lithospheric structures*. *Annali di Geofisica*, 36, 249-260.
- Cita M.B., Aloisi G. (2000). *Deep-sea tsunami deposits triggered by the explosion of Santorini (3500 y BP), eastern Mediterranean*. *Sedimentary Geology*, 135, 181-203.
- Clark N. (2007). *Living through the tsunami: vulnerability and generosity on a volatile earth*. *Geoforum*, 32, 1127-1139.
- Clews J.E. (1989). *Structural controls on basin evolution: Neogene to Quaternary of the Ionian zone, western Greece*. *Journal of the Geological Society*, 146, London, 447-457.
- Cocard M., Kahle H.G., Peter Y., Geiger A., Veis G., Felekis S., Paradissis D., Billiris H. (1999). *New constraints on the rapid crustal motion of the Aegean region: recent results inferred from GPS measurements (1993-1998) across the West Hellenic Arc, Greece*. *Earth and Planetary Science Letters* 172, 39-47.
- Cochard R., Ranamukhaarachchi S. L., Shivakoti G. P., Shipin O. V., Edwards P. J., Seeland K. T. (2008). *The 2004 tsunami in Aceh and Southern Thailand: A review on coastal ecosystems, wave hazards and vulnerability*. *Perspectives in Plant Ecology, Evolution and Systematics*, 10, 1, 3-40.

- Colantoni P., Gallignani P. (1978). *Quaternary evolution of the continental shelf of the coast of Bari (South Adriatic Sea): shallow seismic, sedimentological and faunal evidences*. Géologie Méditerranée, 5 (3), 327-338.
- Colantoni P., Noto P., Taviani M. (1975). *Prime datazioni assolute di una fauna fossile a P. septemradiatum dragata nel Basso Adriatico*. Giornale di Geologia, 40 (2), 133-140.
- Colizza E., Corradi N., Cuppari A., Fanucci F., Morelli D., Del Ben A. (2005). *Rischi geologici ed ambientali sul margine continentale ligure e sul margine della Calabria Ionica*. - In: Sleijko D., Rebez A. (2005). 24° Convegno Nazionale GNGTS, Roma, 15-17 novembre 2005, 301-304.
- Collignon M. (1886). *Torses archaïques en marbre provenant d'Actium*. Gazette Archéologique, 11, 235-243.
- Console R., Di Giovambattista R., Favali P., Presgrave B.W., Smriglio G. (1993). *Seismicity of the Adriatic microplate*. Tectonophysics, 218, 343-354.
- Console R., Di Giovambattista R., Favali P., Smriglio G. (1989). *Lower Adriatic Sea seismic sequence (January 1986): spatial definition of the seismogenic structure*. Tectonophysics, 166, 23-246.
- Coppa M.G., De Castro P., Marino M., Rosso A., Sanfilippo R. (2001). *The Pleistocene with Aequipecten opercularis (Linneo) of "Campo d'Imare" (Brindisi, Italy)*. Bollettino della Società Paleontologica Italiana, 40(3), 405-429.
- Coppola D. (1977). *Civiltà antiche nel territorio di T.S. Sabina (Carovigno - Brindisi). Ricostruzione topografica ed avvicendamenti culturali*. Ricerche e Studi, 10, 47-110.
- Coppola D., Costantini L. (1987). *Le néolitique ancien littoral et la diffusion des céréales dans le Poulles durant le VI millénaire: les sites de Fontanelle, Torre Canne et de Le Macchie*. Premières Communautés Paysannes en Méditerranée Occidentale. Colloque du CNRS, Montpellier 1983, 249-253.
- Coppola D., Denoyelle M., Dewailly M., Lepetz S., Poccetti P., Van Andringa W. (2008). *La grotte de Santa Maria di Agnano (Ostuni) et ses abords: à propos des critères d'identification d'un sanctuaire messapien, in "Saturnia tellus. Definizioni dello spazio consacrato in ambiente etrusco, italico, fenicio-punico, iberico e celtico*, CNR, Roma 2008, p.208.
- Corsini S., Guiducci F., Inghilesi R. (2002). *Statistical Extreme Wave Analysis of the Italian Sea Wave Measurement Network Data in the period 1989-1999*. Servizio Idrografico e Mareografico Nazionale, Dipartimento per i Servizi Tecnici Nazionali, Rome, Italy.
- Cotecchia V., Canitano A. (1954). *Sull'affioramento delle "Pietre Nere" al Lago di Lesina*. Bollettino Società Geologica Italiana, 73, 1-19.
- Cotecchia V., Dai Pra G., Magri G. (1977). *Morfogenesi litorale olocenica tra Capo Spulico e Taranto nella prospettiva della protezione costiera*. Geologia Applicata e Idrogeologia, 6.
- Crichton D. (1999). *The Risk Triangle*. In: Ingleton J. (ed.), Natural disaster management, Tudor Rose, pp. 102-103, London.
- Cundy A. B., Kortekaas S., Dewez T., Stewart I. S., Collins P. E. F., Croudace I. W., Maroukian D., Papanastassiou D., Gaki-Papanastassiou P., Pavlopoulos K., Dawson A. (2000). *Coastal wetlands as recorders of earthquake subsidence in the Aegean: a case study of the 1894 Gulf of Atalanti earthquakes, central Greece*. Marine Geology, 170, 3-26.
- Dai Pra G., Hearty J. P. (1988). *I livelli marini pleistocenici del Golfo di Taranto*. Sintesi Geocronostratigrafica e tettonica. Memorie Società Geologica Italiana, 41, 637-644.
- D'Alessandro A., Iannone A. (1982). *Pleistocene carbonate deposits in the area of Monopoli (Bari Province): sedimentology and palaeocology*. Geologica Romana, 21, 603-653.
- D'Alessandro A., Iannone A. (1984). *Prime considerazioni sedimentologiche e paleoecologiche su alcune sezioni della Calcarenite di Gravina (Pleistocene) nei pressi di Monopoli*. Studi di Geologia e Geofisica, 27, 1-16.
- D'Alessandro A., Massari F. (1997). *Pliocene and Pleistocene depositional environments in the Pesculuse area (Salento, Italy)*. Rivista Italiana di Paleontologia e Stratigrafia 103, 221-258.
- D'Alessandro A., Mastronuzzi G., Palmentola G., Sansò P. (1994). *Pleistocene deposits of Salento leccese (Southern Italy): problematic relationships*. Boll. Soc. Paleont. It., 33 (2), 257-263.
- D'Alessandro A., Palmentola G. (1978). *Sabbie e Brachiopodi, una nuova unità del Salento leccese (aspetti litostatigrafici e paleoambientali)*. Rivista Italiana Paleontologia e Stratigrafia, 84, 1083-1120.
- Damiani V., Bianchi C.N., Ferretti O., Bedulli D., Morri C., Viel M., Zurlini G. (1988). *Risultati di una ricerca ecologica sul sistema marino costiero pugliese*. Thalassia Salentina, 18, 153-169.
- Dawson A.G. (1994). *Geomorphological effects of tsunami run-up and backwash*. Geomorphology, 10, 83-94.
- Dawson A. G. (1999). *Linking tsunami deposits, submarine slides and offshore earthquakes*, Quaternary International, 60, 119-126.
- Dawson A. G., Shi S. (2000). *Tsunami deposits*. Pure and Applied Geophysics, 157, 875-897.
- Dawson S., Smith D.E. (2000). *The sedimentology of Middle Holocene tsunami facies in northern Sutherland, Scotland, UK*. Marine Geology, 170, 69-79.

- De Lange W.P., Moon V.G. (2007). *Tsunami washover deposits, Tawharanui, New Zealand*. *Sedimentary Geology*, 200, 3-4, 232-247.
- De Martini P.M., Burrato P., Pantosti D., Maramai A., Graziani L., Abramson H. (2003). *Identification of tsunami deposits and liquefaction features in the Gargano area (Italy): paleosismological implication*. *Annals of Geophysics*, 46 (5), 883-902.
- De Pippo T., Donadio C., Pennetta M. (2001). *Morphological evolution of Lesina Lagoon (Southern Adriatic, Italy)*. *Geografia Fisica Dinamica Quaternaria*, 24, 29-41.
- De Santis V. (2005). *Stato ed evoluzione di alcuni apparati dunali della costa pugliese*. Tesi di Dottorato in Geomorfologia e Dinamica Ambientale, Dipartimento di Geologia e Geofisica, Facoltà di Scienze Matematiche, Fisiche e Naturali, Università degli Studi di Bari.
- Del Gaudio V., Pierri P. (2001). *Seismicity and seismic hazard of Apulia (Southern Italy)*. Abstract VI Workshop Italy-Romania, Bari 9-12 maggio 2001.
- Del Gaudio V., Pierri P., Calcagnile G., Venisti N. (2005). *Characteristics of the low energy seismicity of central Apulia (southern Italy) and hazard implications*. *Journal of Seismology*, 9, 39-59.
- Del Gaudio V., Pierri P., Frepoli A., Calcagnile G., Venisti N., Cimini G.B. (2007). *A critical revision of the seismicity of Northern Apulia (Adriatic microplate - Southern Italy) and implications for the identification of seismogenic structures*. *Tectonophysics*, 436, 9-35.
- Di Bucci D., Caputo R., Fracassi U., Mastronuzzi G., Sansò P., Selleri G. (2007). *Middle-Late Quaternary brittle deformation of the Southern Adriatic foreland (Southern Apulia) and geodynamic implications*. 26° Convegno Nazionale GNGTS, Roma, 13/15.11.2007. Extended abstracts, 85-86.
- Di Bucci D., Mazzoli S. (2003). *The October-November 2002 Molise seismic sequence (southern Italy): an expression of Adria intraplate deformation*. *Journal of Geological Society of London*, 160, 503-506.
- Di Bucci D., Ravaglia A., Seno S., Toscani G., Fracassi U., Valensise G. (2006). *Seismotectonics of the Southern Apennines and Adriatic foreland: insights on active regional E-W shear zones from analogue modeling*. *Tectonics*, 25, TC4015, doi: 10.1029/2005TC001898.
- Di Luccio F., Fukuyama E., Pino N.A. (2005). *The 2002 Molise earthquake sequence: what can we learn about the tectonics of southern Italy?* *Tectonophysics*, 405, 141-154.
- Dini M., Mastronuzzi G., Sansò P. (2000). *The Effects of Relative Holocene Sea Level Changes on the Coastal Morphology of Southern Apulia (Italy) during the Holocene*. In: Slaymaker O. (ed.). *Geomorphology and Global Environmental Change*. John Wiley & Sons: Chichester, U.K., 43-65.
- Di Perna G. (1998). *Lesina dal Paleolitico all'anno Mille*. Ed. Torraco.
- DISS Working Group (2007). *Database of Individual Seismogenic Sources (DISS), Version 3.0.3: A compilation of potential sources for earthquakes larger than M 5.5 in Italy and surrounding areas*. <http://www.ingv.it/DISS/>, © INGV 2005, 2007.
- Dogliani C., Merlini S., Cantarella G. (1999) - *Foredeep geometries at the front of the Apennines in the Ionian Sea (central Mediterranean)*. *Earth and Planetary Science Letters*, 168, 243-254.
- Dogliani C., Mongelli F., Pieri P. (1994). *The Puglia uplift (SE-Italy): an anomaly in the foreland of the Apenninic subduction due to buckling of a thick continental lithosphere*. *Tectonics*, 13, 1309-1321.
- Dominey-Howes D.T.M. (2002). *Documentary and geological records of tsunamis in the Aegean Sea region of Greece and their potential value to risk assessment and disaster management*. *Natural Hazards* 25, 195-224.
- Dominey-Howes D.T.M., Papadopoulos G.A., Dawson A.G. (2000a). *Geological and historical investigation of the 1650 Mt. Columbo (Thera Island) eruption and tsunami, Aegean Sea, Greece*. *Natural Hazards* 21, 83-96.
- Dominey-Howes D.T.M., Cundy A., Croudace I. (2000b). *High energy marine flood deposits on Astypalaea Island, Greece: possible evidence for the AD 1956 southern Aegean tsunami*. *Marine Geology* 163, 303-315.
- Donato S.V., Reinhardt E.G., Boyce J.I., Rothaus R., Vosmer T. (2008). *Identifying tsunami deposits using bivalve shell taphonomy*. *Geology*, 36/3, 199-202.
- D'Onofrio S. (1972). *Foraminiferi di carote e campioni di fondo nell' Adriatico meridionale*. *Giornale di Geologia*, 2, XXXVIII, fasc.II, 499-512.
- Douglas B.C. (2001). *An Introduction to Sea Level*. In: Douglas B.C., Kearney M.S., Leatherman S.P. (eds) *Sea Level Rise. History and consequences*. Academic Press, USA, 1-11.
- Doutsos T., Kokkalas S. (2001). *Stress and deformation patterns in the Aegean region*. *Journal of Structural Geology*, 23, 455-472.
- Earthquake Engineering Research Institute (2003). *Preliminary observations on the August 14, 2003, Lefkada Island (Western Greece) earthquake*. EERI Special Earthquake Report, 11 pp. http://www.eeri.org/lfe/pdf/greece_lefkada_eeri_preliminary_rpt.pdf [access: May 24, 2008].

- Einsele G. (2000). *Sedimentary basins. Evolution, facies, and sediment budget*. 2nd edition, Springer, Berlin, Heidelberg, 792 pp.
- Emanuel K. A. (2005). *Increasing destructiveness of tropical cyclones over the past 30 years*. Nature, 436, 686-688.
- Ernst J.A. Matson M. (1983). *A Mediterranean tropical storm?* Weather, 38, 332-337.
- Eva C., Rabinovich A. (1997). *The 23 February 1887 tsunami recorded on the Ligurian coast, western Mediterranean*. Geophysical Research Letters, 24, 17, 2211-2214.
- Fabbri A., Gallignani P. (1972). *Ricerche geomorfologiche e sedimentologiche nell'Adriatico Meridionale*. Giornale di Geologia, 38 (2), 453-498.
- Facorellis Y, Maniatis Y, Kromer B. (1998). *Apparent ¹⁴C ages of marine mollusc shells from a Greek Island: calculation of the marine reservoir effect in the Aegean Sea*. Radiocarbon 40(2), 963-73.
- Favali P., Funicello R., Mattiotti G., Mele G., Salvini F. (1993). *An active margin across the Adriatic Sea (central Mediterranean Sea)*. Tectonophysics, 219, 109-117.
- Felton E.A., Crook K.A.W., Keating B.H. (2000). *The Hulopoe Gravel, Lanai, Hawaii, new sedimentological data and their bearing on the "giant wave" (mega-tsunami) emplacement hypothesis*. Pure and Applied Geophysics, 157 (6-8), 1257-1284.
- Felton E. A., Crook K.A.W. (2003). *Evaluating the impacts of huge waves on rocky shorelines: an essay review of the book 'Tsunami - The Underrated Hazard'*. Marine Geology, 197, 1-4, 1-12.
- Felton E. A., Crook K.A.W., Keating B.H., Kay E.A. (2006). *Sedimentology of rocky shorelines: 4. Coarse gravel lithofacies, molluscan biofacies, and the stratigraphic and eustatic records in the type area of the Pleistocene Hulopoe Gravel, Lanai, Hawaii*. Sedimentary Geology, 184, 1-2, 1-76.
- Ferranti L., Antonioli F., Mauz B., Amorosi A., Dai Pra G., Mastronuzzi G., Monaco C., Orrù P., Pappalardo M., Radtke U., Renda P., Romano P., Sansò P., Verrubbi V. (2006). *Markers of the last interglacial sea-level high stand along the coast of Italy: Tectonic implications*. Quaternary International, 145-146, 30-54.
- Fita L., Romero R., Luque A., Emanuel K., Ramis C. (2007). *Analysis of medicane environments using a tropical cloud model*. Natural Hazards Earth System Sciences, 7, 41-56.
- Fracassi U., Valensise G. (2007). *Unveiling the sources of the catastrophic 1456 multiple earthquake: Hints to an unexplored tectonic mechanism in Southern Italy*. Bulletin of Seismological Society America, 97 (3), 725-748.
- Fukui Y., Nakamura M., Shiraishi H., Sasaki Y. (1963). *Hydraulic study on tsunami*. Coastal Engineering in Japan, 6, 67-82.
- Funicello R., Montone P., Parotto M., Salvini F., Tozzi M. (1991). *Geodynamical evolution of an intra-orogenic foreland: the Apulia case history (Italy)*. Bollettino della Società Geologica Italiana, 110, 419-425.
- Gaillard J.-C., Clavé E., Kelman I. (2008). *Wave of peace? Tsunami disaster diplomacy in Aceh, Indonesia*. Geoforum, 39, 511-526.
- Gaki-Papanastassiou K., Maroukian H., Papanastassiou D., Palyvos N., Lemeille F. (2001). *Geomorphological study in the Lokrian coast of northern Evoikos Gulf (central Greece) and evidence of palaeoseismic destructions*. Rapports et Procès-verbaux des Réunions, Commission Internationale pour l'Exploration Scientifique de la Mer Méditerranée 36, 25.
- Galanopoulos A. (1952). *Die Seismizität der Insel Leukas*. I. Allgemeine historische Übersicht. Gerlands Beiträge zur Geophysik 62 (4), 256-263 Leipzig.
- Galanopoulos A. (1954). *Die Seismizität der Insel Leukas*. II. Die Erdbeben vom 22. April und 30 Juni 1948. Gerlands Beiträ ge zur Geophysik 63 (1), 1-15 Leipzig.
- Galanopoulos A.G., Ekonomides A. (1973). *Rapid diapir growth, a triggering agent of a 6 1/2 magnitude earthquake on October 29, 1966, in Acarnania (Greece)*. Annali di Geofisica XXVI, Rome, pp. 605-612.
- Galvin Jr. C.J. (1972). *Wave breaking in shallow water*. In: Meyer R.E. (Ed.), Waves on Beaches, Academic Press, New York, 413-456.
- Gentile G. M., Monterisi L. (1994). *Un esempio di dinamica costiera: l'arretramento della falesia a sud della città di Brindisi*. Abstr. 77° Congresso Società Geologica Italiana, Bari 28/09/1994.
- Geyh M.A. (2005). *Handbuch der physikalischen und chemischen Altersbestimmung*. Wissenschaftliche Buchgesellschaft, Darmstadt, p. 211.
- Gianfreda F., Mastronuzzi G., Sansò P. (2001). *Impact of historical tsunamis on a sandy coastal barrier: an example from the northern Gargano coast, southern Italy*. Natural Hazard and Earth System Science, 1, 213-219.
- Gianfreda F., Miglietta M.M., Sansò P. (2005). *Tornadoes in southern Apulia*. Natural Hazards, 34, 71-89.
- Goff J. R., Chagué-Goff C. (1999). *A late Holocene record of environmental changes from coastal wetlands: Abel Tasman National Park, New Zealand* Quaternary International, 56, 1, 39-51.

- Goff J.R., Rouse H.L., Jones S.L., Hayward B.W., Cochran V., Mclea W., Dickinson W.W., Morley M.S. (2000). *Evidence for an earthquake and tsunami about 3100-3400 yr ago, and other catastrophic saltwater inundations recorded in a coastal lagoon, New Zealand*. Marine Geology, 170, 231-249.
- Goto K., Chavanich S. A., Imamura F., Kunthasap P., Matsui T., Minoura K., Sugawara D., Yanagisawa H. (2007). *Distribution, origin and transport process of boulders deposited by the 2004 Indian Ocean tsunami at Pakarang Cape, Thailand*. Sedimentary Geology, 202, 841-837.
- Granger K. T., Leiba J. M., Scott G. (1999). *Community Risk in Cairns: A Multihazard Risk Assessment*. AGSO (Australian Geological Survey Organisation) Cities Project, Department of Industry, Science and Resources, Australia.
- Gravina A., Mastronuzzi G., Sansò P. (2005). *Historical and prehistorical evolution of the Fortore River coastal plain and the Lesina Lake area (Southern Italy)*. Mediterranean, 1.2, 107-117.
- Gruppo di Lavoro CPTI (2004). *Catalogo Parametrico dei Terremoti Italiani, versione 2004 (CPTI04)*. INGV, Bologna, <http://emidius.mi.ingv.it/CPTI/>.
- Guerricchio S. (1983). *Strutture tettoniche di compressione nel Gargano d'elevato interesse applicativo evidenziate da immagini da satellite*. Geologia Applicata ed Idrogeologia, 18 (1), 1-14.
- Guidoboni E., Comastri A. (2007). *Catalogue of Earthquakes and Tsunamis in the Mediterranean Area from the 11th to the 15th Centur*. Istituto Nazionale di Geofisica e Vulcanologia, Bologna, pp. 1037.
- Guidoboni E., Ferrari G. (2004). *Revisione e integrazione di ricerca riguardante il massimo terremoto storico della Puglia: 20 febbraio 1743*. RPT 272A/05, SGA - Storia Geofisica Ambiente, Bologna, 103 pp.
- Guidoboni E., Tinti S. (1987). *I maremoti garganici del seicento*. Atti. VI Conv. Naz. GNGTS, Rome, 491-504.
- Guidoboni E., Tinti S. (1988). *A review of the historical 1627 tsunami in the southern Adriatic*. Science of Tsunami Hazards, 1, 11-17.
- Gunatillake D. (2007). *The 2004 tsunami in Sri Lanka: destruction and recovery*. Geography, 92(3), 285-293.
- Hall A.M., Hansom J.D., Williams D.M., Jarvis P. (2006). *Distribution, geomorphology and lithofacies of cliff-top storm deposits: Examples from the high-energy coasts of Scotland and Ireland*. Marine Geology, 232, 131-155.
- Hamilton S., Shennan I., Combellick R., Mulholland J., Noble C. (2005). *Evidence for two great earthquakes at Anchorage, Alaska and implications for multiple great earthquakes through the Holocene*. Quaternary Science Reviews, 24, 2050-2068.
- Hansom J.D., Barltrop N.D.P., Hall A.M. (2008). *Modelling the processes of cliff-top erosion and deposition under extreme storm waves*. Marine Geology, 253, 1-2, 36-50.
- Harmelin-Vivien M.L., Laboute P. (1986). *Catastrophic impact of atoll outer reef slopes in the Tuamotu (French Polynesia)*. Coral Reefs 5, 55-62.
- Harvard University (2006). *Harvard Centroid Moment Tensor Project*. <http://www.seismology.harvard.edu/projects/CMT/>.
- Haslinger F., Kissling E., Ansorge J., Hatzfeld D., Papadimitriou E., Karakostas V., Makropoulos K., Kahle H.-G., Peter Y. (1999). *3D crustal structure from local earthquake tomography around the Gulf of Arta (Ionian region, NW Greece)*. Tectonophysics, 304, 201-218.
- Hatzfeld D., Kassaras I., Panagiotopoulos D., Amorese D., Makropoulos K., Karakaisis G., Coutant O. (1995). *Microseismicity and strain pattern in northwestern Greece*. Tectonics 14, 773-785.
- Hearty J.P. (1997). *Boulder deposits from large waves during the last interglaciation on North Eleuthera Island, Bahamas*. Quaternary Research, 48, 326-338.
- Hearty J.P. (1998). *Chevron ridges and runup deposits in the Bahamas from storms late in Oxygen-Isotope Substage 5e*. Quaternary Research, 50, 309-322.
- Hearty J.P., Dai Pra G. (1992). *The age and stratigraphy of Quaternary coastal deposits along the gulf of Taranto (south Italy)*. Journal of Coastal Research, 8 (4), 882-905.
- Heck N.H. (1947). *List of Seismic Sea Waves*. Bulletin of Seismological Society of America, 37(4), 269-286.
- Helley E.J. (1969). *Field measurement of the initiation of large bed particle motion in blue creek near Klamath, California*. U.S. Geological Survey Professional Paper 562-G, 19 pp.
- Hesse R., Von Rad U., Fabricius F.H. (1971). *Holocene sedimentation in the strait of Otranto between the Adriatic and Ionian seas (Mediterranean)*. Marine Geology, 10, 293-355.
- Hills J.G., Mader C.L. (1997). *Tsunami produced by the impacts of the small asteroids*. Annals of the New York Academy of Sciences, 822, 381-394.
- Hippolyte J.C., Angelier J., Roure F. (1994). *A major geodynamic change revealed by Quaternary stress patterns in the Southern Apennines (Italy)*. Tectonophysics, 230, 199-210.
- Iannone A., Pieri P. (1979). *Considerazioni critiche sui "Tufo calcarei" delle Murge*. Nuovi datii litostratigrafici e paleoambientali. Geografia Fisica e Dinamica Quaternaria, 2, 173-186.
- Imamura F., Synolaks C.E., Gica E., Titov V., Listanco E., Lee H.J. (1995). *Field survey of the 1994 Mindoro Island, Philippines, Tsunami*. Pure and Applied Geophysics, 144, (3/4), 875-890.

- Institute of Computational Mathematics and Mathematical Geophysics. *On-line catalogs*. http://tsun.sgcc.ru/On_line_Cat.htm
- Institute of Geology and Mineral Exploration (IGME, 1996). *Geological map of Greece*, 1:50.000. Vonitsa Sheet, Athens.
- International Tsunami Information Center (2008). *Tsunami Database*. http://ioc3.unesco.org/itic/categories.php?category_no=72.
- Istituto Idrografico della Marina (1982). *Il vento e lo stato del mare lungo le coste italiane e dell'Adriatico*. Genova, Vol. III.
- Jahns S. (2005). *The Holocene history of vegetation and settlement at the coastal site of Lake Voukaria in Acarnania, western Greece*. *Vegetation History and Archaeobotany*, 14/1, 55-66.
- Jennings J.N. (1985). *Karst Geomorphology*. Basil Blackwell, Oxford, pp. 1-293.
- Jing Z., Rapp G. (Rip) (2003). *The coastal evolution of the Ambracian embayment and its relationship to archaeological settings*. In: Wiseman, J., Zachos K. (Eds.). *Landscape Archaeology in Southern Epirus, Greece I*. The American School of Classical Studies at Athens, Hesperia Supplement, Athens, 12, 157-198.
- Jones B., Hunter I.G. (1992). *Very large boulders on the Coast of Grand Cayman, the effects of giant waves on rocky shorelines*. *Journal of Coastal Research*, 8, 763-774.
- Kahle H.G., Müller M.V., Mueller St., Veis G. (1993). *The Kefalonia transform fault and the rotation of the Apulian Platform: evidence from satellite geodesy*. *Geophysical Research Letters* 20 (8), 651-654.
- Kahle H.G., Müller M.V., Geiger A., Danuser G., Mueller St., Veis G., Billiris H., Paradissis G. (1995). *The strain field in NW Greece and the Ionian Islands: results inferred from GPS measurements*. *Tectonophysics* 249, 41-52.
- Kahle H., Cocard M., Peter Y., Geiger A., Reilinger R., Barka A., Veis G. (2000). *GPS-derived strain rate field with the boundary zones of the Eurasian, African and Arabian Plates*. *Journal of Geophysical Research* 105 (B10), 23353-23370.
- Kapsimalis V., Pavlakis P., Poulos S.E., Alexandri S., Tziavos C., Sioulas A., Filippas D., Lykousis V. (2005). *Internal structure and evolution of the Late Quaternary sequence in a shallow embayment: The Amvrakikos Gulf, NW Greece*. *Marine Geology*, 222-223, 399-418.
- Karakostas V.G., Papadimitriou E.E., Papazachos C.B. (2004). *Properties of the 2003 Lefkada, Ionian Islands, Greece, earthquake seismic sequence and seismicity triggering*. *Bulletin of the Seismological Society of America*, 94/5, 1976-1981.
- Kawana T., Pirazzoli P. (1990). *Re-examination of the Holocene emerged shorelines in Orabu and Shimoji Islands, the South Ryukyus, Japan*. *Quaternary Research* 28, 419-426.
- Kelletat D. (2005). *Neue Beobachtungen zu Paläo-Tsunami im Mittelmeergebiet: Mallorca und Bucht von Alanya, türkische Südküste*. In: Beck, N. (Ed.), *Neue Ergebnisse der Meeres- und Küstenforschung. Beiträge der 23. Jahrestagung des Arbeitskreises "Geographie der Meere und Küsten"* (AMK), Koblenz, 28-30 April 2005. *Schriften des Arbeitskreises Landes- und Volkskunde Koblenz (ALV)* 4, 1-14.
- Kelletat D., Scheffers A. (2005). *Ergänzende Informationen zum Sumatra-Andaman-Tsunami vom 26.12.2004*. *Geographische Rundschau* 57 (9), 64-65.
- Kelletat D., Scheffers A., Scheffers S. (2005). *Paleo-Tsunami Relics on the Southern and Central Antillean Island Arc (Grenada, St. Lucia and Guadalupe)*. *Journal of Coastal Research*, 21 (2), 263-273.
- Kelletat D., Schellmann G. (2001). *Sedimentologische und geomorphologische Belege starker Tsunami-Ereignisse jung-historischer Zeitstellung im Westen und Südosten Zyperns*. *Essener Geographische Arbeiten* 32, 1-74.
- Kelletat D., Schellmann G. (2002). *Tsunami in Cyprus, field evidences and ¹⁴C dating results*. *Zeitschrift für Geomorphologie*, NF 46 (1), 19-34.
- Keulegan G.H., Patterson G.W. (1940). *Mathematical theory of irrotational translation waves*. *Journal of Research of the National Bureau of Standards*, 24, 47-101.
- Kolbe W. (1902). *Neue Grabinschriften aus Leukas*. *Mitteilungen des Kaiserlichen Deutschen Archäologischen Instituts* 1902, 368.
- Kontopoulos N., Avramidis P. (2003). *A late Holocene record of environmental changes from the Aliko lagoon, Egeion, North Peloponnesus, Greece*. *Quaternary International*, 111, 75-90.
- Kor P. S. G., Shaw J., Sharpe D. R. (1991). *Erosion of bedrock by subglacial meltwater, Georgian Bay, Ontario: a regional view*. *Canadian Journal of Earth Sciences*, 28, 623-642.
- Kortekaas S. (2002). *Tsunamis, storms and earthquakes: Distinguishing coastal flooding events*. Phd Thesis, University of Coventry. Coventry, 171 pp.
- Kortekaas S., Dawson A.G., (2007). *Distinguishing tsunami and storm deposits: An example from Martinhal, SW Portugal*. *Sedimentary Geology*, 200, 3-4, 208-221.

- Kortekaas S., Papadopoulos G.A., Ganas A., Diakantoni A. (2005). *Geological identification of historical tsunamis in the Gulf of Corinth, Greece*. In: Poster Presented at the Workshop “Tsunami Deposits and their Role in Hazard Mitigation” National Science Foundation and Department of Earth and Space Sciences at the University of Washington, Seattle /<http://earthweb.ess.washington.edu/tsunami2/deposits/downloads.htmS> [access 13 December 2006].
- Laborel J., Laborel-Deguen F. (1994). *Biological indicators of relative sea-level variations and of co-seismic displacements in the Mediterranean region*. Journal of Coastal Research, 10 (2), 395-415.
- Lambeck K., Anzidei M., Antonioli F., Benini A., Esposito E. (2004). *Sea level in Roman time in the Central Mediterranean and implications for modern sea level rise*. Earth and Planetary Science Letter, 224, 563-575.
- Laigle M., Hirn A., Sachpazi M., Clément C. (2002). *Seismic coupling and structure of the Hellenic subduction zone in the Ionian Islands region*. Earth and Planetary Science Letters 200, 243–253.
- Laigle M., Sachpazi M., Hirn A. (2004). *Variation of seismic coupling with slab detachment and upper plate structure along the western Hellenic subduction zone*. Tectonophysics, 391, 85–95.
- Lang F., Schwandner E.-L., Funke P., Kolonas L., Freitag K. (2007). *Das Survey-Projekt auf der Plaghiá-Halbinsel 2000-2002*. In: Lang F., Schwandner E.-L., Funke P., Kolonas L., Jahns S., Vött A. (Eds.): Interdisziplinäre Landschaftsforschungen im westgriechischen Akarnanien. Archäologischer Anzeiger, 2007/1, 97-178.
- Lavigne F., Paris R., Wassmer P., Gomez C., Brunstein D., Grancher D., Vautier F., Sartohadi J., Setiawan A., Syahnan T.G., Fachrizal B.W., Mardiatno D., Widagdo A., Cahyadi R., Lespinasse N., Mahieu L. (2006). *Learning from a Major Disaster (Banda Aceh, December 24th, 2004): A Methodology to Calibrate Simulation Codes for Tsunami Inundation Models*. Zeitschrift für Geomorphologie, NF, Suppl. Volume 146, 253-265.
- Louvari E., Kiratzi A.A., Papazachos B.C. (1999). *The Cephalonia Transform Fault and its extension to western Lefkada Island (Greece)*. Tectonophysics, 308, 223–236.
- Le Roux J. P., Gómez C., Fenner J., Middleton H. (2004). Sedimentological processes in a scarp-controlled rocky shoreline to upper continental slope environment, as revealed by unusual sedimentary features in the Neogene Coquimbo Formation, north-central Chile. Sedimentary Geology, 165, 1-2, 67-92.
- Lort J. M. (1971). *The tectonics of the Eastern Mediterranean: A geophysical review*. Reviews of Geophysics and Space Physics, 9, 189-216.
- Mader C.L. (1974). *Numerical simulation of tsunamis*. Journal Physical Oceanography, 4(1), 74-82.
- Magagnosc J.S. (1984). *Observations géomorphologiques dans la zone épicertrale du séisme d'Ech Chélif (ex El Asam, Algérie) et leurs implications dans la pianification de l'aménagement*. Méditerranée, 1-2, 33-41.
- Maiorano P., Aiello G., Barra D., Di Leo P., Joannin S., Lirer F., Marino M., Pappalardo A., Capotondi L., Ciaranfi N., Stefanelli S. (2007). *Paleoenvironmental changes during sapropel 19 (i-cycle 90) deposition: Evidences from geochemical, mineralogical and micropaleontological proxies in the mid-Pleistocene Montalbano Jonico land section (southern Italy)*. Palaeogeography, Palaeoclimatology, Palaeoecology, in press.
- Maracchione M.I., Mastronuzzi G., Sansò P., Sergio A., Walsh N. (2001). *Approccio semiquantitativo alla dinamica delle coste rocciose fra Monopoli e Mola di Bari (Puglia Adriatica)*. Studi Costieri, 4, 3-17.
- Maramai A., Graziani L., Tinti S. (2005). *Tsunamis in the Aeolian Islands (southern Italy), a review*. Marine Geology 215, 11–21.
- Maramai A., Tinti S. (1997). *The 3 June 1994 Java Tsunami: a post-event survey of the coastal effects*. Natural Hazards, 15, 31-49.
- Marées W. Von (1907). *Karten von Leukas*. Beiträge zur Frage Leukas-Ithaka. Berlin.
- Margottini C. (1981). *Il terremoto del 1743 nella Penisola Salentina*. Memorie Convegno Annuale Progetto Finalizzato Geofisica - Consiglio Nazionale delle Ricerche, 251-279.
- Martinis B. (1962). *Lineamenti strutturali della parte meridionale della Penisola salentina*. Geol. Rom., 1, 11-23, Roma.
- Marino M. (1996). *Quantitative calcareous nannofossil biostratigraphy of the Lower-Middle Pleistocene, Montalbano Jonico section (Southern Italy)*. Palaeopelagos, 6, 347-360.
- Marsico A., Selleri G., Mastronuzzi G., Sansò P., Walsh N. (2003). *Cryptokarst: a case-study of the Quaternary landforms of southern Apulia (southern Italy)*. Acta Carsologica, 32 (2), 147-159.
- Marzo P., Mastronuzzi G., Palmentola G., Sansò P. (1998). *Le Isole Chéradi*. Rivista Marittima, 35, 99-118.
- Massel S.R. (1997). *Prediction of the largest surface wave height in water of constant depth*. - In: Saxena N. (Ed.), Recent Ad.in Marine Science and Technology 96, PACON International, Honolulu, USA, 141-151.
- Mastronuzzi G., Caputo R., Di Bucci D., Fracassi U., Pignatelli C., Sansò P., Selleri G. (2008). *Morphological data and definition of tsunamigenic areas between Apulia (Italy) and the Ionian Islands (Greece)*. Abstract Book 2nd International Tsunami Field Symposium, GI²S Coast, Research Publication 6.

- Mastronuzzi G., Palmentola G., Ricchetti G. (1989). *Aspetti dell'evoluzione olocenica della costa pugliese*. Memorie Società Geologica Italiana, 42, 287-300.
- Mastronuzzi G., Palmentola G., Sansò P. (1992). *Morphological types of rocky coast on Southeastern Apulia*. International Coastal Congress - ICC, Kiel, 7-12 September 1992, 784 - 797.
- Mastronuzzi G., Palmentola G., Sansò P. (1994). *Le tracce di alcune variazioni del livello del mare olocenico tra Torre dell'Orso e Otranto (Lecce)*. Geografia Fisica e Dinamica Quaternaria, 17, 55-60.
- Mastronuzzi G., Palmentola G., Sansò P. (2002). *Lineamenti e dinamica della costa pugliese*. Studi Costieri, 5, 9-22.
- Mastronuzzi G., Pignatelli C., Sansò P. (2006). *Boulder fields: a valuable morphological indicator of paleotsunamis in the Mediterranean Sea*. Zeitschrift für Geomorphologie, NF Suppl.-Bd. 146, 173-194.
- Mastronuzzi G., Pignatelli C., Sansò P., Selleri G. (2007a). *Boulder accumulations produced by the 20th February 1743 tsunami along the coast of southeastern Salento (Apulia region, Italy)*. Marine Geology, 242 (1-3), 191-205.
- Mastronuzzi G., Pignatelli C., Stamatopoulos L. (in prep.). *New data on Holocene coseismic uplift in the Kerkira Island (Greece)*.
- Mastronuzzi G., Pye K., Sansò P., Sergio A. (1997). *The impact of dam construction and coast protection works on beach sediment budgets and erosional accretion trends: examples from Apulia, Southern Italy, and Eastern and Southern England*. Environmental Sedimentology IAS-SEPM, Meeting on Environmental Sedimentology, Venice, Italy, 27-29 October.
- Mastronuzzi G., Quinif Y., Sansò P., Selleri G. (2007b). *Middle-Late Pleistocene polycyclic evolution of a geologically stable coastal area (southern Apulia, Italy)*. Geomorphology, 86, 393-408.
- Mastronuzzi G., Sansò P. (1998). *Morfologia e genesi delle Isole Chéradi e del Mar Grande (Taranto, Puglia, Italia)*. Geografia Fisica e Dinamica Quaternaria, 21, 131-138.
- Mastronuzzi G., Sansò P. (2000). *Morphological effects of catastrophic waves along the Ionian coast of Apulia (southern Italy)*. Marine Geology, 170, 93-103.
- Mastronuzzi G., Sansò P. (2002a). *Holocene uplift rates and historical rapid sea-level changes at the Gargano promontory, Italy*. Journal of Quaternary Science, 17 (5-6), 593-606.
- Mastronuzzi G., Sansò P. (2002b). *Holocene coastal dune development and environmental changes in Apulia (southern Italy)*. Sedimentary Geology, 150, 139-152.
- Mastronuzzi G., Sansò P. (2002c). *Pleistocene sea level changes, sapping processes and development of valleys network in Apulia region (southern Italy)*. Geomorphology, 46, 19-34.
- Mastronuzzi G., Sansò P. (2003). *Field Guide. Puglia 2003 — Final Conference Quaternary Coastal Morphology and Sea Level Changes*. IGCP 437 Project, Otranto/Taranto 22-28 settembre 2003, GI²S Coast, Brizio srl, Taranto. 184 pp.
- Mastronuzzi G., Sansò P. (2004). *Large boulder accumulations by extreme waves along the Adriatic coast of Southern Apulia (Italy)*. Quaternary International, 120, 173-184.
- May S.M., Vött A., Brückner H., Brockmüller S. (2007). *Evidence of tsunamigenic impact on Actio headland near Preveza, NW Greece*. In: Gönnert G., Pflüger B., Bremer J.-A. (Eds.). *Von der Geoarchäologie über die Küstendynamik zum Küstenzonenmanagement*. Coastline Reports, 9, 115-125.
- McClusky S., Balassanian S., Barka A., Demir C., Ergintav S., Georgiev I., Gurkan O., Hamburger M., Hurst K., Kahle, H., Kastens K., Kekelidze G., King R., Kotzev V., Lenk O., Mahmoud S., Mishin A., Nadariya M., Ouzounis A., Paradissis D., Peter Y., Prilepin M., Reilinger R., Sanli I., Seeger H., Tealeb A., Toksoz M.N., Veis G. (2000). *Global Positioning System constraints on plate kinematics and dynamics in the eastern Mediterranean and Caucasus*. Journal of Geophysical Research, Solid Earth V, 105/3, 5695-5719.
- McCoy F.W., Heiken G. (2000). *Tsunami generated by the Late Bronze Age eruption of Thera (Santorini), Greece*. Pure Applied Geophysics, 157, 1227-1256.
- McSaveney M.J., Goff J.R., Darby D.J., Goldsmith P., Barnett A., Elliott S., Nonckas M. (2000). *The 17 July 1998 tsunami, Papua New Guinea: evidence and initial interpretation*. Marine Geology, 170, 81-92.
- Meehl G.A., Stocker T.F., Collins W.D., Friedlingstein P., Gaye A.T., Gregory J.M., Kitoh A., Knutti R., Murphy J.M., Noda A., Raper S.C.B., Watterson I.G., Weaver A.J., Zhao Z.-C., (2007). *Global Climate Projections*. In: *Climate Change 2007: The Physical Science Basis*. Contribution of Working Group I to the Fourth Assessment Report of the Intergovernmental Panel on Climate Change [Solomon S., Qin D., Manning M., Chen Z., Marquis M., Averyt K.B., Tignor M., Miller H.L. (eds.)]. Cambridge University Press, Cambridge, United Kingdom and New York, NY, USA.
- Menardi Noguera A., Rea G. (2000). *Deep structure of the Campanian-Lucanian Arc (southern Apennines)*. Tectonophysics, 324, 239-265.
- Merlini S., Cantarella G., Doglioni C. (2000). *On the seismic profile Crop M5 in the Ionian Sea*. Bollettino Società Geologica Italiana, 119, 227-236.

- Milella M., De Santis V., Pignatelli C., Cacciapaglia G., Selli G., Fozzati L., Mastronuzzi G., Sansò P., Palmentola G. (2008). *Sensibilità della costa pugliese ad ondate estreme*. Atti del Convegno Nazionale "Coste: Prevenire, Programmare, Pianificare", Maratea 15-17 Maggio 2008, 477-487.
- Minoura K., Imamura F., Kuran U., Nakamura T., Papadopoulos G.A., Takahashi T., Yalciner A.C. (2000). *Discovery of Minoan tsunami deposits*. *Geology*, 28, 59-62.
- Minoura K., Imamura F., Takahashi T., Shuto N. (1997). *Sequence of sedimentation processes caused by the 1992 Flores tsunami: Evidence from Babi island*. *Geology*, 25 (6), 523-526.
- Minoura K., Nakaya S. (1991). *Traces of tsunami preserved in inter-tidal lacustrine and marsh deposits: some examples from Northeast Japan*. *Journal of Geology* 99, 265-287.
- Miyoshi H., Iida K., Suzuki H., Osawa Y. (1983). *The largest tsunami in the Sanriku District*. In: Iida K., Iwasaki T. (Eds.), *International Tsunami Symposium 1981*, IUGG Tsunami Commission, May 1981. *Advances in Earth and Planetary Science*. Terra Publishing, Sendai, Japan, pp. 205-211.
- Molin D., Margottino C. (1981). *Il terremoto del 1627 nella Capitanata settentrionale*, *Memorie Conv. Ann. PFG-CNR*, 251-279 (in Italian).
- Monserrat S., Vilibić I., Rabinovich A. B. (2006). *Meteotsunamis: atmospherically induced destructive ocean waves in the tsunami frequency band*. *Nat. Haz. Earth Syst. Sci.*, 6, 1035-1051.
- Montone P., Mariucci M.T., Pondrelli S., Amato A. (2004). *An improved stress map for Italy and surrounding regions (central Mediterranean)*. *Journal of Geophysical Research*, 109.
- Moore G.W., Moore J.G. (1984). *Deposit from a giant wave on the island of Lanai, Hawaii*. *Science* 226, 1311-1315.
- Moore G.W., Moore J.G. (1988). *Large-scale bedforms in boulder gravel produced by giant waves in Hawaii*. In: Clifton H.E. (Ed.), *Sedimentologic Consequences of Convulsive Geologic Events*. Geological Society of America, Special Papers, 229, 101-110.
- Moretti M. (2000). *Soft-sediment deformation structures interpreted as seismites in middle-late Pleistocene aeolian deposits (Apulian foreland, Southern Italy)*. *Sedimentology*, 135, 167-179.
- Moretti M., Tropeano M. (1996). *Strutture sedimentarie deformative (sismiti) nei depositi tirreniani di Bari*. *Memorie Società Geologica Italiana*, 51, 485-500.
- Morhange C., Marriner N., Pirazzoli P.A. (2006). *Evidence of Late-Holocene Tsunami Events in Lebanon*. *Zeitschrift für Geomorphologie, NF, Suppl. Volume 146*, 81-95.
- Mörner N.-A. (1988). *Terrestrial variations within given energy, mass and momentum budgets; Paleoclimate, sea level, paleomagnetism, differential rotation and geodynamics*. In: Stephenson F.R., Wolfendale A.W. (eds.), *Secular Solar and Geomagnetic Variations in the last 10,000 years*. Dordrecht/Boston/London: Kluwer Acad. Press, 455-478.
- Mörner N.-A. (1994). *Recorded sea level variability in the Holocene and expected future changes*. *Bull. INQUA Neotectonic Commission*, 17, 48-53.
- Mörner N.-A. (1996). *Sea level variability*. *Zeitschrift für Geomorphologie N.S.* 102, 223-232.
- Morton R. A., Goff J.R., Nichol S.L. (2008). *Hydrodynamic implications of textural trends in sand deposits of the 2004 tsunami in Sri Lanka*. *Sedimentary Geology*, 207, 1-4, 56-64.
- Mostardini F., Merlini S. (1986). *Appennino centro-meridionale. Sezioni Geologiche e Proposta di Modello Strutturale*. *Memorie Società Geologica Italiana*, 35, 177-202.
- Murray W. M. (1982). *The coastal sites of western Akarnania: a topographical-historical survey*. Ph.D. Thesis, University of Pennsylvania, 587 pp.
- Murray W.M. (1985). *The ancient harbour of Palairos*. In: Raban A. (Ed.): *Harbour Archaeology. Proceedings of the first international Workshop on ancient Mediterranean Harbours*. *British Archaeological Reports, International Series*, 257, 67-80.
- Myroie J. E. (2008). *Late Quaternary sea-level position: Evidence from Bahamian carbonate deposition and dissolution cycles*. *Quaternary International*, 183, 1, 61-75.
- Nakata T., Kawana T. (1993). *Historical and prehistoric large tsunamis in the southern Ryukyus, Japan*. In: *Tsunami '93. Proceedings IUGG/IOC, International Tsunami Symposium, Wakayama; Japan, August 23-27*, 297-307.
- Narayan J.P., Sharma M.L., Maheshwar B.K. (2005). *Run-up and Inundation Pattern Developed During the Indian Ocean Tsunami of December 26, 2004 Along the Coast of Tamilnadu (India)*. *Gondwana Research*, 8(4), 611-616.
- National Geophysical Data Center (2008). *Tsunami data at NGDC*. http://www.ngdc.noaa.gov/hazard/tsu_db.shtml.
- National Observatory of Athens, Institute of Geodynamics (2008). *Seismicity catalogs*. [Http://www.gein.noa.gr/services/info-en.html](http://www.gein.noa.gr/services/info-en.html) [access May 24, 2008].
- Naval Intelligence Division (Ed.) (1944). *Greece*. Vol. I. *Physical Geography, History, Administration and Peoples*. *Geographical Handbook Series B. R. 516 (Restricted)*. Andover, Hants.

- Négris P. (1903). *Régression et transgression de la mer depuis l'époque glaciaire jusqu'à nos jours*. Revue universelle des mines de la métallurgie, des travaux publics etc., Tome III, 3.
- Négris P. (1904). *Vestiges antiques submergés*. Athener Mitteilungen 1904/29, 340-369.
- Nichol S.L., Lian O.B., Carter C.H. (2003). *Sheet-gravel evidence from a late Holocene tsunami run-up on beach dunes, Great Barrier Island; New Zealand*. Sedimentary Geology, 155, 129-145.
- Nicholls R.J., Leatherman S.P. (1995). *The implication of accelerated sea level rise for developing countries: A discussion*. Journal of Coastal Research, S I, 14, 303-323.
- Nicholls R.J., Leatherman S.P., Dennis K.C., Volonte C.R. (1995). *Impacts and responses to sea level rise: qualitative and quantitative assessments*. Journal of Coastal Research, SI, 14, 26-43.
- Nishimura Y., Miyaji N. (1995). *Tsunami deposits from the 1993 Southwest Hokkaido earthquake and the 1640 Hokkaido Komagatake eruption, northern Japan*. - In: Satake K., Imamura F. (Eds.), *Tsunamis: 1992-1994, their Generation, Dynamics, and Hazard*. Pure and Applied Geophysics, 144 (3-4), 719-733.
- Noji M., Imamura N., Shuto N. (1985). *Numerical simulation of movement of large rocks transported by tsunamis*. Proceedings of the IUGG/IOC International Tsunami Symposium, Wakayama, Japan, pp. 189-197.
- Noormets R, Crook K.A.W., Felton E.A. (2004). *Sedimentology of rocky shorelines:3. Hydrodynamics of megaclast emplacement and transport on a shore platform, Oahu, Hawaii*. Sedimentary Geology, 172, 41-65.
- Noormets R, Felton E.A., Crook K.A.W. (2002). *Sedimentology of rocky shorelines: 2. Shoreline megaclasts on the north shore of Oahu, Hawaii - origins and history*. Sedimentary Geology, 150, 31-45.
- Nott J.F. (1997). *Extremely high wave deposits inside the Great Barrier Reef, Australia; determining the cause tsunami or tropical cyclone*. Marine Geology, 141, 193-207.
- Nott J.F. (2003a). *Waves, coastal boulders and the importance of the pre-transport setting*. Earth and Planetary Science Letters, 210, 269-276.
- Nott J. (2003b). *Tsunami or Storm Waves? – Determining the Origin of a Spectacular Field of Wave Emplaced Boulders Using Numerical Storm Surge and Wave Models and Hydrodynamic Transport Equations*. Journal of Coastal Research, 19, 2, 348-356.
- Nott J.F. (2004). *The tsunami hypothesis — comparison of field evidence against the effects, on the Western Australia coasts, of some of the most powerful storms on Earth*. Marine Geology, 208, 1-12.
- Nott J.F. (2006). *Extreme Events: A Physical reconstruction and Risk Assessment*. Cambridge University Press, New York - USA, 297 pp.
- Ortolani F., Pagliuca S. (1987). *Tettonica transpressiva nel Gargano e rapporti con le catene Appenninica e Dinarica*. Memorie Società Geologica Italiana, 38, 205-224.
- Palmentola G. (1987). *Lineamenti geologici e morfologici del Salento leccese*. Atti “Convegno sulle conoscenze geologiche del territorio salentino. Quaderni di Ricerca del Centro Studi Geotecnica e d'Ingegneria, 11, 173-202.
- Palmentola G., Vignola N. (1980). *Dati di neotettonica sulla penisola salentina*. Fogli 204 Lecce, 213 Maruggio, 214.
- Pantosti D., Barbano M.S., Smedile A., De Martini P.M., Tigano G. (2008). *Geological Evidence of Paleotsunamis at Torre degli Inglesi (northeast Sicily)*, Geophysical Research Letters, 35, 105311 doi:10.1029/2007GL032935, in press.
- Panza G.F., Craglietto A., Suhadolc P. (1991). *Source geometry of historical events retrieved by synthetic isoseismals*. Tectonophysics, 193, 173-184.
- Papadatou-Giannopoulou H. (1999). *Leukada Euronontas*. Achaikes Ekdoseis, Patras.
- Papadimitriou P., Kaviris G., Makropoulos K. (2006). *The Mw = 6.3 2003 Lefkada earthquake (Greece) and induced stress transfer changes*. Tectonophysics, 423, 73-82.
- Papadopoulos G.A. (2003). *Tsunami hazard in the eastern Mediterranean: strong earthquakes and tsunamis in the Corinth Gulf, Central Greece*. Natural Hazards, 29, 437-464.
- Papadopoulos G.A., Karastathis V. K., Ganas A., Pavlides S., Fokaefs A., Orfanogiannaki K. (2003). *The Lefkada, Ionian Sea (Greece), shock (Mw 6.2) of 14 August 2003: Evidence for the characteristic earthquake from seismicity and ground failures*. Earth, Planets and Space, 55/11, 713-718.
- Papathanassiou G., Pavlides S., Ganas A. (2005). *The 2003 Lefkada earthquake: Field observations and preliminary microzonation map based on liquefaction potential index for the town of Lefkada*. Engineering Geology, 85, 12-31.
- Papazachos B. C., Papazachou C. B. (1997). *The earthquakes of Greece*. Ziti Edit., Thessaloniki, 304 pp.
- Papazachos B.C., Dimitriou P.P. (1991). *Tsunamis in and near Greece and their relation to the earthquake focal mechanism*. In: Bernard E.N. (Ed.). *Tsunami hazard. A practical guide for tsunami hazard reduction*. Natural Hazards, 4/2+3, 161-170.

- Pararas-Carayannis G. (1986). *The Pacific tsunami warning system*. Earthquakes and Volcanoes, 18, 3, US Geological Survey, Reston, Virginia, USA, 120-130.
- Pareschi M. T., Boschi E., Mazzarini F., Favali M. (2006). *Large submarine landslides offshore Mt. Etna*. Geomorphology Research Letters, 33, L13302, doi:10.1029/2006GL026064.
- Paris R., Lavigne F., Wassmer P., Sartohadi J. (2007). *Coastal sedimentation associated with the December 26, 2004 tsunami in Lhok Nga, west Banda Aceh (Sumatra, Indonesia)*. Marine Geology, 238, 1-4, 93-106.
- Paris R., Wassmer P., Sartohadi J., Lavigne F., Barthomeuf B., Desgages E., Grancher D., Baumert P., Vautier F., Brunstein D., Gomez C. (2008). *Tsunamis as geomorphic crises: Lessons from the December 26, 2004 tsunami in Lhok Nga, West Banda Aceh (Sumatra, Indonesia)*. Geomorphology, in press.
- Parroni F., Silenzi S. (1997). *Paleoeustatismo e geomorfologia nel settore costiero emerso e sommerso di Marina di Novaglie (LE)*. Bollettino Società Geologica Italiana, 116, 421-433.
- Partsch J. (1889). *Die Insel Leukas*. Eine geographische Monographie. Petermanns Geographische Mitteilungen, Ergänzungsheft 95. Gotha.
- Partsch J. (1907). *Das Alter der Inselnatur von Leukas*. Petermanns Geographische Mitteilung 53, 269-278 Gotha.
- Paschos P., Papadakis J., Rondoyanni-Tsiambaou Th. (1991). *Neotectonic study of Preveza-Aktio area*. Institute of Geology and Mineral Exploration, Athens, 23 pp.
- Paskoff R. (1991). *Likely occurrence of a Mega Tsunami in the Middle Pleistocene, near Coquimbo, Chile*. Rev. Geol. Chile 18, 87-91.
- Patacca E., Scandone P. (1989). *Post-Tortonian mountain building in the Apennines. The role of the passive sinking of a relic lithospheric slab*. In: Boriani A.M., Bonafede M., Piccardo G.B., Vai G.B. (Ed.), *The Lithosphere in Italy*. Atti dei Convegni Lincei, 80, 157-176.
- Patacca E., Scandone P. (2004a). *The 1627 Gargano earthquake (Southern Italy): Identification and characterization of the causative fault*. Journal of Seismology, 8, 259-273.
- Patacca E., Scandone P. (2004b). *The Plio-Pleistocene thrust belt - foredeep system in the Southern Apennines and Sicily (Italy)*. In: Crescenti U., D'Offizi S., Merlini S., Lacchi L. (Ed.), *Geology of Italy*. Società Geologica Italiana, Roma, 93-129.
- Pelinovsky E., Kharif C., Riabov I., Francius M. (2001). *Study of tsunami propagation in the Ligurian Sea*. Natural Hazards Earth Systems Sciences, 1, 195-201.
- Pelinovsky E., Kharif C., Riabov I., Francius M. (2002). *Modelling of Tsunami Propagation in the Vicinity of the French Coast of the Mediterranean*. Natural Hazards, 25, 2, 135-159.
- Pelinovsky E., Yuliadi D., Prasetya G., Hmayat R. (1997). *The 1996 Sulawesi Tsunami*. Natural Hazards, 16, 29-38.
- Pennetta L. (1988). *Ricerche sull'evoluzione recente del delta deU'Ofanto*. Bollettino del Museo Storia Naturale Lunigiana, 6-7, 41-45.
- Pennetta M. (1985). *La sedimentazione attuale. Analisi granulometriche*. C.N.R. - Consiglio Nazionale delle Ricerche, Progetto finalizzato Oceanografia e Fondi Marini. Sottoprogetto "Utilizzazione e gestione della piattaforma continentale: rapporto tecnico finale". Roma.
- Péres J.M. (1967). *The Mediterranean Benthos*. Oceanographic Marine Biology Annual Review, 5, 449-553.
- Péres J.M., Picard J. (1964). *Nouveau manuel de bionomie benthique de la Mer Méditerranée*. Recueil des Travaux de la Station Marine d'Endoume, 14(23), 1-114.
- Peter Y., Kahle H.G., Cocard M., Veis G., Felekis S., Paradissis D. (1998). *Establishment of a continuous GPS network across the Kefalonia Fault Zone, Ionian Islands, Greece*. Tectonophysics, 294, 253-260.
- Piccardi L. (1998). *Cinematica attuale, comportamento sismico e sismologia storica della faglia di Monte Sant'Angelo (Gargano, Italia): la possibile rottura superficiale del "leggendario" terremoto del 493 d.C.*. Geografia Fisica e Dinamica Quaternaria, 21, 155-166.
- Piccardi L. (2005). *Paleoseismic evidence of legendary earthquakes: the apparition of Archangel Michael at Monte Sant'Angelo (Italy)*. Tectonophysics, 408, 113-128.
- Pieri P., Sabato L., Tropeano M. (1996). *Significato Geodinamico dei caratteri deposizionali e strutturali della Fossa Bradanica nel Pleistocene*. Memorie della Società Geologica Italiana, 51, 501-515.
- Piper D.J.W., Kontopoulos N., Panagos A.G. (1988). *Deltaic sedimentation and stratigraphic sequences in post-orogenic basins, western Greece*. Sedimentary Geology, 55, 283-294.
- Piper D.J.W., Panagos A.G., Kontopoulos N. (1982). *Some observations on surficial sediments and physical oceanography of the Gulf of Amvrakia*. Thalassographica, 5, 63-80.
- Pirazzoli P.A. (1996). *Sea Level Changes*. J. Wiley & Sons Ltd, Chichester, 212 pp.
- Pirazzoli P.A. (1998). *A comparison between Postglacial Isostatic Predictions and Late Holocene Sea-Level Field Data from Mediterranean and Iranian Coastal Areas*. GeoResearch Forum, 3-4, 401-420.
- Pirazzoli P.A. (2005). *A review of possible eustatic, isostatic and tectonic contributions in eight Late-Holocene relative sea-level histories from Mediterranean area*. Quaternary Science Reviews, 24, 1989-2001.

- Pirazzoli P.A., Laborel J., Saliège J.F., Erol O, Kaian I., Person A. (1991). *Holocene raised shorelines on the Hatay coasts (Turkey): palaeological and tectonic implications*. Marine Geology, 96, 295-311.
- Pirazzoli P.A., Mastronuzzi G., Saliège J. F., Sansò P. (1997). *Late Holocene emergence in Calabria, Italy*. Marine Geology, 141 (1-4), 61-70.
- Pirazzoli P. A., Stiros S. C., Arnold M., Laborel J., Laborel-Deguen F. (1999). *Late Holocene Co-seismic Vertical Displacements and Tsunami Deposits Near Kynos, Gulf of Euboea, Central Greece*. Physical and Chemistry of Earth, 24 (4), 361-367.
- Pirazzoli P.A., Stiros S.C., Arnold M., Laborel J., Laborel-Deguen F., Papageorgiou S. (1994a). *Episodic uplift deduced from Holocene shorelines in the Perachora Peninsula, Corinth area, Greece*. Tectonophysics, 229, 201-209.
- Pirazzoli P.A., Stiros S.C., Arnold M., Laborel J., Laborel-Deguen F., Papageorgiou S., Morhange C. (1994b). *Late-Holocene shoreline changes related to palaeoseismic events in the Ionian Islands, Greece*. The Holocene, 4, 397-405.
- Pirazzoli P.A., Tomasin A. (1999). *L'evoluzione recente delle cause meteorologiche dell'acqua alta*. Atti Istituto Veneto di Scienze, Lettere ed Arti, CLVII, 317-344.
- Poppe G.T., Goto Y. (2000). *European seashells*. Vol. II: Scaphopoda, Bivalvia, Cephalopoda. ConchBooks, Hackenheim, 221 pp.
- Poulos S. E., Lykousis V., Collins M.B. (1995). *Late Quaternary evolution of Amvrakikos Gulf, Western Greece*. Geomarine Letters, 15/1, 9-16.
- Poulos S.E., Kapsimalis V., Tziavos C., Pavlakis P., Leivaditis G., Collins M. (2005). *Sea-level stands and Holocene geomorphological evolution of the northern deltaic margin of Amvrakikos Gulf (western Greece)*. Zeitschrift für Geomorphologie N.F., Suppl. Vol. 137, 125-145.
- Pytharoulis I., Craig G. C., Ballard S. P. (1999). *Study of the Hurricane-Like Mediterranean Cyclone of January 1995*. Phys. Physical and Chemistry of Earth, 24 (6), pp. 627-632.
- Rabinovich A. B., Monserrat S. (1998). *Generation of meteorological tsunamis (large amplitude seiches) near the Balearic and Kuril Islands*. Nat. Hazards, 18(1), 27-55.
- Rasmussen E., Zick C. (1987). *A subsynoptic vortex over the Mediterranean with some resemblance to polar lows*. Tellus, 39A, 408-425.
- Reale O., Atlas R. (1998). *A tropical-like cyclone in the extratropics*. International Centre for Theoretical Physics preprint, Trieste, Italy. No. IC98007.
- Reimer P.J., Baillie M.G.L., Bard E., Bayliss A., Beck J.W., Bertrand C., Blackwell P.G., Buck C.E., Burr G., Cutler K.B., Damon P.E., Edwards R.L., Fairbanks R.G., Friedrich M., Guilderson T.P., Hughen K.A., Kromer B., McCormac F.G., Manning S., Bronk Ramsey C., Reimer R.W., Remmele S., Southon J.R., Stuiver M., Talamo S., Taylor F.W., van der Plicht J., Weyhenmeyer C.E. (2004). *IntCal04 Terrestrial Radiocarbon Age Calibration, 0-26 cal kyr BP*. Radiocarbon, 46(3), 1029-1058.
- Reimer P.J., McCormac F.G. (2002). *Marine radiocarbon reservoir corrections for the Mediterranean and Aegean Seas*. Radiocarbon, 44, 159-166.
- Reineck H.E., Singh I.B. (1980). *Depositional sedimentary environments. With reference to terrigenous clastics*. 2nd edition. Springer, Berlin, Heidelberg, New York, 551 pp.
- Reinhardt E.G., Goodman B.N., Boyce J. I., Lopez G., van Henstum P., Rink W. J., Mart Y., Raban A. (2006). *The tsunami of 13 December A.D. 115 and the destruction of Herod the Great's harbor at Caesarea Maritima, Israel*. Geology, 34, 12, 1061-1064.
- Ricchetti G. (1967). *Osservazioni preliminari sulla geologia e morfologia dei depositi quaternari nei dintorni del Mar Piccolo (Taranto)*. Atti Accademia Gioenia Scienze Naturali in Catania, 6, XVIII, 123-130.
- Ricchetti G. (1972). *Osservazioni geologiche e morfologiche preliminari sui depositi quaternari affioranti nel F. 203 (Brindisi)*. Bollettino Società Naturalisti in Napoli, LXXXI, 543-566.
- Ricchetti G. (1980). *Contributo alla conoscenza strutturale della Fossa Bradanica e delle Murge*. Bollettino Società Geologica Italiana, 99, 421-430.
- Ricchetti G., Ciaranfi N., Luperto Sinni E., Mongelli F., Pieri P. (1992). *Geodinamica ed evoluzione sedimentaria e tettonica dell'Avampese apulo*. Memorie Società Geologica Italiana, 41, 57-82.
- Richmond B.M., Jaffe B.E., Gelfenbaum G., Morton R.A. (2006). *Geologic Impacts of the 2004 Indian Ocean Tsunami on Indonesia, Sri Lanka, and the Maldives*. Zeitschrift für Geomorphologie, NF, Suppl. Volume 146, 235-251.
- Robertson E., Rowe D.H., Khan S. (2006). *Wave-Emplaced boulders on Jamaica's Rocky shores*. In: Scheffers, A. & Kelletat, D. (eds.) (2006): Extreme Events in the Coastal Environment. Proceedings of the IGCP 495. First Tsunami Field Symposium, Bonaire 2006.
- Ruiz F., Rodríguez-Ramírez A., Cáceres L. M., Rodríguez Vidal J., Carretero M. I., Abad M., Olías M., Pozo M. (2005). *Evidence of high-energy events in the geological record: Mid-holocene evolution of the*

- southwestern Doñana National Park (SW Spain)*. Palaeogeography, Palaeoclimatology, Palaeoecology, 229, 3, 212-229.
- Russo F., Valletta M. (1995). *Rischio ed impatto ambientale: considerazioni e precisazioni*. Bollettino Servizio Geologico d'Italia, CXII, 103-126.
- Sachpazi M., Hirn A., Clément C., Haslinger F., Laigle M., Kissling E., Charvis P., Hello Y., Lépine J.-C., Sapin M., Ansorge J. (2000). *Western Hellenic subduction and Cephalonia transform: local earthquakes and plate transport and strain*. Tectonophysics, 319 (4), 301–319.
- Salvi S., Quattrocchi F., Brunori C.A., Doumaz F., Angelone A., Billi A., Buongiorno F., Funicello R., Guerra M., Mele G., Pizzino L., Salvini F. (1999). *A Multidisciplinary Approach to Earthquake Research: Implementation of a Geochemical Geographic Information System for the Gargano Site, Southern Italy*. Natural Hazards, 20, 255-278.
- Sato H., Shimamoto T., Tsutsumi A., Kawamoto E. (1995). *Onshore Tsunami Deposits Caused by the 1993 Southwest Hokkaido and 1983 Japan Sea Earthquakes*. PAGEOPH, 144, 693-71.
- Schäfer A. (2005). *Klastische Sedimente. Fazies und Sequenzstratigraphie*. Elsevier, München, 414 pp.
- Scheffers A. (2002a) *Paleotsunamis in the Caribbean. Field evidences and datings from Aruba, Curaçao and Bonaire*. Essener Geographische Arbeiten, Band 33, 186 pp.
- Scheffers A. (2002b). *Paleotsunami evidences of tsunami from boulder deposits on Aruba, Curaçao and Bonaire*. Science of Tsunami Hazards, 20 (1), 26-37.
- Scheffers A. (2004). *Tsunami imprints on the leeward Netherlands Antilles (Aruba, Curaçao and Bonaire) and their relation to other coastal problems*. Quaternary International, 120 (1), 163-172.
- Scheffers A. (2005). *Coastal response to extreme wave events. Hurricanes and tsunami on Bonaire*. Essener Geographische Arbeiten, Band, vol. 37. Auflage-Essen, Selbstverlag, 100 pp.
- Scheffers A. (2006a). *Coastal transformation during and after a sudden neotectonic uplift in western Crete (Greece)*. Zeitschrift für Geomorphologie N.F., 146 (Suppl.), 97–124.
- Scheffers A. (2006b). *Argumente und Methoden zur Unterscheidung von Sturm- und Tsunamischnitt und das Problem der Datierung von Paläo-Tsunami*. Die Erde, 136 (4), 413–429.
- Scheffers A., Kelletat D. (2003). *Sedimentologic and geomorphic tsunami imprints worldwide - a review*. Earth-Science Reviews, 63, 83-92.
- Scheffers A., Kelletat D. (2003). *Sedimentologic and geomorphologic tsunami imprints worldwide—a review*. Earth-Science Reviews, 63, 83–92.
- Scheffers A., Kelletat D. (2004). *Bimodal tsunami deposits—a neglected feature in palaeo-tsunami research*. In: Schernewski G., Dolch T., (Eds.), Geographie der Meere und Küsten. 22. AMK-Jahrestagung, 28-30.04.2004. Coastline Reports, 1, 67–75.
- Scheffers A., Kelletat D. (2005). *Tsunami Relics On The Coastal Landscape West Of Lisbon, Portugal*. Science of Tsunami Hazards, 23 (1), 3-16.
- Scheffers A., Kelletat D. (2006). *Preface: Tsunami- and palaeo-tsunami research: Where are we now and where do we go?* Zeitschrift für Geomorphologie N.F., 146 (Suppl.), 1–5.
- Scheffers, A., Kelletat, D., Vött, A., May, S.M., Scheffers, S. (2008). *Late Holocene tsunami traces on the western and southern coastlines of the Peloponnesus (Greece)*. Earth Planetary Science Letters 269, 271-279.
- Scheffers A, Scheffers S. (2007). *Tsunami deposits on the coastline of west Crete (Greece)*. Earth and Planetary Science Letters, 259, 613-624.
- Schielein P., Schellmann G., Zschau J., Woith H. (2008). *Tsunamigefährdung im Mittelmeer - eine Analyse geomorphologischer und historischer Zeugnisse*. Bamberger Geographische Schriften, 22, 153-199.
- Schubert C. (1994). *Tsunami in Venezuela. Some observations on their occurrence*. In: Finkl Ch.F. (Ed.), *Coastal Hazards. Perception, Susceptibility and Mitigation*. Journal of Coastal Research, Special Issue, 12, 189-195.
- Scicchitano G., Antonioli F., Castagnino Berlinghieri E. F., Dutton A., Monaco C. (2008). *Submerged archaeological sites along the Ionian coast of southeastern Sicily (Italy) and implications for the Holocene relative sea-level change*. Quaternary Research, in press.
- Scicchitano G., Monaco C., Tortorici L. (2007). *Large boulder deposits by tsunami waves along the Ionian coast of south-eastern Sicily (Italy)*. Marine Geology, 238(1-4), 75-91.
- Scordilis E., Karakaisis G., Panagiotopoulos D., Papazachos B. (1985). *Evidence for transform faulting in the Ionian Sea: the Cephalonia Island earthquake sequence of 1983*. Pageoph, 123, 387–397.
- Sella M., Turci C., Riva A. (1988). *Sintesi geopetrolifera della Fossa Bradanica (avanfossa della catena appenninica)*. Memorie Società Geologica Italiana, 41, 87-107.
- Sella G.F., Dixon T.H., Mao A. (2002) - *REVEL: a model for Recent plate velocities from space geodesy*. Journal of Geophysical Research, 107.

- Senatore M.R., Diplomatico G., Mirabile L., Pescatore T., Tramotuoli M. (1982). *Franamenti sulla scarpata continentale pugliese del Golfo di Taranto (Alto Ionio - Italia)*. Geologia Romana, 21, 497-510.
- Sergio A. (1999). *Dinamica costiera: linee-guida allo studio del modellamento marino e analisi qualitative quantitative dei fenomeni di instabilità*. Tesi di Dottorato in Geomorfologia e Dinamica Ambientale, Dipartimento di Geologia e Geofisica, Facoltà di Scienze Matematiche, Fisiche e Naturali, Università degli Studi di Bari, 290 pp.
- Serpelloni E., Anzidei M., Baldi P., Casula G., Galvani A. (2005). *Crustal velocity and strain-rate fields in Italy and surrounding regions: new results from the analysis of permanent and non-permanent GPS networks*. Geophysical Journal International, 161, 861-880.
- Serpelloni E., Vannucci G., Pondrelli S., Argnani A., Casula G., Anzidei M., Baldi P. And Gasperini P. (2007) - *Kinematics of the Western Africa-Eurasia plate boundary from focal mechanisms and GPS data*. Geophysical Journal International (Online-Early Articles). doi:10.1111/j.1365-246X.2007.03367X.
- Shaw J. (1994). *Hairpin erosional marks, horseshoe vortices and subglacial erosion*. Sedimentary Geology, 91, 269-283.
- Shi S., Dawson A.G., Smith D.E. (1993). *Geomorphological impact of the Flores tsunami of 12th December, 1992*. In: Tsuchiya Y., Shuto N. (Ed.). Tsunami '93. Proceedings of the IUGG/IOC International Tsunami Symposium, Wakayama, Japan, August 23-27, 689-696.
- Shi S., Dawson A.G., Smith D.E. (1995). *Coastal sedimentation associated with the December 12th 1992 tsunami in Flores, Indonesia*. In: Satake K., Imamura F. (Ed.). Tsunami 1992-1994. Their Generation, Dynamics and Hazard - Pure and Applied Geophysics. Topical Volume, 525-536.
- Shimamoto T., Tsutsumi A., Kawamoto E., Miyawaki M., Sato H. (1995). *Field survey report on tsunami disasters caused by the 1993 Southwest Hokkaido Earthquake*. Pure and Applied Geophysics, 144, (3/4), 665-691.
- Shuto N., Matsutomi H. (1995). *Field survey of the 1993 Hokkaido Nansei-Oki Earthquake Tsunami*, Pure and Applied Geophysics, 144,(3/4), 649-663.
- Simeoni U. (1992). *I litorali tra Manfredonia e Barletta (Basso Adriatico): dissesti, sedimenti, problematiche ambientali*. Bollettino Società Geologica Italiana, 111, 367-398.
- Slejko, D., Camassi, R., Cecic, I., Herak, D., Herak, M., Kociu, S., Kouskouna, V., Lapajne, J., Makropoulos, K., Meletti, C., Muco, B., Papaioannou, C., Peruzza, L., Rebez, A., Scandone, P., Sulstarova, E., Voulgaris, N., Zivcic, M., Zupancic, P., 1999. *Seismic hazard assessment for Adria*. Annali di Geofisica, 42, 1085-1107.
- Smedile A., De Martini P.M., Barbano M.S., Gerardi F., Pantosti D., Pirrotta C., Cosentino M., Del Carlo P., Guarnieri P. (2007). *Identification of paleotsunami deposits in the Augusta Bay area (eastern Sicily, Italy): paleoseismological implication*. XXVI Convegno GNGTS. Extended Abstract, 207-211.
- Soloviev S.L. (1990). *Tsunamigenic Zones in the Mediterranean Seno*. Natural Hazards, 3, 183-202.
- Soloviev S.L., Solovieva O.N., Go C.N., Kim K.S., Shchetnikov N.A. (2000). *Tsunamis in the Mediterranean Sea 2000 B.C.-2000 A.D.*. Advances in Natural and Technological Hazards Research, Kluwer Academic Publisher, 242.
- Srinivasalu S., Thangadurai N., Switzer A. D., Ram Mohan V., Ayyamperumal T. (2007). *Erosion and sedimentation in Kalpakkam (N Tamil Nadu, India) from the 26th December 2004 tsunami*. Marine Geology, 240, 1-4, 65-75.
- Stefatos A., Charalambakis M., Papatheodorou G., Ferentinos G. (2006). *Tsunamigenic sources in an active European half-graben (Gulf of Corinth, Central Greece)*. Marine Geology, 232, 35-47.
- Stiros S.C., Arnold M., Pirazzoli P.A., Laborel J., Laborel-Deguen F., Papageorgiou S. (1992). *Historical coseismic uplift on Euvoea Island, Greece*. Earth and Planetary Science Letters, 108, 109-117.
- Stiros S.C., Pirazzoli P.A. (1995). *Palaeoseismic studies in Greece: a review*. Quaternary International, 25, 57-63.
- Stuiver M., Polach H.A. (1977). *Discussion: reporting of ¹⁴C data*. Radiocarbon, 19 (3), 355-363.
- Stuiver M., Reimer P. J. (1993). *Extended ¹⁴C database and revised CALIB radiocarbon calibration program*. Radiocarbon, 35, 215-230.
- Stuiver M., Reimer P. J. (2005). Calib 5.0 software. <http://radiocarbon.Pa.qub.ac.uk/calib/>.
- Stuiver M., Reimer P. J., Reimer R. W. (2005). CALIB 5.0. <http://www.calib.qub.ac.uk/crev50/manual.html>.
- Stuiver M., Reimer P.J., Reimer R. (2006). *CALIB Radiocarbon Calibration*. [/http://calib.qub.ac.uk/calibS](http://calib.qub.ac.uk/calibS) [access 13 December 2006].
- Stuiver M., Reimer P.J., Bard E., Beck J.W., Burr G.S., Hughen K.A., Kromer B., McCormac G., van der Plicht J., Spurk M. (1998). *INTCAL98 Radiocarbon Age Calibration, 24000-0 cal BP*. Radiocarbon, 40(3), 1041-1083.
- Sukma R. (2006). *Indonesia and the tsunami: responses and foreign policy implications*. Australia Journal of International Affairs, 60(2), 213-228.

- Switzer A.D., Bristow C.S., Jones B.G. (2006). *Investigation of large-scale washover of a small barrier system on the southeast Australian coast using ground penetrating radar*. *Sedimentary Geology*, 183, 145-156.
- Synolakis C.E. (1991). *Tsunami Runup on Steep Slopes: How Good Linear Theory Really is*. *Natural Hazards*, 4, 2-3, 221-234.
- Talandier J., Bourrouilh-Le Jan F.G. (1988). *High energy sedimentation in French Polynesia, cyclone or tsunami?* In: El-Sabh, M.I. & Murty, T.S. (Eds.). *Natural and Man-Made Hazards*. Reidel, Dordrecht, 193-199.
- Taggart B.E., Lundberg J., Carew J.L., Mylroie, J.E. (1993). *Holocene reef-rock boulders on Isla de Mona, Puerto Rico, transported by a hurricane or seismic sea wave*. *Abstracts with Programs, Geological Society of America*, 25 (6), A-61.
- Tanioka Y., Satake K. (1996). *Tsunami Generation by Horizontal Displacement of Ocean Bottom*. *Geophysical Research Letters*, 23, 8, 861-864.
- Taviani M. (1978). *Associazioni a molluschi pleistoceniche - attuali dragate nell' Adriatico meridionale*. *Bollettino di Zoologia*, 45, 297-306.
- Taylor F.W., Lawrence Edwards R., Wasserburg G.J., Frohlich C. (1990). *Seismic recurrence intervals and timing of aseismic subduction inferred from emerged corals and reefs of the Central Vanuatu (New Hebrides) frontal arc*. *Journal of Geophysical Research*, 95 (B1), 393-408.
- Thatcher T. (1984). *The earthquakes deformation cycle, recurrence and the time predictable model*. *Journal of Geophysical Research*, 89, 5674-5680.
- Tinti S., Armigliato A. (2003). *The Use of Scenarios to Evaluate Tsunami Impact in South Italy*. *Marine Geology*, 199, 3-4, 221-243.
- Tinti S., Maramai A. (1996). *Catalogue of tsunamis generated in Italy and in Cote d'Azur, France: a step towards a unified catalogue of tsunamis in Europe*. *Annali di Geofisica*, 39 (6), 1523-1300.
- Tinti S., Maramai A., Favali P. (1995). *The Gargano promontory: An important Italian seismogenic - tsunamigenic area*. *Marine Geology*, 122, 227-241.
- Tinti S., Maramai A., Graziani L. (2004). *The new catalogue of Italian tsunamis*. *Natural Hazards*, 33, 439-465.
- Tinti S., Maramai A., Graziani L. (2007). *The Italian Tsunami Catalogue (ITC), Version 2*. Available on-line at: http://web1.ingv.it:8080/portale_ingv/servizi-e-risorse/cartella-banche-dati/catalogo-tsunami/catalogo-degli-tsunami-italiani.
- Tinti S., Platanesi A. (1996). *Numerical simulation of the tsunami induced by the 1627 earthquake affecting Gargano, southern Italy*. *Journal of Geodynamics*, 21(2), 141-160.
- Tinti S., Platanesi A., Maramai A. (1997). *Numerical simulations of the 1627 Gargano tsunami (Southern Italy) to locate the earthquake source, Perspective on Tsunami Hazard Reduction: Observation, theory and planning*, G.T. Hebenstreit (Ed.), Kluwer Academic Publishers, Dordrecht, The Netherlands, 115-131.
- Titov V., González F.I. (1997). *Implementation and testing of the Method of Splitting Tsunami (MOST) model*. NOAA Tech. Memo. ERL PMEL-112 (PB98-122773), NOAA/Pacific Marine Environmental Laboratory, Seattle, WA, 11 pp.
- Titov V., Synolakis C.E. (1998). *Numerical modeling of tidal wave runup*. *Journal of Waterwall Port Coastal Ocean Engineering*, 124(4), 157-171.
- Tropeano M., Pieri P., Moretti M., Festa V., Calcagnile G., Del Gaudio V., Pierri P. (1997). *Tettonica quaternaria ed elementi di sismotettonica nell'area delle Murge (Avampaese Apulo)*. *Il Quaternario*, 10 (2), 543-548.
- Tropeano M., Spalluto L., Moretti M., Pieri P., Sabato L. (2004). *Depositi carbonatici infrapleistocenici di tipo Foramol in sistemi di scarpata (Salento, Italia Meridionale)*. *Il Quaternario, Italian Journal of Quaternary Sciences*, 17(2/2) 537-546.
- Tsuji Y., Imamura F., Matsutomi H., Synolakis C.E., Nanang P.T., Jumadi, Harada S., Han S.S., Arai K., Cook B. (1995a). *Field survey of the East Java Earthquake and Tsunami of June 3, 1994*. *Pure and Applied Geophysics*, 144 (3/4), 839-854.
- Tsuji Y., Matsutomi H., Imamura F., Takeo M., Kawata Y., Matsuyama M., Takahashi T., Sunarj O., Haraji P. (1995b). *Damage to coastal villages due to the 1992 Flores Island Earthquake Tsunami*. *Pure and Applied Geophysics*, 144 (3/4), 481-524.
- Tziavos C. (1997). *Paleogeographic evolution of the Amvrakikos Gulf, Western Greece*. - Marinos P.G., Koukis G.C., Tsiambaos G.C., Stournaras G.C. (Eds.). *Engineering Geology and the Environment*. Proceedings International Symposium on Engineering Geology and the Environment, organized by the Greek group of IAEG, Athens, Greece, 23-27 June 1997. 425-430.
- Ullmann A., Pirazzoli P.A., Moron V. (2007). *Sea surges around the Gulf of Lions and atmospheric conditions*. *Global and Planetary Change*, in press.
- Umitsu M., Tanavud C., Patanakanog B. (2007). *Effects of landforms on tsunami flow in the plains of Banda Aceh, Indonesia, and Nam Khem, Thailand*. *Marine Geology*, 242, 1-3, 141-153.

- Underhill J. (1988). *Triassic evaporates and Plio-Quaternary diapirism in western Greece*. Journal of the Geological Society (London), 145, 269–282.
- UN-DHA (1992). *Hierarchy of disaster management fermi*. United Nations Department of Humanitarian Affairs, New York.
- UNESCO (1972). *Report on consultative meeting of experts on the statistical study of natural hazard and their consequences*. Document SC/WS/500, 11 pp., Parigi.
- United States Geological Services (USGS, 2008). M 6.9 - SOUTHERN GREECE. http://earthquake.usgs.gov/eqcenter/pager/master.php?Event_id=2008nkan&network_id=us.
- Valensise G., Pantosti D. (eds.) (2001). *Database of Potential Sources for Earthquakes Larger than M 5.5 in Italy*. Annals of Geophysics, 44, with CD-ROM.
- Valensise G., Pantosti D., Basili R. (2004). *Seismology and Tectonic Setting of the Molise Earthquake Sequence of October 31-November 1, 2002*. Earthquake Spectra, 20, 23-37.
- Van Hinsbergen D.J.J., Langereis C.G., Meulenkamp J.E. (2005). *Revision of the timing, magnitude and distribution of Neogene rotations in the western Aegean region*. Tectonophysics, 396, 1–34.
- Van Straaten L.M.J.U. (1985). *Molluscs and sedimentation in the Adriatic Sea during late-Pleistocene and Holocene times*. Giornale di Geologia, 3, 47 (1-2), 181-202.
- Vannucci G., Gasperini P. (2004). *The new release of the database of Earthquake Mechanisms of the Mediterranean Area (EMMA Version 2)*. Annals of Geophysics, Suppl. 47, 307-334.
- Vocino M. (1930). *L'avventura della Contessa Matilde*. In: *A orza a poggia. Curiosità di storia e leggenda*. Edizioni Fratelli Palombi, Roma, 79-91.
- Von Seidlitz W. (1927). *Geologische Untersuchung der Inselnatur von Leukas*. In: Dörpfeld W. (Ed.), *Alt-Ithaka. Ein Beitrag zur Homer-Frage*. Uhde, Munich, 352–372.
- Vött A. (2007). *Relative sea level changes and regional tectonic evolution of seven coastal areas in NW Greece since the mid-Holocene*. Quaternary Science Reviews, 26, 894-919.
- Vött A., Handl M., Brüückner H. (2002). *Rekonstruktion holozäner Umweltbedingungen in Akarnanien (Nordwestgriechenland) mittels Diskriminanzanalyse von geochemischen Daten*. Geologica et Palaeontologica (Marburg), 36, 123–147.
- Vött A., Brüückner H., Handl M. (2003). *Holocene environmental changes in coastal Akarnania (northwestern Greece)*. In: Daschkeit A., Sterr H. (Eds.), *Aktuelle Ergebnisse der Küstenforschung*. 20. AMK-Tagung, Kiel, 30.05 - 01.06.2002. Berichte Forschungs- und Technologiezentrum Westküste Christian-Albrechts-Universität zu Kiel (Büsum), 28, 117–132.
- Vött A., May M., Brüückner H., Brockmüller S. (2006a). *Sedimentary evidence of late Holocene tsunami events near Lefkada Island (NW Greece)*. Zeitschrift für Geomorphologie N.F. Suppl. Vol. 146, 139-172
- Vött A., Brüückner H., Schriever A., Luther J., Handl M., Van der Borg K. (2006b). *Holocene palaeogeographies of the Palairos coastal plain (Akarnania, NW Greece) and their geoarchaeological implications*. Geoarchaeology, 21/7, 649-664.
- Vött A., Brüückner H., Handl M., Schriever A. (2006c). *Holocene palaeogeographies and the geoarchaeological setting of the Mytikas coastal plain (Akarnania, NW Greece)*. Zeitschrift für Geomorphologie N.F., Suppl. Vol., 142, p. 85-108.
- Vött A., Brüückner H., Handl M., Schriever A. (2006d). *Holocene palaeogeographies of the Astakos coastal plain (Akarnania, NW Greece)*. Palaeogeography, Palaeoclimatology, Palaeoecology 239, 126–146.
- Vött A., Brüückner H., May M., Lang F., Brockmüller S. (2007a). *Late Holocene tsunami imprint on Actio headland at the entrance to the Ambrakian Gulf*. Méditerranée 108, 43-57. Aix-en-Provence.
- Vött A., Brüückner H., Georg C., Handl M., Schriever A., Wagner H.J. (2007b). *Geoarchäologische Untersuchungen zum holozänen Landschaftswandel der Küstenebene von Palairos (Nordwestgriechenland)*. In: Lang F., Schwandner E.-L., Funke P., Kolonas L., Jahns S., Vött A. (Eds.): *Interdisziplinäre Landschaftsforschung im westgriechischen Akarnanien*. Archäologischer Anzeiger 1/2007: 191-213.
- Vött A., Brüückner H., May M., Lang F., Herd R., Brockmüller S. (2008a). *Strong tsunami impact on the Bay of Aghios Nikolaos and its environs (NW Greece) during Classical-Hellenistic times*. Quaternary International 181, 105-122.
- Vött A., Brüückner H., Brockmüller S., Handl M., May S.M., Gaki-Papanastassiou K., Herd R., Lang F., Maroukian H., Nelle O., Papanastassiou D. (2008b). *Traces of Holocene tsunamis across the Sound of Lefkada, NW Greece*. Global and Planetary Change (accepted).
- Vött A., Brüückner H., Brockmüller S., May M., Fountoulis I., Gaki-Papanastassiou K., Herd R., Lang F., Maroukian H., Papanastassiou D., Sakellariou D. (2008c). *Tsunami impacts on the Lefkada coastal zone during the past millennia and their palaeogeographical implications*. In: Papadatou-Giannopoulou H. (Ed.). *Proceedings of the International Conference Honouring Wilhelm Dörpfeld, August 6-9, 2006, Lefkada*, in press.

- Ward S.N., Valensise G. (1994). *The Palos Verdes terraces, California; Bathtub rings from a buried reverse fault*. Journal of Geophysical Research, 99 (B3), 85-94.
- Weiss R., Wünnemann K., Bahlburg H. (2006). *Numerical modelling of generation, propagation and run-up of tsunamis caused by oceanic impacts: model strategy and technical solutions*. Geophysical Journal International 167(1), 77-88.
- Whelan F., Kelletat D. (2002). *Geomorphologic evidence and relative and absolute dating results for tsunami events on Cyprus*. Science of Tsunami Hazards, 20 (1), 3–18.
- Whelan F., Kelletat D. (2003). *Analysis of Tsunami Deposits at Cabo de Trafalgar, Spain, Using GIS and GPS Technology*. Essener Geographische Arbeiten, 35, 11-25.
- Williams D. M., Hall A. M. (2004). *Cliff-top megaclast deposits of Ireland, a record of extreme waves in the North Atlantic—storms or tsunamis?* Marine Geology, 206, 101-117.
- Yeh H., Imamura F., Synolakis C., Tsuji Y., Liu P., Shi S. (1993). *The Flores Island tsunamis*. EOS, Transactions American Geophysical Union, 74 (33), 369, 371-373.
- Yeh H., Titov V., Gusiakov V., Pelinovsky E., Khrumushin V., Kai-Strenko V. (1995). *The 1994 Shitokan earthquake tsunamis*. Pure and Applied Geophysics, 144, 855-874.
- Young R. W., Bryant E.A. (1993). *Coastal rock platforms and ramp of Pleistocene and Tertiary age in Southern New South Wales, Australia*. Zeitschrift für Geomorphologie, N.F., 37, 257-272.
- Young R.W., Bryant E.A., Price D.M. (1996). *Catastrophic wave (tsunami?) Transport of boulders in southern New South Wales, Australia*. Zeitschrift für Geomorphologie, N.F., 40 (2), 191-207.
- Yu K.-F., Zhao J.-X., Shi Q., Meng Q.-S. (2008). *Reconstruction of storm/tsunami records over the last 4000 years using transported coral blocks and lagoon sediments in the southern South China Sea*. Quaternary International, in press.
- Zander A.-M., Fülling A., Brückner H., Mastronuzzi G. (2003). *Lumineszenzdatierungen an litoralen Sedimenten der Terrassentreppe von Metapont, Süditalien*. Essener Geographische Arbeiten, 35, 77-94, Essen.
- Zander A.-M., Fülling A., Brückner H., Mastronuzzi G. (2006). *OSL dating of Upper Pleistocene littoral sediments: a contribution to the chronostratigraphy of raised marine terraces bordering the Gulf of Taranto, Southern Italy*. Geografia Fisica e Dinamica Quaternaria, 29 (2) 33-50.
- Zeza F. (1981). *Morfogenesi litorale e fenomeni d'instabilità della costa a Falesia del Gargano tra Vieste e Manfredonia*. Geologia Applicata e Idrogeologia, 16, 193-227.
- Zeza F., Bruno G. (1991). *Caratteristiche geomorfologiche e problemi di instabilità della falesia di Porto Miggianno (Puglia)*. Geologia Applicata e Idrogeologia, 26, 273-291.

Index

Preface	5
CHAPTER 1: Central Mediterranean Area: An Overview	9
1.1. Introduction.....	9
1.2. Geomorphological and sedimentological traces of tsunami impact in the central Mediterranean area.....	10
CHAPTER 2: Geological, Geodynamic and Morphological features of Apulia (Italy)	15
2.1. Geological and geodynamic setting	15
2.1.1. Tectonic outline	18
2.1.2. Quaternary setting.....	19
2.1.3. Bradanic foredeep cycle.....	19
2.1.4. Marine Terraced Deposits.....	20
2.1.5. Quaternary vertical motions.....	21
2.2. Apulian Coastal morphology.....	22
2.2.1. Introduction.....	22
2.2.2. The continental shelf.....	23
2.2.3. Hydrogeological features	25
2.2.4. Meteo-marine features	25
2.2.5. Coastal types	30
2.2.6. Causes of coastal erosion	34
2.3. The effects of the impact of catastrophic waves on the coasts of Apulia.....	36
CHAPTER 3: The Fortore River Area	37
3.1. An introduction	37
3.2. Geomorphological features	38
3.3. The influence of large seismic events on the coastal landscape evolution.....	41
3.4. Conclusions.....	45
CHAPTER 4: The Ostuni-Carovigno coastal area	49
4.1. The Bari-Brindisi coast	49
4.1.1. The boulder accumulation at Torre Santa Sabina: STOP 1.....	50
4.1.2. Discussions	55
4.1.3. Conclusions.....	57
4.2. The Costa Merlata Area: STOP 2.....	58
4.2.1. Anthropogenic vs catastrophic origin of an enigmatic bioclastic deposit.....	58
4.2.2. Discussions	60
4.2.3. Conclusions.....	62
CHAPTER 5: The Western Coast of Salento peninsula	67
5.1. The coast Between Taranto and Santa Maria di Leuca	67
5.1.1. The deposit of Torre Squillace: STOP 3	68

5.1.2. The La Strea Peninsula.....	70
5.1.3. Discussions.....	71
5.1.4. Conclusions.....	73
5.2. The Torre Castiglione coast: STOP 4.....	73
5.2.1. The deposits of Torre Castiglione	74
5.2.2. Discussions.....	76
5.2.3. Conclusions.....	76
5.3. The Baia d'Argento (Silver Bay): STOP 5.....	76
5.3.1. Discussions.....	80
5.3.2. Conclusions.....	82
CHAPTER 6: The Eastern Coast of Salento peninsula.....	87
6.1. The Santa Maria di Leuca – Otranto coast	87
6.2. Torre Sasso boulder accumulation: STOP 6.....	88
6.3. Out-of-size coastal landform: the Torre S.Emiliano boulder accumulation: STOP 7	89
6.3.1. Inferred chronology of Torre S.Emiliano tsunami	94
6.3.2. Conclusions	98
6.4. Out-of-place landforms in a foreland stable area: the raised shore platforms of Otranto - Torre dell'Orso: STOP 8.....	98
6.4.1. Geological and morphological setting of the area.....	99
6.4.2. The raised shore platforms of Torre dell'Orso	101
6.4.3. The morphological evidences of recent tectonic activity	103
6.4.4. Discussions.....	106
6.4.5. Conclusions.....	106
CHAPTER 7: Tsunami flooding and vulnerability	107
7.1. The effects of tsunamis on coasts.....	107
7.1.1. Cliffs and convex rocky coasts.....	107
7.1.2. Rocky gently sloping coasts.....	108
7.1.3. Beaches	108
7.1.4. Pocket beach.....	108
7.1.5. Beach/lagoon system.....	109
7.1.6. River mouth.....	109
7.1.7. Discussions.....	109
7.1.8. Conclusions.....	111
CHAPTER 8: Geomorphological, sedimentological and geoarchaeological traces of Holocene tsunami impact between Lefkada and Lake Voukaria (NW Greece).....	115
8.1. Around the Sound of Lefkada	115
8.1.1. The Gyrapetra chevron: STOP 1	118
8.1.2. The Bay of Aghios Ioannis: STOP 2.....	119
8.1.3. Santa Maura Castle and the mouth of the modern channel: STOP 3	120
8.1.4. Teki Castle and the Canali Stretti washover plain: STOP 4.....	121

8.1.5. The central Sound of Lefkada near the ancient bridgehead: STOP 5	122
8.1.6. The southern Sound of Lefkada near Alexandros spit: STOP 6	123
8.1.7. The castle of Aghios Georgios at Nea Plaghia: STOP 7	124
8.2. The Bay of Aghios Nikolaos and the Lake Voulkaria.....	124
8.2.1. The Plaka beach ridge ruin: STOP 8.....	124
8.2.2. The Cheladivaron Promontory: STOP 9.....	125
8.2.3. The inner Bay of Cheladivaron and the ancient watchtower at Vigla: STOP 10.....	126
8.2.4. The Cleopatra Canal and the Lake Voulkaria: STOP 11	127
CHAPTER 9: Geomorphological, sedimentological and geoarchaeological traces of Holocene tsunami impact between Palairos and Preveza (NW Greece)	129
9.1. The Bay of Palairos-Pogonia.....	129
9.1.1. The ancient polis of Palairos: STOP 12	129
9.1.2. The submerged mole and geoarchaeological cliff deposits at Pogonia: STOP 13.....	129
9.2. Actio Headland.....	130
9.2.1. The Phoukias tsunami sequence and the Phoukias sand spit: STOP 14.....	130
9.2.2. The tsunami ripples at Paliokoulio: STOP 15	130
9.2.3. The spit of Actio and Actio Castle: STOP 16	131
9.2.4. The Strait of Preveza: STOP 17	133
9.2.5. The eastern shore of Actio Headland: STOP 18	134
CHAPTER 10: Strong tsunami impact on the Bay of Aghios Nikolaos and its environs (NW Greece) during Classical–Hellenistic times	135
10.1. Introduction	135
10.2. Topography and geotectonic setting.....	136
10.3. Materials and methods	138
10.4. Geomorphological and geoarchaeological records of extreme events and geochronological data.....	139
10.4.1. Washover deposits east of the Canali Stretti	139
10.4.2. Dislocated beachrock slabs at the Santa Maura beach ridge complex	141
10.4.3. Sublittoral disturbances in the Bay of Aghios Nikolaos	141
10.4.4. Evidence of strong landfall	143
10.4.4.1. Cheladivaron promontory	143
10.4.4.2. Pine forest beach.....	144
10.4.4.3. Paliokoulio on Actio headland.....	146
10.5. Discussion	147
10.5.1. Tsunami versus storm or sea level high stand deposits.....	147
10.5.1.1. Environs of the Canali Stretti.....	147
10.5.1.2. Santa Maura beach ridge complex	147
10.5.1.3. Bay of Aghios Nikolaos.....	148
10.5.1.4. Cheladivaron promontory	148
10.5.1.5. Pine forest beach.....	149
10.5.1.6. Paliokoulio.....	149

10.5.2. Strong tsunami impact during Classical–Hellenistic times	149
10.6. Conclusions	151
CHAPTER 11: Late Holocene tsunami imprint at the entrance of the Ambrakian gulf (NW Greece).....	153
11.1. Introduction	153
11.2. Topography and geotectonic setting.....	153
11.3. Materials and methods.....	155
11.4. Event deposits at Aktio headland	155
11.4.1. Phoukias and the Phoukias sand spit – transect A.....	155
11.4.2. Underwater geomorphology at Skoupeloi Achilleos.....	156
11.4.3. Paliokoulio and Koumaros – transect B	158
11.4.4. Northeastern shore of the Lagoon of Saltini.....	159
11.4.5. Vasiliko – transect C	159
11.5. Ages derived from ceramic findings and radiocarbon data	161
11.6. Discussion	162
11.6.1. Tsunami sediments versus storm or sea level high stand deposits	162
11.6.2. Geochronology of tsunami landfalls at Aktio headland	164
11.6.2.1. The mid-Holocene environment and the 2870-2350 cal BC tsunami event.....	165
11.6.2.2. Intermediary events.....	165
11.6.2.3. The 840 cal AD and (sub-) recent events	166
11.7. Conclusions	166
References.....	169
Index	189

Address of the Authors

Giuseppe Mastronuzzi, Cosimo Pignatelli
Dipartimento di Geologia e Geofisica
Università degli Studi "Aldo Moro"
Campus Universitario
Via E. Orabona, 4 – 70125 Bari, Italy
e.mail: g.mastronuzzi@geo.uniba.it
c.pignatelli@geo.uniba.it

Paolo Sansò
Dipartimento di Scienza dei Materiali
Università del Salento
Campus universitario
Via per Arnesano – 73100 Lecce, Italy
e.mail: paolo.sanso@unile.it

Helmut Brückner, Simon Matthias May
Faculty of Geography
Philipps-Universität Marburg
Deutschhausstr 10 - 35032 Marburg, Germany
e.mail: h.brueckner@staff.uni-marburg.de
maysi@staff.uni-marburg.de

Andreas Vött
Department of Geography
Universität zu Köln
Albertus-Magnus-Platz - 50923 Köln (Cologne), Germany
e.mail: andreas.voett@uni-koeln.de

Riccardo Caputo
Dipartimento di Scienze della Terra
Università degli Studi di Ferrara
Via Saragat, 1 - 44100 Ferrara, Italy
e.mail: rcaputo@unife.it

Donato Coppola
Dipartimento di Beni Culturali, Musica e Spettacolo
Università di Roma "Tor Vergata"
Via Columbia 1 - 00150 Roma, Italy
Museo di Civiltà Preclassiche della Murgia Meridionale
Via Cattedrale 15 - 72017 Ostuni (Br), Italy
e.mail: museo.ostuni@libero.it

Daniela Di Bucci
Dipartimento della Protezione Civile
Via Vitorchiano, 4 – 00189 Roma, Italy
e.mail: daniela.dibucci@protezionecivile.it

Umberto Fracassi
Istituto Nazionale di Geofisica e Vulcanologia
Via di Vigna Murata, 605 – 00143 Roma, Italy.
e.mail: fracassi@ingv.it

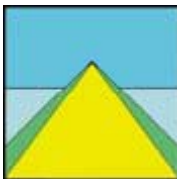
Maurilio Milella
Collaboratore Esterno Dipartimento di Geologia e Geofisica
Università degli Studi "Aldo Moro"
Via Giulio Petroni, 117/B – 70124 Bari, Italy
e.mail: maurisismo@email.it

Gianluca Selleri
G.D.S. - GEO DATA SERVICE s.r.l.
Via Scoglio del Tonno 70 ed.6/A - 74100 Taranto, Italy
e.mail: gianluca.selleri@yahoo.it

Publication designer and art copy editor:

Dr. Cosimo Pignatelli & Dr. Maurilio Milella

GDS – Geo Data Service, Taranto, Italy

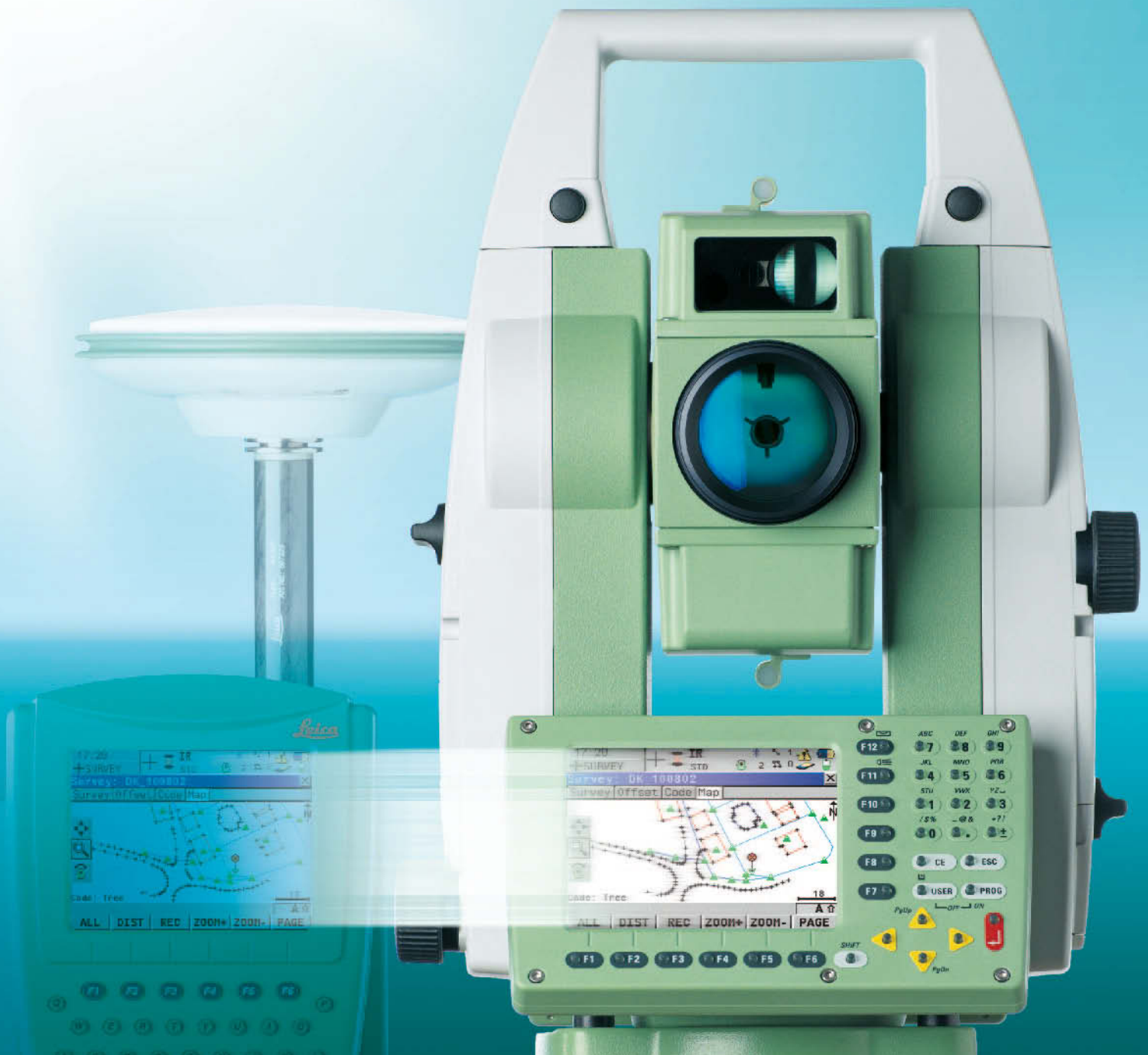


Copyright 2008

GI²S Coast – gruppo Informale Interuniversitario di Studi Costieri

Part of this publication may be reproduced if the source is clearly reported.
This book is out of print. It is available from editors.

Leica TPS1200+ Series High performance Total Station



- when it has to be **right**

Leica
Geosystems

Leica TPS1200+

Technical specifications and system features



Models and options

	TC	TCR	TCRM	TCA	TCP	TCRA	TCRP
Angle measurement	•	•	•	•	•	•	•
Distance measurement (IR-Mode)	•	•	•	•	•	•	•
PinPoint reflectorless dist. measur. (RL-Mode)		•	•			•	•
Motorized			•	•	•	•	•
Automatic Target Recognition (ATR)				•	•	•	•
PowerSearch (PS)					•		•
Guide Light (EGL)	◦	◦	◦	•	•	•	•
Remote Control Unit / RadioHandle	◦	◦	◦	◦	◦	◦	◦
GUS74 Laser Guide				◦		◦	
SmartStation (ATX1230 GG)	◦	◦	◦	◦	◦	◦	◦

• = Standard ◦ = Optional

Angle measurement



		Type 1201+	Type 1202+	Type 1203+	Type 1205+
Accuracy (std.dev., ISO 17123-3)	Hz, V	1" (0.3 mgon)	2" (0.6 mgon)	3" (1 mgon)	5" (1.5 mgon)
	Display resolution:	0.1" (0.1 mgon)	0.1" (0.1 mgon)	0.1" (0.1 mgon)	0.1" (0.1 mgon)
Method	absolute, continuous, diametrical				
Compensator	Working range:	4' (0.07 gon)	4' (0.07 gon)	4' (0.07 gon)	4' (0.07 gon)
	Setting accuracy:	0.5" (0.2 mgon)	0.5" (0.2 mgon)	1.0" (0.3 mgon)	1.5" (0.5 mgon)
	Method:	centralized dual axis compensator			

Distance measurement (IR-Mode)



Range (average atmospheric conditions)	Round prism (GPR1):	3000 m
	360° reflector (GRZ4):	1500 m
	Mini prism (GMP101):	1200 m
	Reflective tape (60 mm x 60mm)	250 m
	Shortest measurable distance:	1.5 m
Accuracy / Measurement time (standard deviation, ISO 17123-4)	Standard mode:	1 mm + 1.5 ppm / typ. 2.4 s
	Fast mode:	3 mm + 1.5 ppm / typ. 0.8 s
	Tracking mode:	3 mm + 1.5 ppm / typ. <0.15 s
	Display resolution:	0.1 mm
Method	Special phase shift analyzer (coaxial, visible red laser)	

PinPoint R400/R1000 reflectorless distance measurement (RL-Mode)



Range (average atmospheric conditions)	PinPoint R400:	400 m / 200 m (Kodak Gray Card: 90 % reflective / 18 % reflective)
	PinPoint R1000:	1000 m / 500 m (Kodak Gray Card: 90 % reflective / 18 % reflective)
	Shortest measurable distance:	1.5 m
	Long Range to round prism (GPR1):	1000 m – 7500 m
Accuracy / Measurement time (standard deviation, ISO 17123-4) (object in shade, sky overcast)	Reflectorless < 500 m:	2 mm + 2 ppm / typ. 3 – 6 s, max. 12 s
	Reflectorless > 500 m:	4 mm + 2 ppm / typ. 3 – 6 s, max. 12 s
	Long Range:	5 mm + 2 ppm / typ. 2.5 s, max. 12 s
Laser dot size	At 20 m:	approx. 7 mm x 14 mm
	At 100 m:	approx. 12 mm x 40 mm
Method	PinPoint R400 / R1000: System analyzer (coaxial, visible red laser)	

Motorized



Maximum speed	Rotating speed:	45° / s
----------------------	-----------------	---------

Automatic Target Recognition (ATR)



Range ATR mode / LOCK mode (average atmospheric conditions)	Round prism (GPR1):	1000 m / 800 m
	360° reflector (GRZ4, GRZ122):	600 m / 500 m
	Mini prism (GMP101):	500 m / 400 m
	Reflective tape (60 mm x 60 mm):	55 m (175 ft)
	Shortest measurable distance:	1.5 m / 5 m
Accuracy / Measure time (std. dev. ISO 17123-3)	ATR angle accuracy Hz, V:	1" (0.3 mgon)
	Base positioning accuracy:	± 1mm
	Measure time for GPR1:	3 – 4 s
Maximum speed (LOCK mode)	Tangential (standard mode):	5 m / s at 20 m, 25 m / s at 100 m
	Radial (tracking mode):	4 m / s
Method	Digital image processing (laser beam)	

PowerSearch (PS)



Range (average atmospheric conditions)	Round prism (GPR1):	300 m
	360° reflector (GRZ4, GRZ122):	300 m (perfectly aligned to instrument)
	Mini prism (GMP101):	100 m
	Shortest distance:	5 m
Search time	Typical search time:	< 10 s
Maximum speed	Rotating speed:	45° / s
Method	Digital signal processing (rotating laser fan)	

Guide Light (EGL)



Range (average atmospheric conditions)	Working range:	5 m – 150 m
	Accuracy	Positioning accuracy:

General data



Telescope	
Magnification:	30 x
Free objective aperture:	40 mm
Field of view:	1°30' (1.66 gon) / 2.7 m at 100 m
Focusing range:	1.7 m to infinity
Keyboard and Display	
Display:	1/4 VGA (320*240 pixels), graphic LCD, colour, illumination, touch screen
Keyboard:	34 keys (12 function keys, 12 alphanumeric keys), illumination
Angle display:	360° ' ", 360° decimal, 400 gon, 6400 mil, V%
Distance display:	meter, int. ft, int. ft/inch, US ft, US ft/inch
Position:	face I standard / face II optional
Data storage	
Internal memory:	64 MB (optional)
Memory card:	CompactFlash cards (64 MB and 256 MB)
Number of data records:	1750 / MB
Interfaces:	RS232, Bluetooth® Wireless-Technology (optional)
Circular Level	
Sensitivity:	6' / 2 mm

Laser plummet	
Centering accuracy:	1.5 mm at 1.5 m
Laser dot diameter:	2.5 mm at 1.5 m
Endless drives	
Number of drives:	1 horizontal / 1 vertical
Battery (GEB221)	
Type:	Lithium-Ion
Voltage:	7.4 V
Capacity:	3.8 Ah
Operating time:	typ. 5 – 8 h
Weights	
Total station:	4.8 – 5.5 kg
Battery (GEB221):	0.2 kg
Tribrach (GDF121):	0.8 kg
Environmental specifications	
Working temperature range:	-20° C to +50° C
Storage temperature range:	-40° C to +70° C
Dust / water (IEC 60529):	IP54
Humidity:	95 %, non-condensing

Remote Control Unit (RX1250T/Tc)



Communication	via integrated radio modem	
Control unit	Display:	1/4 VGA (320*240 pixels), graphic LCD, touch screen, illumination
	Keyboard:	62 keys (12 function keys, 40 alphanumeric keys), illumination
	Interface:	RS232
Battery (GEB211)	Type:	Lithium-Ion
	Voltage:	7.4 V
	Capacity:	1.9 Ah
	Operating time:	RX1250T: typ. 9 h, RX1250Tc: typ. 8 h
	Weights	Control unit RX1250T/Tc:
	Battery (GEB211):	0.1 kg
	Reflector pole adapter:	0.25 kg
Environmental specifications	Working temperature range:	RX1250T -30° C to +65° C / RX1250Tc -30° C to +50° C
	Storage temperature range:	-40° C to +80° C
	Protection against water, dust and sand (IEC 60529, MIL-STD-810F)	IP67
		waterproof to 1 m temporary submersion, dust tight

Whether you want to survey a parcel of land or a construction site, a facade or indoors to create as-built plans or carry out high-precision measurements of bridge and tunnel constructions – Leica Geosystems' surveying instruments provide the right solution for all measuring tasks.

The System 1200 Series instruments as well as the software are designed to meet the daily challenges of modern surveying. They all have outstanding, easy to read and user-friendly interfaces. Their straightforward menu structures, their clearly outlined scope of functions and high technology perfectly mate GNSS and TPS applications in the field. Whether you use the advantages of both technologies combined or each separately – due to the exceptional flexibility of Leica Geosystems instruments, reliable and productive surveying is assured.

When it has to be right.

Illustrations, descriptions and technical specifications are not binding and may change. Printed in Switzerland – Copyright Leica Geosystems AG, Heerbrugg, Switzerland, 2007. 738582en – IX.07 – RDV



Total Quality Management – our commitment to total customer satisfaction.

Ask your local Leica Geosystems dealer for more information about our TQM program.

Distance meter (PinPoint R400 / R1000):
Laser class 3R in accordance with IEC 60825-1 resp. EN 60825-1

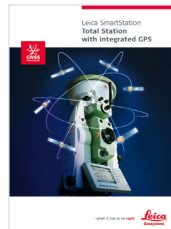
Laser plummet:
Laser class 2 in accordance with IEC 60825-1 resp. EN 60825-1

Distance meter (IR), ATR and PowerSearch:
Laser class 1 in accordance with IEC 60825-1 resp. EN 60825-1

The **Bluetooth®** word mark and logos are owned by Bluetooth SIG, Inc. and any use of such marks by Leica Geosystems AG is under license. Other trademarks and trade names are those of their respective owners.



Leica SmartPole
Product brochure



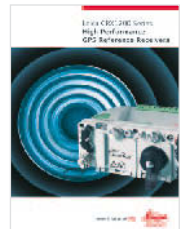
Leica SmartStation
Product brochure



Leica GPS1200
Product brochure



Leica System 1200 Software
Product brochure



Leica GRX1200
Product brochure

Our values for building the future



Our corporate culture is the result of shared values, a heritage that represents the company's strength and our commitment to the future. It has always been our policy **to protect the environment**, through the restoration and reutilization of the land; to develop our ideas by investing in **research** and **technology**; and to establish relations based on trust, constantly maintaining professional standards and **guaranteeing the excellency of our products**.

At present, Colacem is one of the most important industrial groups in Italy:

progress and corporate culture are encouraged, helping our communities to grow up and develop.

Colacem company profile

Colacem currently represents an avant-garde Italian industrial group, which has been able to grow and transform itself during the years, thanks to an always modern and innovative company policy and philosophy.

The company is present all across Italy with 7 full-cycle production plants: Caravate (VA), Rassina (AR), Ghigiano-Gubbio (PG), Sesto Campano (IS), Galatina (Le), Ragusa and Modica (Rg); 2 grinding centers: Acquasparta (TR) and Limatola (BN); 1 production plant for pre-mixed products : Salone (Roma), 2 terminals: Savona and Mestre (VE) and 3 warehouses in Ravenna, Ancona and Ascoli Piceno.

The 3 full-cycle plants located in Tunisi (Tunisia), Sabana Grande de Palenque (Dominican Republic) and Kilmar-Grenville sur la Rouge (Canada), and the terminals of Alicante and Cartagena in Spain , well represent the international dimension of the whole Group.

The 2007 turnover exceeded 493 million Euro (the consolidated aggregated turnover of the Financo Group is equal to 866 million Euro), with an increase of over 2% compared to the year 2006.

The number of employees exceeds 1450 people.

The entrepreneurial history of the Colaicovo Family is the result of hard working, new ideas and expertise : the Colaicovo brothers, Pasquale, Giovanni, Franco and Carlo, have been able to create such a company in a few decades, which is now among the first Italian producers and distributors of cement.

Colacem style is clear: a firm commitment aimed to enabling any division and department of the Company to grow and develop. This has led the company to attain very prestigious goals in the technologic and innovation field, which are recognized internationally: future-oriented dynamics; a unique know-how that has allowed the company to achieve important organization and technological results even in the design, construction and management of their production plants.

A winning strategy constantly marked by success, thanks to a company policy that has always seen the research activity as the basis of its development process. It resulted in a highly valuable background of knowledge and experience aimed to performing a correct management of both natural and human resources .

An active and reliable approach towards social and environmental subjects , centered around industrial purposes that combine ecologic preservation with economic growth.